Denitrification and the hypoxic response in obligate aerobic methane-oxidizing bacteria

By

Kerim Dimitri Kits

A thesis submitted in partial fulfillment of the requirements for the degree of

Doctor of Philosophy

In

Microbiology and Biotechnology

Department of Biological Sciences

University of Alberta

Abstract

Aerobic methanotrophic bacteria lessen the impact of the greenhouse gas methane (CH_4) not only because they are a sink for atmospheric methane but also because they oxidize it before it is emitted to the atmospheric reservoir. Aerobic methanotrophs, unlike anaerobic methane oxidizing archaea, have a dual need for molecular oxygen (O_2) for respiration and CH_4 oxidation. Nevertheless, methanotrophs are highly abundant and active in environments that are extremely hypoxic and even anaerobic. While the O_2 requirement in these organisms for CH_4 oxidation is inflexible, recent genome sequencing efforts have uncovered the presence of putative denitrification genes in many aerobic methanotrophs. Being able to use two different terminal electron acceptors – hybrid respiration – would be massively advantageous to aerobic methanotrophs as it would allow them to halve their O_2 requirement. But, the function of these genes that hint at an undiscovered respiratory anaerobic metabolism is unknown. Moreover, past work on pure cultures of aerobic methanotrophs ruled out the possibility that these organisms denitrify. An organism that can couple CH_4 oxidation to NO_3^- respiration so far does not exist in pure culture. So while the role of aerobic methanotrophs in the carbon cycle is appreciated, the hypoxic metabolism and contribution of these specialized microorganisms to the nitrogen cycle is not understood. Here we demonstrate using cultivation dependent approaches, microrespirometry, and whole genome, transcriptome, and proteome analysis that an aerobic methanotroph – *Methylomonas denitrificans* FJG1 – couples CH_4 oxidation to NO_3^- respiration with N_2O as the terminal product via the intermediates NO_2^- and NO. Whole transcriptome and proteome analysis reveals that respiratory nitrate (Nar, Nap), nitrite (Nir), and nitric oxide (Nor) reductases are expressed and upregulated at the transcript and protein levels under denitrifying conditions. Physiological analysis of denitrifying cultures of *M. denitrificans* FJG1 also confirms

that NO_3^- respiration is bioenergetically advantageous. We also confirm denitrification activity and upregulation of denitrification gene expression in another obligate methanotroph – *Methylomicrobium album* BG8 – and also show that this activity is supported by a diverse array of energy sources. Formaldehyde fermentation has been identified by others as an important adaptation of aerobic methanotrophs to hypoxia. We additionally illustrate here that *M. denitrificans* FJG1 can also ferment formaldehyde and that nitrate respiration and fermentation occur simultaneously during hypoxia. The work herein is a significant contribution to our knowledge of how aerobic methanotrophs affect greenhouse gas flux though CH_4 oxidation in low O_2 environments and through N_2O production via denitrification.

Preface

This thesis is an original work by Kerim Kits and serves as a compendium of original research articles that are either currently published in peer reviewed journals or are currently in preparation for submission. The research objectives and background for these research articles are detailed in the opening chapter. The closing chapter – Chapter 5 – provides a synopsis of the conclusions, contributions, and major findings of this thesis and the articles contained within. The original research articles that contribute to this thesis have been reformatted from the original publication style and are as follows:

Chapter 2: **Kits, K. D**., Klotz, M. G., and Stein, L. Y. (2015). Methane oxidation coupled to nitrate reduction under hypoxia by the Gammaproteobacterium *Methylomonas denitrificans*, sp. nov. type strain FJG1. *Environ. Microbiol.* 17, 3219–3232. doi:10.1111/1462-2920.12772. (*in press*)

Chapter 3: **Kits, K. D**., Campbell, D. J., Rosana, A. R., and Stein, L. Y. (2015). Diverse electron sources support denitrification under hypoxia in the obligate methanotroph *Methylomicrobium album* strain BG8. *Front. Microbiol.* 6, 1072. doi:10.3389/fmicb.2015.01072. (*in press*)

Chapter 4: **Kits, K.D**., Manuel, K., Liu, D., and Stein, L. Y. (2016). Simultaneous expression of denitrifying and fermentation pathways in the methanotroph, *Methylomonas denitrificans* FJG1. (*in preparation*)

Additional original research articles in which the thesis author is the primary author but that do not contribute to the individual outlined chapters are included as appendices:

Appendix A: Kits, K. D., Kalyuzhnaya, M. G., Klotz, M. G., Jetten, M. S. M., Op den Camp, H. J. M., Vuilleumier, S., et al. (2013). Genome Sequence of the Obligate Gammaproteobacterial Methanotroph Methylomicrobium album Strain BG8. *Genome Announc* 1, e0017013–e00170–13. doi:10.1128/genomeA.00170-13. (*in press*)

Publications in which the thesis author was a co-author and not the primary author and are therefore not included in the thesis are:

Stein, L. Y., F. Bringel, A. A. DiSpirito, S. Han, M. S. M. Jetten, M. G. Kalyuzhnaya, **K. D. Kits**, M. G. Klotz, H. J. M. O. den Camp, J. D. Semrau, S. Vuilleumier, D. C. Bruce, J. Cheng, K. W. Davenport, L. Goodwin, S. Han, L. Hauser, A. Lajus, M. L. Land, A. Lapidus, S. Lucas, C. Medigue, S. Pitluck, and T. Woyke. (2011). Genome sequence of the methanotrophic Alphaproteobacterium, Methylocystis sp. Rockwell (ATCC 49242). *J. Bacteriol.* 193, 2668–2669. doi:10.1128/JB.00278-11.

Boden, R., Cunliffe, M., Scanlan, J., Moussard, H., **Kits, K. D**., Klotz, M. G., et al. (2011). Complete genome sequence of the aerobic marine methanotroph Methylomonas methanica MC09. *J. Bacteriol.* 193, 7001–7002. doi:10.1128/JB.06267-11.

Hamilton, R., **Kits, K. D**., Ramonovskaya, V. A., Rozova, O. N., Yurimoto, H., Iguchi, H., et al. (2015). Draft genomes of gammaproteobacterial methanotrophs isolated from terrestrial ecosystems. *Genome Announc* 3, e00515–15. doi:10.1128/genomeA.00515-15.

Kozlowski, J. A., **Kits, K. D**., and Stein, L. Y. (2016a). Genome Sequence of Nitrosomonas

communis Strain Nm2, a Mesophilic Ammonia-Oxidizing Bacterium Isolated from Mediterranean Soil. *Genome Announc* 4, e01541–15. doi:10.1128/genomeA.01541-15.

Kozlowski, J. A., **Kits, K. D**., and Stein, L. Y. (2016b). Complete Genome Sequence of Nitrosomonas ureae Strain Nm10, an Oligotrophic Group 6a Nitrosomonad. *Genome Announc* 4, e00094–16. doi:10.1128/genomeA.00094-16.

The contribution of the thesis author to the aforementioned published journal articles was as follows. For chapter 2, the thesis author performed all of the physiology, genome sequencing, transcriptome sequencing and all of the data analysis while Martin G. Klotz performed the phylogenetic analysis of the *M. denitrificans* FJG1 genome. The thesis author wrote the manuscript (Chapter 2) with input and guidance from M. G. Klotz and L. Y. Stein. For chapter 3, the thesis author performed all of the physiology, all of the data analysis, and a portion of the expression analysis while Albert R. R. Rosana finished the expression analysis. Chapter 3 was written by the thesis author with input from L. Y. Stein who also helped develop experimental design for this chapter. For chapter 4, the thesis author carried out the transcriptome sequencing and all data analysis, and Manuel Kleiner and Dan Liu performed the proteomics. In all cases, Lisa Y. Stein contributed guidance and editorial comments on written manuscripts.

With regard to the publications in which the thesis author was a co-author and not a primary author, the contributions from the thesis author were as follows. The thesis author performed the main bioinformatics role, assembled, and closed genome sequences for Kozlowski *et al.,* (2016a) and Kozlowski *et al.,* (2016b). In all other co-authored original research articles, the author contributed to genome annotation.

Acknowledgements

First, I would like to thank my supervisor – Dr. Lisa Stein. When I first started working in your lab, during my third undergraduate year, my CV was not that of a promising future research assistant or graduate student. You recognized something in me and you then played an enormous role in the development of my skills and interests as a then (very) junior scientist. Thank you for accepting me as a graduate student, thank you for providing me with funding and space to do research, and thank you for always giving me the independence to pursue my interests. Also, I have to thank you for always allowing and encouraging me to attend meetings and meet other scientists – these experiences gave me immeasurable maturity and perspective.

I also have to levy a massive thank you to the other members of my graduate studies committee – Dr. Yan Boucher and Dr. George Owttrim. Thank you both so much for taking the time to read over my work and assessing my progress during our committee meetings. You were both valuable committee members and I am incredibly grateful for your suggestions, advice, and support. It is also important that I mention Dr. Martin Klotz, although Martin wasn't officially part of my committee; Martin, your approach to critical thinking massively influenced me and ignited in me a true appreciation for exactitude of meaning, nomenclature, and logic.

I have to recognize the contribution that other members of the University of Alberta had to my work. Thank you to the storeroom staff – Shelley Scott, Ben McDonald, and Debbie Preston; it would have been difficult to do the work I did without your expertise – from ordering complex gas mixtures to shipping sensitive samples. I also really have to thank Troy Locke and Cheryl Nargang; you both went above what was necessary in training me and answering my questions. I also want to thank the funding agencies that supported me throughout my degree - The National Science and Engineering Research Council (NSERC) and Alberta Innovates (AI).

On a more personal note, I'd like to thank my parents and my little brother. Mom and Dad, you both put up with me visiting too infrequently and the generally high levels of stress and despair throughout my PhD. I'm very proud to continue our family tradition of getting an advanced degree. I didn't always know where I was going, but thanks to you I always knew that knowledge is valuable.

I cannot be grateful enough to my incredible colleague, wife, companion, and best friend – Dr. Jessica Ann Kozlowski. You are all that matters. It really would not have been possible for me to finish this work without you; you helped me with experiments, you edited much of my writing, you offered me good advice, you gave me emotional support, and you helped generally pave the road for me during this degree. Because of you I understand the relative significance of life and work, including the general incompatibility between those two things and the overwhelming importance of the former. This last fact unfailingly always made me a better scientist - the realization that the human effort to understand the world is *only* enlightening in the short run but totally futile in the long run allowed me to enjoy life, to enjoy work, and ultimately enabled me to stay sane enough to finish this degree.

Table of Contents

Table of Figures

Tables of Tables

List of symbols, nomenclature, and abbreviations

Δp: proton motor force

1D: one dimensional

2D: two dimensional

ABC: ammonium bicarbonate

ADP: adenosine diphosphate

AMS: ammonia mineral salts

ANAMMOX: Anaerobic ammonium oxidation

ANI: average nucleotide identity

ANME: Anaerobic methane oxidizing euryarchaeota

ATP: adenosine triphosphate

Ack: acetate kinase

Adh: alcohol dehydrogenase

bc_1: respiratory complex III

Bfr: bacterioferritin

Bp: base pairs

C1 compound: a compound that has no carbon to carbon bonds and only one carbon atom

C2: compound with two carbon atoms

C_2H_6: ethane

C_2H_6O: ethanol

CBB: Calvin-Benson-Bassham cycle or the Calvin cycle

CCCP: Carbonyl cyanide m-chlorophenyl hydrazone

cDNA: complementary DNA

CH_2O: formaldehyde

CH_3OH: methanol

CH_4: Methane

CHOOH: formate

cNOR: cytochrome c linked nitric oxide reductase

CO_2: Carbon dioxide

Cu-MMO/CuMMO: copper containing monooxygenase

Cu^{2+}: copper (II) oxide

Cu: copper

Cyt: cytochrome

D.O.: dissolved oxygen

DHAP: dihydroxyacetone phosphate

DNA: deoxyribonucleic acid

dO_2: dissolved O_2

Da: dalton

dsDNA: double stranded DNA

ED: Enter-Doudoroff pathway

EIP: environmental information processing

EMP: Embden-Meyerhof-Parnas pathway

ESI: electrospray ionization

EtOH: ethanol

F6P: fructose-6-phosphate

FAD: Flavin adenine dinucleotide

FASP: filter-aided sample preparation

FBPA: fructose bisphosphate aldolase pathway

FDR: false discovery rate

Fae: formaldehyde activating enzyme

Fba: fructose bisphosphate aldolase

Fdh: formate dehydrogenase

Fum: fumarate hydratase

G3P: glyceraldehyde-3-phosphate

GC-TCD: gas chromatography with a thermal conductivity detector

gDNA: genomic DNA

Gap: glyceraldehyde-3-phosphate dehydrogenase

Gck: glucokinase

Gpd: glucose phosphate dehydrogenase

Gpi: glucose phosphate isomerase

H_2: hydrogen gas

H_2O: dihydrogen oxide or water

H_2S: hydrogen sulfide

H_4MPT: tetrahydromethanopterin

Hpi: hexulose phosphate isomerase

Hps: hexulose phosphate synthase

ICM: intracytoplasmic membrane

iTraq: isobaric tags for absolute and relative quantification

KDPG: 2-keto-3-deoxy-6-phosphogluconate

KDPGA: KDPG pathway

KEGG: Kyoto Encyclopedia of Genes and Genomes

KNO_3: potassium nitrate

Kat: catalase

LC: liquid chromatography

m/z: mass to charge ratio

MCR: Methyl coenzyme M reductase

MDH: methanol dehydrogenase

MMO: methane monooxygenase

MR: microrespiration

mRNA: messenger ribonucleic acid

MS/MS: tandem mass spectrometry

MS: mass spectrometry

MWCO: molecular weight cutoff

N-DAMO: nitrite-dependent anaerobic methane oxidation

N_2: dinitrogen

N_2O: nitrous oxide

N: nitrogen

NAD+: nicotinamide adenine dinucleotide phosphate (oxidized)

NADH: nicotinamide adenine dinucleotide phosphate (reduced)

NADP+: nicotinamide adenine dinucleotide phosphate (oxidized)

NADPH: nicotinamide adenine dinucleotide phosphate (reduced)

NH_4^+: ammonium

NH_4Cl: ammonium chloride

NMS: nitrate mineral salts

NO_2^-: nitrite

NO_3^-: nitrate

NO: nitric oxide

NO_x: nitrogen oxide

NSAF: normalized spectral abundance factors

$NaNO_2$: sodium nitrite

Nap: nitrate reductase (periplasmic)

Nar: nitrate reductase (membrane bound)

Nas: assimilatory nitrate reductase (cytoplasmic)

Ndh: NADH dehydrogenase

NiFe: nickel iron

Nir: nitrite reductase

NirK: copper containing nitrite reductase

NirS: cytochrome cd_1 containing nitrite reductase

Nor: nitric oxide reductase

NorCB: cytochrome *c* linked nitric oxide reductase

Nos: nitrous oxide reductase

NosZ: nitrous oxide reductase

O.D.: optical density

O_2: dioxygen

O: oxygen

OH: hydroxyl

PAGE: polyacrylamide gel electrophoresis

PCR: polymerase chain reaction

PEP: phosphoenolpyruvate

pMMO: particulate methane monooxygenase

PQQ: pyrroloquinoline quinone

PSM: peptide spectral match

PTA-ACK: phosphate acetyl transferase – acetate kinase

pXMO: uncharacterized monooxygenase encoded by the *pxmABC* gene cluster

Pdc: pyruvate decarboxylase

Pdh: pyruvate dehydrogenase

Pfk: phosphofructokinase

Pfl: pyruvate formate lyase

Pgm: phosphoglycerate mutase

Pi: inorganic phosphate

pmf: proton motor force

ppb: parts per billion

Ppc: phosphoenolpyruvate carboxylase

Ppk: polyphosphate kinase

ppm: part per million

Pps: phosphoenolpyruvate synthase

Proli-NONOate: 1-(hydroxy-NNO-azoxy)-L-proline, disodium salt

Pta: phosphate acetyltransferase

Pyc: pyruvate carboxylase

qNOR: quinol linked nitric oxide reductase

qPCR: quantitative PCR

R: Pearson correlation coefficient

RIN: RNA integrity number

RNA: ribonucleic acid

ROS: reactive oxygen species

RPKM: reads per kilobase of transcript per million mapped reads

rRNA: ribosomal RNA

Rpi: ribose-5-phosphate isomerase

R_s: Spearman correlation coefficient

RuMP: ribulose monophosphate

SBPase: sedoheptulose-1,7-bisphosphate aldolase pathway

SIP: stable isotope probing

sMMO: soluble methane monooxygenase

SO_4^{2-}: sulfate

SRB: sulfate reducing bacteria

Sod: superoxide dismutase

str.: strain

TA: transaldolase

TCA: tricarboxylic acid cycle

THF: tetrahydrofolate

TPM: transcripts per million transcripts

tRNA: transfer RNA

Tg: teragrams

Tkt: transketolase

U: units

Ydbk: pyruvate ferredoxin oxidoreductase

Chapter 1: General Introduction

1.1: The global methane budget and significance of methane

Methane (CH_4) is the second most important anthropogenically produced greenhouse gas after carbon dioxide (CO_2) and accounts for about one quarter to one third of the global warming effect (Nazaries et al., 2013). Aside from abiotic sources, methane is produced by methanogenic archaea that ferment degraded organic matter under anoxic conditions (Conrad, 2009). The concentration of CH_4 in the atmosphere was 722 ± 25 ppb prior to the industrial revolution and has since increased 150% in the atmosphere to a concentration of 1803 ppb (IPCC, 2013). From 1999-2006, the increase of CH_4 in the atmosphere was stalled at around 1774 ppb but began to surge again in 2007 (IPCC, 2013). The concentration of CH_4 in the atmosphere in 2011 was 1803 ± 2 ppb (IPCC, 2013). Although CH_4 has a short lifetime in the atmosphere (11.2 ± 1.3 years), it is 25 times more potent at trapping heat than CO_2 over a century due to its very high ability to absorb and emit infrared radiation (Nazaries et al., 2013). Man-made CH_4 emissions now make up 63% of the total global emissions; the sources being fossil fuels (18%), emission by ruminants (17%), rice cultivation (10%), landfills (7%), biomass burning (7%), and treatment of waste (4%) with most of these sources being microbial in nature (Conrad, 2009).

The vast majority of CH_4 in the atmosphere is abiotically removed through a reaction with OH radicals (88%) (Nazaries et al., 2013). Stratosphere loss is responsible for another 7% and the microbial sink is estimated to be at only 5-7% (Nazaries et al., 2013). However, is it estimated that about 50-90% of the CH_4 produced by the anaerobic methanogens is oxidized prior to reaching the atmosphere (Colin Murrell and Jetten, 2009). So, although the microbial sink for atmospheric CH_4 oxidation is small, understanding the sources and sinks of CH_4 is critical to comprehending not only how we can attenuate emissions but also how future

emissions will be impacted by a warming planet. Methane-oxidizing microbes are very diverse and fall into two domains of life – Archaea and Bacteria. Perhaps the most significant distinction between the two different groups of methane consumers is whether O_2 is required for methane oxidation; all methane-oxidizing bacteria (including the candidate phylum NC10, which is discussed near the closing of this chapter) require O_2 to oxidize CH_4 while the methane consuming archaea are all strict anaerobes, operate the typical methanogenesis pathway in reverse using methyl coenzyme M reductase (MCR), and thus do not require O_2 for CH_4 oxidation. Though the focus of this thesis is only on aerobic methanotrophic bacteria, due to the immense importance of archaea for global methane consumption I will briefly address them in the next section before addressing the bacteria in detail.

1.2: Methane oxidizing microorganisms

1.2.1: Anaerobic methane-oxidizing archaea

As mentioned in the previous section, up to 90% of the 300 Tg of CH_4 produced by methanogenesis globally is oxidized by anaerobic archaea referred to as ANME (**AN**aerobic **M**ethane-oxidizing **E**uryarchaeota) before this methane reaches oxygenated environments (Reeburgh, 2007). Anaerobic methane oxidation was first proposed by Martens and Berner as a way to rationalize why dissolved CH_4 concentrations were so low in anoxic Long Island Sound sediments when sulfate was high and suddenly increases when sulfate was depleted (Martens and Berner, 1974). One of the initial explanations was that sulfate reducing bacteria (SRB) could be consuming the methane and respiring sulfate. However, even though the reaction was energetically plausible, pure cultures of SRB could not perform the process and all known methane-oxidizers at the time were obligate aerobic bacteria (Martens and Berner, 1974). Later, Hoehler et al and others suggested that the process could involve a bacterial consortium of

several partners that included an association between reversely operating methanogenic archaea and SRB (Hoehler et al., 1994). The process is now better understood and it is generally agreed that anaerobic methanogens oxidize the CH_4 to CO_2 and share the energy yield with SBR that reduce sulfate (SO_4^{2-}) to hydrogen sulfide (H_2S) in an apparently tight syntrophic physical association characterized by the ANME residing at the centre of a round aggregate surrounded by Desulfobacteriaceae (Boetius et al., 2000; Hinrichs et al., 1999). Since then, culture independent approaches have suggested that direct interspecies electron transfer occurs between the ANME and SRB to fuel the partnership and, most recently, that the ANME and SRB can be decoupled using soluble artificial terminal electron acceptors (McGlynn et al., 2015; Scheller et al., 2016; Wegener et al., 2015). However, it also appears that another strategy involves ANME reducing SO_4^{2-} to H_2S and consuming methane without a syntrophically linked partner; this metabolism would involve only a single organism (ANME) and would allow all of the energy from the oxidation of CH_4 to be conserved by the ANME (Milucka et al., 2012).

Critically, it has also been demonstrated that anaerobic methane oxidation can involve terminal electron acceptors other than SO_4^{2-}. Beal et al showed using $^{13}CH_4$ that anaerobic methane oxidation activity is detectable in CH_4 marine seep sediment samples in the absence of sulfate if either manganese or iron are added to the incubations (Beal et al., 2009). This is clear evidence that anoxic CH_4 oxidation is linked to more terminal electron acceptors than just SO_4^{2-} – though we do not yet know what microorganisms may be cooperating to perform this manganese and iron linked metabolism. Finally, anaerobic methane oxidation by ANME can also be linked to nitrate (NO_3^-) respiration (Haroon et al., 2013). In a lengthy 350-day experiment, a bioreactor fed with nitrate, ammonium, and methane indicated that a single dominant ANME-2d population (*Candidatus Methanoperedens nitroreducens*) apparently oxidized $^{13}CH_4$ and coupled

this to NO_3^- reduction (Haroon et al., 2013). The NO_3^- was reduced to NO_2^- which was then consumed by syntrophically linked anaerobic ammonium oxidizing bacteria (ANAMMOX) (Haroon et al., 2013). The metagenome and metatranscriptome of the bioreactor community as well as single cells showed that the *M. nitroreducens* genome encoded a membrane-bound nitrate reductase (*narGH*) which was highly transcribed and apparently acquired laterally by the ANME from a Gammaproteobacterial donor.

1.2.2: Aerobic methane oxidizing bacteria

Aerobic methanotrophic bacteria are a specialized category of microorganisms that are capable of utilizing methane (a reduced gaseous substrate) as their only source of carbon and energy – meaning that the carbon in all of their cellular components must be made from a C1 compound (a compound that has just 1 carbon atom and no carbon to carbon bonds). The aerobic methanotrophs as a functional guild are phylogenetically diverse; representatives exist in the Gammaproteobacteria, Alphaproteobacteria, and Verrucomicrobia (Knief, 2015). There are three known phyla, each with subfamilies: within the Alphaproteobacteria: Methylocystaceae, Beijerinckiaceae (Knief, 2015); within the Gammaproteobacteria: Methylococcaceae, Methylothermaceae, Crenotrichaceae (Knief, 2015); within the Verrucomicrobia: Methylacidiphilaceae.

The ability to grow solely on a reduced C1 compound means that this functional group of microorganisms requires a unique set of biochemical pathways to generate energy and oxidize/assimilate carbon. There are three major C1 carbon assimilation pathways that aerobic methanotrophs can use: the ribulose monophosphate pathway (RuMP), The Serine pathway, and the Calvin-Benson-Bassham (CBB) cycle (Chistoserdova and Lidstrom, 2013). A distinguishing feature of carbon assimilation pathways in aerobic methanotrophs is the important role of

formaldehyde. This molecule is a central intermediate in their carbon metabolism and in most methanotrophs, the formaldehyde generated as a result of methane oxidation is split into two parts: one that is oxidized further to CO_2 for energy generation and a second part that is assimilated into cellular carbon(Trotsenko and Murrell, 2008). Some use a more than one pathway or a combination thereof.

The Gammaproteobacterial methanotrophs all contain a RuMP pathway but some also use Serine or CBB in addition (Chistoserdova and Lidstrom, 2013). The Alphaproteobacterial methanotrophs all utilize the Serine pathway, sometimes together with CBB (Chistoserdova and Lidstrom, 2013). The Verrucomicrobial methanotrophs only utilize the CBB for C1 assimilation (Khadem et al., 2011). Methanotrophs that only utilize CBB to fix carbon are known as autotrophic methanotrophs and this group does not assimilate formaldehyde. Nearly all aerobic methanotrophs possess intracytoplasmic membranes (ICM) – known exceptions are facultative methanotrophs that contain only the soluble form of methane monooxygenase (sMMO) (Murrell, 2010). These highly folded membrane invaginations contain the particulate methane monooxygenase (pMMO) enzyme, which is responsible for O_2 dependent CH4 oxidation to CH_3OH (Trotsenko and Murrell, 2008).

Aerobic methanotrophic bacteria, since they help to attenuate net flux of the greenhouse gas CH_4 to the atmosphere from the terrestrial and aquatic reservoirs, are ubiquitous in the environment and inhabit a very diverse variety of ecosystems. Methanotrophs thrive in mesophilic environments but can also be present in high abundance in extreme environments; ergo, methanotrophs have been found to grow in environments that range from 0°C-75°C, pH 1-12, 0-5% salinity (Murrell, 2010). These include freshwater and marine water columns as well as sediments, ground water, wastewater and sewage sludge, rice paddies, landfill cover soil, upland

soils, forest soil, tundra, artic soil, permafrost, floodplains, aquifers and extreme environments such as hot springs, Antarctic lakes, soda lakes and volcanic mud pots (Knief, 2015; Murrell, 2010). Some aerobic methanotrophs also function as symbionts in deep-sea mussels, hydrothermal-vent sails, hydrothermal-vent crabs, tubeworms, sponges and sphagnum moss (Murrell, 2010).

1.3: Central carbon metabolism of aerobic methane-oxidizing bacteria

1.3.1: Methane (CH_4) oxidation to methanol (CH_3OH)

Aerobic methanotrophs oxidize CH_4 to CO_2 and H_2O via methanol, formaldehyde and formate (Fig. 1). The first step, the oxidation of CH_4 to CH_3OH, is catalyzed by the methane monooxygenase (MMO) enzyme. This enzyme is an oxidase that utilizes reducing power and O_2 to activate and oxidize methane. In this mechanism one O atom is put into CH_4 to form CH_3OH and the other O atom is incorporated into H_2O (Trotsenko and Murrell, 2008) (Fig. 1). There are different types of MMO in aerobic methanotrophs; a cytoplasmic soluble type (known as sMMO) and a membrane bound particulate type (pMMO). All methanotrophs except for *Methylocella* species have a pMMO while only some methanotrophs have both the sMMO and pMMO (Theisen and Murrell, 2005). The pMMO is nearly universal among methanotrophs while the presence of the sMMO is somewhat limited (Chistoserdova and Lidstrom, 2013). The pMMO requires Cu^{2+} for activity and the expression of pMMO and sMMO in methanotrophs is tightly regulated by Cu:biomass ratio – a high Cu:biomass ratio leads to expression of pMMO while a low Cu:biomass ratio favours the sMMO (Trotsenko and Murrell, 2008).

Much work has been done recently to elucidate the structure and mechanism of pMMO. The pMMO enzyme has been purified in its active form from several methanotrophs, including representatives of both the Alpha- and Gammaproteobacteria; the crystal structure revealed that a

dicopper center plays a central role in CH_4 catalysis (Balasubramanian et al., 2010; Lieberman and Rosenzweig, 2005; Zahn and DiSpirito, 1996). The enzyme is encoded by a single *pmoCAB* operon, although many methanotrophs contain multiple copies of the operon that often have significant sequence divergence (Tavormina et al., 2011; Ward et al., 2004). Though it is known that pMMO requires reducing power to function, the source of this reductant *in vivo* has not yet been elucidated (Chistoserdova and Lidstrom, 2013).

The sMMO has also been purified from both the Alpha- and Gammaproteobacterial methanotrophs. It is made up of three constituent parts: a hydroxylase which itself is made up of three polypeptides and non-heme iron centre, a reductase which accommodates an iron-sulfur cluster as well as FAD, and a third component (called component B) (Lipscomb, 1994). Unlike the pMMO, the source of reducing power for the sMMO *in vivo* is known – it uses NADH (Trotsenko and Murrell, 2008). The sMMO is a catalytically loose enzyme and it is known to have an exceedingly broad substrate specificity; sMMO can oxidize a wide variety of alkanes – straight chain, branched, aromatic – and has been the focus of many bioremediation studies (Lipscomb, 1994; Semrau et al., 2010). The sMMO is encoded by a group of genes (*mmo* genes) that are usually found together in on a chromosome.

1.3.2: Methanol (CH_3OH) oxidation to formaldehyde (CH_2O)

CH_3OH produced by the methane monooxygenase is oxidized by methanotrophs via a methanol dehydrogenase (MDH) (Fig. 1). There are two systems for this; 1) a periplasmic, calcium dependent, pyrroquinoline quinone (PQQ)-linked methanol dehydrogenase and 2) an alternative periplasmic methanol dehydrogenase that may be lanthanide dependent (Pol et al., 2014; Trotsenko and Murrell, 2008). The calcium dependent methanol dehydrogenase is encoded by *mxaFI* (the large and small subunits, respectively) and also requires a cytochrome c electron

acceptor (encoded by *mxaF*), and other structural components (encoded by *mxaLCKA*) responsible for calcium incorporation into the protein (Chu and Lidstrom, 2016). The MxaFI is the traditional well-studied methanol dehydrogenase. Electrons from the oxidation of methanol are transferred to the PQQ cofactor and then from the cofactor to a discrete cytochrome *c* protein and further, via other electron carriers, to complex IV (the terminal oxidase)(Trotsenko and Murrell, 2008).

The presence and function of XoxF in methanotrophs has just recently been uncovered by several groups which showed that rare-earth lanthanides (such as lanthanum, cerium, etc) regulate the transcriptional expression of the *xoxF* gene (Chu and Lidstrom, 2016; Gu et al., 2016). It has also recently come to light that *xoxF* is more widely distributed in methylotrophic bacteria than *mxaFI* (Chistoserdova and Lidstrom, 2013). Most recently, Chu and Lidstrom (2016) demonstrated that lanthanides stimulate *xoxF* expression and depress *mxaFI* expression in a Gammaproteobacterial methanotroph, *Methylomicrobium buryatense* 5GB1C, despite an excess of calcium in the growth medium(Chu and Lidstrom, 2016). Further, they demonstrated that XoxF is actually the principal methanol dehydrogenase in this strain.

1.3.3: Formaldehyde (CH_2O) oxidation to formate (CHOOH)

There are several pathways present in methanotrophs for the oxidation of formaldehyde. One of the most significant is the tetrahydromethanopterin (H_4MPT)-linked CH_2O oxidation pathway. This pathway utilizes H_4MPT as a cofactor (Trotsenko and Murrell, 2008). The formaldehyde activating enzyme (Fae) condenses CH_2O with H_4MPT to form methylene-H_4MPT in step 1 (Chistoserdova and Lidstrom, 2013). The oxidation of methylene-H_4MPT is catalyzed by a $NADP^+$ dependent methylene-H_4MPT dehydrogenase (MtdB) in step 2. Then, methenyl-H_4MPT cyclohydrolase (Mch) in step 3 performs the conversion of methenyl-H_4MPT into

formyl-H_4MPT. Finally, the formyltransferase-hydrolase (encoded by *fhcABCD*) converts formyl-H_4MPT to formate (CHOOH) in step 4 of the pathway (Trotsenko and Murrell, 2008).

1.3.4: Formate (CHOOH) oxidation to CO_2

The concluding step of the methane oxidation pathway of methanotrophs is the oxidation of CHOOH to CO_2 (Fig. 1). This reaction is catalyzed in known methanotrophs by an NAD^+ dependent formate dehydrogenase (Fdh) in the cytoplasm (Trotsenko and Murrell, 2008). This is an important step because it results in the conversion of NAD^+ to NADH, which is a critical physiological reductant (Fig. 1).

1.3.5: Carbon assimilation

1.3.5.1: Ribulose monophosphate (RuMP pathway) for formaldehyde assimilation

Methanotrophs assimilate C1 carbon the Ribulose monophosphate (RuMP) and Serine pathways (Fig. 3 & 4). The RuMP pathway allows for the assimilation of formaldehyde into cellular biomass whereas the serine pathways incorporates formaldehyde and CO_2 (Hanson and Hanson, 1996; Trotsenko and Murrell, 2008). In the RuMP pathway, CH_2O (a C-1 compound) condensation with ribulose monophosphate (a C-5 compound) is catalyzed by the enzyme hexulose phosphate synthase (Hps) yielding a C-6 hexulose phosphate (White et al., 2012) (Fig. 3). Then, hexulose phosphate isomerase (Hpi) isomerizes the hexulose phosphate to fructose-6-phosphate. CH_2O is a C1 compound, so to synthesize a C-3 compound from the condensation of CH_2O and ribulose monophosphate, this first part of the pathway is performed three times yielding three fructose-6-phosphate molecules.

In the second major stage of the RuMP pathway, the fructose-6-phosphate formed from the first state is then cleaved into two C-3 compounds (Fig. 3). There are two different pathways

for this. In the first variant, fructose-6-phosphate is phosphorylated by phosphofructokinase to form fructose-1,6-bisphosphate and then this molecule is then cleaved into 3-phosphoglyceraldehyde and dihydroxyacetone phosphate (DHAP) by a critical enzyme called fructose bisphosphate aldolase (Fba) (White et al., 2012). This first variant on fructose-6-phosphate cleavage is called the FBPA pathway – for Fructose BisPhosphate Aldolase. In the second variant, the fructose-6-phosphate rearranged to glucose-6-phosphate by glucose phosphate isomerase (Gpi). The glucose-6-phosphate is then converted to 6-phosphogluconate and then 2-keto-3-deoxy-6-phosphogluconate (KDPG) via glucose-6-phosphate dehydrogenase and 6-phosphogluconate-dehydratase, respectively (White et al., 2012). As a final step of the second variant of stage two, the KDPG is split into pyruvate and 3-phosphoglyceraldehyde (Hanson and Hanson, 1996). The second variant is called the KDPGA pathway and shares many enzymes with the Entner-Doudoroff pathway (Chistoserdova and Lidstrom, 2013).

In the third major stage of the RuMP pathway, sugar molecules are rearranged so that the phosphoglyceraldehyde formed from stage two, along with two fructose-6-phosphate molecules, can be used to replenish the supply of ribulose-5-phosphate(White et al., 2012) (Fig. 3). There are two different pathways among methanotrophs for this third major stage as well; the first is called the TA pathway (which stands for the critical TransAldolase enzyme) and the second is SBPase pathway (which stands for the critical enzyme sedoheptulose-1,7-bisphosphate aldolase)(White et al., 2012). The critical differentiating enzyme for the TA pathway is the transaldolase while there are two critical differentiating enzymes for the SBPase pathway – sedoheptulose-1,7-bisphosphate aldolase and sedoheptulose-1,7-bisphosphatase. The net result of the assimilation of three CH_2O molecules is the production of one C-3 compound – either a DHAP (if the organism is using the FBPA pathway) or pyruvate (if the organism is using the

KDPGA pathway) (Trotsenko and Murrell, 2008). Due to the various routes that carbon can take, there are four possible variants of the RuMP pathway that a methanotroph can utilize, corresponding to the two different ways to split sugar and two alternatives for the ribulose monophosphate replenishment (Chistoserdova and Lidstrom, 2013). It is very important to note that some methanotrophs can utilize multiple versions of the RuMP pathway and that the variants are not mutually exclusive of one another. Overall, the RuMP pathway requires 1 ATP and 3 CH_2O molecules to make 1 C-3 unit (White et al., 2012) (Fig. 3).

1.3.5.2: Serine pathway for formaldehyde assimilation

As in the RuMP pathway, the serine pathway involves a condensation reaction between CH_2O and a multicarbon compound to yield, after the replenishment of the C-accepting molecule, a compound with >1 C atom (Fig. 4). However, unlike the RuMP pathway, the Serine pathway provides one acetyl-CoA (a 2-C unit) from CH_2O and CO_2(Trotsenko and Murrell, 2008) (Fig. 4). In addition to producing only a C-2 carbon unit rather than a C-3 unit, the Serine pathway also requires more energy – 2 NADH and 2 ATP (as well as 1 CoA unit) are required to form 1 molecule of acetyl-CoA and 2 molecules of H_2O from 1 CH_2O and 1 CO_2 (Trotsenko and Murrell, 2008) (Fig. 4).

First, CH_2O reacts with tetrahydrofolic acid to form methylene-THF (Fig. 4). This compound then transfers the C1 unit to a molecule of glycine, forming serine and thus replenishing the tetrahydrofolic acid (Chistoserdova and Lidstrom, 2013). A transaminase then converts the serine to hydroxypyruvate and also transfers an amine group to glyoxylate to replenish glycine (White et al., 2012). Then, stepwise, hydroxypyruvate is reduced and phosphorylated by hydroxypryuvate reductase and glycerate kinase, respectively, to form 3-phosphoglycerate (White et al., 2012). Phosphoglycerate mutase is then responsible for 3-

phosphoglycerate conversion to 2-phosphoglycerate. The 2-phosphoglycerate is further dehydrated to phosphoenolpyruvate by an enolase and the resulting phosphoenolpyruvate is carboxylated to form oxaloacetate by PEP carboxylase. The oxaloacetate is reduced by malate dehydrogenase to malate. The enzyme malyl-CoA synthase then converts malate to malyl-CoA which is then split to acetyl-CoA and glyoxylate by malyl-CoA lyase (Trotsenko and Murrell, 2008).

1.4: Bioenergetics of aerobic methanotrophic bacteria

Methanotrophs generate Δp by pumping protons out of the cell while electrons flow into the cell to oxygen, as well as the liberation of protons in the periplasm and consumption of protons in the cytoplasm (Fig. 1). As with most bacteria, the electron transport chains of methanotrophs utilize quinone to accept electrons from dehydrogenases and then transfer those electrons to terminal oxidase complexes that then reduce the terminal electron acceptor – O_2 in the case of aerobic respiration (Fig. 2). Up until this thesis, methanotrophs were considered obligate aerobes without the capacity to perform anaerobic respiration using alternative electron acceptors. In addition to requiring O_2 for respiration, methanotrophs also require O_2 for methane oxidation. Thus, there is a dual need for O_2 in aerobic methanotrophic bacteria (Hanson and Hanson, 1996) (Fig. 1).

To understand the bioenergetics of methanotrophs we must identify the relevant coupling sites – spots in the electron transport chain where redox reactions occur that facilitate proton extrusion to create a Δp. In terms of oxidative phosphorylation, methanotrophs possess in their electron transport chains the typical assortment of complex I (NADH dehydrogenase), complex II (succinate dehydrogenase), complex III (ubiquinol-cytochrome c reductase or the bc_1 complex), complex IV (cytochrome aa_3 complex or the terminal oxidase), complex V (ATP

synthase) (Ward et al., 2004) (Fig. 1). As in most bacteria, the coupling sites for methanotrophs are at the NADH dehydrogenase, the bc1 complex, and the terminal oxidase – these are the sites were protons are extruded from the cell (Fig. 2). The cytochrome c oxidase (complex IV) is especially important for oxidative phosphorylation as it is responsible for using inward flowing electrons to reduce O_2 to H_2O and pump protons out of the cell (White et al., 2012) (Fig. 2). However, methanotrophs can utilize a variety of different terminal oxidases(Ward et al., 2004). In addition to the cytochrome *aa*$_3$ oxidase (or cytochrome c oxidase) that falls into the heme-copper oxidase superfamily of oxidases, some methanotrophs like *Methylococcus capsulatus* strain Bath have a two-subunit cytochrome *bd* oxidase(Ward et al., 2004). The cytochrome *bd* oxidase is a quinol oxidase meaning that it oxidizes quinol instead of cytochrome c. Moreover, this enzyme is also not a member of the heme-copper oxidase superfamily (Borisov et al., 2011). The capability to utilize a variety of O_2 reducing oxidases enables bacteria to have some metabolic flexibility and adaptability if environmental conditions change (Chen and Strous, 2013). In terms of the variety of terminal oxidases that methanotrophs can synthesize, the cytochrome *aa*$_3$ oxidase and cytochrome *bd* oxidase differ in their affinity for O_2. The cytochrome *bd* oxidase has a higher affinity for O_2 than the cytochrome *aa*$_3$ oxidase (Borisov et al., 2011). Generally, the cytochrome *bd* oxidase allows aerobic and microaerophilic bacteria to continue O_2 respiration even when O_2 tension in the environment decreases beyond the affinity of the cytochrome *aa*$_3$ oxidase (Borisov et al., 2011). This is critical for obligate aerobes, like all aerobic methanotrophs, because O_2 is necessary to assure that the reoxidation of NADH and reduced quinones/cytochromes occurs so that the oxidation of the provided energy source can continue. Essentially, high affinity oxidases like the cytochrome *bd* oxidase may allow methanotrophs to prevent cellular asphyxia when O_2 is scarce.

1.5: The problem

The dual dependency of aerobic methanotrophic bacteria for O_2 (CH_4 oxidation and respiration) makes O_2 starvation one of the principal environmental stressors for this group of bacteria. On the other hand, aerobic methanotrophs consume a substrate that is produced in the absence of O_2 by methanogenic archaea(Murrell and Jetten, 2009). It is evident then that aerobic methanotrophs have a respiratory requirement that is at odds with the sole energy source they consume. Nevertheless, there is a colossal amount of evidence that aerobic methanotrophs prefer low oxygen environments and that they are present in high abundance and have high activity in low oxygen environments. In the lab, aerobic methanotrophs starved under anoxic conditions survived much longer, had higher viability, had a significantly smaller biomass decrease, and degraded less of their cellular protein when compared to cells starved under aerobic conditions (Roslev and King, 1994; 1995). Aerobic methanotrophs have been found in high abundance in anoxic thawing permafrost soils (Mackelprang et al., 2011), anoxic arctic peat soils (Tveit et al., 2014), and hypoxic oil sands tailings ponds (Saidi-Mehrabad et al., 2013). Thus, the ability to utilize alternative terminal electron acceptors to O_2 would be hugely advantageous to aerobic methanotrophs. This would alleviate the need for O_2 at the terminal oxidase for respiration and direct the limiting amount of O_2 to CH_4 activation. Furthermore, anaerobic respiration would prevent cellular asphyxia in methanotrophs by allowing their metabolism to remain in respiratory mode.

O_2 is a great terminal electron acceptor because the reduction of O_2 to H_2O has a very positive standard electrode potential (+815 mV) (Thauer et al., 1977). However, in the absence of O_2, NO_3^- reduction to N_2 has a standard electrode potential that is nearly as positive (+740 mV) and NO_3^- is the next preferred electron acceptor in NO_3^- supplemented cultures of *E. coli* if

O_2 is not available (Thauer et al., 1977). Denitrification is the reduction of NO_3^- or NO_2^- to a gasous N-product (NO, N_2O, N_2). The general pathway of denitrification including the intermediates and involved enzymes are illustrated in Fig. 5A. Denitrification as a metabolic module in widespread in bacteria, archaea, and even eukaryotes but has not yet been conclusively identified in aerobic methanotrophs. It should be noted, however, that anaerobic methanotrophic bacteria belonging to the candidate phylum NC10 and anaerobic methanotrophic archaea belonging to the ANME 2d can reduce NO_2^- and NO_3^-, respectively (Ettwig et al., 2010; Haroon et al., 2013). Candidatus *Methylomirabilis oxyfera* reduces NO_2^- to NO which is then seemingly dismutated to N_2 and O_2, the latter of which the organism uses for canonical aerobic methane oxidation via pMMO (Ettwig et al., 2010). Though Candidatus *Methylomirabilis oxyfera* utilizes O_2 for CH_4 oxidation, like canonical aerobic methanotrophs, this organism will be referred to as an anaerobe for the duration of the thesis since it does not require exogenously supplied O_2 and grows under strictly anaerobic conditions. The anaerobic archaeon Candidatus *Methanoperedens nitratireducens* utilizes a respiratory NarGHJI nitrate reductase, evidently acquired from a Gammaproteobacterial source by horizontal gene transfer, to reduce NO_3^- to NO_2^- which is then apparently consumed by ANAMMOX bacteria in consortium (Haroon et al., 2013). It is just an important to note that both of these anaerobic methane-consuming microorganisms are currently not in axenic culture and have only been studied in a consortium.

Denitrification in aerobic methanotrophs has been studied before but the results are largely controversial. As long ago as 1985, Yoshinari and showed that the obligate methanotrophs *Methylosinus trichosporium* strain OB3b consumes NO_2^- and produces N_2O under hypoxic conditions (Yoshinari, 1985). However, Yoshinari concluded that the N_2O was abiotic and resulted from an enzyme-bound nitroxyl intermediate driven by the anaerobic

oxidation of hydroxylamine. Later, Ren et al showed that three obligate methanotrophs – *Methylobacter luteus*, *Methylosinus trichosporium* OB3b, and *Methylobacter* sp. strain T20 all consumed NO and produced small quantities of N_2O (Ren et al., 2000). This activity prevailed in nitrate supplemented medium only under anaerobic conditions and was chlorate sensitive. However, since no denitrification genes could be detected by PCR, the authors concluded that denitrification activity was unlikely and that the NO produced originated from the abiotic chemical degradation of NO_2^- (Ren et al., 2000).

Just one year later Ye and Thomas published the first report of putative homologs of nitrite and nitric oxide reductases that were found encoded in the genomes of aerobic methanotrophs (Ye and Thomas, 2001). However, not only were the observations based on personal communication and unpublished data, no expression or function of the genes was demonstrated. Later, Roger Knowles again pursued denitrification in aerobic methanotrophs and concluded that methanotrophs cannot perform denitrification but that they do export carbon compounds into the surrounding medium that associated heterotrophic bacteria can utilize as substrates for growth and denitrification (Knowles, 2005). As a direct result of these findings, it was widely concluded that methane-dependent denitrification involving aerobic methanotrophs was driven by a collaboration between the methanotrophs which excrete organic compounds (acetate, citrate, formate, methanol, formaldehyde) and associated heterotrophic bacteria (Costa et al., 2000; Liu et al., 2014). Notwithstanding, it was recently demonstrated that the facultative methanotroph *Methylocystis* sp. strain SC2 can use methanol as a substrate to produce heavy $^{30}N_2$ from $^{15}NO_3^-$ under anoxic conditions (Dam et al., 2013). Corresponding with these observations were several reports of nitrite and nitric oxide reductases in the sequenced genomes of aerobic methanotrophs (Boden et al., 2011; Kits et al., 2013; Stein et al., 2011; Svenning et

al., 2011; Ward et al., 2004). Ergo, at this point it remained unclear whether aerobic methanotrophs could couple methane oxidation to respiratory NO_3^- and NO_2^- reduction. The functional of the putative nitrite and nitric oxide reductases encoded in the genomes of aerobic methanotrophs was unclear. And more essentially, it was not understood what environmental conditions might stimulate methane-dependent nitrogen oxide formation in aerobic methanotrophs.

1.6: Denitrification – a brief review

1.6.1: Nitrate (NO_3^-) reduction to nitrite (NO_2^-)

The nitrate reductase enzyme complex catalyzes the first step of denitrification which is the two electron reduction of nitrate (NO_3^-) to nitrite (NO_2^-) for which the standard reduction potential is +430 mV (Thauer et al., 1977) (Fig. 5). All nitrate reductases fall into the molybdopterin oxidoreductase family and contain Molybdenum in the active site(González et al., 2006). There are three general classes of nitrate reductase: respiratory (Nar), periplasmic (Nap), and assimilatory (Nas) (González et al., 2006). Since the assimilatory nitrate reductase participates only in the assimilatory reduction of NO_3^- to NO_2^- rather than denitrification, it will no longer be mentioned it in this portion of chapter 1. The Nar enzyme, encoded by *narGHJI*, is membrane bound but the active site is in the cytoplasm while the Nap, encoded by *napABC*, is located in the periplasm(Richardson et al., 2001) (Fig. 5). Since the reduction of NO_3^- to NO_2^- consumes two electrons and two protons, the Nar allows for the conservation of energy and the generation of Δp because protons are consumed in the cytoplasm(Richardson et al., 2001) (Fig. 5). Consequently, the Nar is generally only utilized by bacteria for growth via respiratory denitrification while the Nap can serve a variety of functions in redox balancing, denitrification, or fermentation (Chen and Strous, 2013). Another differentiating characteristic of the Nar system

is that, because the catalytic subunit is cytoplasmic, nitrate must be imported into the cell. This is performed by a nitrate:nitrite antiporter NarK (encoded by *narK*) which allows nitrate reduction to operate at a steady state – imported NO_3^- molecules are reduced to NO_2^- and exchanged for more NO_3^-(González et al., 2006).

1.6.2: Nitrite (NO_2^-) reduction to nitric oxide (NO)

There are two different but non-homologous enzymes that catalyze the one electron reduction of NO_2^- to NO: a haem based cytochrome cd_1 nitrite reductase NirS (encoded by *nirSCFLGHJ*) and a copper-containing nitrite reductase NirK (encoded by *nirK*) (Wei et al., 2015) (Fig. 5). Both of these enzymes are periplasmic and thus do not directly contribute to Δp (Fig. 5). Other than the different metal requirements, these enzymes are thought to be isofunctional and it is not known if either one bestows a kinetic or bioenergetic advantage under specific conditions(Chen and Strous, 2013; Wei et al., 2015).

1.6.3: Nitric oxide (NO) reduction to nitrous oxide (N_2O)

All known nitric oxide reductase (NOR) enzymes fall into the heme-copper oxidase superfamily (complex IV also falls into this category) (Zumft, 2005). As with the nitrate reductases, several different types of NORs exist; there are two main classes based on whether the enzyme accepts electrons from quinol (qNORs) or cytochrome c (cNOR) (Fig. 5). The heterodimeric nitric oxide reductase NorBC (encoded by *norBC*) is the most common cNOR while the NorZ (encoded by *norZ*) is a known qNOR (Zumft, 2005).

1.6.4: Nitrous oxide (N_2O) reduction to dinitrogen (N_2)

The terminal step in denitrification is the reduction of N_2O to N_2 (Fig. 5). This reaction is catalyzed by nitrous oxide reductase (Nos) which is encoded by *nosZ*. All nitrous oxide reductases are cytochrome c linked and none of them contribute to Δp directly (Zumft, 1997)

(Fig. 5). The Nos enzyme has previously always been considered to be extremely sensitive to O_2, as the copper based active site is inactivated by oxygen; however, O_2-insensitive Nos enzymes still of the NosZ type have been characterized (Teraguchi and Hollocher, 1989; Tsugawa et al., 2012).

1.7: Research objectives and hypotheses

As previously mentioned, the genomes of some aerobic methanotrophs contain putative dissimilatory nitrite (*nirK* and *nirS*) and nitric oxide reductases (*norB*) with no known function. Previous research has suggested that CH_4-linked denitrification in aerobic methanotrophs may be possible but rigorous evidence for this metabolism in methanotrophs was nonexistent. The hypothesis of my dissertation is that aerobic methanotrophs that contain the genetic inventory for the respiration of NO_3^-, NO_2^-, or NO can denitrify at the expense of CH_4 under oxygen limiting conditions. Further, I hypothesize that the putative denitrification genes will be transcribed and translated at higher levels under denitrifying conditions.

The overall goals of this thesis were (**i**) to determine whether aerobic methanotrophs can denitrify at the expense of methane, (**ii**) to unravel what genes and enzymes are involved in methane-dependent denitrification, (**iii**) what environmental conditions govern methane-dependent denitrification in aerobic methanotrophs, (**iv**) to assess the diversity of denitrification in aerobic methanotrophs in terms of energy sources and terminal electron acceptors, (**v**) to elucidate the bioenergetic function of denitrification in aerobic methanotrophs (i.e. is hybrid respiration bioenergetically advantageous in aerobic methanotrophs?), and (**v**) to characterize the genome wide metabolic regulation by oxygen in a model aerobic methanotroph using transcriptomics, proteomics, and metabolomics.

1.8: Figures

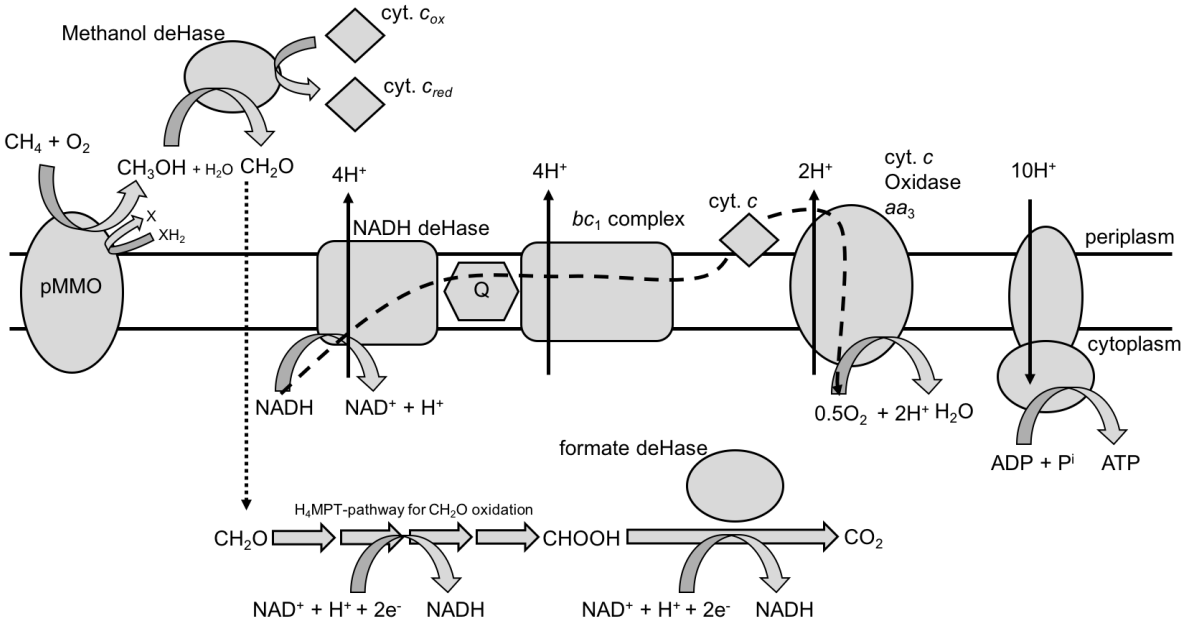

Figure 1: **Scheme for generalized electron transport in aerobic methanotrophic bacteria during aerobic respiration.**

Electrons are transferred down the electron transport chain from low electrode potential to high electrode potential. CH_4 is the electron source and O_2 is the terminal electron acceptor. Dashed line represents electron flow, solid arrows indicate proton flow, dotted line indicates transport. Abbreviations: cyt. *c*, cytochrome *c*; deHase, dehydrogenase; H_4MPT, tetrahydromethanopterin; pMMO, particulate methane monooxygenase;

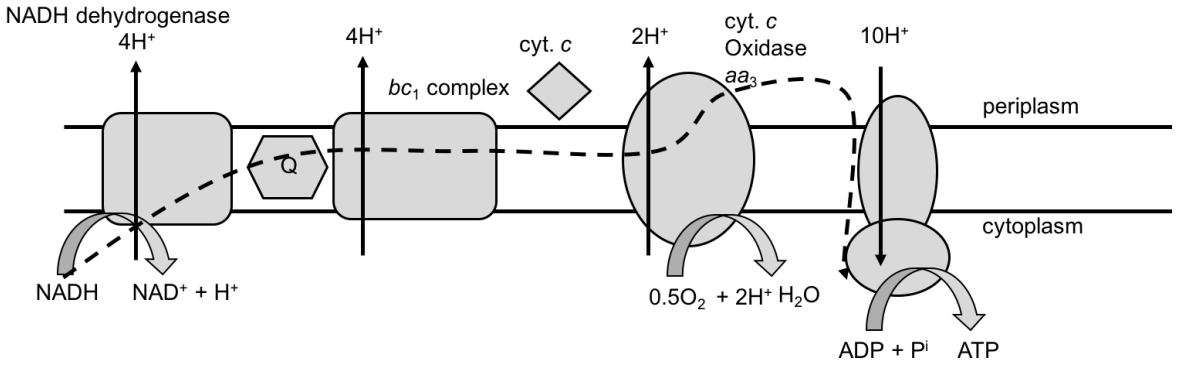

Figure 2: **Scheme for generalized electron transport in bacteria during aerobic respiration.**

Electrons are transferred down the electron transport chain from low electrode potential to high electrode potential. NADH is the electron source and O_2 is the terminal electron acceptor. Dashed line represents electron flow while the solid arrows indicate proton flow. Abbreviations: cyt. *c*, cytochrome *c*.

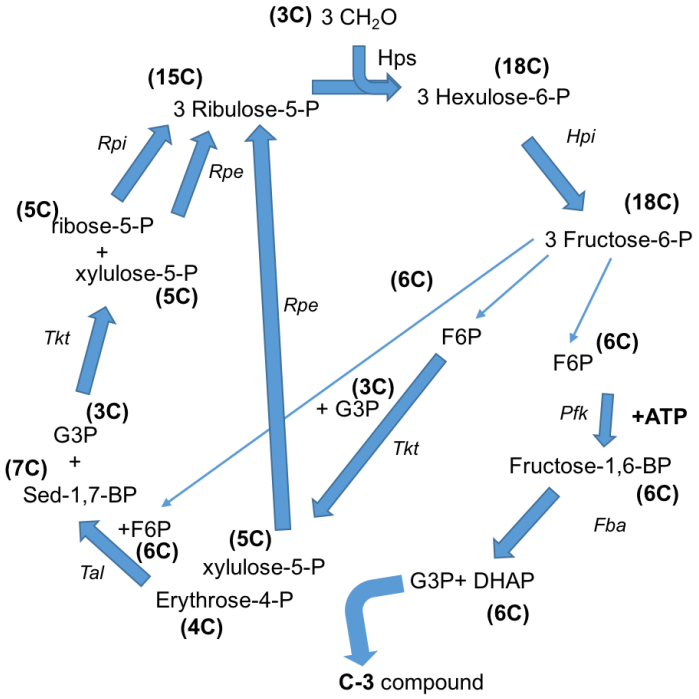

Figure 3: **The ribulose monophosphate (RuMP) cycle.**

Depicted with the FBPA pathway for fructose cleavage and TA pathway for sugar rearrangment. Enzymes: *Hps*, hexulose phosphate synthase; *Hpi*, hexulose phosphate isomerase; *Pfk*, phosphofructokinase; *Fba*, fructose bisphosphate aldolase; *Tkt*, transketolase; *Tal*,

transaldolase; *Rpi*, ribose-5- phosphate isomerase; *Rpe*, ribulose-5-phosphate epimerase. The number of carbon atoms is depicted in parenthesis near each compound.

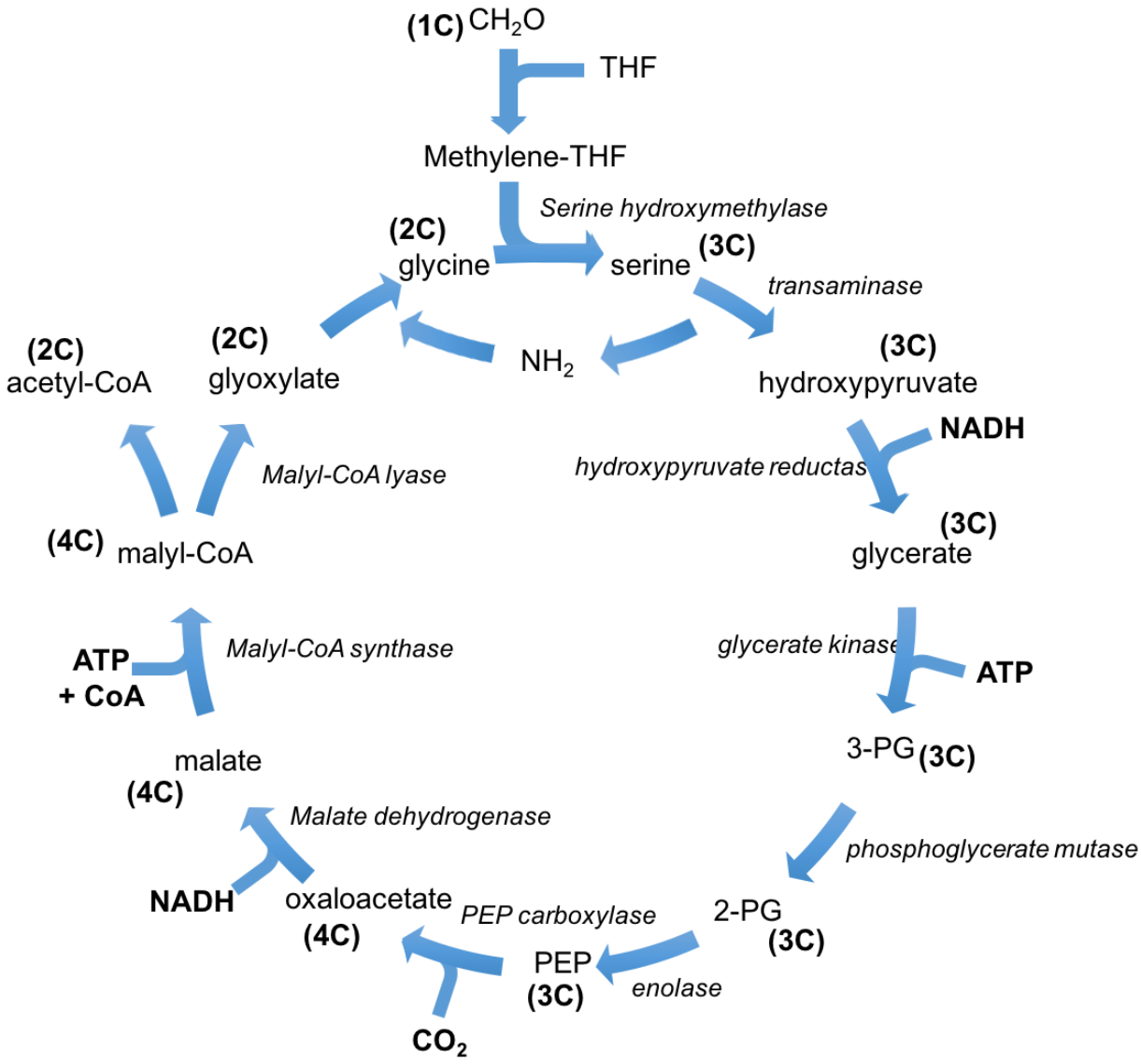

Figure 4: **The Serine cycle.**

The serine pathway produces 1 acetyl-CoA (2-C unit) from 1 molecule of CH_2O and 1 molecule of CO_2 using 2 ATP, 2 NADH, and CoA. The number of carbon atoms is depicted in parenthesis near each compound.

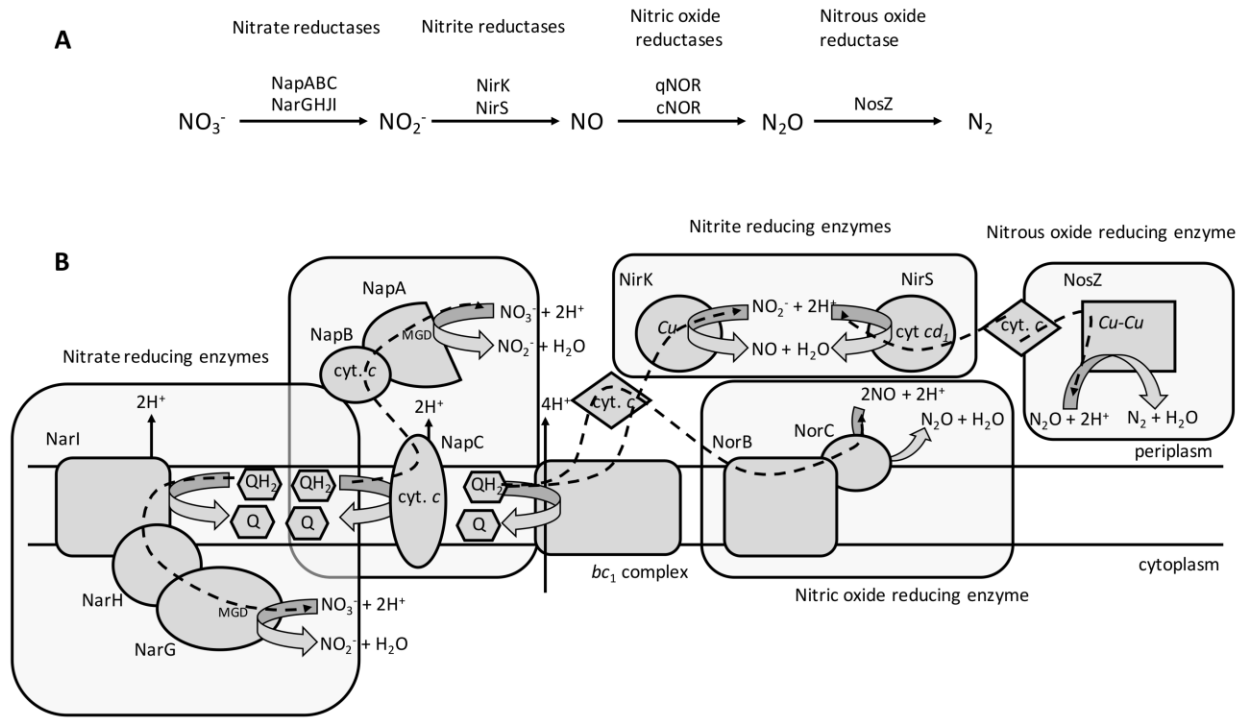

Figure 5: **The general denitrification pathway (A) and topological cellular organization of some dissimilatory denitrification enzymes (B) that may play a role in aerobic methanotrophs**.

Depicted are two classes of nitrate reductase (Nar and Nap), two classes of NO-forming nitrite reductase (NirK and NirS), a membrane bound nitric oxide reductase (NorC), and a periplasmic nitrous oxide reductase (NosZ). Abbreviations: MDG, *bis*-molybdopterin guanine dinucleotide; Q, quinone; cyt. c, cytochrome *c*; Cu, copper; cyt. cd_1, cytochrome cd_1; bc_1 complex, ubiquinol cytochrome c oxidoreductase.

1.9: References

Balasubramanian, R., Smith, S. M., Rawat, S., Yatsunyk, L. A., Stemmler, T. L., and Rosenzweig, A. C. (2010). Oxidation of methane by a biological dicopper centre. *Nature* 465, 115–119. doi:10.1038/nature08992.

Beal, E. J., House, C. H., and Orphan, V. J. (2009). Manganese- and iron-dependent marine methane oxidation. *Science* 325, 184–187. doi:10.1126/science.1169984.

Boden, R., Cunliffe, M., Scanlan, J., Moussard, H., Kits, K. D., Klotz, M. G., et al. (2011). Complete genome sequence of the aerobic marine methanotroph *Methylomonas methanica* MC09. *J. Bacteriol.* 193, 7001–7002. doi:10.1128/JB.06267-11.

Boetius, A., Ravenschlag, K., Schubert, C. J., Rickert, D., Widdel, F., Gieseke, A., et al. (2000). A marine microbial consortium apparently mediating anaerobic oxidation of methane. *Nature* 407, 623–626. doi:10.1038/35036572.

Borisov, V. B., Gennis, R. B., Hemp, J., and Verkhovsky, M. I. (2011). The cytochrome bd respiratory oxygen reductases. *Biochimica et Biophysica Acta (BBA) - Bioenergetics* 1807, 1398–1413. doi:10.1016/j.bbabio.2011.06.016.

Chen, J., and Strous, M. (2013). Denitrification and aerobic respiration, hybrid electron transport chains and co-evolution. *Biochimica et Biophysica Acta (BBA) - Bioenergetics* 1827, 136–144. doi:10.1016/j.bbabio.2012.10.002.

Chistoserdova, L., and Lidstrom, M. E. (2013). "Aerobic methylotrophic prokaryotes," in *The Prokaryotes: Prokaryotic Physiology and Biochemistry* (Berlin, Heidelberg: Springer Berlin Heidelberg), 267–285. doi:10.1007/978-3-642-30141-4_68.

Chu, F., and Lidstrom, M. E. (2016). XoxF acts as the predominant methanol dehydrogenase in the type I methanotroph *Methylomicrobium buryatense*. *J. Bacteriol.* 198, 1317–1325.

doi:10.1128/JB.00959-15.

Colin Murrell, J., and Jetten, M. S. M. (2009). The microbial methane cycle. *Environ Microbiol Rep* 1, 279–284. doi:10.1111/j.1758-2229.2009.00089.x/asset/j.1758-2229.2009.00089.x.pdf.

Conrad, R. (2009). The global methane cycle: Recent advances in understanding the microbial processes involved. *Environ Microbiol Rep* 1, 285–292. doi:10.1111/j.1758-2229.2009.00038.x/asset/j.1758-2229.2009.00038.x.pdf.

Costa, C., Dijkema, C., Friedrich, M., García-Encina, P., Fernández-Polanco, F., and Stams, A. J. (2000). Denitrification with methane as electron donor in oxygen-limited bioreactors. *Appl. Microbiol. Biotechnol.* 53, 754–762.

Dam, B., Dam, S., Blom, J., and Liesack, W. (2013). Genome Analysis Coupled with Physiological Studies Reveals a Diverse Nitrogen Metabolism in *Methylocystis* sp. Strain SC2. *PLoS ONE* 8, e74767. doi:10.1371/journal.pone.0074767.

Ettwig, K. F., Butler, M. K., Le Paslier, D., Pelletier, E., Mangenot, S., Kuypers, M. M. M., et al. (2010). Nitrite-driven anaerobic methane oxidation by oxygenic bacteria. *Nature* 464, 543–548. doi:10.1038/nature08883.

González, P. J., Correia, C., Moura, I., Brondino, C. D., and Moura, J. J. G. (2006). Bacterial nitrate reductases: Molecular and biological aspects of nitrate reduction. *J. Inorg. Biochem.* 100, 1015–1023. doi:10.1016/j.jinorgbio.2005.11.024.

Gu, W., Haque, M. F. U., Dispirito, A. A., and Semrau, J. D. (2016). Uptake and Effect of Rare Earth Elements on Gene Expression in *Methylosinus trichosporium* OB3b. *FEMS Microbiology Letters*. doi:10.1093/femsle/fnw129.

Hanson, R. S., and Hanson, T. E. (1996). Methanotrophic bacteria. *Microbiol. Rev.* 60, 439–471.

Haroon, M. F., Hu, S., Shi, Y., Imelfort, M., Keller, J., Hugenholtz, P., et al. (2013). Anaerobic oxidation of methane coupled to nitrate reduction in a novel archaeal lineage. *Nature* 500, 567–570. doi:10.1038/nature12375.

Hinrichs, K. U., Hayes, J. M., Sylva, S. P., Brewer, P. G., and DeLong, E. F. (1999). Methane-consuming archaebacteria in marine sediments. *Nature* 398, 802–805. doi:10.1038/19751.

Hoehler, T. M., Alperin, M. J., Albert, D. B., and Martens, C. S. (1994). Field and laboratory studies of methane oxidation in an anoxic marine sediment: Evidence for a methanogen-sulfate reducer consortium. *Global Biogeochemical Cycles* 8, 451–463. doi:10.1029/94GB01800.

Khadem, A. F., Pol, A., Wieczorek, A., Mohammadi, S. S., Francoijs, K.-J., Stunnenberg, H. G., et al. (2011). Autotrophic methanotrophy in verrucomicrobia: *Methylacidiphilum fumariolicum* SolV uses the Calvin-Benson-Bassham cycle for carbon dioxide fixation. *J. Bacteriol.* 193, 4438–4446. doi:10.1128/JB.00407-11.

Kits, K. D., Kalyuzhnaya, M. G., Klotz, M. G., Jetten, M. S. M., Op den Camp, H. J. M., Vuilleumier, S., et al. (2013). Genome Sequence of the Obligate Gammaproteobacterial Methanotroph *Methylomicrobium album* Strain BG8. *Genome Announc* 1, e0017013–e00170–13. doi:10.1128/genomeA.00170-13.

Knief, C. (2015). Diversity and Habitat Preferences of Cultivated and Uncultivated Aerobic Methanotrophic Bacteria Evaluated Based on pmoA as Molecular Marker. *Front. Microbiol.* 6, 1346. doi:10.3389/fmicb.2015.01346.

Knowles, R. (2005). Denitrifiers associated with methanotrophs and their potential impact on the nitrogen cycle. *Ecological Engineering* 24, 441–446. doi:10.1016/j.ecoleng.2005.01.001.

Lieberman, R. L., and Rosenzweig, A. C. (2005). Crystal structure of a membrane-bound

metalloenzyme that catalyses the biological oxidation of methane. *Nature* 434, 177–182. doi:10.1038/nature03311.

Lipscomb, J. D. (1994). Biochemistry of the soluble methane monooxygenase. *Annual Reviews in Microbiology*.

Liu, J., Sun, F., Wang, L., Ju, X., Wu, W., and Chen, Y. (2014). Molecular characterization of a microbial consortium involved in methane oxidation coupled to denitrification under micro-aerobic conditions. *Microb Biotechnol* 7, 64–76. doi:10.1111/1751-7915.12097.

Mackelprang, R., Waldrop, M. P., DeAngelis, K. M., David, M. M., Chavarria, K. L., Blazewicz, S. J., et al. (2011). Metagenomic analysis of a permafrost microbial community reveals a rapid response to thaw. *Nature* 480, 368–371. doi:10.1038/nature10576.

Martens, C. S., and Berner, R. A. (1974). Methane production in the interstitial waters of sulfate-depleted marine sediments. *Science* 185, 1167–1169. doi:10.1126/science.185.4157.1167.

McGlynn, S. E., Chadwick, G. L., Kempes, C. P., and Orphan, V. J. (2015). Single cell activity reveals direct electron transfer in methanotrophic consortia. *Nature* 526, 531–535. doi:10.1038/nature15512.

Milucka, J., Ferdelman, T. G., Polerecky, L., Franzke, D., Wegener, G., Schmid, M., et al. (2012). Zero-valent sulphur is a key intermediate in marine methane oxidation. *Nature* 491, 541–546. doi:10.1038/nature11656.

Murrell, J. C. (2010). The aerobic methane oxidizing bacteria (methanotrophs). *Handbook of Hydrocarbon and Lipid Microbiology*. doi:10.1007/978-3-540-77587-4_143.pdf.

Murrell, J. C., and Jetten, M. S. M. (2009). The microbial methane cycle. *Environ Microbiol Rep* 1, 279–284. doi:10.1111/j.1758-2229.2009.00089.x.

Nazaries, L., Murrell, J. C., and Millard, P. (2013). Methane, microbes and models: fundamental

understanding of the soil methane cycle for future predictions - Nazaries - 2013 - Environmental Microbiology - Wiley Online Library. *Environmental* .... doi:10.1111/1462-2920.12149/pdf.

Pol, A., Barends, T. R. M., Dietl, A., Khadem, A. F., Eygensteyn, J., Jetten, M. S. M., et al. (2014). Rare earth metals are essential for methanotrophic life in volcanic mudpots. *Environ. Microbiol.* 16, 255–264. doi:10.1111/1462-2920.12249.

Reeburgh, W. S. (2007). Oceanic Methane Biogeochemistry. *Chem. Rev.* 107, 486–513. doi:10.1021/cr050362v.

Ren, T., Roy, R., and Knowles, R. (2000). Production and consumption of nitric oxide by three methanotrophic bacteria. *Appl. Environ. Microbiol.* 66, 3891–3897.

Richardson, D. J., Berks, B. C., Russell, D. A., Spiro, S., and Taylor, C. J. (2001). Functional, biochemical and genetic diversity of prokaryotic nitrate reductases. *Cell. Mol. Life Sci.* 58, 165–178.

Roslev, P., and King, G. M. (1994). Survival and recovery of methanotrophic bacteria starved under oxic and anoxic conditions. *Appl. Environ. Microbiol.* 60, 2602–2608.

Roslev, P., and King, G. M. (1995). Aerobic and anaerobic starvation metabolism in methanotrophic bacteria. *Appl. Environ. Microbiol.* 61, 1563–1570.

Saidi-Mehrabad, A., He, Z., Tamas, I., Sharp, C. E., Brady, A. L., Rochman, F. F., et al. (2013). Methanotrophic bacteria in oilsands tailings ponds of northern Alberta. *ISME J* 7, 908–921. doi:10.1038/ismej.2012.163.

Scheller, S., Yu, H., Chadwick, G. L., McGlynn, S. E., and Orphan, V. J. (2016). Artificial electron acceptors decouple archaeal methane oxidation from sulfate reduction. *Science* 351, 703–707. doi:10.1126/science.aad7154.

Semrau, J. D., Dispirito, A. A., and Yoon, S. (2010). Methanotrophs and copper. *FEMS Microbiol. Rev.* 34, 496–531. doi:10.1111/j.1574-6976.2010.00212.x.

Stein, L. Y., Bringel, F., Dispirito, A. A., Han, S., Jetten, M. S. M., Kalyuzhnaya, M. G., et al. (2011). Genome sequence of the methanotrophic Alphaproteobacterium, *Methylocystis* sp. Rockwell (ATCC 49242). *J. Bacteriol.* 193, 2668–2669. doi:10.1128/JB.00278-11.

Svenning, M. M., Hestnes, A. G., Wartiainen, I., Stein, L. Y., Klotz, M. G., Kalyuzhnaya, M. G., et al. (2011). Genome sequence of the Arctic methanotroph *Methylobacter tundripaludum* SV96. *J. Bacteriol.* 193, 6418–6419. doi:10.1128/JB.05380-11.

Tavormina, P. L., Orphan, V. J., Kalyuzhnaya, M. G., Jetten, M. S. M., and Klotz, M. G. (2011). A novel family of functional operons encoding methane/ammonia monooxygenase-related proteins in gammaproteobacterial methanotrophs. *Environ Microbiol Rep* 3, 91–100. doi:10.1111/j.1758-2229.2010.00192.x.

Teraguchi, S., and Hollocher, T. C. (1989). Purification and some characteristics of a cytochrome c-containing nitrous oxide reductase from *Wolinella succinogenes*. *J. Biol. Chem.* 264, 1972–1979.

Thauer, R. K., Jungermann, K., and Decker, K. (1977). Energy conservation in chemotrophic anaerobic bacteria. *Bacteriol Rev* 41, 809–180.

Theisen, A. R., and Murrell, J. C. (2005). Facultative methanotrophs revisited. *J. Bacteriol.* 187, 4303–4305. doi:10.1128/JB.187.13.4303-4305.2005.

Trotsenko, Y. A., and Murrell, J. C. (2008). Metabolic aspects of aerobic obligate methanotrophy. *Adv. Appl. Microbiol.* 63, 183–229. doi:10.1016/S0065-2164(07)00005-6.

Tsugawa, W., Shimizu, H., Masahiro Tata, R. A., Ueno, Y., Kojima, K., and Sode, K. (2012). Nitrous oxide sensing using oxygen-Insensitive direct-electron-transfer- type nitrous oxide

reductase. *Electrochemistry* 80, 371–374. doi:10.5796/electrochemistry.80.371.

Tveit, A. T., Urich, T., and Svenning, M. M. (2014). Metatranscriptomic analysis of arctic peat soil microbiota. *Appl. Environ. Microbiol.* 80, 5761–5772. doi:10.1128/AEM.01030-14.

Ward, N., Larsen, Ø., Sakwa, J., Bruseth, L., Khouri, H., Durkin, A. S., et al. (2004). Genomic Insights into Methanotrophy: The Complete Genome Sequence of *Methylococcus capsulatus* (Bath). *PLoS Biol* 2, e303. doi:10.1371/journal.pbio.0020303.

Wegener, G., Krukenberg, V., Riedel, D., Tegetmeyer, H. E., and Boetius, A. (2015). Intercellular wiring enables electron transfer between methanotrophic archaea and bacteria. *Nature* 526, 587–590. doi:10.1038/nature15733.

Wei, W., Isobe, K., Nishizawa, T., Zhu, L., Shiratori, Y., Ohte, N., et al. (2015). Higher diversity and abundance of denitrifying microorganisms in environments than considered previously. *ISME J*. doi:10.1038/ismej.2015.9.

White, D., Drummond, J., and Fuqua, C. (2012). "The Physiology and Biochemistry of Prokaryotes," in (New York: Oxford University Press), 358–382.

Ye, R. W., and Thomas, S. M. (2001). Microbial nitrogen cycles: physiology, genomics and applications. *Curr. Opin. Microbiol.* 4, 307–312. doi:10.1016/S1369-5274(00)00208-3.

Yoshinari, T. (1985). Nitrite and nitrous oxide production by *Methylosinus trichosporium*. *Can. J. Microbiol.* 31, 139–144.

Zahn, J. A., and DiSpirito, A. A. (1996). Membrane-associated methane monooxygenase from *Methylococcus capsulatus* (Bath). *J. Bacteriol.* 178, 1018–1029.

Zumft, W. G. (1997). Cell biology and molecular basis of denitrification. *Microbiol. Rev.* 61, 533–616.

Zumft, W. G. (2005). Nitric oxide reductases of prokaryotes with emphasis on the respiratory,

heme-copper oxidase type. *J. Inorg. Biochem.* 99, 194–215.

doi:10.1016/j.jinorgbio.2004.09.024.

Chapter 2: Methane oxidation coupled to nitrate reduction under hypoxia by the Gammaproteobacterium *Methylomonas denitrificans*, sp. nov. Type Strain FJG1

This chapter has been published as: Kits, K. D., Klotz, M. G., and Stein, L. Y. (2015). Methane oxidation coupled to nitrate reduction under hypoxia by the Gammaproteobacterium *Methylomonas denitrificans*, sp. nov. type strain FJG1. *Environ. Microbiol.* 17, 3219–3232. doi:10.1111/1462-2920.12772.

2.1: Abstract

Obligate methanotrophs belonging to the Phyla Proteobacteria and Verrucomicrobia require oxygen for respiration and methane oxidation; nevertheless, aerobic methanotrophs are abundant and active in low oxygen environments. While genomes of some aerobic methanotrophs encode putative nitrogen oxide reductases, it is not understood whether these metabolic modules are used for NO_x detoxification, denitrification, or other purposes. Here we demonstrate using microsensor measurements that a gammaproteobacterial methanotroph *Methylomonas denitrificans* sp. nov. strain FJG1^T couples methane oxidation to nitrate reduction under oxygen limitation, releasing nitrous oxide as a terminal product. Illumina RNA-Seq data revealed differential expression of genes encoding a denitrification pathway previously unknown to methanotrophs as well as the *pxmABC* operon in *M. denitrificans* sp. nov. strain FJG1^T in response to hypoxia. Physiological and transcriptome data indicate that the genetic inventory encoding the denitrification pathway is upregulated only upon availability of nitrate under oxygen limitation. In addition, quantitation of ATP levels demonstrates that the denitrification pathway employs inventory such as nitrate reductase NarGH serving *M. denitrificans* sp. nov. strain FJG1^T to conserve energy during oxygen limitation. This study unraveled an unexpected metabolic flexibility of aerobic methanotrophs thereby assigning these bacteria a new role at the metabolic intersection of the carbon and nitrogen cycles.

2.2: Introduction

Atmospheric methane (CH_4) levels have more than doubled since pre-industrial times, increasing from 722 ± 25 ppb in 1750 to 1803 ± 2 ppb in 2011, making CH_4 the second most important anthropogenic greenhouse gas after carbon dioxide (CO_2) (Myhre *et al.*, 2013). Microorganisms play a central role in the global carbon cycle; 69% of the atmospheric CH_4

budget originates from the activity of methanogenic archaea in wetlands through decomposition of organic matter in the absence of oxygen (Murrell & Jetten, 2009). Aerobic and anaerobic methane-oxidizing microorganisms play a key role in controlling global methane flux by attenuating methane emissions from terrestrial and aquatic environments thereby serving as a biological methane filter.

Oxygen starvation is one of the main environmental stresses that aerobic methanotrophs experience due to their dependency on molecular oxygen for methane oxidation and respiration. It has been shown that aerobic methanotrophs are abundant and active under oxygen limiting conditions, such as in the Costa Rica oxygen minimum zone, oil sand tailings ponds, thawing permafrost soils, and high-arctic peat soils (MacKelprang *et al.*, 2011; Saidi-Mehrabad *et al.*, 2013; Tavormina *et al.*, 2013; Tveit *et al.*, 2014). Fermentation has been recently identified as one possible adaptation of some aerobic methanotrophs to mitigate oxygen starvation (Kalyuzhnaya *et al.*, 2013). However, fermentation inventory is not encoded in all genomes of aerobic methanotrophs and little is known about additional mechanisms that allow aerobic methanotrophs to survive and grow in low oxygen environments.

The utilization of multiple terminal electron acceptors (also known as hybrid respiration) is a strategy of many microorganisms in oxycline habitats; however, no such catabolism has been reported for aerobic methanotrophs. The ability of methanotrophs to utilize alternate terminal electron acceptors in addition to oxygen during times of transient hypoxia would maintain their metabolism in respiratory mode and increase their survival by eliminating the oxygen dependency of the respiratory chain (Chen & Strous, 2013). Substitution of O_2 with NO_3^- in the methanotroph respiratory chain would decrease the O_2 requirement of a cell by half, thereby allowing the O_2 that would have been required for respiration to be used for CH_4 oxidation. For

instance, denitrifying chemoorganoheterotrophic bacteria utilize this strategy to maximize respiration under oxygen limitation or to dissipate excess reductant (Ferguson & Richardson, 2004). Furthermore, due to the industrial manufacture and use of nitrogenous fertilizers in agriculture, increased nitratation has created a significant new source of nitrate (NO_3^-), one of the most energetically favorable terminal electron acceptors next to oxygen (Canfield *et al.*, 2010). The ratio of available nitrite (NO_2^-) to NO_3^- and the availability of sources for energy and reductant, which determine growth and succession in natural microbial communities, govern the flow of nitrogen towards nitrogenous gases or ammonium (NH_4^+). Since bioenergetics and N-saturation favor denitrification over ammonification, the importance of denitrification as a form of anaerobic respiration in terrestrial and aquatic habitats continues to increase (Kraft *et al.*, 2014).

Nitrite-dependent Anaerobic Methane Oxidation (N-DAMO) facilitated by intra-oxygenic methane-oxidizing bacteria in the NC10 phylum has been recently identified as a major process in oxygen depleted habitats (Ettwig *et al.*, 2010). While denitrification coupled to aerobic methane-oxidation has also been studied previously, these studies focused on microbial consortia in which chemoorganoheterotrophic denitrifiers utilize organic compounds released by methanotrophs as sources of energy, reductant and carbon (Costa *et al.*, 2000; Knowles, 2005; Liu *et al.*, 2014). In contrast, the study of methane-dependent denitrification in pure cultures of aerobic methanotrophs has been largely controversial in that previous studies of aerobic methanotrophy in hypoxic culture concluded that nitrous oxide (N_2O) production from NO_3^- or NO_2^- was the result of abiotic processes (Yoshinari, 1985; Ren *et al.*, 2000; Knowles, 2005). Recently, it was shown that cultures of aerobic methanotrophs produce N_2O when cultivated on NH_4^+ or NO_3^- as the sole nitrogen source and that this phenotype varied widely within closely

related strains (Hoefman *et al.*, 2014). The facultative methanotroph *Methylocystis* sp. strain SC2 was demonstrated to produce N_2 from NO_3^- under anoxia with methanol rather than methane as a carbon source (Dam *et al.*, 2013). Hence, methane oxidation coupled to respiratory nitrate reduction with NO and N_2O as products has yet to be demonstrated in an axenic culture. The molecular inventory that obligate methanotrophs use to reduce NO_3^- to N_2O is presently uncharacterized and the expression of putative denitrification genes has not been investigated, even though many aerobic methanotroph genomes encode nitrogen oxide reductases (Campbell *et al.*, 2011). More fundamentally, the environmental conditions that govern denitrification by aerobic methanotrophs and the carbon sources that support it remain uncharacterized (Stein & Klotz, 2011).

For the present study, we hypothesized that a gammaproteobacterial methanotroph possessing the genetic inventory for reduction of NO_3^- to N_2O can couple denitrification to methane oxidation in a bioenergetically favorable manner under hypoxia. We further hypothesized that the predicted gene inventory supporting respiratory denitrification was expressed only in the presence of NO_3^-. We demonstrate here that a strain of a new species in the *Methylomonas* genus is capable of linking methane oxidation to NO_3^- reduction in a bioenergetically favorable manner to produce N_2O as a terminal product. Ecological implications of this metabolism in light of recent studies showing an abundance of gammaproteobacterial methanotrophs in extremely hypoxic to anoxic ecosystems are discussed.

2.3: Materials and Methods

Culture conditions: *Methylomonas denitrificans* sp. nov. strain FJG1^T was cultured at 30°C in 100 mL of nitrate (10 mM KNO_3) or ammonium (10 mM NH_4Cl) mineral salts medium (Whittenbury et al., 1970) in 300 mL septum topped glass Wheaton bottles that were shaken at

200 rpm. Growth conditions were identical for the batch culture experiments, the batch culture activity assays, and for transcriptome analysis. The initial gas-mixing ratio in the headspace was 3:7, CH_4 to air. Rate of N_2O production (60 h -120 h) was calculated by subtracting the amount of N_2O in the culture bottles at 120 h from the 60 h sample. The resulting number was divided by the time difference (60 h) and then divided by the number of cells in the culture, which yielded mol N_2O/cell/h. Cell density was determined at 60 h and 120 h using phase contrast microscopy by direct count with a Petroff-Hausser counting chamber. Cell density did not change significantly from 60 h to 120 h (Figure 6a) in the NMS cultures.

Gas analysis: Headspace of each batch culture was sampled immediately after inoculation (t = 0) and at 12, 24, 36, 48, 72, 96, and 120 h using gas chromatography (GC-TCD, Shimadzu GC-8A; equipped with molecular sieve and Hayesep Q columns, Alltech). The headspace O_2, CH_4, and N_2O concentrations in each vessel were calculated from standard curves using pure gases (Sigma-Aldrich).

Batch culture activity assays: Using a filtration manifold and 0.2 μm filters (Supor 200, 47mm, Pall Corporation), ~1×10^{11} cells were harvested from cultures grown for 120 h in NMS or AMS as described above. The biomass was washed three times with fresh mineral salts medium and resuspended in 10 mL of mineral salts medium. The cells were transferred into a 10 mL double-port MicroRespiration (MR) chamber leaving no headspace in the chamber. The MR chamber was fitted with an OX-MR O_2 sensor (Unisense) and either a N_2O-500 N_2O sensor (Unisense) or an amiNO-700 NO sensor (Innovative Instruments). A Microsensor multimeter (Unisense) was used as the D/A converter to measure the signals from the OX-MR and N_2O-500 microsensors while the amiNO-700 sensor was connected to the Microsensor multimeter through a One-Channel Free Radical Analyzer (World Precision Instruments). SensorTrace BASIC

software was used to log the output from all of the microsensors in real time. Procedures were identical for data in figure 8 except that only ~4×10^{10} cells were used.

Addition of NO_3^- (final concentration -1 mM), NO_2^- (final concentration -1 mM) and an NO donor (6 nM [final concentration] Proli-NONOate/injection/2.5 min) was through direct injection into the 10 mL MicroRespiration Chamber using an injection lid and a 10 µL glass syringe (Hamilton). CH_4 was added to the MicroRespiration Chamber with a 50 µL gastight syringe (SGE Analytical Science).

ATP determination: Mineral salts media (9 mL) supplemented with either 1 mM KNO_3 or 1 mM NH_4Cl was transferred to 37 mL glass vessels capped with a grey butyl rubber stopper and aluminum crimp seal. The media-containing vessels were sparged with N_2 gas for 30 minutes and backfilled with CH_4 and O_2 to achieve headspace concentrations of approximately 30% and 1.5%, respectively. Approximately 1.3×10^9 cells were harvested with a filtration manifold using 0.22 µm filters from the NMS medium cultures (at 120 h) cultivated as described above. After washing three times, cells were transferred to the prepared closed hypoxic (1.5% starting headspace O_2) glass vials and incubated at 30°C in a rotary shaker at 150 rpm. Subsamples (100 µL) were harvested immediately after the addition of biomass (t = 0 minutes) and 30 minutes, 90 minutes, and 180 minutes after the addition of biomass. ATP concentrations were determined with the BacTiter-Glo Microbial Cell Viability Assay (Promega) according to manufacturer's instructions at each time point using a POLARstar OPTIMA microplate reader (BMG LABTECH). Headspace O_2 was measured at each time point by GC-TCD (molecular sieve 5A column, Alltech).

Nucleic acid extraction: Cells were cultivated as described above and collected from six independent cultures after 24, 36, 48, 72, and 120 h growth in both NMS and AMS media and

immediately treated with STOP solution: 95% anhydrous EtOH (Commercial Alcohols), 5% water Sat. Phenol, (Sigma Aldrich) to a final concentration of 50% STOP v/v. DNA and RNA were extracted according to manufacturer's instructions using the MasterPure Complete DNA and RNA Purification Kit (Epicentre). DNA and RNA yields were quantified using the Quant-iT dsDNA HS assay kit (Invitrogen) or the Quant-iT RNA assay kit (Invitrogen), respectively, as per manufacturer's instructions.

Genome sequencing and Assembly: Genomic DNA extracted from the batch cultures was sheared to approximately 200bp using a Covaris-S2 instrument (Covaris) and a single end library was prepared using the Ion AmpliSeq library 2.0 kit. The library was sequenced on the Ion-Torrent PGM system generating 200bp single-end reads. Reads were filtered based on quality score. Filtered reads were assembled using CLC's *de novo* assembler using a word size of 20 and bubble size of 50 with a minimum contig length of 1000 bp. The Whole Genome Shotgun project has been deposited at DDBJ/EMBL/GenBank under the accession JTDD00000000.

Transcriptomics: Total RNA from the batch cultures was treated once with recombinant DNase I (Ambion) to remove gDNA and then purified using the RNA Clean and Concentrator-25 kit (Zymo Research). To assess whether there was any contaminating gDNA, end point PCR was performed on 1 μL of the extracted total RNA in triplicate using a home-made mastermix with the following PCR parameters: denaturation at 94C for 3 min, 40 cycles consisting of 94C for 15s, 60C for 15s and 72 for 15s. Primers used to check for gDNA contamination targeted the *norB* gene: F-5'-CGGTTTGCAGTTCATCTTCC-3' and R-5'- CGCTTTCATCTTCCAG-AAACC-3'. Integrity of the total RNA was confirmed using a RNA Nano Chip on the Bioanalyzer 2100 (Agilent). The total RNA was then rRNA depleted using the Ribo-Zero rRNA Removal Kit for Gram-Negative Bacteria (Epicentre) according to manufacturer's instructions.

The efficiency of the rRNA removal was assessed by analysis of the rRNA depleted mRNA samples on a RNA Pico chip on the Bioanalyzer 2100 (Agilent). The rRNA depleted mRNA samples were quantified prior to library preparation with the Quant-iT RNA assay kit (Invitrogen).

Single-end Illumina RNA-Seq was done by the Center for Genome Research and Bioinformatics (Oregon State University, Oregon, USA). Libraries were prepared using the TruSeq RNA Sample Prep Kit v2 (Illumina) according to manufacturer's instructions. Quantification of the libraries was performed by qPCR and fluorometry. The libraries were then transferred and immobilized onto a flow cell using a cBot (Illumina) followed by sequencing on the Illumina HiSeq 200 (1 × 100bp reads) using the TruSeq v3 kit. Reads that passed the internal quality control filter then were used for subsequent RNA-Seq analysis.

The non-rRNA reads were trimmed and quality checked using CLC Genomic Workbench using quality scores (limit 0.05) and length (>30 bp). Then, the rRNA-depleted reads that passed trimming and quality control were mapped against the genome using CLC's RNA-seq assembler using the default parameters. Reads that mapped to greater than one location in the genome were randomly distributed among the matching locations. Gene expression was calculated using transcript abundance and differential expression using CLC Genomic Workbench. The number of reads that mapped against a gene was normalized by the length of the gene to generate a number of reads per kilobase of transcript per million mapped reads (RPKM) and were then reported as normalized gene expression levels. The total number of reads mapped was 6,443,134 million for NMS 24 h (1), 8,729,341 million for NMS 24 h (2), 6,393,707 million for NMS 48 h (1), 6,437,865 million for NMS 48 h (2), 6,459,649 million for AMS 24 h (1), 6,441,177 million for AMS 24 h (2), 6,553,723 million for AMS 48 h (1), 8,266,066 million for AMS 48 h (2). We

considered genes as differentially expressed only when the n-fold change value was > | 2 | and the P-value was < 0.001 as calculated by CLC Genomics Workbench. The raw transcriptome data sequence reads were deposited at DDBJ/EMBL/GenBank under the accession SRX696231.

2.4: Results

Taxonomic characterization: Strain FJG1 was obtained in 2002 **F**rom **J**ay **G**ulledge (University of Louisville, Kentucky). This name was effectively published with previous physiological work (Nyerges *et al.*, 2010); however, recent complete genome sequencing combined with physiological experimentation presented here revealed that strain FJG1 is not the same as what was deposited as *Methylomonas methanica* str. Rubra in the ATCC. The average nucleotide identity (ANI) comparison between the genome of strain FJG1 and the genomes of other gammaproteobacterial methane-oxidizing bacteria resulted in values considerably lower than 95%, an ANI that corresponds to 70% species level cut-off based on DNA-DNA hybridization (Goris *et al.*, 2007): *Methylomonas methanica* MC09 (GI:333981747): 81.9%, *Methylomicrobium album* BG8 (GI:381150023): 79.3%, *Methylomicrobium alcaliphilum* 20Z (GI:357403388): 78.79%; *Methylobacter marinus* A45 (GI:487735769): 79.27%, *Methylococcus capsulatus* Bath (GI:77128441): 78.22% . The following comparisons yielded insufficient hits to estimate ANI: *Methylomonas* sp. MK1 (GI:478730390), *Methylomonas* sp. 11b (GI:570990514), *Methylomicrobium buryatense* 5G (GI:452012734), *Methylobacter luteus* IMV-B-3098 (GI:523611614), *Methylobacter tundripaludum* SV96 (GI:343788098), *Methylovulum miyakonense* HT12 (GI:481782133), *Methylosarcina lacus* LW1 (GI:570956030), *Methylohalobius crimeensis* 10Ki (GI:522811456) and *Methylocaldum szegediense* O-12 (GI:523611165). Based on this significant difference in genome sequence, physiological characteristics such as the red color of pelleted cells as well as its nitrate-dependent denitrifying

activity, a new species name has been proposed: *Methylomonas denitrificans* sp. nov. with strain FJG1^T as the type strain. Future research will investigate whether strains physiologically and genetically similar to FJG1^T differ enough from other strains in the genus *Methylomonas* to consider classification as a new genus.

Growth phenotype of *Methylomonas denitrificans* sp. nov. FJG1^T cultivated on NO_3^- versus NH_4^+ as the nitrogen source. To determine how growth is affected by nitrogen source, *Methylomonas denitrificans* sp. nov. FJG1^T was cultured in batch in either nitrate (10 mM KNO_3) mineral salts (NMS) medium or ammonium (10 mM NH_4Cl) mineral salts (AMS) medium and growth was compared over 5 days (Figure 6a). The cultures were initiated at an O_2 tension of 17.6 ± 0.6%. Both the AMS- and NMS-based cultures reached stationary phase at 48-60 h (Figure 6a).

Trace gas measurements showed that the AMS-grown cultures consumed O_2 and CH_4 at rates (12 to 36 h) similar to the cultures grown in NMS: 0.043 mmol O_2 h^{-1} and 0.041 mmol CH_4 h^{-1} for AMS cultures and 0.041 mmol O_2 h^{-1} and 0.044 mmol CH_4 h^{-1} for NMS cultures (Figure 6b & 6c). Interestingly, the total amounts of O_2 and CH_4 consumed were not different between the cultures. To test whether O_2 was the limiting factor to growth of the NMS cultures, replicate NMS cultures were supplemented with additional O_2 (1.1 mmol) at 48 h. The OD_{600nm} at 60 h was 70% higher in the O_2 supplemented cultures when compared to the un-supplemented cultures (Figure 6a). Gas analysis of the headspace in both treatments revealed that N_2O was only produced in the NMS-grown culture, with production being measurable in the gas headspace at 60 h and increasing linearly at 4.14×10^{-18} mol N_2O/cell/h until the end of the incubation at 120 h (Figure 6d).

Instantaneous O_2 consumption and nitrogen oxide production by *M. denitrificans* sp.

nov. strain FJG1^T. To experimentally address whether *M. denitrificans* sp. nov. strain FJG1^T can consume and/or produce the nitrogen oxides NO_3^-, NO_2^-, NO, and N_2O, we incubated harvested cells from the batch cultures in a closed 10-mL micro-respiratory (MR) chamber fitted with O_2- and NO- or N_2O-detecting microsensors. Methane was supplied as the sole source of energy, reductant and carbon. Addition of methane (300 μM) led to a concomitant consumption of O_2 and the chamber quickly went anoxic (Figure 7a). The addition of NO_3^- before anoxia led to the production of N_2O only after O_2 was depleted in the chamber (Figure 7b). Treatment of the NO_3^- consuming cells with the protonophore CCCP caused a 75% decrease in the N_2O production rate (Figure 7b).

The addition of NO_2^- (1 mM) also resulted in N_2O production (Figure 7c); although CCCP treatment did not have a significant effect on the rate (Figure 7c). Furthermore, the stepwise addition of NO in the form of an NO-donor (6 nM Proli-NONOate/injection/2.5min) over 1 hour resulted in N_2O production (Figure 7d) and CCCP treatment did not have a significant effect on the rate (Figure 7d). Finally, the addition of 1 mM NO_2^- resulted in the production of ~5 nM NO (Figure 7f). The addition of NO_3^- (1 mM), NO_2^- (1 mM), or NO (20 μM) in the absence of CH_4 to the MR chamber did not lead to N_2O production, indicating a dependence on CH_4 as an electron donor (data not shown). When 10 mL of cells were supplied with a known and limiting amount of NO_3^- (30 μM) in a microelectrode chamber, about 15 μM N_2O was recovered (Figure 7e). As a control, we measured instantaneous O_2 consumption and N_2O production from NO_2^- using the same procedure in *Methylococcus capsulatus* strain Bath, a methanotrophic strain that was shown previously to produce N_2O during growth on NMS medium amended with NH_4^+ (Campbell *et al.*, 2011). *Methylococcus capsulatus* strain Bath did not produce N_2O from NO_2^- in this assay, suggesting that this strain may not possess active

denitrifying inventory (Figure 10).

We also used the MR setup to determine whether *M. denitrificans* sp. nov. strain FJG1^T coupled methane oxidation directly to N_2O production under extremely hypoxic (<50 nM O_2) conditions. Harvested cells were supplied with a limited amount of CH_4 – enough only to reach anoxia (Figure 8). When CH_4 was re-introduced into the MR chamber at <50 nM O_2, the harvested cells produced N_2O until CH_4 was depleted (Figure 8). A second and third addition of CH_4 into the nearly anoxic chamber showed the same effect.

ATP levels in NH_4^+ vs. NO_3^- grown *M. denitrificans* sp. nov. strain FJG1^T. We next measured the intracellular concentration of ATP in denitrifying cells of *M. denitrificans* sp. nov. strain FJG1^T incubated at low O_2 concentrations (1.5%) in the presence of NH_4^+ or NO_3^- and with CH_4 as the sole source of energy, reductant and carbon. We found that such denitrifying cells of *M. denitrificans* sp. nov. strain FJG1^T treated with 1 mM KNO_3 had ~46% more intracellular ATP after 90 minutes of incubation when compared to cells incubated in the presence of an equal concentration of NH_4Cl (0.78 μM/6 x 10^7 cells in the NO_3^-treated, 0.54 μM/6 x 10^7 cells in the NH_4^+ treated, $P < 0.05$) (Figure 9). This difference increased further after 180 and 270 minutes with ~53% and ~74% more ATP, respectively, in the NO_3^--treated versus NH_4^+-treated cells (Figure 9). In contrast, the O_2 consumption profiles over 270 minutes of incubation in the vials treated with equal concentrations of NO_3^- or NH_4^+ were not significantly different (Figure 9).

Analysis of gene expression in *M. denitrificans* sp. nov. strain FJG1^T **under hypoxic conditions.** Transcriptomic analysis of *M. denitrificans* sp. nov. strain FJG1^T cultures grown with either NO_3^- or NH_4^+ as the sole N source was performed after 24 and 48 h of incubation. The objective was to compare expression of methane and nitrogen metabolism pathway genes in

M. denitrificans sp. nov. strain FJG1^T cultured in either NMS or AMS media during the transition from exponential to stationary growth phase with and without O_2 limitation, at the end of which cultures must operate at limited supply of co-substrate (O_2) and under denitrifying conditions. Exponentially growing cultures (24 h) were considered the control and transition to stationary phase (48 h) was the time point at which respiratory nitrate reduction became evident in NMS-grown cells, even though N_2O was not yet measurable in the gas headspace (Fig. 6). The O_2 concentrations in the headspace during exponential phase growth at 24 h in the AMS- and NMS-based cultures were 8.7% and 11.4%, respectively. The O_2 concentrations in the headspace at 48 h, when the cultures were transitioning to stationary phase due to O_2 limitation, were 3.1% in AMS- and 3.5% in NMS-based cultures.

Analysis of the *M. denitrificans* sp. nov. strain FJG1^T genome revealed that it encodes two different putative membrane-associated dissimilatory nitrate reductases in addition to the assimilatory nitrate reductase (*nasA*): the cytoplasmic electrogenic enzyme complex NarGHJI and the periplasmic enzyme complex NapABC. Steady-state levels of *narG* mRNA in NMS-grown cultures were significantly increased after 48 h when compared to the 24 h sample (Table 1). The steady-state mRNA levels of two other subunit-encoding genes (*narHI*) were also significantly higher after 48 h of incubation in the NMS medium. In contrast, steady-state mRNA levels of the *narGHJI* gene cluster did not change in response to O_2 limitation during growth for 48 h in the AMS-grown cultures (Table 1). Steady-state levels of *napABC* mRNA did not change in response to O_2 limitation in either of the AMS- or NMS-grown cultures.

Two genes encoding putative periplasmic NO-forming nitrite reductases were annotated in the genome, the cytochrome cd_1 (*nirS*) and copper-containing (*nirK*) nitrite reductases. Transcript levels of the *nirK* gene were significantly higher at 48 h in the NMS cultures but not

changed in AMS-grown cultures (Table 1). In contrast, transcript levels of the *nirS* gene did not change between 24 and 48 h in cells cultured in either AMS or NMS (Table 1). However, the *nirS* gene showed a high basal level of expression in all samples with RPKM (reads per kilobase of transcript per million mapped reads) values in the top 20% of expressed transcripts. A putative cytochrome *c*-dependent nitric oxide reductase (cNOR; *norBC*) was also annotated in the genome of *M. denitrificans* sp. nov. strain FJG1^T. As with *narG* and *nirK*, steady-state mRNA levels of both *norB* and *norC* genes were significantly elevated in NMS after 48 h when compared to the 24 h sample (Table 1). There was no change in levels of *norBC* transcripts in the AMS-grown culture after 48 h.

Additional genes for which transcript levels were elevated at 48-h in both NMS and AMS media under O_2-limited conditions include the *pxmABC* operon, which encodes a copper-containing membrane monooxygenase (Cu-MMO) related to particulate methane monooxygenase (Tavormina *et al.*, 2011). While mRNA levels were very low in AMS and NMS samples at 24 h, the *pxmABC* transcripts were significantly more abundant in both the NMS and AMS samples after 48 h in response to hypoxia (Table 1). Interestingly, the increase in steady-state *pxmABC* transcript levels after 48 h was significantly greater in the O_2 limited NMS samples when compared to the AMS samples ($P<0.001$). So while the abundance of *pxmABC* transcripts increased in response to hypoxia in general, the increase in the presence of NO_3^- was significantly greater than with NH_4^+. In contrast to *pxmABC*, transcript levels of the canonical *pmoCAB* operon were high at 24-h and 48-h in both AMS and NMS and did not exhibit any significant change in response to hypoxia at 48-h in either medium (Table 1).

In addition to *pxmABC*, transcript levels of a hemoglobin-like cyanoglobin-encoding gene increased in response to hypoxia at 48 h in NMS. While the genome of *M. denitrificans* sp.

nov. strain FJG1^T encodes a total of 4 cyanoglobin-encoding genes, transcript abundance of only one of these genes (HbN_3) was significantly increased in NMS and AMS cultures after 48 h due to limited oxygen (Table 1).

2.5: Discussion

***Methylomonas denitrificans* sp. nov. strain FJG1^T produces N_2O only under hypoxia in the presence of NO_3^- and CH_4.** The observation of N_2O production in the NMS- but not in the AMS-grown cultures (Fig. 6d) suggests that N_2O originated from the reduction of NO_3^- via a dissimilatory pathway. During growth on NMS, N_2O was only measurable once the cultures reached hypoxia. This suggests that N_2O production occurred in the presence of NO_3^- in response to O_2 limitation due to either enzyme activation or induced gene expression. N_2O production under low O_2 tension by *M. denitrificans* sp. nov. FJG1^T is similar to two other microbial processes: nitrifier denitrification in ammonia-oxidizing bacteria and aerobic denitrification in chemoorganoheterotrophic bacteria such as *Paracoccus denitrificans*, which both utilize alternative terminal electron acceptors to O_2 during hypoxia (Stein, 2011; Kozlowski *et al.*, 2014). Extrapolation using the linear rate of N_2O production from 60-120 h (0.414 μmol L-1 hr-1) provided for the estimate that N_2O production began 48 h after inoculation of culture into the NMS medium. A 70% increase in $O.D._{600nm}$ in replicate NMS cultures supplemented with O_2 after 60 h demonstrated that the limiting growth factor in the cultures was O_2.

***Methylomonas denitrificans* sp. nov. strain FJG1^T reduces NO_3^- to N_2O via the intermediates NO_2^- and NO.** The ability of *Methylomonas denitrificans* sp. nov. strain FJG1^T to reduce NO_3^-, NO_2^-, and NO to N_2O in the presence of CH_4 as a sole energy source demonstrates that this organism has a functional denitrifying pathway and that the respiratory electron flow is linked to CH_4 oxidation. Denitrification only occurred at O_2 concentrations below the detection

limit of our O_2 sensor (50 nM) and only with sufficient CH_4. The minute amount of O_2 present in the MR chamber was enough to sustain methane oxidation. Since the only energy source supplied was CH_4 and we were unable to grow *Methylomonas denitrificans* sp. nov. strain FJG1^T under anoxia, we conclude that O_2 is still required for CH_4-dependent denitrification in this organism. The O_2 present in the MR chamber below the detection limit of the electrode was likely supplied by leakage of atmospheric O_2 into the chamber. Our batch culture data support this hypothesis, as the batch incubations did not reach anoxia (ca. 0.5 mM O_2 in the headspace after 120 h of growth). Nevertheless, denitrification was CH_4 dependent at <50 nM O_2 (Figure 8). These results demonstrate that *M. denitrificans* sp. nov. strain FJG1^T is able to scavenge O_2 for CH_4 oxidation at low O_2 concentrations and that CH_4 is the direct electron donor for denitrification under O_2-limiting conditions.

The protonophore CCCP decreased the rate of N_2O-forming activity from NO_3^- by 75%. Both dissimilatory nitrate reductases, NAR and NAP, rely on the quinone pool for reductant (González *et al.*, 2006) but only the proton-motive force-generating activity of the NAR protein will contribute to energy conservation (Simon & Klotz, 2013). Thus, the decrease in denitrification (N_2O-formation from NO_3^-) effected by CCCP suggests that *Methylomonas denitrificans* sp. nov. strain FJG1^T utilizes the predicted energy-conserving NAR protein rather than the electro-neutral NAP and NasA complexes for the reduction of NO_3^- to NO_2^-. In agreement with this conclusion, we confirmed that CCCP did not affect the rate of N_2O production from NO_2^-, which is facilitated by the soluble and thus electro-neutral copper type (*nirK*) and cytochrome cd_1 (*nirS*) nitrite reductases; both receive reductant from the cytochrome *c* pool rather than the quinone pool (Ferguson & Richardson, 2004). These results and conclusions agree with our finding that denitrifying conditions increase steady-state transcript

levels of *norB*, *nirK* and *nar* but not *nap* genes in a generally high expression background of *nirS* genes (see below).

The 2:1 stoichiometry of NO_3^- conversion to N_2O indicates that N_2O was the sole product of the denitrification pathway. The absence of a nitrous oxide reductase-encoding gene (*nosZ*) in the genome of *Melylomonas denitrificans* sp. nov. strain FJG1^T genetically verifies the detection of N_2O as the end product of the denitrification pathway. The only known methanotroph encoding a *nosZ* gene on a plasmid is *Methylocystis* sp. strain SC2, although this bacterium has not been shown to denitrify with CH_4 as the electron donor (Dam *et al.*, 2013).

Previous studies showed that CH_4 is an adequate electron donor for denitrification in mixed communities at micro-aerobic conditions in both engineered systems and natural environments (Costa *et al.*, 2000; Knowles, 2005; Liu *et al.*, 2014). These studies concluded that the observed denitrification process was driven by collaboration of at least two different cohorts in the microbial consortium: methane-oxidizing bacteria that export organic compounds (acetate, formaldehyde, methanol, citrate) under O_2 limitation and heterotrophic bacteria that use the reduced organic compounds to denitrify. Our results clearly demonstrate that *M. denitrificans* sp. nov. FJG1^T can couple CH_4 oxidation to respiratory nitrate reduction on its own and in pure culture during O_2 limitation. This suggests that aerobic methanotrophs may, in addition to heterotrophic denitrifiers, contribute directly to denitrification and N_2O emission in natural environments.

Denitrification is bioenergetically advantageous for *Methylomonas denitrificans* sp. nov. strain FJG1^T during O_2 limitation. Identification of two different dissimilatory nitrate reductases in the genome of *Methylomonas denitrificans* sp. nov. strain FJG1^T raises questions about the physiological role of denitrification in this organism. The periplasmic nitrate

reductases are widespread in bacteria and can fulfill a variety of physiological functions such as dissipating excess energy during aerobic growth as in *Paracoccus denitrificans*, redox balance in the photosynthetic electron transfer chain of *Rhodococcus capsulatus*, fermentation, and also denitrification (Ferguson & Richardson, 2004). The periplasmic nitrate reductase has also been implicated in assimilatory nitrate ammonification in the hydrothermal vent bacterium *Nautilia profundicola* (Hanson *et al.*, 2013). In contrast, the respiratory nitrate reductase is much less common in bacteria and used solely by denitrifiers for anaerobic respiration because it allows for the conservation of energy through pmf-driven ATP synthesis (Richardson *et al.*, 2001; Simon & Klotz, 2013). ATP abundance measurements in cells of *Methylomonas denitrificans* sp. nov. strain FJG1^T during low O_2 batch incubations, indeed, revealed higher levels of ATP in cells that were actively respiring NO_3^- at the expense of CH_4 oxidation when compared to those that were not respiring NO_3^-. Thus, denitrification provides a means of energy conservation under O_2 limitation. This result further suggests that *Methylomonas denitrificans* sp. nov. strain FJG1^T utilizes primarily the NAR nitrate reductase during denitrification rather than NAP since NAR contributes to energy conservation (Richardson *et al.*, 2001).

Transcript levels of predicted nitrate, nitrite, and nitric oxide reductases increase in response to O_2 limitation and NO_3^- availability. Increased levels of steady-state *narGHI* mRNA in response to denitrifying conditions and the known electrogenic nature of NAR complexes in other bacteria suggests that this nitrate reductase is involved in the denitrification pathway and supports our above hypothesis that nitrate respiration in *M. denitrificans* sp. nov. strain FJG1^T is connected to energy conservation. We define denitrifying conditions as requiring both hypoxia and NO_3^- since those are the two main environmental factors that control the onset of denitrifying activity in our bacterium. The lack of a change in *napABC* transcript levels in

cells grown in 10 mM NMS medium was consistent with previous findings that *nap* genes are only expressed under nitrate-limiting growth conditions in *E. coli* specifically for high affinity nitrate respiration (Ferguson & Richardson, 2004). On the other hand, steady-state levels of *nap* gene transcripts were elevated in *Nautilia* upon availability of NO_3^- (Hanson *et al.*, 2013) indicating that NO_3^- can serve as a signal to initiate the expression of genes encoding either dissimilatory nitrate reductase. While the *Nautilia* genome encodes only the NAP complex, the genome of *Methylomonas denitrificans* sp. nov. FJG1^T represents the rare situation of a genome encoding all three known nitrate reductases, which requires differential regulation. Whether the *nap* gene cluster is expressed in *Methylomonas denitrificans* sp. nov. strain FJG1^T during hypoxia under nitrate-limiting conditions has yet to be investigated.

The second step in denitrification, a one-electron reduction of NO_2^- to NO, can be performed by either of two non-homologous NO-forming nitrite reductase enzymes – a cytochrome cd_1 (*nirS*) or a copper-containing (*nirK*) nitrite reductase. Both of these enzymes are localized in the periplasm and appear to be isofunctional; however, no organism until now has been shown to conclusively possess both types of active nitrite reductase (Chen & Strous, 2013). Our finding that *M. denitrificans* sp. nov. strain FJG1^T encodes and expresses both types of nitrite reductase raises questions about whether either enzyme has a catalytic advantage or specialized function. While the presence of predicted *nirS* or *nirK* genes in the genomes of methanotrophs has been reported previously, little is known about their function and expression. Recently, it was shown that the *nirK* gene in *Methylacidiphilum fumariolicum* strain SolV is upregulated in a chemostat under O_2-limiting conditions (Khadem *et al.*, 2012a); however, it remains unknown if *M. fumariolicum* can reduce NO_2^- to NO using this enzyme. The absence of a dissimilatory nitrate reductase-encoding gene in the genome suggests that a functional serial

denitrifying pathway is lacking (Khadem *et al.*, 2012b). The differential expression of *nirK* and not *nirS* in the transcriptome of *Methylomonas denitrificans* sp. nov. strain FJG1^T in response to denitrifying conditions suggests that NirK may be the only operational nitrite reductase for the observed denitrification activity. However, we cannot rule out that NirS may also serve this or some other metabolic function such as detoxification of excess nitrite as the relatively high RPKM values for the *nirS* gene in NMS and AMS samples at both the 24 and 48 h time points suggest constitutive expression. Therefore, NirS might be involved in a process that is apparently not influenced by nitrogen source or O_2 concentration.

The end product of the denitrification pathway of *Methylomonas denitrificans* sp. nov. strain FJG1^T is N_2O and not N_2. Membrane-associated nitric oxide reductases are encoded in the genomes of many obligate aerobic methanotrophs; however, it is not clear from previous work whether methanotrophs utilize it for respiratory denitrification. Chemostat cultures of *M. fumariolicum* strain SolV revealed that the transcription of *norBC* was upregulated in response to O_2 limitation; however, it remains unknown if *M. fumariolicum* strain SolV can metabolize NO (Khadem *et al.*, 2012a). It has also been demonstrated that *norBC* is upregulated 4.8 fold in *M. capsulatus* strain Bath in response to 0.5 mM sodium nitroprusside – a nitrosating agent that releases NO (Campbell *et al.*, 2011). Elevated transcript levels of *norBC* in *Methylomonas denitrificans* sp. nov. strain FJG1^T in response to denitrifying conditions in context with measured N_2O production suggests that this gene cluster encodes inventory (cNOR) that participates in the denitrification pathway, which adds further support for its involvement in low O_2 nitrogen metabolism in methanotrophs in general.

The lack of change in transcript levels of any putative denitrification genes in *Methylomonas denitrificans* gen. nov. strain FJG1^T grown in AMS for 48 hours, when compared

to the 24-hour AMS control, demonstrates that O_2 limitation alone is not sufficient to increase the transcript levels of *narGHJI*, *nirK*, or *norBC*. Furthermore, comparing the 24 h NMS transcriptome to the 24 h AMS transcriptome demonstrates that the presence of NO_3^- alone is also not sufficient to cause a change in transcript levels of denitrification genes in *Methylomonas denitrificans* sp. nov. strain FJG1^T. Taken together, these observations demonstrate that transcript levels of a complete suite of genes encoding the first three steps in the denitrification pathway increase only in response to simultaneous O_2 limitation and NO_3^- availability.

Ancillary genes regulated by hypoxia and NO_3^- include the *pxmABC* operon and cyanoglobin. The *pxmABC* operon was recently discovered in addition to the conventional *pmoCAB* operon in some gammaproteobacterial obligate methanotrophs (Tavormina *et al.*, 2011). This operon is predicted to encode a member of the Cu-MMO protein family, pXMO, which has a novel 'A-B-C' gene organization when compared to the canonical 'C-A-B' organization of characterized conventional *pmo* operons (Tavormina *et al.*, 2011). Although function and substrate of the putative pXMO complex encoded by this operon are still unknown, it has been demonstrated that the *pxm* operon is expressed *in situ* in freshwater peat bog and creek sediment (Tavormina *et al.*, 2011). More recently, *pxmA* sequences were detected in the aerobic layer of oilsands tailings ponds as determined by metagenomic sequencing of the heavy DNA after SIP with $^{13}CH_4$ (Saidi-Mehrabad *et al.*, 2013). The detection of highly elevated transcript levels of *pxmABC* under hypoxia in NMS and AMS media suggests that steady-state mRNA levels of *pxmABC* increase in response to O_2 limitation. Nevertheless, *pxmABC* transcript levels during hypoxia were significantly higher in the presence of NO_3^- when compared to NH_4^+, which implicates NO_3^- as a signal and suggests a physiological connection between denitrification and activity of a putative pXMO protein complex.

In addition to *pxmABC* expression under hypoxia, elevated transcript levels of a hemoglobin-like cyanoglobin-encoding gene suggests that O_2 binding by globins is a possible mechanism for delivering scarce O_2 to the CH_4-monooxygenase. In other bacterial systems globins have been shown to alleviate O_2 limitation by facilitating respiration via O_2 delivery/transport and by detoxifying reactive nitrogen species such as NO (Frey & Kallio, 2003).

Conclusions

Here we report the discovery of nitrate reduction coupled with aerobic methane oxidation under extreme hypoxia in which N_2O production is directly supported by CH_4 oxidation within a single organism. The main conclusions from this study are that (i) *Methylomonas denitrificans* sp. nov. strain FJG1^T is a novel representative of aerobic methanotrophs that couples CH_4 oxidation to NO_3^- reduction; (ii) NO_3^- availability and hypoxia are required for N_2O-forming denitrification activity; (iii) CH_4-dependent denitrification is a means of energy conservation under O_2 limitation; (iv) mRNA levels of predicted denitrification genes encoding a nitrate reductase, nitrite reductase, and nitric oxide reductase exist at significantly elevated levels under denitrifying conditions; and (v) the expression product of the *pxmABC* operon may play a functional role in hypoxic methane oxidation and may be aided by globins to access low levels of O_2. The discovery of CH_4 oxidation coupled to NO_3^- respiration in *Methylomonas denitrificans* sp. nov. strain FJG1^T expands our understanding of methanotrophy and has major implications for the environmental role of methanotrophic bacteria in both the carbon and nitrogen cycle. This metabolism also provides an explanation for the abundance and activity of aerobic methanotrophs in anoxic ecosystems (Tveit *et al.*, 2013; Tveit *et al.*, 2014). In O_2-limited ecosystems, strains that possess similar denitrifying inventory to *Methylomonas denitrificans* sp.

nov. strain FJG1^T could couple the consumption of the greenhouse gas CH_4 to the removal of NO_3^- while releasing N_2O – a more potent and persistent ozone-depleting greenhouse gas. The finding that aerobic methanotrophs can respire NO_3^- under extreme hypoxia suggests a hitherto unknown role of methanotrophs at the intersection of the global carbon and nitrogen cycles.

Description of *Methylomonas denitrificans* sp. nov.: *Methylomonas denitrificans* **(**N.L. part. adj. *denitrificans*, denitrifying, the name referring to its ability to reduce nitrate to nitrous oxide.). Cells utilize methane as sole source of carbon, energy and reductant; they are strictly oxygen-dependent, Gram stain-negative rods, utilize flagella for motility and the genotype is chemotaxis positive. Colonies and liquid cultures appear pale pink. Cultures grow under mesophilic conditions (pH 6.2 – 7.5) with an optimum growth temperature between 27-30°C. The G+C content of the sequenced genome is 51.6%. Strain FJG1^T is the type strain of *Methylomonas denitrificans* sp. nov., which belongs to the family *Methylococcaceae*, the order *Methylococcales*, class *Gammaproteobacteria.*

2.6: Tables and Figures

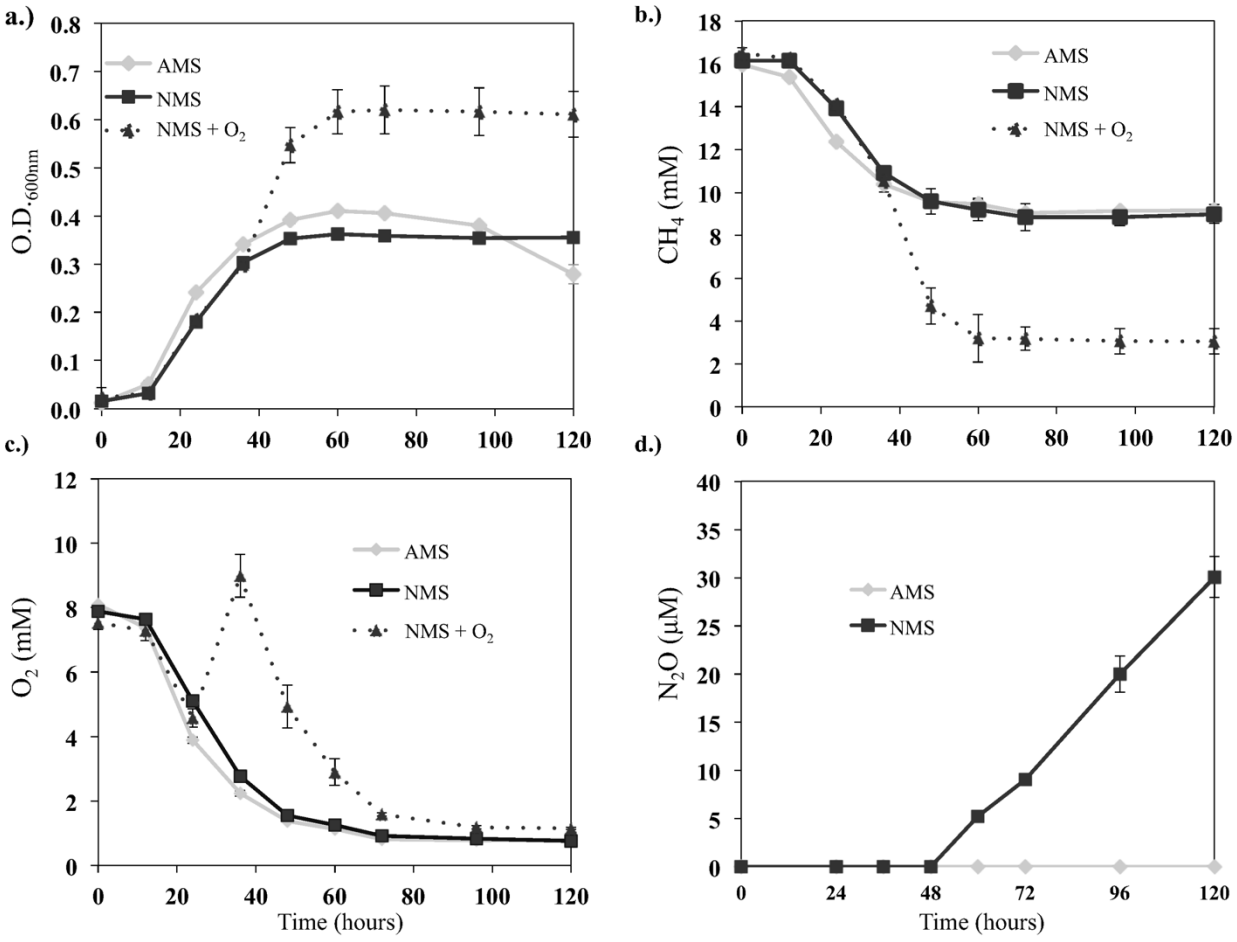

Figure 6: **Growth, CH_4 and O_2 consumption, and N_2O production by *Methylomonas denitrificans* sp. nov. strain FJG1^T cultivated on AMS and NMS.**

M. denitrificans sp. nov. strain FJG1^T was cultivated for 120 h in 100 mL of AMS or NMS media in a 250 mL closed glass Wheaton bottle sealed with a butyl rubber septum cap with a headspace has mixing ratio of 3:7, CH_4 to O_2. Optical density (a) was measured with a plate reader at 600nm and headspace gas concentrations of CH4 (b), O2 (c), and N2O (d) were measured using GC-TCD. AMS (black □) and NMS (grey ■). All data points represent the mean ± standard deviation for an n = 6.

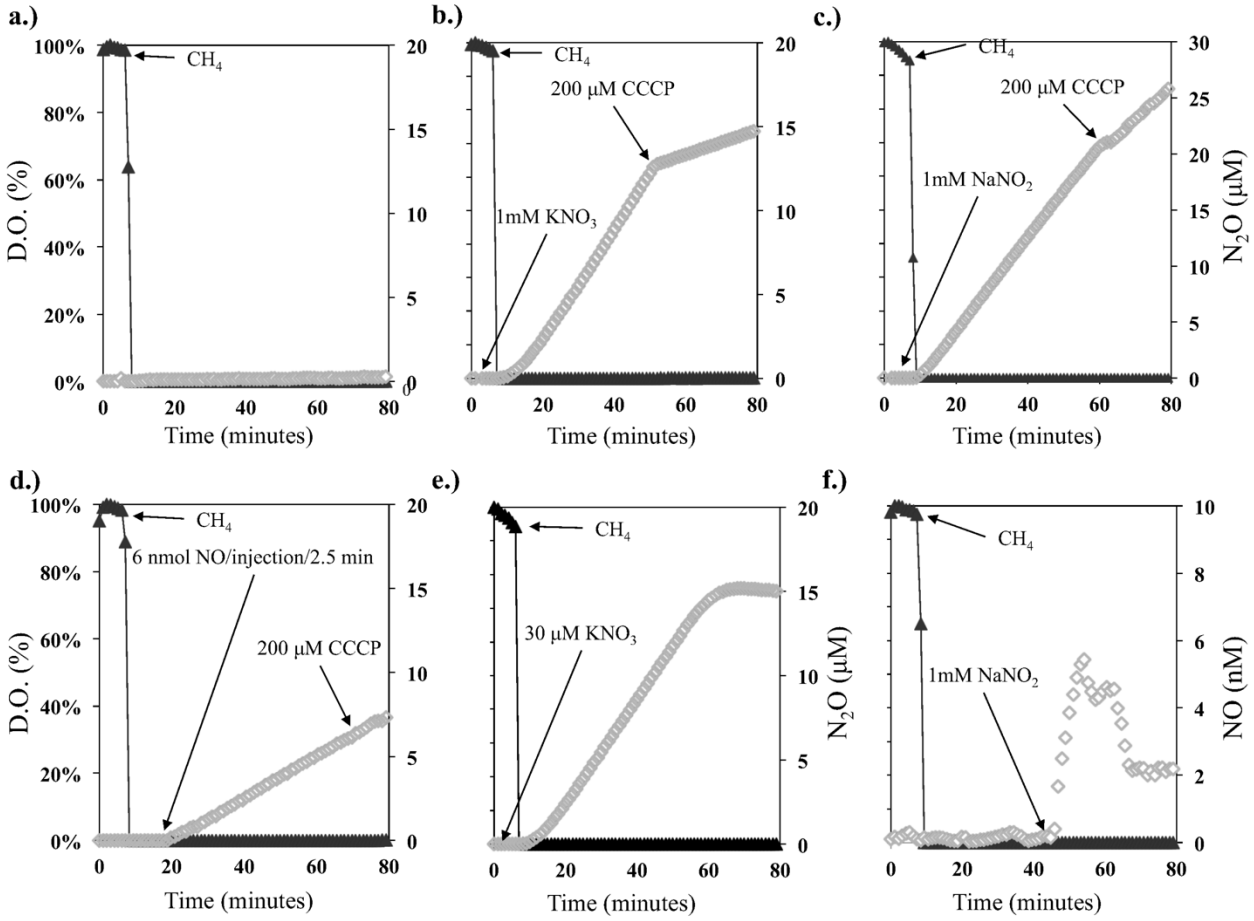

Figure 7: **The coupling of CH_4 oxidation to NO_3^-, NO_2^-, and NO reduction in *Methylomonas denitrificans* sp. nov. strain FJG1^T under O_2 limitation.**

Experiments were performed in a closed 10 mL micro-respiratory chamber outfitted with an O_2 and NO or N_2O microsensors and logged with Sensor Trace Basic software. O_2 (black ▲) and N_2O/NO (grey ◆). Arrows mark the addition of CH_4, KNO_3 (1 mM), CCCP (200 µM), $NaNO_2$ (1 mM), or Proli NONOate (6 nmol/injection/2.5 min) in all panels. The x-axes (time in minutes) as well as left y-axes (% dissolved O_2) are identical in all panels. The right y-axes are identical in panels a, b, c, d, and e - µM N_2O). It should be noted that the right y-axis is different in panel f – nM NO.

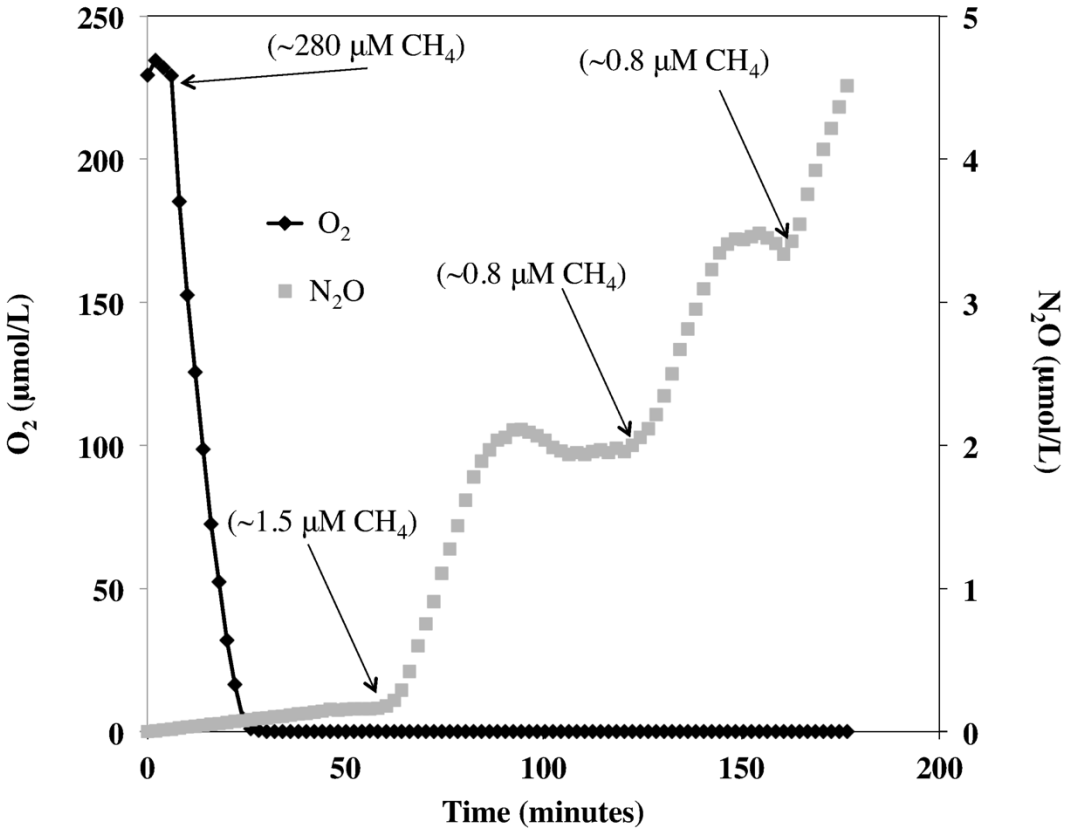

Figure 8: **NO_3^- reduction to N_2O is CH_4 dependent at <50 nM O_2.**

Experiments were performed in a closed 10 mL micro-respiratory chamber outfitted with O_2 and N_2O microsensors and logged with Sensor Trace Basic software. O_2 (black ◆) and N_2O (grey ■). Arrows mark the addition of CH_4.

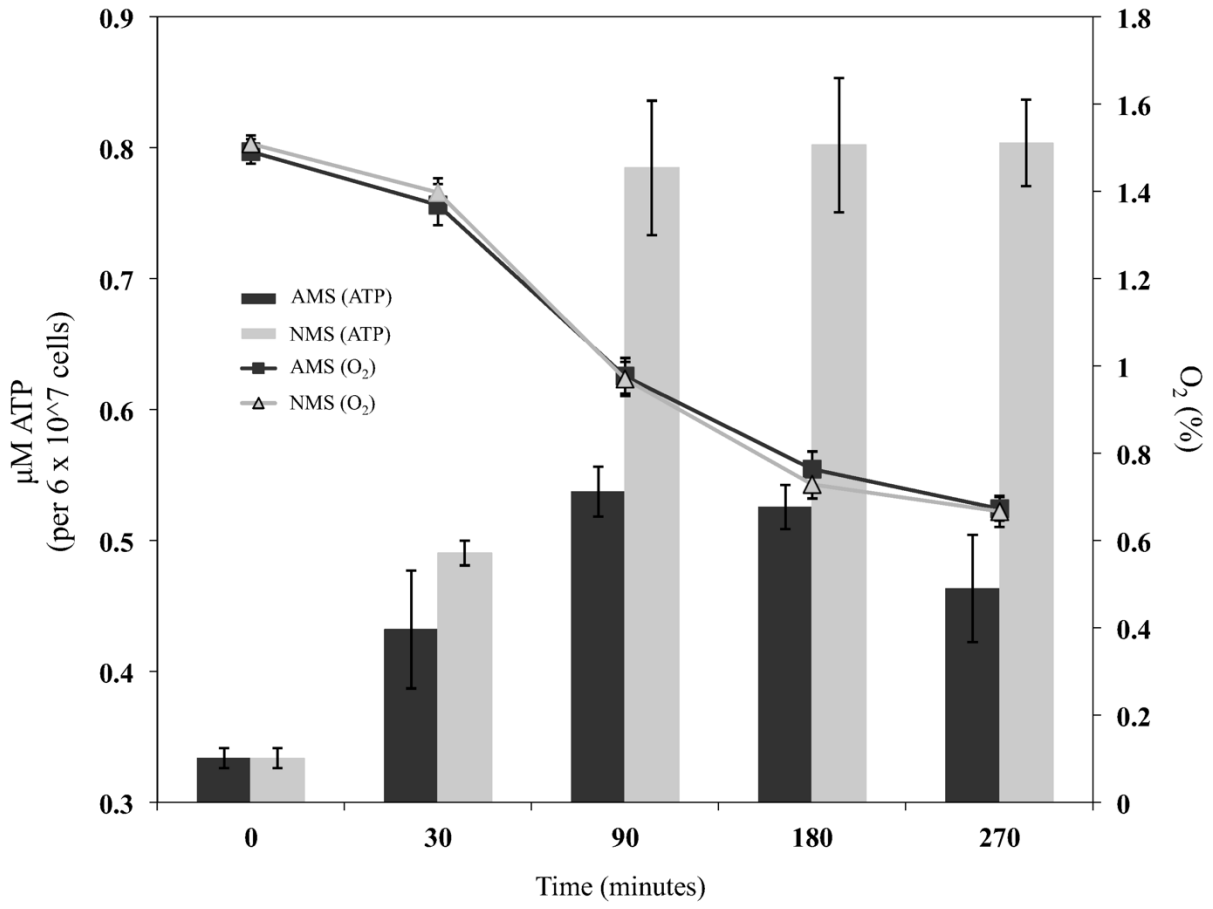

Figure 9: **ATP production and O_2 consumption by denitrifying cells of *Methylomonas denitrificans* sp. nov. strain FJG1^T under O_2 limitation.**

Methylomonas denitrificans sp. nov. strain FJG1^T was cultivated in 100 mL of NMS media in a closed 250 mL glass Wheaton bottle for 120 h at a headspace gas mixing ratio of 3:7, CH_4 to O_2. Columns represent ATP abundance (black – AMS, grey – NMS) and lines represent headspace O_2 concentration (AMS – black ■, NMS – grey ▲). ATP was measured using the BacTiter-Glo Microbial Cell Viability Assay (Promega) on a luminometer. Headspace O_2 concentrations were measured using GC-TCD. Each data point represents the mean ± standard deviation for n = 6.

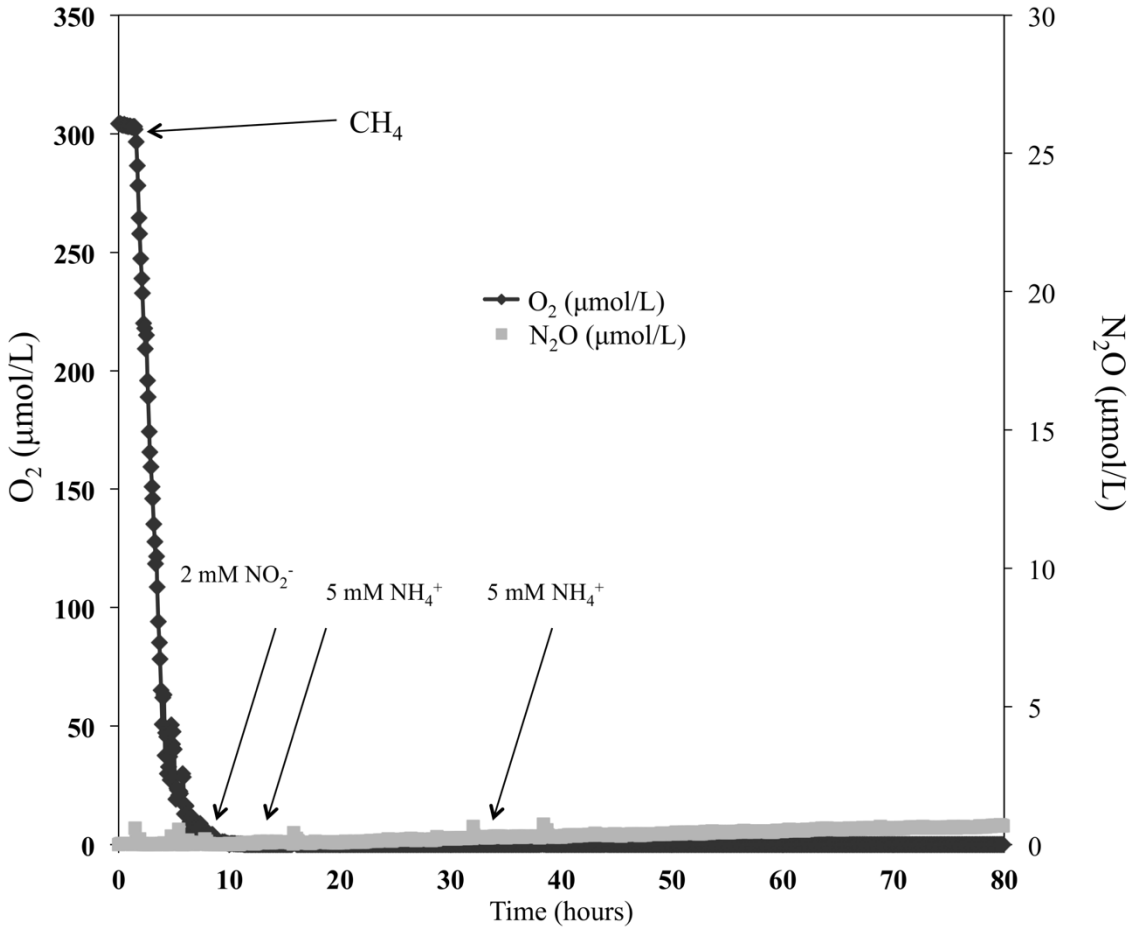

Figure 10: ***M. capsulatus*** **Bath cannot couple CH_4 oxidation to N_2O production under hypoxia in the presence of NO_2^- and NH_4^+.**

Experiments were performed in a closed 10 mL micro-respiratory chamber outfitted with an O_2 and N_2O microsensors and logged with Sensor Trace Basic software. O_2 (black ◆) and N_2O/NO (grey ■). Arrows mark the addition of CH_4, $NaNO_2$ (1 mM), or NH_4Cl (5 mM).

			RPKM				N-fold change of RPKM value		
Gene ID	Gene	Locus Tag	NMS 24 h	NMS 48 h	AMS 24 h	AMS 48 h	NMS 48 h/NMS 24 h	AMS 48 h/AMS 24 h	NMS 24 h/AMS 24 h
Methane oxidation									
Particulate methane monooxygenase subunit C	pmoC	JT25_22645	30597	16089	26464	12746	-1.9	-2.1	1.2
Particulate methane monooxygenase subunit A	pmoA	JT25_22640	84846	84846	80060	80060	-1.0	1.0	1.1
Particulate methane monooxygenase subunit B	pmoB	JT25_22635	52025	30597	41565	29006	-1.7	-1.4	1.3
Sequence divergent particulate monooxygenase subunit A	pxmA	JT25_09560	12	109	15	28	9.1	1.9	-1.3
Sequence divergent particulate monooxygenase subunit B	pxmB	JT25_09565	9	100	12	37	11.1	3.1	-1.3
Sequence divergent particulate monooxygenase subunit C	pxmC	JT25_09570	10	80	12	32	8.0	2.7	-1.2
Dissimilatory nitrogen metabolism									
Respiratory nitrate reductase alpha chain	narG	JT25_19580	38	93	39	22	2.4	-1.8	-1.0
Respiratory nitrate reductase beta chain	narH	JT25_19585	24	54	44	22	2.3	-2.0	-1.8
Respiratory nitrate reductase delta chain	narJ	JT25_18045	40	72	36	28	1.8	-1.3	1.1
Respiratory nitrate reductase gamma chain	narI	JT25_18050	65	153	86	38	2.4	-2.3	-1.3
Periplasmic nitrate reductase subunit A	napA	JT25_07960	18	21	17	22	1.2	1.3	1.1
Periplasmic nitrate reductase subunit B	napB	JT25_07955	10	12	6	8	1.2	1.3	1.7
Periplasmic nitrate reductase subunit C	napC	JT25_07950	12	15	11	16	1.3	1.5	1.1
Copper containing nitrite reductase	nirK	JT25_18055	26	74	27	23	2.8	-1.2	-1.0
Cytochrome cd1 nitrite reductase	nirS	JT25_11725	117	181	233	230	1.5	1.0	-2.0
Nitric oxide reductase subunit B	norB	JT25_07185	108	300	144	57	2.8	-2.5	-1.3
Nitric oxide reductase subunit C	norC	JT25_07190	182	591	222	105	3.2	-2.1	-1.2
Ancillary									
Cyanoglobin; hemoglobin like protein	glbn_3	JT25_21145	144	319	163	331	2.2	2.0	-1.1

a. Only some genes involved in nitrogen metabolism and methane metabolism are displayed.

b. RPKM values represent the mean of two biological replicates

c. Annotated and expressed genes for which the N-fold change of RPKM values was >= |2| and for which the P-value was <0.01 are highlighted in grey.

Table 1: **Expression and differential expression of major methane and nitrogen metabolism genes in response to oxygen limitation**

2.7: References

References

Campbell, M. A., Nyerges, G., Kozlowski, J. A., Poret-Peterson, A. T., Stein, L. Y., & Klotz, M. G. (2011) Model of the molecular basis for hydroxylamine oxidation and nitrous oxide production in methanotrophic bacteria. *FEMS Microbiol Lett* **322:** 82-89.

Canfield, D. E., Glazer, A. N., & Falkowski, P. G. (2010) The evolution and future of earth's nitrogen cycle. *Science* **330:** 192-196.

Chen, J., & Strous, M. (2013) Denitrification and aerobic respiration, hybrid electron transport chains and co-evolution. *Biochim Biophys Acta-Bioenerg* **1827:** 136-144.

Costa, C., Dijkema, C., Friedrich, M., Garcia-Encina, P., Fernandez-Polanco, F., & Stams, A. J. M. (2000) Denitrification with methane as electron donor in oxygen-limited bioreactors. *Appl Microbiol Biotechnol* **53:** 754-762.

Dam, B., Dam, S., Blom, J., & Liesack, W. (2013) Genome Analysis Coupled with Physiological Studies Reveals a Diverse Nitrogen Metabolism in *Methylocystis* sp. Strain SC2. *PLoS ONE* **8:**

Dunfield, P., & Knowles, R. (1995) Kinetics of Inhibition of Methane Oxidation by Nitrate, Nitrite, and Ammonium in a Humisol. *Appl Environ Microbiol* **61:** 3129-3135.

Ettwig, K. F., Butler, M. K., Le Paslier, D., Pelletier, E., Mangenot, S., Kuypers, M. M. M. et al. (2010) Nitrite-driven anaerobic methane oxidation by oxygenic bacteria. *Nature* **464:** 543-+.

Ferguson, S. J., & Richardson, D. J. (2004) The enzymes and bioenergetics of bacterial nitrate, nitrite, nitric oxide and nitrous oxide respiration. In *Respiration in archaea and bacteria.* Netherlands, Springer, pp. 169-206.

Frey, A., & Kallio, P. (2003) Bacterial hemoglobins and flavohemoglobins: versatile proteins and their impact on microbiology and biotechnology. *FEMS Microbiol Rev* **27:** 525-545.

González, P. J., Correia, C., Moura, I., Brondino, C. D., & Moura, J. J. G. (2006) Bacterial nitrate reductases: Molecular and biological aspects of nitrate reduction. *J Inorg Biochem* **100:** 1015-1023.

Goris, J., Konstantinidis, K. T., Klappenbach, J. A., Coenye, T., Vandamme, P., & Tiedje, J. M. (2007) DNA-DNA hybridization values and their relationship to whole-genome sequence similarities. *Int J Syst Evol Microbiol* **57:** 81-91.

Hanson, T. E., Campbell, B. J., Kalis, K. M., Campbell, M. A., & Klotz, M. G. (2013) Nitrate ammonification by Nautilia profundicola AmH: experimental evidence consistent with a free hydroxylamine intermediate. *Frontiers in Microbiology* **4:** 180.

Hoefman, S., Ha, D. v. d., Boon, N., Vandamme, P., Vos, P. d., & Heylen, K. (2014) Niche differentiation in nitrogen metabolism among methanotrophs within an operational taxonomic unit. *BMC Microbiology* **14:** (4 April 2014)-(4 April 2014).

Kalyuzhnaya, M. G., Yang, S., Rozova, O. N., Smalley, N. E., Clubb, J., Lamb, A. et al. (2013) Highly efficient methane biocatalysis revealed in a methanotrophic bacterium. *Nat Commun* **4:** 2785.

Khadem, A. F., Pol, A., Wieczorek, A. S., Jetten, M. S. M., & Op den Camp, H. J. M. (2012a) Metabolic regulation of "Ca. *Methylacidiphilum fumariolicum*" soIV cells grown under different nitrogen and oxygen limitations. *Frontiers in Microbiology* **3:**

Khadem, A. F., Wieczorek, A. S., Pol, A., Vuilleumier, S., Harhangi, H. R., Dunfield, P. F. et al. (2012b) Draft genome sequence of the volcano-inhabiting thermoacidophilic methanotroph *Methylacidiphilum fumariolicum* strain SoLV. *J Bacteriol* **194:** 3729-3730.

Knowles, R. (2005) Denitrifiers associated with methanotrophs and their potential impact on the nitrogen cycle. *Ecol Eng* **24:** 441-446.

Kozlowski, J. A., Price, J., & Stein, L. Y. (2014) Revision of N_2O-Producing Pathways in the Ammonia-Oxidizing Bacterium *Nitrosomonas europaea* ATCC 19718. *Appl Environ Microbiol* **80:** 4930-4935.

Kraft, B., Tegetmeyer, H. E., Sharma, R., Klotz, M. G., Ferdelman, T. G., Hettich, R. L. et al. (2014) The environmental controls that govern the end product of bacterial nitrate respiration. *Science* **345:** 676-679.

Krämer, M., Baumgärtner, M., Bender, M., & Conrad, R. (1990) Consumption of NO by methanotrophic bacteria in pure culture and in soil. *FEMS Microbiol Lett* **73:** 345-350.

Liu, J., Sun, F., Wang, L., Ju, X., Wu, W., & Chen, Y. (2014) Molecular characterization of a microbial consortium involved in methane oxidation coupled to denitrification under micro-aerobic conditions. *Microbial Biotechnology* **7:** 64-76.

MacKelprang, R., Waldrop, M. P., Deangelis, K. M., David, M. M., Chavarria, K. L., Blazewicz, S. J. et al. (2011) Metagenomic analysis of a permafrost microbial community reveals a rapid response to thaw. *Nature* **480:** 368-371.

Murrell, J. C., & Jetten, M. S. M. (2009) The microbial methane cycle. *Environ Microbiol Rep* **1:** 279-284.

Myhre, G., Shindell, D., Bréon, F. -., Collins, W., Fuglestvedt, J., Huang, J. et al. (2013) Anthropogenic and natural radiative forcing. in: Climate change 2013: The physical science basis. contribution of working group I to the fifth assessment report of the intergovernmental panel on climate change. In Stocker, T.F., D. Qin, G.-K. Plattner, M. Tignor, S.K. Allen, J. Boschung, A. Nauels, Y. Xia, V. Bex and P.M. Midgley (ed). Cambridge, United Kingdom and New York, NY, USA, Cambridge University Press,

Nyerges, G., Han, S., & Stein, L. Y. (2010) Effects of Ammonium and Nitrite on Growth and Competitive Fitness of Cultivated Methanotrophic Bacteria. *Appl Environ Microbiol* **76:** 5648-5651.

Ren, T., Roy, R., & Knowles, R. (2000) Production and consumption of nitric oxide by three methanotrophic bacteria. *Appl Environ Microbiol* **66:** 3891-3897.

Richardson, D. J., Berks, B. C., Russell, D. A., Spiro, S., & Taylor, C. J. (2001) Functional, biochemical and genetic diversity of prokaryotic nitrate reductases. *Cellular and Molecular Life Sciences* **58:** 165-178.

Saidi-Mehrabad, A., He, Z., Tamas, I., Sharp, C. E., Brady, A. L., Rochman, F. F. et al. (2013) Methanotrophic bacteria in oilsands tailings ponds of northern Alberta. *ISME Journal* **7:** 908-921.

Simon, J., & Klotz, M. G. (2013) Diversity and evolution of bioenergetic systems involved in microbial nitrogen compound transformations. *Biochimica Et Biophysica Acta-Bioenergetics* **1827:** 114-135.

Stein, L. Y., & Klotz, M. G. (2011) Nitrifying and denitrifying pathways of methanotrophic bacteria.

Biochem Soc Trans **39:** 1826-1831.

Stein, L. Y. (2011) Heterotrophic Nitrification and Nitrifier Denitrification. *Nitrification* 95-114.

Tavormina, P. L., Orphan, V. J., Kalyuzhnaya, M. G., Jetten, M. S. M., & Klotz, M. G. (2011) A novel family of functional operons encoding methane/ammonia monooxygenase-related proteins in gammaproteobacterial methanotrophs. *Environmental Microbiology Reports* **3:** 91-100.

Tavormina, P. L., Ussler,William,,III, Steele, J. A., Connon, S. A., Klotz, M. G., & Orphan, V. J. (2013) Abundance and distribution of diverse membrane-bound monooxygenase (Cu-MMO) genes within the Costa Rica oxygen minimum zone. *Environ Microbiol Rep* **5:** 414-423.

Tveit, A., Urich, T., & Svenning, M. M. (2014) Metatranscriptomic Analysis of Arctic Peat Soil Microbiota. *Appl Environ Microbiol* **80(18):** 5761.

Tveit, A., Schwacke, R., Svenning, M. M., & Urich, T. (2013) Organic carbon transformations in high-Arctic peat soils: key functions and microorganisms. *Isme J* **7:** 299-311.

Yoshinari, T. (1985) Nitrite and nitrous oxide production by *Methylosinus trichosporium*. *Can J Microbiol* **31:** 139-144.

Chapter 3: Diverse electron sources support denitrification under hypoxia in the obligate methanotroph *Methylomicrobium album* strain BG8

This chapter has been published as: Kits, K. D., Campbell, D. J., Rosana, A. R., and Stein, L. Y. (2015). Diverse electron sources support denitrification under hypoxia in the obligate methanotroph *Methylomicrobium album* strain BG8. *Front. Microbiol.* 6, 1072. doi:10.3389/fmicb.2015.01072.

3.1: Abstract

Aerobic methane-oxidizing bacteria are a diverse group of microorganisms that are ubiquitous in natural environments. Along with anaerobic methane-oxidizing bacteria and archaea, aerobic methanotrophs are critical for attenuating emission of methane to the atmosphere. Clearly, nitrogen availability in the form of ammonium and nitrite have strong effects on methanotrophic activity and their natural community structures. Previous findings show that nitrite amendment inhibits the activity of some cultivated methanotrophs; however, the physiological pathways that allow some strains to transform nitrite, expression of gene inventories, as well as the electron sources that support this activity remain largely uncharacterized. Here we show that *M. album* strain BG8 utilizes methane, methanol, formaldehyde, formate, ethane, ethanol and ammonia to support denitrification activity under hypoxia only in the presence of nitrite. We also demonstrate that transcript abundance of putative denitrification genes, *nirS* and one of two *norB* genes, increased in response to nitrite. Furthermore, we found that transcript abundance of *pxmA*, encoding the alpha subunit of a putative copper-containing monooxygenase, increased in response to both nitrite and hypoxia. Our results suggest that expression of denitrification genes, found widely within genomes of aerobic methanotrophs, allow the coupling of substrate oxidation to the reduction of nitrogen oxide terminal electron acceptors under oxygen limitation. The present study expands current knowledge of the metabolic flexibility of methanotrophs by revealing that a diverse array of electron donors support nitrite reduction to nitrous oxide under hypoxia.

3.2: Introduction

Aerobic methane oxidizing bacteria (MOB) form an important bridge between the global

carbon and nitrogen cycles, a relationship impacted by the global use of nitrogenous fertilizers (Bodelier, Steenbergh 2014). Ammonia (NH_3) and nitrate (NO_3^-) can stimulate the activity of methanotrophs by acting as a nitrogen source for growth and biomass production (Bodelier et al., 2000; Bodelier, Laanbroek 2004). Further, some methanotrophs such as *Methylomonas denitrificans* utilize NO_3^- as an oxidant for respiration under hypoxia (Kits et al., 2015). Evidently, denitrification in aerobic methanotrophs functions to conserve energy during oxygen (O_2) limitation (Kits et al., 2015). Alternatively, NH_3 and nitrite (NO_2^-) can act as significant inhibitors of methanotrophic bacteria (King, Schnell 1994). NH_3 is a competitive inhibitor of the methane monooxygenase enzyme and NO_2^-, produced by methanotrophs that can oxidize NH_3 to NO_2^-, is a toxin with bacteriostatic properties that is known to inhibit the methanotroph formate dehydrogenase enzyme that is essential for the oxidation of formate to carbon dioxide (Cammack et al., 1999; Dunfield, Knowles 1995; Nyerges et al., 2010).

In spite of the recent discovery that aerobic methanotrophs can denitrify, the energy sources, genetic modules and environmental factors that govern denitrification in MOB are still poorly understood. *M. denitrificans* FJG1 respires NO_3^- using methane as an electron donor to conserve energy. However, it is not known whether C_1 energy sources other than CH_4 (methanol, formaldehyde, formate) can directly support denitrification. Another possibility, which has not yet been investigated, is that C_2 compounds (such as ethane and ethanol) and inorganic reduced nitrogen sources (NH_3) support methanotrophic denitrification. Previous work shows that several obligate methanotrophs, including *Methylomicrobium album* strain BG8, oxidize ethane (C_2H_6) and ethanol (C_2H_6O) using particulate methane monooxygenase (pMMO) and methanol dehydrogenase (MDH), respectively, even though neither substrate supports growth (Dalton 1980; Mountfort 1990; Whittenbury et al., 1970). NH_3 may be able to support methanotrophic

denitrification because many aerobic methanotrophs are capable of oxidizing NH_3 to NO_2^-: a process facilitated by the presence of a copper-containing monooxygenase (CuMMO) enzyme and, in some methanotrophs, a hydroxylamine dehydrogenase homolog (Poret-Peterson et al., 2008). The ability to utilize alternative energy sources to support denitrification would augment the metabolic flexibility of methanotrophs and enable them to sustain respiration in the absence of CH_4 and/or O_2.

Methylomicrobium album strain BG8 is an aerobic methanotroph that belongs to the phylum Gammaproteobacteria; the genome lacks a soluble methane monooxygenase but does contain one particulate methane monooxygenase operon (*pmoCAB* – METAL_RS17430, 17425, 17420) and one operon encoding a putative copper monooxygenase (*pxmABC* – METAL_RS06980, 06975, 06970*)* with no known function. The genome also contains gene modules for import and assimilation of NH_4^+ (*amtB* – METAL_RS11045/*gdhB* – METAL_RS11695/*glnA* – METAL_RS11070/*ald* – METAL_RS11565), assimilation of NO_3^- (*nasA* – METAL_RS06040/*nirB* – METAL_RS15330, *nirD* – METAL_RS15325), oxidation of NH_2OH to NO_2^- (*haoA* – METAL_RS13275), as well as putative denitrification genes – cytochrome cd_1 nitrite reductase (*nirS* – METAL_RS10995) and two copies of cytochrome *c*-dependent nitric oxide reductase (*norB1* – METAL_RS03925, *norC1* – METAL_RS03930/*norB2* – METAL_RS13345). The recent release of several genome sequences of aerobic methanotrophs, including *M. album* strain BG8, points to the frequent presence of putative nitrite and nitric oxide reductases, while only three cultivated methanotrophs possess a respiratory nitrate reductase (Khadem et al., 2012b; Kits et al., 2013; Stein, Klotz 2011; Svenning et al., 2011; Stein et al., 2011; Vuilleumier et al., 2012). It is also unclear whether methanotrophs that lack a respiratory nitrate reductase but possess dissimilatory

nitrite and nitric oxide reductases are still capable of denitrification from NO_2^-. Moreover, due to the significant divergence of the methanotroph *nirS* from known sequences, it is not known whether *nirS* is the operational nitrite reductase in the methanotrophs that lack a *nirK* (Wei et al., 2015). While the genome of the nitrate respiring *M. denitrificans* FJG1 encodes both *nirS* and *nirK* nitrite reductases, transcript levels of only *nirK* increased in response to denitrifying conditions(Kits et al., 2015).

The goal of the present study was to test whether a variety of C_1, C_2 and inorganic energy sources can directly support denitrification, characterize the environmental factors that regulate NO_2^--dependent N_2O production in *M. album* strain BG8 and to assess the expression of its putative denitrification inventory.

3.3: Materials and Methods

Cultivation. *Methylomicrobium album* strain BG8 was cultivated in 100 mL of nitrate mineral salts medium containing 11 mM KNO_3 (NMS) or 10 mM KNO_3 plus 1 mM $NaNO_2$ (NMS + NO_2^-) in 300 mL glass Wheaton bottles topped with butyl rubber septa (Whittenbury et al., 1970). The NMS media was buffered to pH 6.8 using a phosphate buffer (0.26 g/L KH_2PO_4, 0.33 g/L Na_2HPO_4). The final concentration of copper ($CuSO_4$) was 5 µM. Using a 60 mL syringe (BD) and a 0.22µm filter/needle assembly, CH_4 (99.998%) was added into the sealed bottles as a sole carbon source. The initial gas-mixing ratio in the headspace was adjusted using O_2 gas (99.998%, Praxair) to 1.6:1, CH_4 to O_2 (or ca. 28% CH_4, 21% O_2); The initial pressure in the gas tight bottles was adjusted to ca. 1.3 atm to prevent a vacuum from forming during growth as gas samples and liquid culture samples were withdrawn every 12 h for analysis. Cultures were incubated at 30°C and shaken at 200 rpm. To track growth, the cultures were periodically sampled using a needle fitted syringe (0.5 mL) and cell density was determined by direct count

with phase contrast microscopy using a Petroff-Hausser counting chamber. Six biological replicates were grown on separate days and data was collected on each replicate (n=6). Culture purity was assessed by 16s rRNA gene sequencing, phase contrast microscopy, and plating on nutrient agar and TSA with absence of growth indicating no contamination. We assessed purity of the cultures prior to beginning all of the experiments and then assessed it again for each replicate at the conclusion of each experiment.

Gas analysis. Concentrations of O_2, CH_4, and N_2O were determined by sampling the headspace of each culture using gas chromatography (GC-TCD, Shimadzu GC8A; outfitted with a molecular sieve 5A and a Hayesep Q column, Alltech). The headspace of each batch culture was sampled with a 250 µL gastight syringe (SGE Analytical Science; 100 µL/injection) at 0 (immediately post inoculation), 6, 12, 16, 20, 24, 30, 36, 42, 48, 60, 72, 96, and 120 h; A total of 200 µL was sampled from each replicate at every time point. We determined the bottles were gastight by leaving a replicate set of bottles uninoculated throughout the experiment and measuring headspace gas concentrations; leakage was <1% over 120 h. Standard curves using pure gases O_2, CH_4, and N_2O (Praxair) were generated and used to calculate the headspace concentrations in the batch cultures.

Instantaneous micro-sensor assays. *M. album* strain BG8 was grown in NMS + NO_2^- medium as described above. At 96 h of growth, when denitrification activity was highly evident, 4×10^{10} cells were harvested using a filtration manifold onto 0.2 µm filters (Supor 200, 47mm, Pall Corp). The biomass was washed three times with sterile, nitrogen-free mineral salts medium – identical to the mineral salts medium used for cultivation but devoid of NH_4Cl, KNO_3, or $NaNO_2$. For data presented in Figs. 12 & 14, the washed biomass was resuspended in the same nitrogen-free medium and transferred to a gastight 10mL micro-respiration chamber equipped

with an OX-MR O_2 micro-sensor (Unisense) and an N_2O-500 N_2O micro-sensor (Unisense). For data presented in Fig. 13, biomass was resuspended in mineral salts medium amended with 100 μM $NaNO_2$. Data was logged using SensorTrace Basic software. CH_4 gas, 0.001% CH_3OH (HPLC grade methanol, Fisher Scientific), 0.01% CH_2O (Methanol free 16% formaldehyde, Life technologies), 10 mM HCO_2H, C_2H_6 gas (99.999%), 0.01% C_2H_6O (Methanol free 95% ethyl alcohol, Commercial Alcohols), 200 mM NH_4Cl and/or 1 M NO_2^- was injected directly into the chamber through the needle injection port with a gas-tight syringe (SGE Analytical Science). For panels b) - e) in Fig. 13, the dissolved O_2 was decreased to <100 μmol/L (panel b) and <25 μmol/L (panels c-e), respectively, with additions of CH_4 (a), CH_3OH (b), CH_2O (c), HCO_2H (d), C_2H_6 (e), C_2H_6O (f) before data logging was enabled to limit the traces to <100 min and to reduce the number of sampling points. NO_2^- concentration was determined using a colorimetric method (Bollmann et al., 2011). Experiments were performed 3-4 times to demonstrate reproducibility of results and a single representative experiment was selected for presentation.

RNA extraction. Total RNA was extracted from ca. 10^9 *M. album* strain BG8 cells grown in NMS or NMS + NO_2^- medium at 24, 48, and 72 h using the MasterPure RNA purification kit (Epicentre). Briefly, cells were harvested by filtration through a 0.22 μm filter and inactivated with phenol-ethanol stop solution (5% phenol, 95% EtOH). Total nucleic acid was purified according to manufacturers instructions with the following modifications: 6 U proteinase K (Qiagen) were added to the cell lysis step and the total precipitated nucleic acid was treated with 30 units of DNase I (Ambion). The total RNA was then column-purified using RNA clean & concentrator (Zymo Research). RNA quality and quantity was assessed using BioAnalyzer (Agilent Technologies) and Qubit (Life Technologies). Residual genomic DNA contamination was assessed by quantitative PCR (qPCR) targeting *norB1* or *nirS* genes (primers

listed in Table 1). PCR conditions are described below. The total RNA samples were deemed free of genomic DNA if no amplification was detected after 40 cycles of qPCR. High quality RNA (RIN number $\geq$ 9, no gDNA detected) was converted to first strand cDNA using Superscript III reverse transcriptase (Life Technologies), according to manufacturer's instructions.

Quantitiative PCR. Gene copy standards were created using the genomic DNA of *M. album* strain BG8 using universal and gene-specific primers (Table 1). A ten-fold dilution series (10^0 to 10^8 copies/20 µl reaction) of purified amplicons was prepared and used to establish an optimized qPCR condition. Each 20 µl reaction contained 10 µl of 2X qPCR SYBR based master mix (MBSU, University of Alberta), 0.2 µM of forward and reverse primer, 1 µl diluted cDNA, and nuclease-free water. Amplification was performed on a StepOne Plus qPCR system (Applied Biosystems) with an initial activation at 95^{o}C for 3 minutes and fluorescence emission data collected from 40 cycles of amplification (95^{o}C for 15 sec, 60^{o}C for 15 sec, and 72^{o}C for 15 sec). Target specificity was assessed by melt curve analysis, which ensured that a single peak was obtained. Gene copy number was estimated from cDNA diluted from 10^{-3} to 10^{-5} copies for 16S rRNA and *pmoA* transcript analyses and dilutions from 10^{-1} to 10^{-3} copies for *nirS, norB1, norB2* and *pxmA* transcript analyses. The transcript abundance of each functional gene was normalized to that of 16s rRNA to yield a copy number of transcripts per 1 billion copies of 16s rRNA. Then, to calculate the N-fold change, we divided the transcript abundance (per 1 billion copies of 16s rRNA) in the NMS + NO_2^- cultures by transcript abundance (per 1 billion copies of 16s rRNA) in the NMS cultures. Samples were run in triplicate with three dilutions each on at least 3 biological replicates from cells grown and processed on separate dates. Quantitative PCR efficiencies ranged from 95-102% with r^2 values of at least 0.99 for all assays (Table 1).

Statistics. A Student's t-Test (two tailed) was used to calculate the P-level between the control (NMS alone) and experimental (NMS + NO_2^-) replicates as indicated for each experiment. Equal variance between the control and experimental groups was determined using a two sample F-Test for variance. The doubling time, O_2 & CH_4 consumption, cell density, and total headspace O_2 & CH_4 consumed (Table S1) all had equal variance between the control and experimental ($F<F_{crit}$); thus a homoscedastic T-Test was calculated for the aforementioned comparisons. For qPCR, comparisons between NMS + NO_2^- and NMS alone at 48 h for *pmoA*, *pxmA*, *nirS*, and *norB1*, as well as for *pxmA* and *nirS* at 72 h showed unequal variance ($F>F_{crit}$); thus a heteroscedastic T-Test was used to calculate the P-level for these comparisons. The variance between NMS + NO_2^- and NMS alone for all other genes at all other time points was equal ($F<F_{crit}$).

3.4: Results

Growth phenotype of *Methylomicrobium album* strain BG8 in the absence or presence of NO_2^-. *M. album* strain BG8 was cultivated in NMS or NMS supplemented with NO_2^- over 120 h to determine the effect of NO_2^- on growth, O_2 and CH_4 consumption, and N_2O production (Fig. 11). The total amount of nitrogen was kept constant to eliminate a difference in N-availability and salt concentration between treatments. All of the cultures were initiated at an oxygen (O_2) tension of 19.5 ± 0.7% (Fig. 11b). As observed previously (Nyerges et al., 2010), NO_2^- amendment (1 mM) did not have an inhibitory effect on growth or substrate consumption of *M. album* strain BG8 (Fig. 11a-c). The limiting substrate in all treatments was O_2, as demonstrated by supplementing cultures with additional O_2 (20 mL) after 48 h of growth and observing a significant increase in optical density in comparison to cultures not receiving additional O_2 (Fig. 17). N_2O production occurred only in the NMS plus NO_2^- cultures (Fig. 11d).

N_2O production was first apparent in the headspace of NO_2^- amended cultures at 72 h of growth when O_2 reached ca. 1.8% of the headspace and continued up to the termination of the experiment (120 h) at a rate of 9.3×10^{-18} mol N_2O per cell per hour (Fig. 11d). After 120 h of growth, the N_2O yield percentage from the added NO_2^- (100 μmol) was 5.1±0.2% (5.1±0.2 μmol) in the NMS+NO_2^- cultures.

O_2 consumption and N_2O production by resting cells of *M. album* strain BG8 with single or double carbon substrates or ammonium under atmospheric and hypoxic O_2 tensions. To determine which conditions govern N_2O production in *M. album* strain BG8, we measured instantaneous O_2 consumption and N_2O production by *M. album* strain BG8 with CH_4 as the sole carbon and energy source in a closed 10-mL micro-respiratory (MR) chamber outfitted with O_2 and N_2O-detecting microsensors. Introduction of CH_4 (300 μM) into the chamber led to immediate O_2 consumption; O_2 declined to below the detection limit of the sensor (<50 nM O_2) after ca. 3 min (Fig. 12a). Addition of NO_2^- to the chamber led to production of N_2O shortly after O_2 declined below the detection limit at a rate of 7.9×10^{-18} mol $cell^{-1}$ h^{-1} (Fig. 12b). In the absence of NO_2^-, we observed no measureable N_2O production (Fig. 12a). Though the O_2 concentration is < 50nM O_2 when N_2O production is evident, it is important to note that *M. album* strain BG8 still requires O_2 for methane oxidation and cannot grow on CH_4 anaerobically.

Using the same setup described above, we supplemented resting cells in the MR chamber with CH_3OH, CH_2O, HCO_2H, C_2H_6, or C_2H_6O to experimentally address whether carbon-based reductant sources other than CH_4 support denitrification in *M. album* strain BG8. Also, to substantiate that the one- and two-carbon sources we tested can all serve as direct electron donors for denitrification by *M. album* strain BG8 under hypoxia, we provided resting cells only

enough reductant to consume the dissolved O_2 (ca. 234 μmol/L) present in the MR chamber sparing no reductant to support denitrification (Fig. 13). We then measured instantaneous N_2O production through serial addition of small quantities of CH_4, CH_3OH, CH_2O, HCO_2H, C_2H_6, or C_2H_6O to the MR chamber, which contained medium supplemented with $NaNO_2$ (100 μM) (Fig. 13). For all six substrates, N_2O production was stoichiometric with the amount of added substrate (Fig. 13).

Many methanotrophs, including *M. album* BG8, can oxidize NH_3 to NO_2^- due to homologous inventory to ammonia-oxidizing bacteria (Bedard, Knowles 1989; Campbell et al., 2011; Holmes et al., 1995; King, Schnell 1994; Poret-Peterson et al., 2008; Stein, Klotz 2011; Yoshinari 1985). We aimed to test whether reductant and NO_2^- from NH_3 oxidation could also drive denitrification by *M. album* strain BG8. Resting cells in the MR chamber consumed the dissolved O_2 promptly after NH_4Cl (200 μM) was injected into the chamber (Fig. 14). After ca. 70 min, the biomass depleted the dissolved O_2 to <50 nM and NO_2^- concentration reached 163 ± 5 μM. The rate of N_2O production following O_2 depletion was 1.2×10^{-18} mol cell^{-1} h^{-1}.

Expression of predicted denitrification genes in *M. album* strain BG8 under denitrifying conditions. The genome of *M. album* strain BG8 encodes several genes predicted to be involved in denitrification. The first step in respiratory denitrification is the one-electron reduction of NO_3^- to NO_2^-; a reaction performed by one of two membrane-associated dissimilatory nitrate reductase enzymes, neither of which is encoded in the *M. album* strain BG8 genome (Kits et al., 2013). The second step in denitrification, the one-electron reduction of NO_2^- to NO is carried out by one of two non-homologous nitrite reductases, either a copper containing (*nirK*) or a cytochrome cd_1 containing (*nirS*) nitrite reductase, of which the latter was annotated in the genome (Kits et al., 2013). The genome of *M. album* strain BG8 also contains two copies

of a putative cytochrome *c*-dependent nitric oxide reductase (*norB1* and *norB2,* respectively). We also investigated expression of the *pxmA* gene of the *pxmABC* operon that encodes a CuMMO with evolutionarily relatedness to particulate methane monooxygenase (Tavormina et al., 2011). We chose to examine expression of *pxmA* in *M. album* strain BG8 to determine whether this gene responded similarly to that of *M. denitrificans* FJG1; expression of the *pxmABC* operon in *M. denitrificans* FJG1 significantly increased in response to denitrifying conditions (Kits et al., 2015).

To assess the effect of NO_2^- amendment on gene expression, we used cultures grown in NMS alone as the control. The O_2 concentration in the headspace of NMS and NMS+NO_2^- cultures after 24 h growth was ca. 17.2% and 16.9%, respectively (Fig. 11b).
The transcript levels of *pmoA, pxmA, nirS,* and *norB1* were significantly higher at the 24 and 48 h time points in the NO_2^- amended cultures when compared to the NMS alone (Fig. 15). At the 72 h time point, levels of *pmoA* and *nirS* transcript levels remained significantly elevated in the NMS + NO_2^- relative to the NMS only cultures, whereas expression of *norB1* was no longer significantly elevated (Fig. 15). Most interestingly, the transcript abundance of *pxmA* at 72 h was 19.8-fold higher in NMS + NO_2^- relative to NMS only cultures (Fig. 15). The second copy of *norB* (*norB2*) was unresponsive (below 2 fold) to NO_2^- amendment at all time points sampled.

3.5: Discussion

***Methylomicrobium album* strain BG8 produces N_2O only as a function of hypoxia and NO_2^-.** Batch cultivation of *M. album* BG8 clearly revealed that both NO_2^- and low O_2 were required for denitrification, as measured by N_2O production. Although batch cultures of *M. album* strain BG8 have been shown to produce N_2O previously in end-point assays (Nyerges et al., 2010), the mechanism and required conditions for denitrification by this strain were not

determined until now. N_2O production by *Methylomonas denitrificans* FJG1 was also shown to be dependent on hypoxia (Kits et al., 2015); however, this strain was able to respire NO_3^- in addition to NO_2^- likely due to the presence of a *narGHJI* dissimilatory nitrate reductase that is absent in the genome of *M. album* strain BG8. The genome of *M. album* strain BG8 encodes putative dissimilatory nitrite (*nirS*) and nitric oxide (*norB*) reductases (Kits et al., 2013) like *M. denitrificans* FJG1; hence, it is likely that N_2O by *M. album* strain BG8 is from the enzymatic reduction of NO_2^- to N_2O via the intermediate NO.

The correlation between N_2O production and low O_2 tension is similar to two other microbial processes, aerobic denitrification in heterotrophic bacteria such as *Paracoccus denitrificans* and nitrifier denitrification in ammonia-oxidizing bacteria (Kozlowski et al., 2014; Richardson et al., 2001). Aerobic denitrification in chemoorganoheterotrophs and nitrifier-denitrification in ammonia-oxidizing bacteria is a tactic used to maximize respiration during O_2 limitation or to expend surplus reductant (Richardson et al., 2001; Stein 2011). Utilization of NO_2^- in combination with or instead of O_2 in the respiratory chain of *M. album* strain BG8 would reduce the overall cellular O_2 demand, thus conserving O_2 for additional CH_4 oxidation. Thus, it is possible that *M. album* strain BG8 uses NO_2^- as a terminal electron acceptor under O_2 limitation to maximize total respiration. The N_2O yield percentage from NO_2^- by *M. album* strain BG8 (5.1±0.2%) is similar to that of *Nitrosomonas europaea* ATCC 19718 (ca. 4.8%) and one order of magnitude higher than that of *Nitrosospira multiformis* ATCC 25196 (0.27±0.05%) (Stieglmeier et al., 2014; Kozlowski et al., 2014).

Denitrification by *M. album* strain BG8 is enzymatically supported by diverse reductant sources. Resting cells of *M. album* strain BG8 reduced NO_2^- to N_2O at the expense of any of four tested C_1 substrates (CH_4, CH_3OH, CH_2O, HCO_2H), the two C_2 substrates (C_2H_6,

C_2H_6O), and NH_4Cl. These data show that intermediates of the methanotrophic pathway and co-substrates of pMMO, methanol dehydrogenase, and likely hydroxylamine dehydrogenase support respiratory denitrification. These results agree with previous work on the methanotroph *Methylocystis* sp. strain SC2, which couples CH_3OH oxidation to denitrification under anoxia (Dam et al., 2013). Remarkably, both C_2 compounds we tested - C_2H_6 and C_2H_6O - supported denitrification. The ability of C_2 compounds to support denitrification in methanotrophs may have environmental significance as natural gas consists of ~1.8-5.1% (vol%) C_2H_6 (Demirbas 2010). Further, C_2H_6O is a significant product of fermentation by primary fermenters during anoxic decomposition of organic compounds (Reith et al., 2002). The results also demonstrate that electrons derived from the oxidation of NH_3 to NO_2^- were effectively utilized by nitrite and nitric oxide reductases in *M. album* strain BG8, which represents yet another pathway for methanotrophic N_2O production that is not directly dependent on single-carbon metabolism, provided that the methane monooxygenase can access endogenous reductant (Stein, Klotz 2011; King, Schnell 1994; Dalton 1977).

Instantaneous O_2 consumption and N_2O production measurements (Figs. 12, 13 & 14) provide strong support that catabolism of C_1 - C_2 substrates and ammonia is directly coupled to NO_2^- reduction under hypoxia in *M. album* strain BG8. Some aerobic methanotrophs ferment CH_4 and excrete organic compounds such as citrate, acetate, succinate, and lactate (Kalyuzhnaya et al., 2013). Some studies also suggest that methanotrophs only support denitrification within CH_4-fed consortia by supplying these excreted organics to denitrifying bacteria, since methanotrophs were thought incapable of denitrification by themselves (Liu et al., 2014; Knowles 2005; Costa et al., 2000). Although *M. album* strain BG8 may excrete organic compounds under hypoxia when provided with CH_4, the ability of CH_3OH, CH_2O, HCO_2H,

C_2H_6, C_2H_6O or NH_3 oxidation to support denitrification unequivocally demonstrates the linkage between methanotroph-specific enzymology and denitrifying activity within a single organism.

Transcription of predicted denitrification genes, *nirS* and *norB1*, increased in response to NO_2^- but not hypoxia. The expression of a *nirS* homolog in an aerobic methanotroph has been investigated so far only in the NO_3^- respiring *M. denitrificans* FJG1 (Kits et al., 2015). Interestingly, the genome of *M. denitrificans* FJG1 encodes both the copper-containing (*nirK*) and cytochrome cd_1 containing (*nirS*) nitrite reductases and only the steady state mRNA levels of *nirK* increased in this strain in response to simultaneous O_2 limitation and NO_3^- availability (Kits et al., 2015). In the case of *M. album* strain BG8, which only possesses a *nirS* homologue, we showed that the abundance of this *nirS* transcript responded positively to NO_2^- treatment but not to O_2 limitation. This suggests that NO_2^- availability alone elicits the expression of *nirS*, even though hypoxia was required for NO_2^- reduction to occur.

The cytochrome *c* dependent nitric oxide reductase (*norB*) is widely found in the genomes of aerobic methanotrophs (Stein, Klotz 2011). This may in part be due to the need to detoxify NO that is produced during aerobic ammonia oxidation by reducing it to N_2O (Sutka et al., 2003). The expression of *norB* in *Methylococcus capsulatus* strain Bath increased 4.8 fold after treatment with 0.5 mM sodium nitroprusside, a NO releasing compound (Campbell et al., 2011). It is possible that the NorB protein is involved in detoxification of NO during NH_3 oxidation in *M. capsulatus* strain Bath, since the genome lacks a dissimilatory nitrite reductase. More recently, it was demonstrated in *M. fumariolicum* strain SolV that transcription of *norB* was upregulated during O_2 limitation during chemostat growth (Khadem et al., 2012a); however, it is unknown whether *M. fumariolicum* strain SolV can consume NO_2^- or NO. The transcription of *norB* in *M. denitrificans* FJG1 increased 2.8-fold in response to NO_3^- and hypoxia (Kits et al.,

2015). While the genome of *M. album* strain BG8 encodes two copies of the *norB* gene, only one copy (*norB1*) is followed by *norC* - the essential cytochrome *c*-containing subunit (Mesa et al., 2002). Although some organisms like *Cupriavidus necator* possess two independent functional nitric oxide reductases (Cramm et al., 1997), the present work illustrates that expression of only *norB1* in *M. album* strain BG8 is responsive to NO_2^- treatment. Although the function of NorB may differ between *M. album* strain BG8 and *M. capsulatus* strain Bath, both bacteria show a similar transcriptional response of *norB* genes to NO_2^- (Campbell et al., 2011).

Transcript abundance of *pxmA* significantly increased in response to both NO_2^- and hypoxia. Genomes of some aerobic methanotrophs belonging to the phylum *Gammaproteobacteria* have been shown to encode a sequence divergent CuMMO protein complex, pXMO (Tavormina et al., 2011). The function and substrate of the putative pXMO protein encoded by the *pxm* operon remains unknown. Previous studies on the *pxm* operon have shown that it is expressed at low levels during growth in *Methylomonas* sp. strain LW13 as well as in freshwater peat bog and creek sediment (Tavormina et al., 2011). Metagenomic sequencing of the SIP-labeled active community in an oilsands tailings pond revealed that *pxmA* sequences were present in the active methanotroph community (Saidi-Mehrabad et al., 2013). Analysis of the transcriptome of *M. denitrificans* FJG1 revealed that steady state mRNA levels of the *pxmABC* operon increased ~10-fold in response to denitrifying conditions (Kits et al., 2015).

We now demonstrate that expression of *pxmA* in *M. album* strain BG8 is significantly increased in response to both NO_2^- and hypoxia. We did not observe any increase in the expression of *pxmA* in O_2 limited NMS-only cultures where denitrification was not occurring, suggesting that hypoxia alone is not sufficient to illicit an increase in the steady state mRNA levels. This study adds further support to the observation that expression of *pxmA* is responsive

to denitrifying conditions. However, it must be noted that at 72 h in the NO_2^- amended media, absolute transcript abundance of *pxmA* (1×10^3 copies *pxmA*/1×10^9 copies 16s rRNA) was three orders of magnitude lower than absolute transcript abundance of *pmoA* (1×10^6 copies *pxmA*/1×10^9 copies 16s rRNA).

Conclusions. The present study demonstrates that an aerobic methanotroph - *M. album* strain BG8 - couples the oxidation of C_1 (CH_4, CH_3OH, CH_2O, HCO_2H), C_2 (C_2H_6, C_2H_6O), and inorganic (NH_3) substrates to NO_2^- reduction under O_2 limitation resulting in release of the potent greenhouse gas N_2O. The ability to couple C_1, C_2, and inorganic energy sources to O_2 respiration and denitrification gives *M. album* strain BG8 considerable metabolic flexibility. We propose a model for methane driven denitrification in *M. album* strain BG8 (Fig. 16). This discovery has implications for the environmental role of methanotrophic bacteria in the global nitrogen cycle in both N_2O emissions and N-loss. Comparing the genome and physiology of the NO_2^- respiring *M. album* strain BG8 to NO_3^- respiring *M. denitrificans* FJG1 suggests that the inability of *M. album* strain BG8 to reduce NO_3^- to N_2O is likely due to the absence of a dissimilatory nitrate reductase in the genome, but that expression of predicted denitrification genes, *nirS* and *norB1,* enable this aerobic methanotroph to respire NO_2^-.

Acknowledgements:

This work was supported by a grant to L.Y.S. from the Natural Sciences and Engineering Research Council of Canada (RGPIN-2014-03745) and fellowship support to K.D.K. from Alberta Innovates Technology Futures.

3.6: Tables and Figures

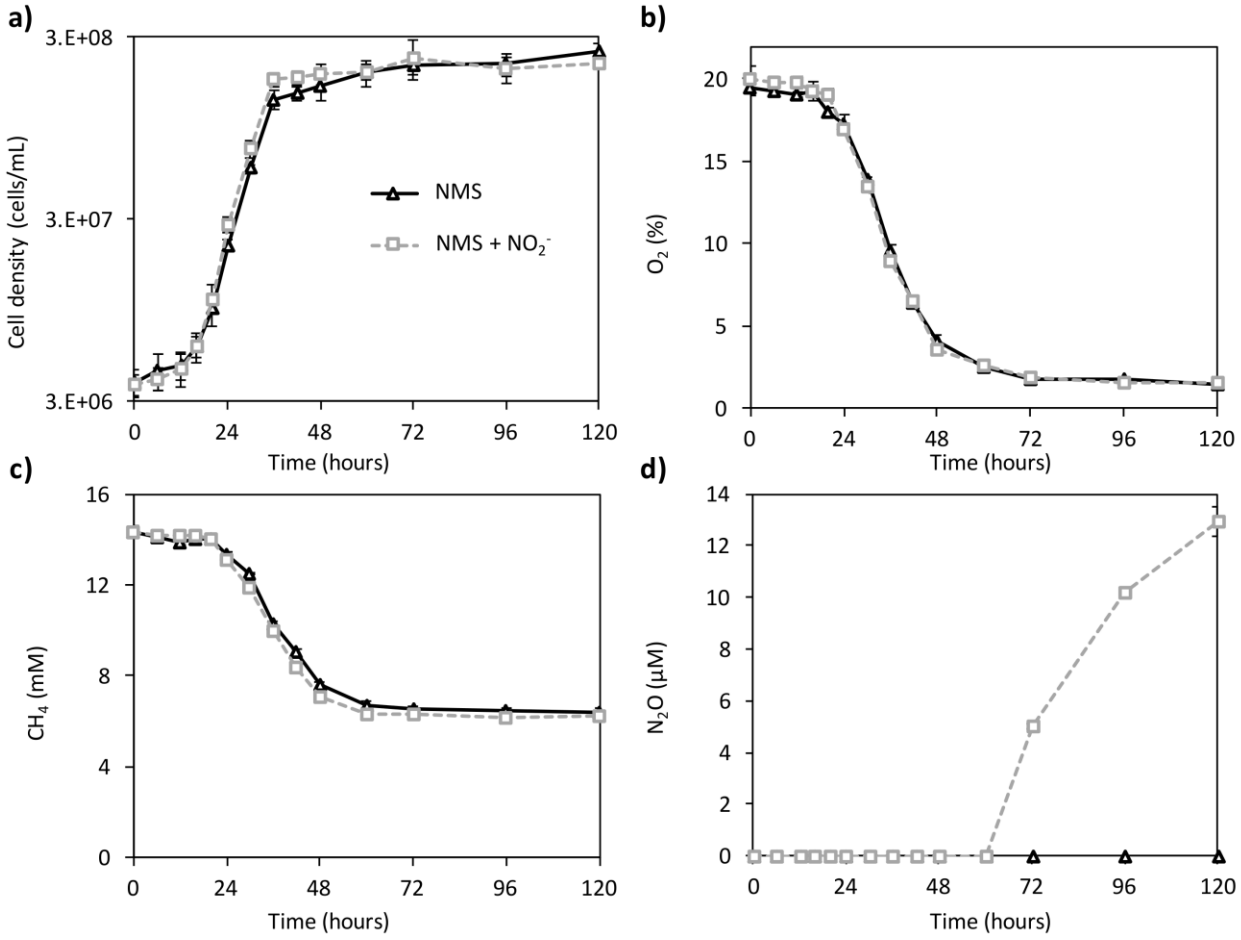

Figure 11: **Growth, CH_4 & O_2 consumption, and N_2O production by *Methylomicrobium album* strain BG8 cultivated on NMS and NMS plus 1 mM $NaNO_2$.**

Methylomicrobium album strain BG8 was cultivated for 5 days in 100 mL of NMS (black triangles) or NMS + 1 mM NO_2^- (gray dashed squares) media in 300 mL closed glass Wheaton bottles sealed with a butyl rubber septum caps. The initial headspace gas-mixing ratio of CH_4 to O_2 was 1.6:1. Cell density (a) was measured using direct count with a Petroff-Hausser counting chamber and headspace gas concentrations of O_2 (b), CH_4 (c) and N_2O (d) were measured using GC-TCD. All data points represent the mean ± standard deviation for 6 biological replicates (n = 6).

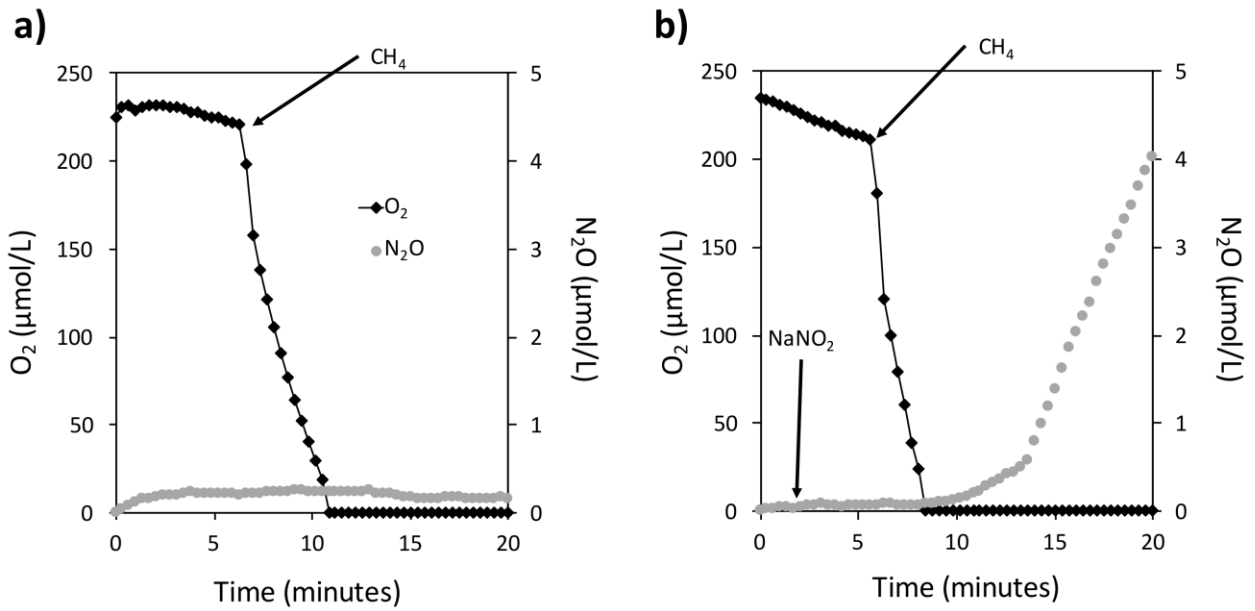

Figure 12: **The instantaneous coupling of CH_4 oxidation to NO_2^- reduction in *Methylomicrobium album* BG8 under hypoxia.**

Experiments were performed in a closed 10 mL micro-respiratory chamber outfitted with an O_2 and N_2O microsensor and logged with Sensor Trace Basic software. O_2 (black triangles) and N_2O (grey circles) were measured using microsensors. Cells of *M. album* strain BG8 were harvested as described in the materials and methods and resuspended in nitrogen free mineral salts medium. Arrows mark the addition of CH_4 (~300 µM) and $NaNO_2$ (1 mM) to the micro-respiratory chamber in all panels. There is no measureable denitrification activity in the absence of NO_2^- (panel **a**); denitrification activity is dependent on CH_4 and NO_2^- (panel **b**).

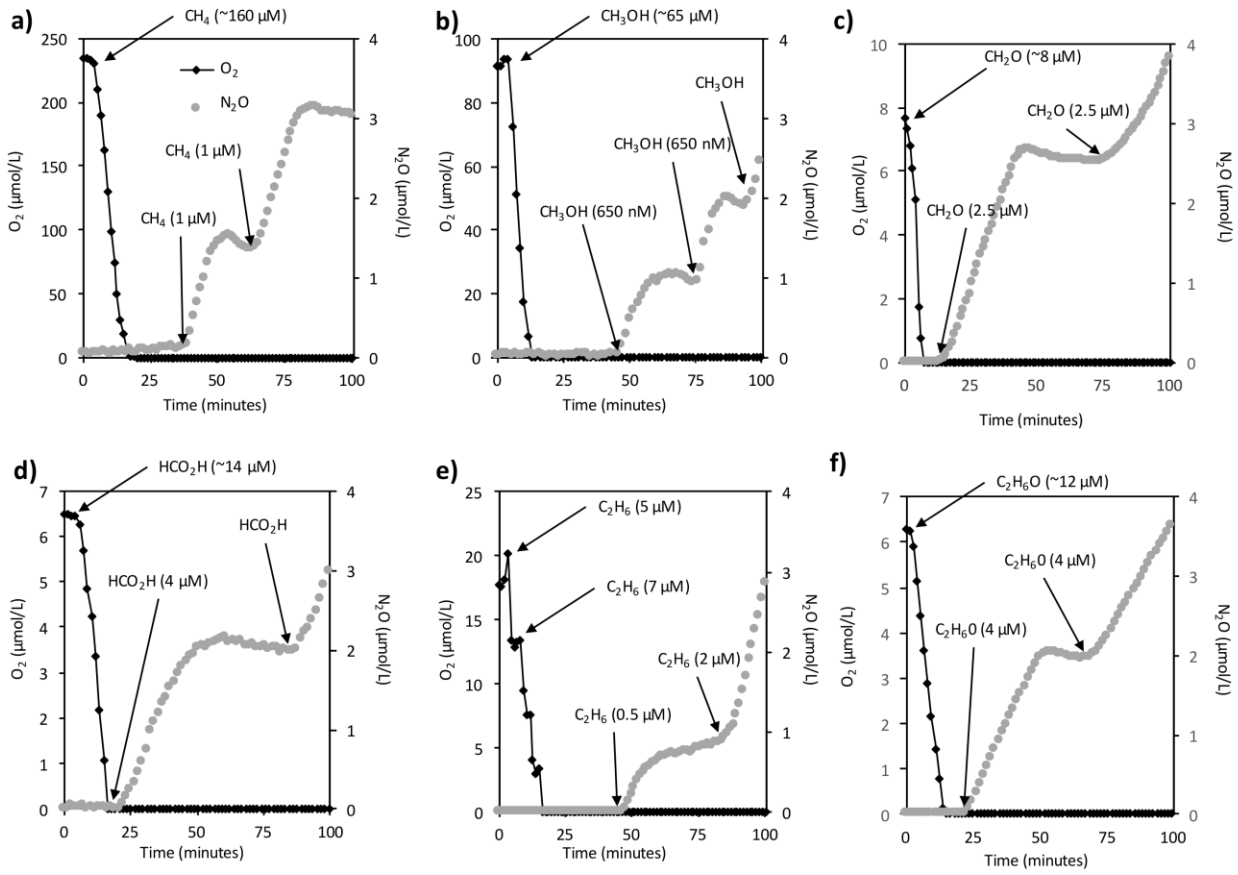

Figure 13: **NO_2^- reduction to N_2O by *M. album* strain BG8 is dependent on an energy source at <50 nM O_2.**

Experiments were performed in a closed 10 mL micro-respiratory chamber outfitted with an O_2 and N_2O microsensor and logged with Sensor Trace Basic software. O_2 (black triangles) and N_2O (grey circles). Cells of *M. album* strain BG8 were harvested as described in the materials and methods and resuspended in mineral salts medium containing 100 µM NO_2^-. Arrows mark the addition of either CH_4 (panel **a**), CH_3OH (**b**), CH_2O (**c**), HCO_2H (**d**), C_2H_6 (**e**), C_2H_6O (**f**), in all panels. The right y-axis is identical in all panels. However, it should be noted that the left y-axis differs in all panels.

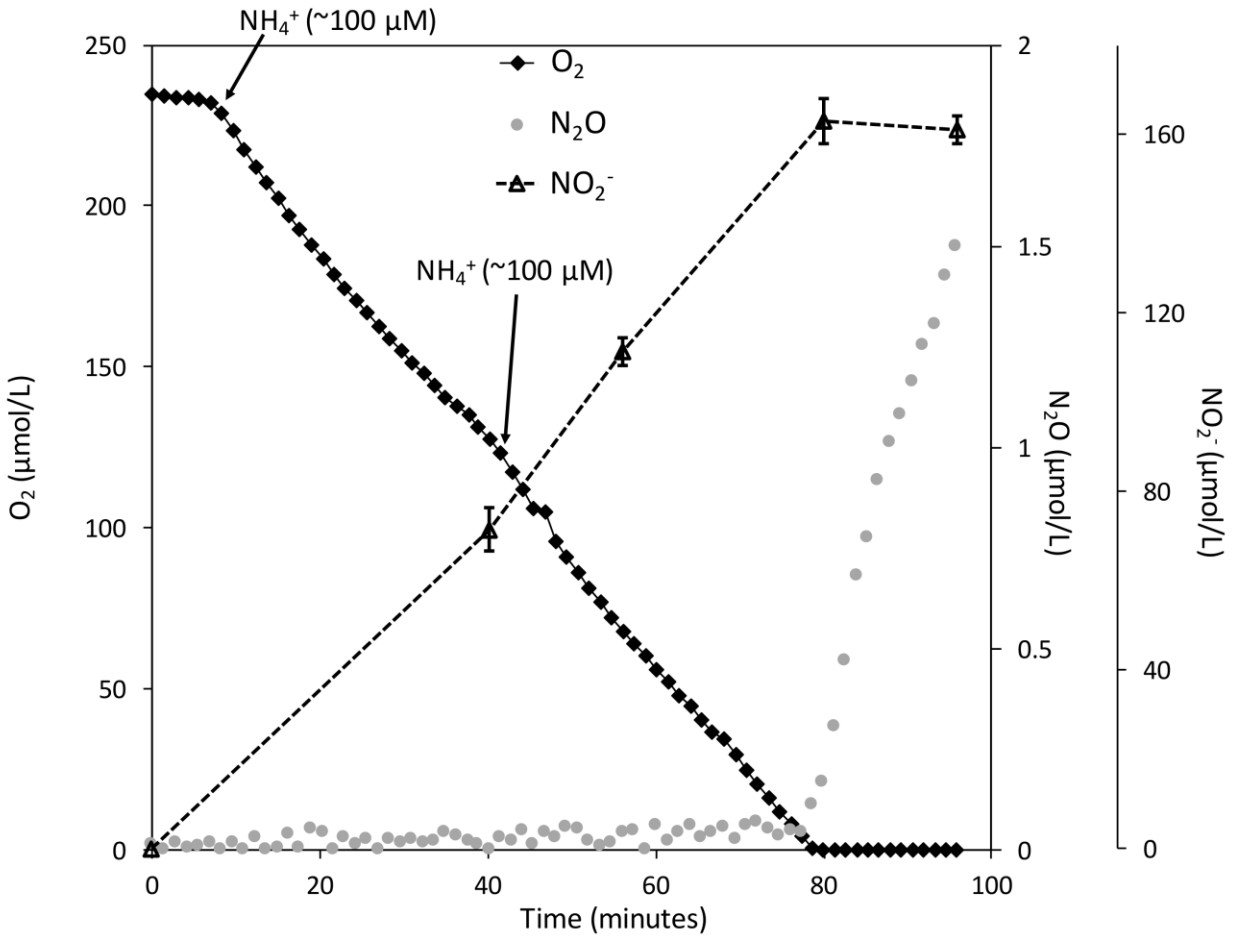

Figure 14: **The coupling of NH_3 oxidation to NO_2^- reduction in *Methylomicrobium album* strain BG8 under hypoxia.**

Experiments were performed in a closed 10 mL micro-respiratory chamber outfitted with an O_2 and N_2O microsensors and logged with Sensor Trace Basic software. O_2 (black diamonds), N_2O (grey circles), NO_2^- (black dashed triangles). Cells of *M. album* strain BG8 were grown and harvested as described in the materials and methods and resuspended in nitrogen free mineral salts medium. Arrows mark the addition of NH_4^+ (100 µM) to the closed micro-respiratory chamber. Traces (O_2 + N_2O) are single representatives of reproducible results from cultures grown on different days. NO_2^- was measured using a colorimetric method as described in the materials and methods and data points represent the mean ± standard deviation for 3 technical replicates.

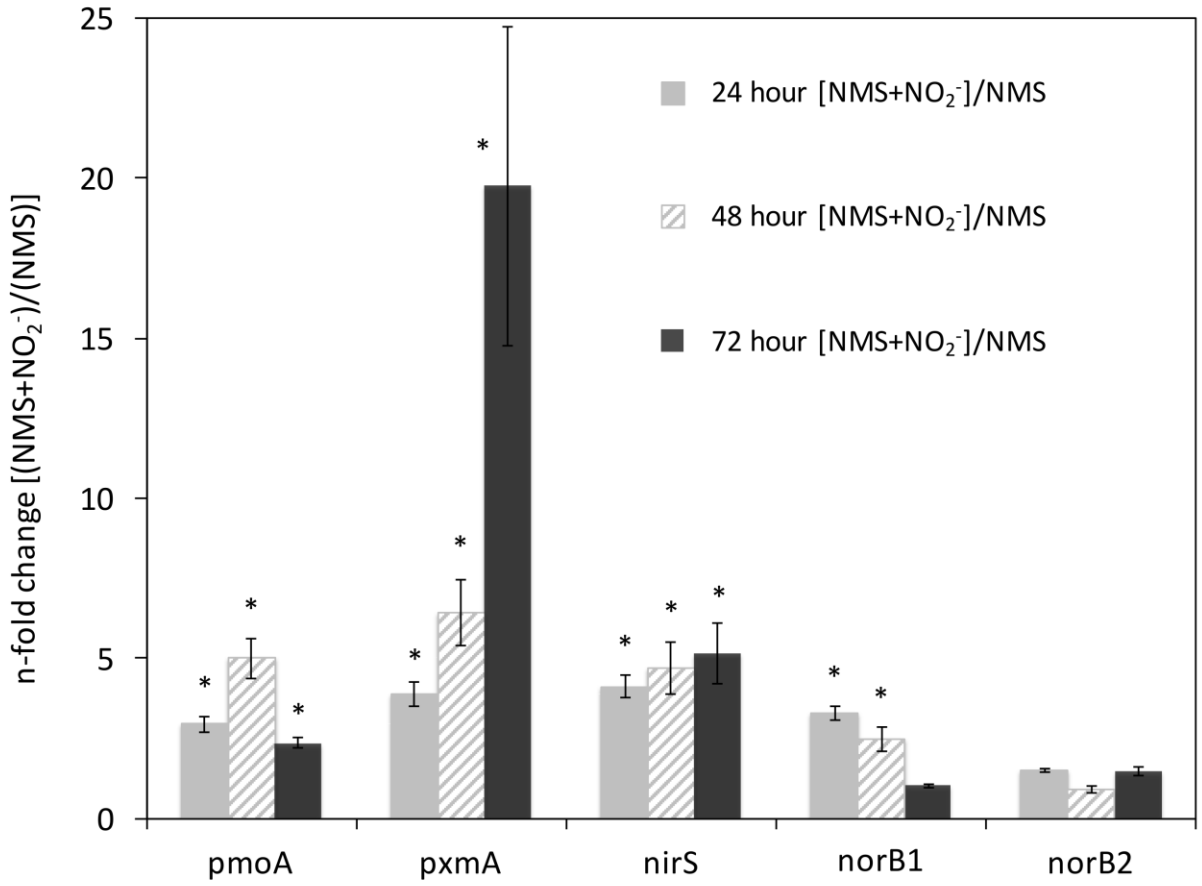

Figure 15: **Expression of *pmoA, pxmA, nirS, norB1* and *norB2* in *Methylomicrobium album* strain BG8 cultivated in NMS or NMS media amended with 1 mM $NaNO_2$.**

Total RNA was extracted from *Methylomicrobium album* strain BG8 at 24 h, 48 h, and 72 h of growth (see Fig. 1) from three separate cultures, converted to cDNA, and the abundance of *pmoA, pxmA, nirS*, *norB1* and *norB2* transcripts was determined using quantitative PCR. The transcript abundance of each gene of interest was normalized to that of 16s rRNA. The n-fold change in transcript abundance of the NO_2^- amended (1 mM $NaNO_2$) NMS cultures relative to the unamended NMS cultures at 24 h of growth (light grey), 48 h of growth (diagonal white/grey), and at 72 h of growth (black). Error bars represent the standard deviation calculated for triplicate qPCR reactions performed on each of the three biological replicates for each treatment. The (*) above the bars designates a statistical significance ($P<0.05$) as determined by t-test between NMS only and NMS + NO_2^- for each time point.

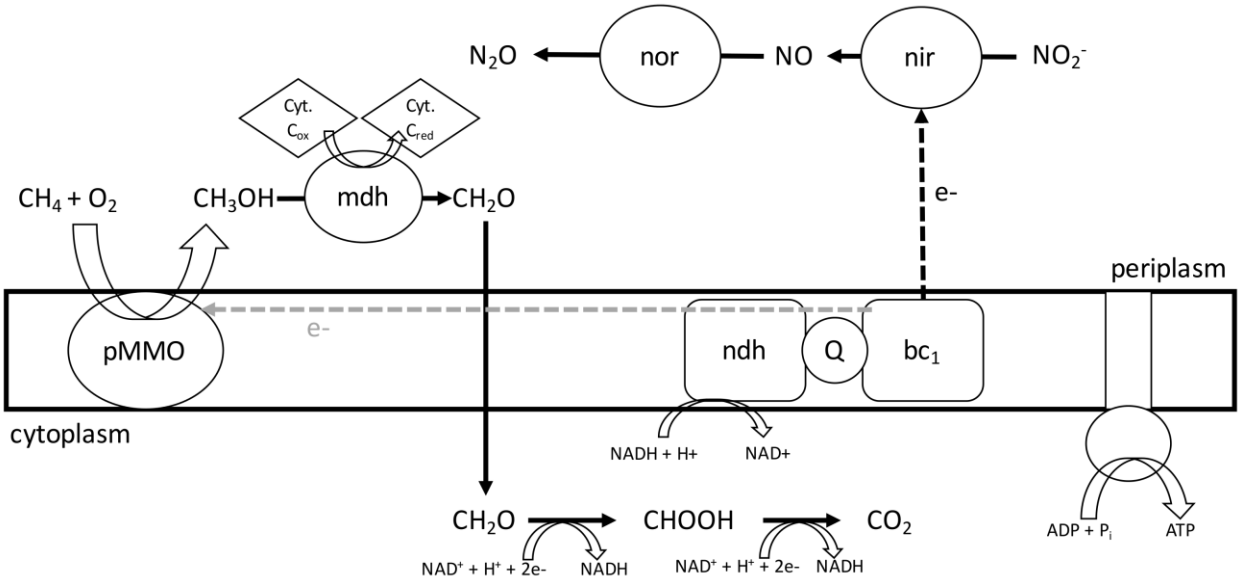

Figure 16: **Proposed model for NO_2^- respiration and central metabolism in *Methylomicrobium album* strain BG8.**

During hypoxia, *M. album* strain BG8 utilizes electrons from aerobic CH_4 oxidation to respire NO_2^-. Abbreviations: pMMO, particulate methane monooxygenase; mdh, methanol dehydrogenase; Cyt, cytochrome; nor, nitric oxide reductase; nir, nitrite reductase; ndh, NAD(P)H dehydrogenase complex; Q, coenzyme Q: bc_1, cytochrome bc_1 complex.

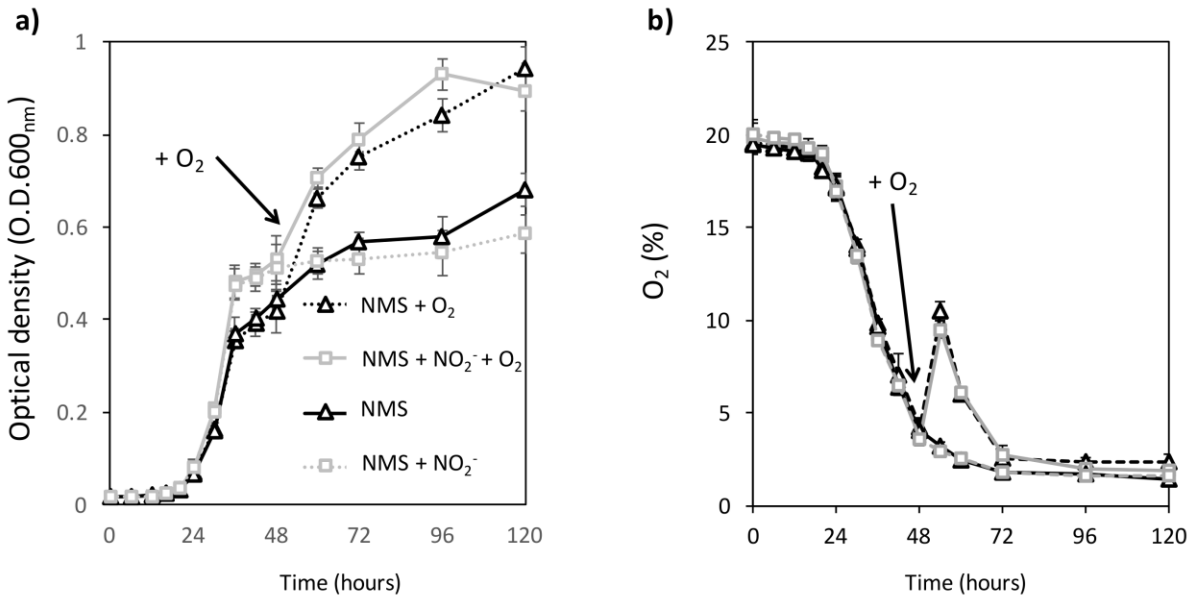

Figure S1 | Effect of O_2 addition on growth and O_2 consumption by *Methylomicrobium album* strain BG8 cultivated on NMS and NMS amended with 1 mM $NaNO_2$. *Methylomicrobium album* strain BG8 was cultivated for 5 days in 100 mL of NMS (black solid triangles), NMS + O_2 (black dashed triangles), NMS + 1 mM NO_2^- (gray dashed squares), or NMS + 1 mM NO_2^- + O_2 (grey solid squares) media in 300 mL closed glass Wheaton bottles sealed with butyl rubber septum caps. All data points represent the mean ± standard deviation for 6 biological replicates (n = 6). The NMS + O_2 and NMS + NO_2^- + O_2 treatments received additional O_2 (20 mL) at 54 h. Optical density (a) of the cultures was measured a spectrophotometer at 600nm and headspace gas concentration of O_2 (b) was measured using GC-TCD.

Figure 17: **Effect of O_2 addition on growth and O_2 consumption by *Methylomicrobium album* strain BG8 cultivated on NMS and NMS amended with 1 mM $NaNO_2$.**

Methylomicrobium album strain BG8 was cultivated for 5 days in 100 mL of NMS (black solid triangles), NMS + O_2 (black dashed triangles), NMS + 1 mM NO_2^- (gray dashed squares), or NMS + 1 mM NO_2^- + O_2 (grey solid squares) media in 300 mL closed glass Wheaton bottles sealed with butyl rubber septum caps. All data points represent the mean ± standard deviation for 6 biological replicates (n = 6). The NMS + O_2 and NMS + NO_2^- + O_2 treatments received additional O_2 (20 mL) at 54 h. Optical density (a) of the cultures was measured a spectrophotometer at 600nm and headspace gas concentration of O_2 (b) was measured using GC-TCD.

Gene Target	Locus Tag[1]	Primer Set	Sequence (5'→3')	qPCR Efficiency	Standard curve - R^2	Reference
pxmA	METAL_RS06980	QpxmA-FWD-3	GCTTGTCAGGGCTTACGATTA	97.7% - 101.8%	0.9989	This study
		QpxmA-REV-3	CTTCCAGTCCACCCAGAAATC			
pmoA	METAL_RS17425	QpmoA-FWD-7	GTTCAAGCAGTTGTGTGGTATC	95.1% - 97.2%	0.9999	This study
		QpmoA-REV-7	GAATTGTGATGGGAACACGAAG			
nirS	METAL_RS10995	QnirS-FWD-1	GTCGACCTGAAGGACGATTT	95.1% - 98.8%	0.9999	This study
		QnirS-REV-1	GTCACGATGCTGTCGTCATA			
norB1	METAL_RS03925	QnorB-FWD-2	ACTGGCGGTGCACTATTT	97.2% - 97.4%	0.9998	This study
		QnorB-REV-2	CATCCGGTTGACGTTGAAATC			
norB2	METAL_RS13345	QnorB-F-1	CACCATGTACACCCTCATCTG	96.2% - 102.2%	0.9999	This study
		QnorB-R-1	CCAAAGTCTGCGCAAGAAAC	96.1% - 101.8%	0.9999	This study
16S rRNA	METAL_RS04240	341F	CCTACGGGAGGCAGCAG	96.9% - 102.2 %	0.9997	Muyzer *et al.*, 1993
		518R	ATTACCGCGGCTGCTGG			

Table 2: **qPCR Primers used in Chapter 3**

[1]: The complete genome sequence of *M. album* strain BG8 is deposited in Genbank (http://www.ncbi.nlm.nih.gov/genbank/) under the accession NZ_CM001475 (http://www.ncbi.nlm.nih.gov/genome/?term=methylomicrobium%20album%20Bg8)

3.7: References

Bédard, C., and Knowles, R. (1989). Physiology, biochemistry, and specific inhibitors of CH_4, NH_4^+, and CO oxidation by methanotrophs and nitrifiers. *Microbiol. Rev.* 53, 68–84.

Bodelier, P. L. E., and Laanbroek, H. J. (2004). Nitrogen as a regulatory factor of methane oxidation in soils and sediments. *FEMS Microbiol. Ecol.* 47, 265–277. doi:10.1016/S0168-6496(03)00304-0.

Bodelier, P. L. E., and Steenbergh, A. K. (2014). Interactions between methane and the nitrogen cycle in light of climate change. *Current Opinion in Environmental Sustainability* 9-10, 26–36.

Bodelier, P. L., Roslev, P., Henckel, T., and Frenzel, P. (2000). Stimulation by ammonium-based fertilizers of methane oxidation in soil around rice roots. *Nature* 403, 421–424. doi:10.1038/35000193.

Bollmann, A., French, E., and Laanbroek, H. J. (2011). Isolation, Cultivation, and Characterization of Ammonia-Oxidizing Bacteria and Archaea Adapted to Low Ammonium Concentrations. *Meth. Enzymol.* 486, Part a 55–88.

Cammack, R., Joannou, C. L., Cui, X.-Y., Torres Martinez, C., Maraj, S. R., and Hughes, M. N. (1999). Nitrite and nitrosyl compounds in food preservation. *Biochimica et Biophysica Acta (BBA) - Bioenergetics* 1411, 475–488. doi:10.1016/S0005-2728(99)00033-X.

Campbell, M. A., Nyerges, G., Kozlowski, J. A., Poret Peterson, A. T., Stein, L. Y., and Klotz, M. G. (2011). Model of the molecular basis for hydroxylamine oxidation and nitrous oxide production in methanotrophic bacteria. *FEMS Microbiology Letters* 322, 82–89. doi:10.1111/j.1574-6968.2011.02340.x.

Costa, C., Dijkema, C., Friedrich, M., García-Encina, P., Fernández-Polanco, F., and Stams, A. J.

(2000). Denitrification with methane as electron donor in oxygen-limited bioreactors. *Appl. Microbiol. Biotechnol.* 53, 754–762.

Cramm, R., Siddiqui, R. A., and Friedrich, B. (1997). Two isofunctional nitric oxide reductases in *Alcaligenes eutrophus* H16. *J. Bacteriol.* 179, 6769–6777.

Dalton, H. (1977). Ammonia oxidation by the methane oxidising bacterium *Methylococcus capsulatus* strain bath. *Arch. Microbiol.* 114, 273–279. doi:10.1007/BF00446873.

Dalton, H. (1980). Oxidation of Hydrocarbons by Methane Monooxygenases from a Variety of Microbes. *Adv. Appl. Microbiol.* 26, 71–87. doi:10.1016/S0065-2164(08)70330-7.

Dam, B., Dam, S., Blom, J., and Liesack, W. (2013). Genome Analysis Coupled with Physiological Studies Reveals a Diverse Nitrogen Metabolism in *Methylocystis* sp. Strain SC2. *PLoS ONE* 8, e74767. doi:10.1371/journal.pone.0074767.

Demirbas, A. (2010). *Methane Gas Hydrate*. London: Springer London doi:10.1007/978-1-84882-872-8.

Dunfield, P., and Knowles, R. (1995). Kinetics of inhibition of methane oxidation by nitrate, nitrite, and ammonium in a humisol. *Appl. Environ. Microbiol.* 61, 3129–3135.

Holmes, A. J., Costello, A., Lidstrom, M. E., and Murrell, J. C. (1995). Evidence that particulate methane monooxygenase and ammonia monooxygenase may be evolutionarily related. *FEMS Microbiology Letters* 132, 203–208.

Kalyuzhnaya, M. G., Yang, S., Rozova, O. N., Smalley, N. E., Clubb, J., Lamb, A., et al. (2013). Highly efficient methane biocatalysis revealed in a methanotrophic bacterium. *Nat Comms* 4, 2785. doi:10.1038/ncomms3785.

Khadem, A. F., Pol, A., Wieczorek, A. S., Jetten, M. S. M., and Op den Camp, H. J. M. (2012a). Metabolic regulation of "Ca. *Methylacidiphilum fumariolicum*" soIV cells grown under

different nitrogen and oxygen limitations. *Front. Microbiol.* 3.

Khadem, A. F., Wieczorek, A. S., Pol, A., Vuilleumier, S., Harhangi, H. R., Dunfield, P. F., et al. (2012b). Draft genome sequence of the volcano-inhabiting thermoacidophilic methanotroph *Methylacidiphilum fumariolicum* strain SolV. *J. Bacteriol.* 194, 3729–3730. doi:10.1128/JB.00501-12.

King, G. M., and Schnell, S. (1994). Ammonium and Nitrite Inhibition of Methane Oxidation by *Methylobacter albus* BG8 and *Methylosinus trichosporium* OB3b at Low Methane Concentrations. *Appl. Environ. Microbiol.* 60, 3508–3513.

Kits, K. D., Kalyuzhnaya, M. G., Klotz, M. G., Jetten, M. S. M., Op den Camp, H. J. M., Vuilleumier, S., et al. (2013). Genome Sequence of the Obligate Gammaproteobacterial Methanotroph *Methylomicrobium album* Strain BG8. *Genome Announc* 1, e0017013–e00170–13. doi:10.1128/genomeA.00170-13.

Kits, K. D., Klotz, M. G., and Stein, L. Y. (2015). Methane oxidation coupled to nitrate reduction under hypoxia by the Gammaproteobacterium *Methylomonas denitrificans*, sp. nov. type strain FJG1. *Environ. Microbiol.* 17, 3219–3232. doi:10.1111/1462-2920.12772.

Knowles, R. (2005). Denitrifiers associated with methanotrophs and their potential impact on the nitrogen cycle. *Ecological Engineering* 24, 441–446. doi:10.1016/j.ecoleng.2005.01.001.

Kozlowski, J. A., Price, J., and Stein, L. Y. (2014). Revision of N_2O-producing pathways in the ammonia-oxidizing bacterium *Nitrosomonas europaea* ATCC 19718. *Appl. Environ. Microbiol.* 80, 4930–4935. doi:10.1128/AEM.01061-14.

Mesa, S., Velasco, L., Manzanera, M. E., Delgado, M. J., and Bedmar, E. J. (2002). Characterization of the *norCBQD* genes, encoding nitric oxide reductase, in the nitrogen fixing bacterium *Bradyrhizobium japonicum*. *J Gen Microbiol* 148, 3553–3560.

Mountfort, D. O. (1990). Oxidation of aromatic alcohols by purified methanol dehydrogenase from *Methylosinus trichosporium*. *J. Bacteriol.* 172, 3690–3694.

Nyerges, G., Han, S.-K., and Stein, L. Y. (2010). Effects of ammonium and nitrite on growth and competitive fitness of cultivated methanotrophic bacteria. *Appl. Environ. Microbiol.* 76, 5648–5651. doi:10.1128/AEM.00747-10.

Poret Peterson, A. T., Graham, J. E., Gulledge, J., and Klotz, M. G. (2008). Transcription of nitrification genes by the methane-oxidizing bacterium, *Methylococcus capsulatus* strain Bath. *ISME J* 2, 1213–1220. doi:10.1038/ismej.2008.71.

Reith, F., Drake, H. L., and Küsel, K. (2002). Anaerobic activities of bacteria and fungi in moderately acidic conifer and deciduous leaf litter. *FEMS Microbiol. Ecol.* 41, 27–35. doi:10.1111/j.1574-6941.2002.tb00963.x.

Richardson, D. J., Berks, B. C., Russell, D. A., Spiro, S., and Taylor, C. J. (2001). Functional, biochemical and genetic diversity of prokaryotic nitrate reductases. *Cell. Mol. Life Sci.* 58, 165–178.

Saidi-Mehrabad, A., He, Z., Tamas, I., Sharp, C. E., Brady, A. L., Rochman, F. F., et al. (2013). Methanotrophic bacteria in oilsands tailings ponds of northern Alberta. *ISME J* 7, 908–921. doi:10.1038/ismej.2012.163.

Stein, L. Y., and Klotz, M. G. (2011). Nitrifying and denitrifying pathways of methanotrophic bacteria. *Biochemical Society Transactions* 39, 1826–1831. doi:10.1042/BST20110712.

Stein, L. Y., Bringel, F., Dispirito, A. A., Han, S., Jetten, M. S. M., Kalyuzhnaya, M. G., et al. (2011). Genome sequence of the methanotrophic Alphaproteobacterium, *Methylocystis* sp. Rockwell (ATCC 49242). *J. Bacteriol.* 193, 2668–2669. doi:10.1128/JB.00278-11.

Stieglmeier, M., Mooshammer, M., Kitzler, B., Wanek, W., Zechmeister-Boltenstern, S.,

Richter, A., et al. (2014). Aerobic nitrous oxide production through N-nitrosating hybrid formation in ammonia-oxidizing archaea. *ISME J* 8, 1135–1146. doi:10.1038/ismej.2013.220.

Sutka, R. L., Ostrom, N. E., Ostrom, P. H., Gandhi, H., and Breznak, J. A. (2003). Nitrogen isotopomer site preference of N_2O produced by *Nitrosomonas europaea* and *Methylococcus capsulatus* Bath. *Rapid Commun. Mass Spectrom.* 17, 738–745. doi:10.1002/rcm.968.

Svenning, M. M., Hestnes, A. G., Wartiainen, I., Stein, L. Y., Klotz, M. G., Kalyuzhnaya, M. G., et al. (2011). Genome sequence of the Arctic methanotroph *Methylobacter tundripaludum* SV96. *J. Bacteriol.* 193, 6418–6419. doi:10.1128/JB.05380-11.

Tavormina, P. L., Orphan, V. J., Kalyuzhnaya, M. G., Jetten, M. S. M., and Klotz, M. G. (2011). A novel family of functional operons encoding methane/ammonia monooxygenase-related proteins in gammaproteobacterial methanotrophs. *Environ Microbiol Rep* 3, 91–100. doi:10.1111/j.1758-2229.2010.00192.x.

Vuilleumier, S., Khmelenina, V. N., Bringel, F., Reshetnikov, A. S., Lajus, A., Mangenot, S., et al. (2012). Genome sequence of the haloalkaliphilic methanotrophic bacterium *Methylomicrobium alcaliphilum* 20Z. *J. Bacteriol.* 194, 551–552. doi:10.1128/JB.06392-11.

Wei, W., Isobe, K., Nishizawa, T., Zhu, L., Shiratori, Y., Ohte, N., et al. (2015). Higher diversity and abundance of denitrifying microorganisms in environments than considered previously. *ISME J*. doi:10.1038/ismej.2015.9.

Whittenbury, R., Phillips, K. C., and Wilkinson, J. F. (1970). Enrichment, Isolation and Some Properties of Methane-utilizing Bacteria. *J Gen Microbiol* 61, 205–218. doi:10.1099/00221287-61-2-205.

Yoshinari, T. (1985). Nitrite and nitrous oxide production by *Methylosinus trichosporium*. *Can.*

J. Microbiol. 31, 139–144.

Chapter 4: Simultaneous expression of denitrifying and fermentation pathways in the methanotroph, *Methylomonas denitrificans* FJG1

K. Dimitri Kits[1], Manuel Kleiner[2], Dan Liu[2] and Lisa Y. Stein[1]*

[1] Department of Biological Sciences, University of Alberta, CW405, Biological Sciences Building, Edmonton, Alberta, T6G 2E9, Canada

[2] Department of Geoscience, University of Calgary, Calgary, 2500 University Drive Northwest, Alberta T2N 1N4, Canada.

* Corresponding Author

4.1: Abstract

Aerobic methanotrophic bacteria are important players in the carbon and nitrogen cycles. Though aerobic methanotrophs depend on molecular oxygen for CH_4 oxidation, these specialized organisms are very abundant and active in oxygen depleted environments. Recently, CH_4-based formaldehyde fermentation was identified as an important adaptation to a low oxygen lifestyle in the obligate methanotroph *Methylomicrobium alcaliphilum* 20Z (Kalyuzhnaya et al., 2013). Additionally, CH_4-dependent respiratory denitrification is a strategy some aerobic methanotrophs like *Methylomonas denitrificans* FJG1 utilize to sustain respiration and alleviate the O_2 dependency of their respiratory chain (Kits et al., 2015b). However, it is not understood whether formaldehyde-based fermentation is common within the Gammaproteobacterial methanotrophs and whether fermentation and respiratory denitrification can occur simultaneously during O_2 starvation. Also, the expression of denitrification genes in aerobic methanotrophs has not been investigated at the protein level. Here we show using RNA-Seq and label-free quantification proteomics that denitrification and formaldehyde fermentation appears to occur simultaneously in *M. denitrificans* FJG1 in response to hypoxia induced stationary phase. In addition to acetate,

succinate, formate, and H_2, we demonstrate that ethanol is likely a fermentation product of *M. denitrificans* FJG1 during hypoxia. Our multi-level omics analysis suggests a critical role for pyruvate and phosphoenolpyruvate in the low oxygen metabolism of *M. denitrificans* FJG1 and adds to our knowledge of CH_4-dependent respiratory denitrification. This study is the first to analyze the global transcriptional and proteomic response of an aerobic methanotroph to hypoxia. Understanding the conditions that control fermentation and denitrification in aerobic methanotrophs informs our knowledge of how methanotrophic bacteria participate in the carbon and nitrogen cycles by elucidating mechanisms that support other community members with consumable exudates and/or produce the greenhouse gas nitrous oxide.

4.2: Introduction

Aerobic methanotrophic bacteria, which require O_2 for methane (CH_4) oxidation, fulfill an important role in the carbon cycle not only because they serve as a microbial sink for atmospheric CH_4 but also because they also attenuate net flux by oxidizing CH_4 before it reaches the atmosphere (Conrad, 2009; Nazaries et al., 2013). While the importance of methanotrophic bacteria in carbon cycling is recognized, their role in the nitrogen cycle is not well understood (Bodelier and Steenbergh, 2014). With regard to nitrogen transformations, aerobic methanotrophs display a tremendous amount of metabolic flexibility; in addition to the assimilation of nitrate and ammonium into biomass, methanotrophs can fix atmospheric nitrogen (N_2) and oxidize ammonia to nitrite (Campbell et al., 2011; Dalton, 1977; Murrell and Dalton, 1983; Nyerges and Stein, 2009; Poret Peterson et al., 2008). Recently, it was demonstrated that an aerobic methanotroph – *Methylomonas denitrificans* FJG1 – can couple CH_4 oxidation to denitrification by respiring NO_3^- (Kits et al., 2015b). This metabolism was demonstrated to be dependent on hypoxia (< 50nM dO_2) and NO_3^-. Since then, it has become clear that NO_3^-

respiration may be much more common in methanotrophs than previously thought and that this metabolism may represent an important component of their low oxygen metabolic response (Hamilton et al., 2015; Skennerton et al., 2015; Zhu et al., 2016).

The use of terminal reductases for respiration by methanotrophs is not the sole metabolic adaptation to hypoxia that this group of specialized bacteria organisms possess. In *Methylomicrobium alcaliphilum* 20Z, a formaldehyde-driven fermentation metabolism occurs under extremely low O_2 tensions that leads to the production and excretion of organic acids (such as acetate, lactate, succinate, and formate), H_2, and 3-hydroxybutyrate (Kalyuzhnaya et al., 2013). When O_2 is extremely scarce, the respiratory pathway in *M. alcaliphilum* 20Z is suppressed and the organism must switch to fermentative metabolism to allow NADH to be reoxidized to NAD^+. This fermentative metabolism involves the fermentation of CH_4-derived formaldehyde in order to discard reducing equivalents. Reducing equivalents are discarded by using organic compounds as electron sinks, thereby resulting in the production and export of the various organic acids listed previously. During this fermentation-based lifestyle, only a small proportion of the oxidized CH_4 is converted into biomass while the rest is excreted (Kalyuzhnaya et al., 2013). This not only displays another critical way that aerobic methanotrophs adapt to hypoxia, but also describes a potentially important role for methanotrophs in attenuation of methane in O_2 depleted environments.

Taken together, it is evident that aerobic methanotrophs have a multitude of ways to deal with oxygen scarcity, yet several questions remain unanswered. First, since formaldehyde fermentation has only been described in two *Methylomicrobium* species, it is not known whether other Gammaproteobacterial methanotrophs have a similar metabolic capability and what other fermentation products they might be produced (Gilman et al., 2015; Kalyuzhnaya et al., 2013). It

is also not known whether O_2 respiration, denitrification, and fermentation represent mutually exclusive lifestyles or whether several strategies can be used simultaneously. With regard to CH_4-driven denitrification, we know that the membrane bound nitrate reductase (*narGHJI*), copper-containing nitrite reductase (*nirK*), and cyctochrome *c* linked nitric oxide (*norBC*) reductase are expressed at the transcript level during denitrification in *Methylomonas denitrificans* FJG1 but we do not know what proteins are made (Kits et al., 2015b).

To answer these questions, we utilized both Illumina RNA-Seq and label free quantification proteomics to investigate the whole transcriptome and proteome of *Methylomonas denitrificans* FJG1 when cultivated under oxic conditions and compared that to hypoxia-induced stationary phase. Previous studies on formaldehyde-based fermentation utilized a continuous cultivation approach under low oxygen conditions; however, off-line batch incubations in N_2-flushed vials accumulated an order of magnitude or more succinate, lactate, and H_2 than the microaerobic reactor (Kalyuzhnaya et al., 2013). Hence, we applied a batch culture approach in which the limiting nutrient is O_2 to assess how mRNA and protein levels change in response to hypoxia induced stationary phase.

4.3: Materials and Methods

Cultivation and biomass collection

Methylomonas denitrificans FJG1 was cultivated as described previously (Kits et al., 2015b). In brief: *M. denitrificans* FJG1 was grown at 30°C in 100 mL of NMS medium (phosphate buffered at pH 6.8) at 200 rpm in 300 mL glass Wheaton bottles sealed with butyl rubber septa; the sole carbon and energy source was CH_4 and the ratio of CH_4 to O_2 in the closed bottles prior to inoculation was: 1.5:1. Growth occurred exactly as described previously (i.e. stationary phase due to O_2 depletion began at 48 hr and N_2O was measureable in the headspace

beginning at 60h) (Kits et al., 2015b). Growth of *M. denitrificans* FJG1 here was confirmed to be consistent with previous growth curves through measurements of optical density ($O.D._{600nm}$), direct cell count, and headspace O_2, CH_4, and N_2O concentrations. Biomass from 6 biological replicates (i.e. 6 bottles inoculated from 6 separate inocula) was harvested using a filtration manifold and 0.22 μm filters (Supor 200) during mid-log phase ("aerobic or oxic growth") and 24 hr after reaching stationary phase ("hypoxia induced stationary phase"). The biomass was quickly washed while on the filter, resuspended in sterile NMS medium, centrifuged at 4°C for 2 minutes at 15,000g, and frozen at -80°C after the supernatant for removed.

RNA extraction, library preparation, Illumina HiSeq sequencing

Approximately 10 mL of culture was removed from the replicate bottles during mid-log phase and 24 hr after reaching stationary phase and harvested by filtration (Kits et al., 2015). The biomass was treated with STOP solution (5% water saturated phenol pH 4.0, 95% anhydrous EtOH) and the RNA extraction, library preparation, and Illumina HiSeq sequencing was performed exactly as described elsewhere (Kits et al., 2015).

Assembly and analysis of transcriptome data

Reads that passed the initial Illumina quality control filter were imported into Geneious R9.1 (Kearse et al., 2012). Reads were mapped onto the closed genome of *M. denitrificans* FJG1 using medium sensitivity, 10 iterations for fine-tuning. Ambiguously mapped reads were counted as partial matches. Mapped reads were then used to calculate a TPM (transcripts per million), a measurement designed to be more consistent across samples and avoid read count bias (Wagner et al., 2012). Differential expression levels were compared on a transcript basis and normalized by the median of gene expression ratios to prevent a few very highly transcribed genes (as is the case in aerobic methanotrophs) from biasing the fraction of total transcripts that belong to genes

that are expressed at a very low or low level (Dillies et al., 2013). Differential expression p-values were calculated by Geneious R9.1; the expected likelihood that a random transcript comes from a given gene, assuming no differential expression, is then factored in (using a Binomial distribution) to calculate the likelihood that a TPM count as least as great as was observed would be observed assuming no differential expression.

Protein extraction and peptide preparation

For each of the two treatments tryptic digests were prepared from six biological replicates following the filter-aided sample preparation (FASP) protocol described by Wisniewski et al (Wiśniewski et al., 2009). In brief, SDT-lysis buffer (4% (w/v) SDS, 100 mM Tris-HCl pH 7.6, 0.1 M DTT) was added in a 1:10 sample/buffer ratio to the sample pellets. Samples were heated for lysis to 95° C for 10 minutes followed by pelleting of debris for 5 min at 21,000 x g. 30 µl of the cleared lysate were mixed with 200 µl of UA solution (8 M urea in 0.1 M Tris/HCl pH 8.5) in a 10 kDa MWCO 500 µl centrifugal filter unit (VWR International) and centrifuged at 14,000 x g for 40 min. 200 µl of UA solution were added again and centrifugal filter spun at 14,000 x g for 40 min. 100 µl of IAA solution (0.05 M iodoacetamide in UA solution) were added to the filter and incubated at 22° C for 20 min. The IAA solution was removed by centrifugation and the filter was washed three times by adding 100 µl of UA solution and then centrifuging. The buffer on the filter was then changed to ABC (50 mM Ammonium Bicarbonate), by washing the filter three times with 100 µl of ABC. 1 µg of MS grade trypsin (Thermo Scientific Pierce, Rockford, IL, USA) in 40 µl of ABC were added to the filter and filters incubated overnight in a wet chamber at 37° C. The next day, peptides were eluted by centrifugation at 14,000 x g for 20 min, followed by addition of 50 µl of 0.5 M NaCl and again centrifugation. Peptides were desalted using C18 spin columns (Thermo Scientific Pierce, Rockford, IL, USA) according to the

manufacturer's instructions. Approximate peptide concentrations were determined using the Pierce Micro BCA assay (Thermo Scientific Pierce, Rockford, IL, USA) following the manufacturer's instructions.

1D-LC-MS/MS

Samples were analyzed by 1D-LC-MS/MS using a block-randomized design as outlined by Oberg and Vitek (Oberg and Vitek, 2009). Two blank runs were done between samples to reduce carry over. For each run 800 ng of peptide were loaded onto a 2 cm, 75 µm ID C18 Acclaim® PepMap 100 pre-column (Thermo Fisher Scientific) using an EASY-nLC 1000 Liquid Chromatograph (Thermo Fisher Scientific) set up in 2-column mode. The pre-column was connected to a 50 cm x 75 µm analytical EASY-Spray column packed with PepMap RSLC C18, 2µm material (Thermo Fisher Scientific), which was heated to 35° C via the integrated heating module. The analytical column was connected via an Easy-Spray source to a Q Exactive Plus hybrid quadrupole-Orbitrap mass spectrometer (Thermo Fisher Scientific). Peptides were separated on the analytical column at a flow rate of 225 nl/min using a 260 min gradient going from buffer A (0.2% formic acid, 5% acetonitrile) to 20% buffer B (0.2% formic acid in acetonitrile) in 200 min, then from 20 to 35% B in 40 min and ending with 20 min at 100% B. Eluting peptides were ionized with electrospray ionization (ESI) and analyzed in the Q Exactive Plus. Full scans were acquired in the Orbitrap at 70,000 resolution. MS/MS scans of the 15 most abundant precursor ions were acquired in the Orbitrap at 17,500 resolution. The mass (m/z) 445.12003 was used as lock mass as described by Olsen et al. (2005) with the modification that lock mass was detected in the full scan rather than by separate SIM scan injection (Olsen et al., 2005). Lock mass use was set to "best". Ions with charge state +1 were excluded from MS/MS analysis. Dynamic exclusion was set to 30 sec. Roughly 160,000 MS/MS spectra were acquired

per sample run.

Protein identification, quantification, and statistics

For protein identification a database was created using all protein sequences from the complete genome of *Methylomonas denitrificans* strain FJG1 (Genbank Identifier CP014476.1). The database was submitted to the PRIDE repository (see below). For protein identification MS/MS spectra were searched against the database using the Sequest HT node in Proteome Discoverer version 2.0.0.802 (Thermo Fisher Scientific) with the following parameters: Trypsin (Full), max. 2 missed cleavages, 10 ppm precursor mass tolerance, 0.1 Da fragment mass tolerance and max. 3 equal dynamic modifications per peptide. The following three dynamic modifications were considered: oxidation on M (+15.995 Da), carbamidomethyl on C (+57.021 Da) and acetyl on protein N-terminus (+42.011 Da). False discovery rates (FDRs) for peptide spectral matches (PSMs) were calculated and filtered using the Percolator Node in Proteome Discoverer. The Percolator algorithm "uses semi-supervised learning and a decoy database search strategy to learn to distinguish between correct and incorrect PSMs" (Spivak et al., 2009). Percolator was run with the following settings: Maximum Delta Cn 0.05, a strict target FDR of 0.01, a relaxed target FDR of 0.05 and validation based on q-value. Search results for all 18 samples were combined into a multiconsensus report using the FidoCT node in Proteome Discoverer to restrict the protein-level FDR to below 5% (FidoCT q-value <0.05) (Serang et al., 2010). Proteins with a FidoCT q-value of <0.01 were classified as high confidence identifications and proteins with a FidoCT q-value of 0.01-0.05 were classified as medium confidence identifications. Based on these filtering criteria a total of 1833 proteins were identified in all samples together. The multiconsensus report was then exported as a tab-delimited file for further processing.

For protein quantification normalized spectral abundance factors (NSAFs) were calculated based on number of PSMs per protein using the method described by Florens et al. (2006) and multiplied by 10,000 (Florens et al., 2006). The NSAFx10,000 gives the relative abundance of a protein in a sample as a fraction of 10,000. The table with NSAFx10,000 values was loaded into the Perseus software (version 1.5.1.6, http://www.perseus-framework.org/doku.php), an annotation row was added to group replicates by treatment and proteins that did not have expression values >0 for all replicates in at least one treatment group were removed (1831 proteins remained) (Cox and Mann, 2012). NSAFx10,000 values were $\log_2$ transformed. Missing values produced by $\log_2(0)$ were replaced by sampling from a normal distribution assuming that the missing values are on the lower end of abundance (normal distribution parameters in Perseus: width 0.3, down shift 1.8, do separately for each column). A t-test with permutation based FDR calculation was used to detect proteins that differed significantly in their expression level between two treatments. The statistical method implemented in Perseus that we used is based on the "significance analysis of microarrays" described by Tusher et al. (2001), which by using a permutation based FDR accounts for the multiple-testing problem inherent in testing for significant expression differences for a large number of genes (Tusher et al., 2001). The following parameters were used for the test: groupings were not preserved for randomizations, both sides, 250 randomizations, FDR of 1% and s0 of 0.

Data availability

The mass spectrometry proteomics data and the protein sequence database have been deposited to the ProteomeXchange Consortium via the PRIDE partner repository with the dataset identifier PXD004041 (Vizcaíno et al., 2014).

KEGG classification

Predicted amino acid coding sequences from the completed genome of *M. denitrificans* FJG1 as well as the amino acid sequences from differentially expressed transcripts/proteins were populated onto the Kyoto Encyclopedia of Genes and Genomes (KEGG) dataset using BlastKOALA (http://www.kegg.jp/blastkoala/) (Kinehisa et al., 2016). Pathways were selected as based on those that would most likely be present in a prokaryotic dataset.

4.4: Results

Gene expression and protein identifications

We identified and quantified 1831 proteins in all 6 replicates of both tested conditions – aerobic growth and hypoxia-induced stationary phase. The 1831 identified proteins represent 39.3% of the 4664 total coding sequences predicted in the genome of *M. denitrificans* FJG1 (Fig. 18). 1829 of the total identified proteins had >1 unique peptide match and all of the identified proteins in our analysis showed >24 peptide spectral matches. The average sequence coverage obtained in our analysis was 64.7% and the average number of unique peptides matched per protein was 21.8. Out of the 1831 quantified proteins, the greatest proportion, representing 12.8% of the total coding sequences, were assigned an "intermediate" expression level based on our classification scheme (Fig. 18). Expression of 669 proteins was altered by hypoxia-induced stationary phase (Fig. 19). 359 of the quantified proteins were stimulated while 310 were depressed (Fig. 19).

In the transcriptome, 45.2% of the coding sequences were expressed based on transcripts/million (TPM) values of >50 (Fig. 18). In contrast to the proteome, the greatest proportion of expressed coding sequences in the transcriptome were assigned a "very low" expression level according to our classification scheme (Fig. 18). Out of the 4664 total coding

sequences, expression of 1085 transcripts was altered by hypoxia-induced stationary phase; 541 transcripts were stimulated while 544 were depressed at hypoxia (Fig. 18 & 19). A comparative analysis of the differentially expressed transcripts and proteins showed that 114 of the stimulated transcripts/proteins and 76 of the depressed transcripts/proteins were shared between the transcriptome and proteome (Fig. 19).

General KEGG classification of differentially expressed transcripts and proteins

Transcripts and proteins with significantly altered abundance under hypoxia-induced stationary phase were populated onto pathways present in the Kyoto Encyclopedia of Genes and Genomes (KEGG) dataset, a subset of which is represented in Fig. 20 and Table 3. Carbohydrate metabolism, energy metabolism, and Environmental Information Processing (EIP) together represented >65% of the classified transcripts and proteins stimulated by hypoxia (Fig. 20 & Table 3). However, those same three categories only made up 29.5% and 30.4% of the depressed transcripts and proteins, respectively (Fig. 20 & Table 3). Genes vastly overrepresented on a relative and absolute basis in the stimulated set of transcripts and proteins belonged to the TCA cycle and pyruvate metabolism (within Carbohydrate metabolism), nitrogen metabolism (within Energy metabolism), and the two-component system response (within EIP) (Table 3). Transcripts and proteins that mapped to cell motility were also much more abundant in the stimulated set (8.2% of stimulated transcripts and 10.9% of the stimulated proteins) than in the depressed set (0.3% of the transcripts and 0.5% of the quantified proteins) (Fig. 20 & Table 3).

Depressed transcripts and proteins mostly populated into the nucleotide metabolism, translation, and replication & repair; these latter categories accounted for 26.6% and 33.2% of the depressed transcripts and proteins, respectively, and for only 3.8% and 2.2% of stimulated transcripts/proteins (Fig. 20 & Table 3). Genes that were greatly overrepresented on a relative

and absolute basis in the depressed set mapped to the ribosome and amino-acyl tRNA synthesis (within the Translation category), as well as DNA replication, mismatch repair, and homologous recombination (all within Replication & Repair) (Table 3 & 4). Finally, a significantly larger proportion of the transcripts and proteins in the depressed set mapped to amino acid metabolism (16.9% of the depressed transcripts and 13.6% of proteins) when compared to the stimulated set in which 7.6% of transcripts and 7.2% of proteins mapped to amino acid metabolism (Fig. 20 & Table 3).

Carbohydrate metabolism: RuMP cycle

Transcripts and proteins for all of the required steps of the ribulose monophosphate (RuMP) cycle were identified in the transcriptome and proteome under oxic conditions (Fig. 22 & 23). Hexulose-6-phosphate synthase (*hps*) and hexulose-6-phosphate isomerase (*hpi*) were expressed at very high and high levels during aerobic growth, respectively, in the transcriptome (Fig. 22). This agreed with the proteome, which indicated that both proteins were present at a very high level during aerobic growth; both proteins were in the top 1% of the most abundant quantified proteins (Fig. 23).

The genome of *M. denitrificans* FJG1 encodes both the FBPA and KDPGA pathways for the cleavage of fructose-6-phosphate into two C-3 compounds and both pathways were expressed at the transcript and protein levels under oxic conditions (Fig. 22 & 23). However, the FBPA pathway showed higher transcript and protein abundance. In the transcriptome, the fructose bisphosphate aldolase (*fba*) was expressed at an intermediate level while all of the transcripts belonging to the genes encoding the KDPGA pathway were expressed at a very low level (Fig. 22). At the protein level, the phosphofructokinase (*pfk*) and fructose bisphosphate aldolase (*fba*) were expressed at a high level while all of the proteins of the KDPGA pathway

were expressed at an intermediate level (Fig. 23).

The sugar rearrangements that incorporate glyceraldehyde-3-phosphate and two fructose-6-phosphate molecules to generate three ribulose-5-phosphate molecules can be catalyzed via the SBPase or TA pathway. The complete genome of *M. denitrificans* FJG1 only encodes the TA pathway since it is lacking the sedoheptulose-1,7-bisphosphatase. All transcripts and proteins involved in the TA pathway were expressed during aerobic growth. At the transcript level, the steady state mRNA levels of all transcripts except those belonging to the transaldolase were detected at a low level, while the steady state mRNA level for transaldolase was high (Fig. 22). In the oxic proteome, all of the enzymes were expressed at an intermediate or high level (Fig. 23).

Several transcripts and proteins showed significantly altered abundance in response to hypoxia induced stationary phase. The quantities of the hexulose-6-phosphate synthase (*hps*), bisphosphate aldolase (*fba*), and phosphofructokinase (*pfk*) were significantly lower at either the mRNA level (*fba*) or protein level (*hps, pfk*) (Fig. 24). In contrast, the steady state mRNA level of the second copy of the glucose phosphate dehydrogenase (*gpd2*) was significantly higher under hypoxia (Fig. 24). Finally, the ribose-5-phosphate isomerase (*rpi*) and transketolase (*tkt*) ribose-5-phosphate isomerase (*rpi*) proteins were also significantly more abundant under hypoxic conditions when compared to the oxic control (Fig. 24).

Carbohydrate metabolism: Entner-Doudoroff and Embden-Meyerhof-Parnas

The genome of *M. denitrificans* FJG1 encodes complete ED and EMP pathways. All of the gene involved in the EMP pathway were expressed at the transcript level and identified in the proteome. The steady state mRNA levels for all genes participating in the EMP pathway were at a very low to low level with the exception of fructose bisphosphate aldolase which was

transcribed at an intermediate level (Fig. 22). However, the respective proteins were all detected at an intermediate to high level with the exception of the glucokinase (*gck*) which was present at a low level (Fig. 23). Steady state transcript levels of glyceraldehyde-3-phosphate dehydrogenase (*gap*) decreased in response to hypoxia; however, the protein abundance did not change (Fig. 24). The genome of *M. denitrificans* FJG1 encodes two copies of phosphoglycerate mutase (*pgm*) which is responsible for the conversion of 3-phosphoglycerate (3-PG) to 2-phosphoglycerate (2-PG). Only the first copy (*pgm1*) was expressed in the transcriptome and proteome during aerobic growth (Fig. 22 & 23). Interestingly, in response to hypoxia, the second copy of phosphoglycerate mutase (*pgm2*) was expressed at a higher abundance in the transcriptome (2 fold) and much higher abundance in the proteome (93 fold) (Fig. 24). It must be noted though that the *pgm1* was still more abundant at the absolute level in the proteome.

All of the transcripts and proteins of the ED pathway were expressed at the mRNA and protein levels. The entire pathway was transcribed at a very low level but present at intermediate levels in the proteome during aerobic growth (Fig. 22 & 23). As discussed previously, the steady state transcript level of the second copy of the glucose phosphate dehydrogenase (*gpd2*) was elevated under hypoxia but all of the other steps were unchanged.

Carbohydrate metabolism: pyruvate metabolism, Krebs cycle, fermentation

There are three well-characterized enzyme systems that decarboxylate pyruvate to acetyl-CoA: pyruvate dehydrogenase (*pdh*), pyruvate ferredoxin oxidoreductase (*ydbk*), and pyruvate formate lyase (*pfl*). All three of the aforementioned pyruvate decarboxylating systems are encoded in the genome of *M. denitrificans* FJG1. However, only the pyruvate dehydrogenase (*pdh*) and pyruvate ferredoxin oxidoreductase (*ydbk*) were expressed at the mRNA and protein level under oxic conditions (Fig. 22 & 23). Steady state mRNA levels of pyruvate dehydrogenase

(*pdh*) were present at a very low level but the protein was quantified at an intermediate level during aerobic growth (Fig. 22 & 23). Under the same conditions, however, pyruvate ferredoxin oxidoreductase was expressed at a very low level in both the transcriptome and proteome. In response to hypoxia induced stationary phase, the pyruvate ferredoxin oxidoreductase (*ydbk*) and pyruvate formate lyase (*pfl*) were both significantly more abundant in the proteome (Fig. 24). The pyruvate formate lyase protein was 19.5 fold more abundant and the pyruvate ferredoxin oxidoreductase was 2.1 fold more abundant in the hypoxic proteome when compared to the oxic control (Fig. 24).

The acetyl-CoA formed by any of the three pyruvate decarboxylating enzymes can be converted to acetyl-P by phosphate acetyltransferase (*pta*) and then to acetate by acetate kinase *(ack*) which transfers the phosphoryl group from acetyl-P to ADP. This system allows bacteria that ferment to get an ATP and excrete acetate into the medium. The genome of *M. denitrificans* FJG1 contains the PTA-ACK system but there was no expression at the mRNA level for both genes during aerobic growth. In the proteome, the abundance of Pta and Ack correspondded to just below the threshold for *very low expression* (Fig. 23). Interestingly, the phosphate acetyltransferase (*pta*) was significantly more abundant (1.6 fold) in the proteome during hypoxia (Fig. 24). The acetate kinase (*ack*) protein was 1.3 fold more abundant under hypoxic conditions when compared to the control but this was not statistically significant ($p = .121$).

The genome of *M. denitrificans* FJG1 also encodes a pyruvate dikinase (*pdk*) and phosphoenolpyruvate synthase (*pps*) which both phosphorylate pyruvate to synthesize phosphoenolpyruvate (PEP). During aerobic growth, the pyruvate dikinase was expressed at a very low level in terms of mRNA but at an intermediate level in terms of protein abundance (Fig. 22 & 23). The PEP synthase, however, was not expressed at all during aerobic growth.

Expression of both pyruvate-phosphorylating enzymes increased in response to hypoxia. Steady state mRNA levels of pyruvate dikinase (*pdk*) increased 1.6 fold during hypoxia and both transcript and protein levels of the PEP synthase were also higher (2 fold and 4.4 fold, respectively) (Fig. 24).

The genome of *M. denitrificans* FJG1 encodes a complete TCA cycle, including α-ketogluterate dehydrogenase (*sucA, sucB, lpd*). All of the genes encoding the TCA cycle enzymes were transcribed at a very low level during aerobic growth with the exception of α-ketogluterate dehydrogenase and fumarate hydratase (*fum*), which were not expressed at the mRNA level (Fig. 22). In the proteome, the citrate synthase, aconitase, isocitrate dehydrogenase, succinyl-CoA ligase, succinate dehydrogenase, and malate dehydrogenase were all present at an intermediate level (Fig. 23). Similar to the transcriptome data, the α-ketogluterate dehydrogenase and fumarate dehydratase were detected at lower quantities than the other TCA cycle enzymes during oxic conditions. However, the α-ketogluterate dehydrogenase and fumarate hydratase proteins were still expressed at a low level and very low level, respectively, during aerobic growth (Fig. 22 & 23).

Expression of the entire TCA cycle, with the exception of α-ketogluterate dehydrogenase and fumarate hydratase, increased in response to hypoxia induced stationary phase (Fig. 24). The transcriptome and proteome both indicated that the expression of citrate synthase, aconitate hydratase, succinate-CoA ligase, and malate dehydrogenase increased under O_2 hypoxia (Fig. 24). Additionally, the isocitrate dehydrogenase and succinate dehydrogenase proteins were more abundant in the proteome under hypoxia when compared to the control.

To keep the TCA cycle operational, oxaloacetate must constantly be replenished. There are two enzymes encoded in the *M. denitrificans* FJG1 genome that could replenish oxaloacetate

– a phosphoenolpyruvate carboxylase (*ppc*) and pyruvate carboxylase (*pyc*). Under oxic conditions, neither gene was expressed in the transcriptome (Fig. 22). However, both were detected in the proteome; the pyruvate carboxylase protein was present at very low levels and the PEP carboxylase was present at an intermediate level in the proteome during aerobic growth (Fig. 23). In response to hypoxia-induced stationary phase, expression of the pyruvate carboxylase increased at the mRNA and protein levels while the expression of the PEP carboxylase decreased in the proteome (Fig. 24).

Ethanol is a typical mixed acid fermentation product in facultative anaerobic bacteria (Clark, 1989). The genome of *M. denitrificans* FJG1 lacks an acetaldehyde dehydrogenase which catalyzes the reduction of acetyl-CoA to acetaldehyde in most facultative anaerobic bacteria (Clark, 1989; Eram and Ma, 2013). However, we were able to annotate a pyruvate decarboxylase (*pdc*) in the genome. This enzyme catalyzes the decarboxylation of pyruvate to acetaldehyde and CO_2. In addition to the pyruvate carboxylase, we annotated three alcohol dehydrogenases (*adh1, adh2, adh2*) in the genome. The pyruvate decarboxylase and all three alcohol dehydrogenases were not expressed at the transcript or protein levels during aerobic growth (Fig. 22 & 23). Yet, two of the three alcohol dehydrogenases and the pyruvate decarboxylase enzymes were all significantly more abundant (2-4 fold) in the proteome extracted from hypoxic cultures (Fig. 24).

Energy metabolism: C1 oxidation – CH_4 oxidation to CH_3OH

The genome of *M. denitrificans* FJG1 contains one *pmoCAB* operon which encodes the O_2 and copper dependent particulate methane monooxygenase (pMMO). Additionally, the genome also contains one *pxmABC* operon with no known function (Tavormina et al., 2011). It has been speculated that Pxm is a membrane bound copper-containing monooxygenase that may play a metabolic role in *M. denitrificans* FJG1 under O_2 depleted conditions (Kits et al., 2015a;

2015b). The *pmoCAB* operon has very high expression values during aerobic growth, making up about 30% of all transcripts, and the PmoCAB peptides are also in the top 5% of all detected peptides under oxic conditions (Fig. 22 & 23). In response to hypoxia induced stationary phase, the expression of *pmoCAB* was asymmetric between the mRNA and protein levels – steady state mRNA levels decreased 1.5-2 fold while the protein levels increased 1.6-1.9 fold (Fig. 24). While we did not detect the Pxm protein in the proteomic analysis, the steady state mRNA levels of *pxmABC* increased 8.4-12.9 fold under hypoxic conditions (Fig. 24).

Energy metabolism: C1 oxidation – CH_3OH oxidation to CH_2O

Two methanol dehydrogenases are present in the genome of *M. denitrificans* FJG1. One is the calcium and PQQ dependent *mxa* methanol dehydrogenase and then second in the lanthanide dependent *xoxF* (Chu and Lidstrom, 2016). The transcript and protein expression levels for *mxaF* under oxic conditions both fell into the very high abundance category with the small subunit in the top 1% most abundant peptides (Fig. 22 & 23). In contrast, the lanthanide depedent *xoxF* had very low expression at the mRNA level and intermediate expression in the proteome under oxic conditions (Fig. 22 & 23). Hypoxia stimulated the expression of both methanol dehydrogenases; MxaF exhibited increased steady state mRNA levels and protein levels while XoxF exhibited an expression increase only in mRNA abundance (Fig. 24).

Energy metabolism: C1 oxidation – CH_2O oxidation to CHOOH

A complete H_4MPT dependent pathway for formaldehyde (CH_2O) oxidation was annotated in the genome of *M. denitrificans* FJG1. The entire pathway was expressed at the transcript and proteins levels under oxic conditions. However, transcription and translation of the various steps was dynamic. The condensation of CH_2O with H_4MPT to form methylene-H_4MPT, encoded by *fae* (formaldehyde activating enzyme), had a high level of expression in the

transcriptome and a very high expression level in the proteome; the formaldehyde activating enzyme was the second most abundant peptide under oxic conditions (Fig. 22 & 23). Then, the stepwise conversion of methylene-H_4MPT to CHOOH was expressed at lower levels in the transcriptome and proteome (Fig. 22 & 23). Only the methylene-H_4MPT dehydrogenase showed altered expression in response to hypoxia – a 1.3 fold decrease in protein abundance (Fig. 24).

Energy metabolism: C1 oxidation – CHOOH oxidation to CO_2

An NAD^+ dependent formate dehydrogenase is responsible for CHOOH oxidation to CO_2 in *M. denitrificans* FJG1. During aerobic growth, steady state mRNA levels of the *fdh* were at a low level in the transcriptome and an intermediate level in the proteome (Fig. 22 & 23). Expression of the formate dehydrogenase was not altered in the hypoxic transcriptome and proteome.

Energy metabolism: oxidative phosphorylation

Complexes I (NADH-ubiquinone oxidoreductase), II (succinate dehydrogenase), III (ubiquinol-cytochrome *c* oxidoreductase), IV (cytochrome *c* oxidase *aa_3*), and V (ATP synthase) were annotate in the genome of *M. denitrificans* FJG1. Furthermore, we identified a cytochrome *bd* ubiquinol oxidase which is a high affinity terminal oxidase. With the exception of the cytochrome *bd* ubiquinol oxidase, every complex was expressed in the transcriptome and proteome during aerobic growth. Under oxic conditions, mRNA and the peptide subunits of complex I were present at a high expression level (Fig. 22 & 23). The expression of complexes II, III, and IV were somewhat lower; all of the complexes were expressed at a very low or low level in the transcriptome and at intermediate or low levels in the proteome (Fig. 22 & 23). The ATP synthase (complex V) was transcribed and translated at intermediate levels under oxic conditions. The complexes altered by O_2 limitation were complexes II, IV, and V (Fig. 24). Two

subunits of the succinate dehydrogenase (*sucAB*) were more abundant in the proteome under hypoxic conditions. Similarly, complex IV showed significantly increased (2-4 fold) abundance in the transcriptome and proteome (Fig. 24). The only depressed complex was the ATP synthase which was 2-4 fold less abundant in the proteome during hypoxia when compared to the oxic control (Fig. 24).

Energy metabolism: Hydrogenases

The genome of *M. denitrificans* encodes two types of [NiFe] hydrogenase: a soluble cytoplasmic reversible NAD^+ reducing hydrogenase (*hoxHYGF*) and a membrane bound [NiFe] hydrogenase (*hoxKGZMLOQFRTVhypABCDEF*). Only the cytoplasmic NAD^+ reducing hydrogenase was expressed during aerobic growth – at very low levels at both the transcript and protein level (Fig. 22 & 23). Components of the cytoplasmic (*hoxYGF*) and membrane bound hydrogenase (*hoxKGQF* – encoding the large and small subunit of the membrane bound complex) were more abundant at the mRNA level in response to hypoxia-induced stationary phase (Fig. 24). In the proteome, while we did not detect the membrane bound hydrogenase, we did observe that three subunits (HoxHGF) of the cytoplasmic hydrogenase were more abundant in the hypoxic samples when compared to the control (Fig. 24).

Nitrogen metabolism

A complete pathway for assimilatory nitrate reduction to ammonia is present in the genome of *M. denitrificans* FJG1, including one NAD(P)H dependent assimilatory nitrate reductase and three copies of the NAD(P)H dependent cytoplasmic nitrite reductase. Although the sole nitrogen source in the batch cultures was NO_3^- (10 mM), the cytoplasmic nitrate reductase was not expressed at the mRNA level during aerobic growth according to our classification scheme (Fig. 22). Nevertheless, the protein was detected at very low levels in every

replicate under oxic conditions (Fig. 23). Of the three cytoplasmic nitrite reductases, only the third copy (*nasB3*) was expressed at both the mRNA and protein level, at a low and intermediate expression level, respectively (Fig. 22 & 23). Two copies of the cytoplasmic NAD(P)H dependent nitrite reductase (*nasB1* and *nasB2*) were not expressed at the mRNA level under oxic conditions but were expressed at intermediate levels in the proteome (Fig. 22 & 23). The protein abundance of the assimilatory, cytoplasmic nitrate reductase decreased in response to hypoxia (Fig. 24). The expression pattern for the ammonia forming nitrite reductase was contradictory between the transcriptome and proteome, with the steady state mRNA more abundant under hypoxia for all three copies and protein levels less abundant when compared to the oxic control for all three copies (Fig. 24).

Glutamine synthase (*gln*) and glutamate synthase (*glt*) homologs were also identified in the complete genome sequence, although glutamate dehydrogenase was not present. These are responsible for ammonia incorporation into amino acids, purines, pyrimidines, and amino sugars. Both the glutamine synthase and glutamate synthase were expressed in the transcriptome and proteome; expression levels for both were higher in the proteome (intermediate to high) than in the transcriptome (very to to intermediate) under oxic conditions (Fig. 22 & 23). The response of glutamine and glutamate synthases to hypoxia was similar to that of the cytoplasmic nitrate and nitrite reductase, with both *gln* and *glt* having a decreased abundance in the proteome (Fig. 24). Interestingly, and similar to the pattern observed for the cytoplasmic nitrite reductase under hypoxic conditions, the steady state mRNA levels of the glutamine synthase contradicted the proteome data.

In addition to a pathway for assimilatory nitrate reduction, the genome of *M. denitrificans* FJG1 encodes a dissimilatory pathway for denitrification. This includes two dissimilatory nitrate

reductases (*narHGJI*, *napABC*), two NO-forming nitrite reductases (*nirK*, *nirS*), and one N_2O-forming cytochrome *c* dependent nitric oxide reductase (*norBC*). It has previously been demonstrated that *M. denitrificans* FJG1 denitrifies by reducing NO_3^- to N_2O at the expense of methane under oxygen depleted conditions (Kits et al., 2015a). During unrestricted aerobic growth, only the nitric oxide reductase was expressed; expression was very low in the transcriptome and low in the proteome (Fig. 22 & 23).

Both dissimilatory nitrate reductases were expressed at higher levels under hypoxia (Fig. 24). The membrane bound, electrogenic nitrate reductase (*narGHJI*) showed increased steady state mRNA levels under hypoxia but was not detected in the proteome (Fig. 24). Conversely, the periplasmic dissimilatory nitrate reductase (*napABC*) did not show elevated mRNA levels but the catalytic NapA subunit was present in significantly higher abundance (4.4 fold) in the hypoxia-induced stationary phase proteome (Fig. 24). Of the two NO-forming nitrite reductases, only the copper-containing NirK responded to hypoxia. Steady state mRNA and protein of the copper containing nitrite reductase was significantly more abundant in the transcriptome (2.8 fold) and proteome (3.4 fold) and, while the periplasmic cytochrome cd_1 containing nitrite reductase was expressed at higher levels in the transcriptome and proteome than NirK, the expression of the cytochrome cd_1 nitrite reductase did not respond to hypoxia (Fig. 24). Finally, responsible for the reduction of NO to N_2O, expression of the nitric oxide reductase (*norBC*) increased in response to hypoxia in the transcriptome and proteome; steady state mRNA abundances of *norB* and *norC* were significantly higher, 2.9 and 3.3 fold respectively, under hypoxia (Fig. 24). We did not detect the membrane bound NorB subunit in the proteome, but NorC protein was 3.4 fold more abundant in the hypoxic samples when compared to the control (Fig. 24).

Storage molecules

The genome of *M. denitrificans* FJG1 contains three copies of bacterioferritin. Under oxic conditions, two are transcribed and translated (Fig. 22 & 23). *Bfr1* and *bfr3* transcripts were at very low and low levels during aerobic growth while *bfr2* was not expressed. Correspondingly, the proteome showed that *bfr1* and *bfr3* proteins were expressed at intermediate levels and that *bfr2* was not expressed at all during aerobic growth. Expression of all three copies of bacterioferritin responded to O_2 deprivation. Steady state mRNA and protein abundance increased for *bfr1* and *bfr2* in response to hypoxia while only the protein abundance increased for *bfr3* (Fig. 24). The second copy (*bfr2*) exhibited the most dynamic change in expression; mRNA abundance was 5.2 fold higher and protein abundance was 15.5 fold higher under hypoxia (Fig. 24). It should, however, be pointed out that the total absolute protein abundance of *bfr1* and *bfr3* were still higher than *bfr2* under hypoxic conditions – though all three proteins were expressed at an intermediate level in the proteome.

Inorganic phosphorus can be stored by bacteria in the form of polyphosphate (poly-P) granules. Polyphosphate is a single linear molecule composed of tens to hundreds of P_i residues which are connected together by energy-rich phosphoanhydride bonds (Achbergerová and Nahálka, 2011). The predominant enzyme responsible for the polymerization and depolymerization of polyphosphate are the polyphosphate kinases (encoded by *ppk*). Many biological roles of polyphosphate storage have been proposed - energy and phosphate storage, biofilm formation, growth and motility - and *ppk* mutants have been shown to be more sensitive to environmental perturbations such as changes in temperature, salt, pH, or exposure to reactive oxygen species (Grillo-Puertas et al., 2012; Rao and Kornberg, 1996; 1999). The genome of *M. denitrificans* encodes one polyphosphate kinase (*ppk*) homolog which is not expressed in the

transcriptome or proteome during aerobic growth (Fig. 22 & 23). However, the protein abundance of the polyphosphate kinase (*ppk*) was stimulated in the proteome under hypoxic conditions 3.8 fold (Fig. 24).

Glycogen is a branched polysaccharide of glucose that functions to store energy and carbon in bacteria as well as animals, often in response to nitrogen limitation (Khadem et al., 2012). The completed genome of *M. denitrificans* FJG1 encodes all genes necessary for glycogen synthesis (*glgA*, *glgB*, *glgC*). All three genes were expressed at a very low level in the transcriptome during oxic growth, while the proteome showed that GlgA and GlgB proteins were expressed at a low abundance (Fig. 22 & 23). The glycogen synthesis genes did not respond at the mRNA or protein level to oxygen deprivation (Fig. 24).

4.5: Discussion

Gene expression and protein identifications

We utilized a combined Illumina RNA-Seq and label-free quantification mass spectrometry (MS) based approach to determine which transcripts and proteins were present under oxic growth and hypoxia-induced stationary phase conditions. Previous proteomic studies on methanotrophic bacteria showed that a label-free quantification approach resulted in a larger number of proteins identified, higher identification confidence, and superior sequence coverage when compared to one-dimensional PAGE and isobaric tags for absolute and relative quantification (iTRAQ)(Patel et al., 2012). Prior proteomic analysis of the soluble protein extracts from *Methylocella silvestris* grown on CH_4 yielded 178 total protein identifications when using a 1D-LC approach and 603 using a 2D-LC approach(Patel et al., 2012). Prior work on *M. silvestris* comparing gel-based, iTRAQ, and label free approaches yielded 425 total protein identifications in the label free approach(Patel et al., 2009). We were able to identify a

significant proportion of the predicted protein coding sequences (40.2%) in all of our samples and our proteome analysis yielded more total protein identifications when compared to previous proteomic studies on pure cultures of methanotrophic bacteria.

Of the expressed transcripts and proteins, hypoxia induced stationary phase altered the expression of the transcriptome more than the proteome; 51.5% of the expressed transcripts were altered in response to the experimental conditions whereas only 36.5% of the quantified proteins were altered in the proteome. Further, the absolute number of open reading frames altered in expression was also greater in the transcriptome than in the proteome (1085 and 669, respectively) in response to hypoxia-induced stationary phase. The ratio of mRNA to protein in a given cell is governed by, among other factors, rates of transcription and translation as well as rates of mRNA and protein degradation. That the transcriptional response to hypoxia is more pronounced than the proteome response suggests that there is some decoupling between the mRNA and protein pools; the observed effect could be due to an increase in the rate of protein degradation, decreased rate of translation, or increased mRNA stability.

To quantitatively investigate how coupled the mRNA and protein pools are under aerobic growth and hypoxia induced stationary phase, we analyzed the protein-to-mRNA expression ratios of 1831 genes that were transcribed and translated under both conditions tested (Fig. 21). We found that there was a weak positive correlation between the mRNA and protein pools for the 1831 genes analyzed during aerobic growth ($R_2 = 0.28$, $R_s = .51$) and hypoxia induced stationary phase ($R^2 = 0.33$, $R_s = .55$) (Fig. 21). These correlation coefficients are lower than those reported for *Escherichia coli* ($R^2 = 0.42$-0.47, $R_s = .64$-$.69$) or *Streptomyces coelicolor* ($R^2 = 0.40$) but similar to values reported for *Desulfovibrio vulgaris* ($R^2 = 0.20$-0.28, $R_s = 0.39$-0.46) (Corbin et al., 2003; de Sousa Abreu et al., 2009; Jayapal et al., 2008; Lu et al., 2007; Nie et al.,

2006). Interestingly, the Pearson and Spearman correlation coefficients for the hypoxic stationary phase cultures are significantly different from the oxic cultures (P = 0.046, 0.048). This suggests, while there is significant decoupling between the mRNA and proteins levels in both tested conditions, that protein expression and mRNA expression corresponded better during hypoxia-induced stationary phase than during oxic growth.

The distribution of transcript and protein expression levels (Fig. 18) also shows that the transcriptome and proteome are decoupled not at just level of single genes but in overall proportional abundance of transcripts and proteins. The very high, high, and low expression levels contain very similar proportional abundances between the transcripts and proteins during oxic growth. However, a much larger proportion of proteins fall into the intermediate protein expression category (12.8%) when compared to the transcriptome (2%) (Fig. 18). And conversely, a much larger proportion of transcripts fall into the very low expression category (34.2%) when compared to the proteome (7.7%) (Fig 18). This discrepancy is likely caused by the generally longer half-life of proteins and very tight transcriptional regulation; once a protein has been made in sufficient quantity, regulatory processes at the transcriptional level generally lead to a rapid decrease in the cognate mRNA pool. Nevertheless, our expression level description scheme for the proteome is in agreement with previously published data; whole transcriptome analysis on *Methylosinus trichosporium* OB3b cultivated on CH_4 under unrestricted growth conditions revealed that the majority of genes fell into the *very low* and *low* expression categories and that less than 3% of total genes fell into the *very high* and *high* expression categories (Matsen et al., 2013).

General KEGG classification of differentially expressed transcripts and proteins

To understand the general response of *M. denitrificans* FJG1 to hypoxia-induced

stationary phase, we classified all of the differentially expressed transcripts and proteins into KEGG categories; the omics data sets were divided into those genes differentially expressed either in the transcriptome or proteome and whether those were stimulated or decreased in response to the experimental condition (Fig. 19 & 20 & Table 3). The genes stimulated under hypoxia are consistent with mixed acid fermentation, denitrification, and cell motility being the prominent responses to O_2 starvation. Some methanotrophic bacteria that can perform formaldehyde-based fermentation use, in addition to other strategies, a complete EMP and TCA cycle to produce various fermentation products under O_2 limitation. The stimulation of TCA cycle and pyruvate metabolism in hypoxic cultures of *M. denitrificans* FJG1 suggests that this organism may also use a formaldehyde-based fermentation metabolism when O_2 is scarce (Table 3). The stimulation of cell motility and two-component signaling system genes under hypoxia-induced stationary phase suggests that *M. denitrificans* FJG1 cells sense their environment for O_2 and upregulate flagella synthesis genes in response to O_2 limitation, presumably to locate more of the substrate that is necessary for CH_4 oxidation and respiration (Table 3 & 4). Denitrification – in this case NO_3^- respiration to N_2O - occurs in O_2 limited cultures of *M. denitrificans* FJG1 as long as NO_3^- is present (Kits et al., 2015b). The hypoxia-induced denitrification metabolism of *M. denitrificans* FJG1 likely explains the greater abundance of stimulated genes in the nitrogen metabolism category (Fig. 20 & Table 3).

The genes depressed under hypoxia-induced stationary phase in *M. denitrificans* FJG1 are all consistent with a slowdown in growth and all cellular processes needed for cell division – such as amino acid synthesis, DNA replication, translation, and DNA repair (Table 3 & 4). The doubling time of *Methylomicrobium alcaliphilum* 20Z was reported to be 23 hours in continuous culture at a dissolved O_2 level of 0.0-0.1%. This is about an order of magnitude slower than

unrestricted growth under oxic conditions for this bacterium. Such a significant decrease in doubling time requires a much slower rate of translation, protein synthesis, and DNA replication & repair. We did not observe cell division in our batch cultures after O_2 depletion, likely because of the nature of batch culture (i.e. no CH_4/O_2 were added to the bottles after O_2 became limiting) and because we only observed the cultures for a short time (48 h) after transition to stationary phase became evident.

Carbohydrate metabolism: RuMP cycle

Aerobic methanotrophs belonging to the phylum Gammaproteobacteria generally fix carbon at the level of formaldehyde using the ribulose monophosphate (RuMP) pathway. However, some Gammaproteobacterial methanotrophs have and can utilize the entire Serine pathway into addition to the RuMP pathway. Within the RuMP cycle, there are two variants for the cleavage of fructose-6-phosphate into two C-3 compounds – the Fructose bisphosphate aldolase (FBPA) pathway and the 2-keto-3-deoxy-6-phosphogluconate (KDPG) pathway – and two different variants for the sugar rearrangements that lead to the regeneration of the CH_2O accepting molecule – the transaldolase pathway and the sedoheptulose-1,7-bisphosphate aldolase pathway. This means that, even in Gammaproteobacterial methanotrophs that only encode the RuMP pathway, four variants of the RuMP pathway are possible.

Though both the FBPA and KDPG pathways are encoded in the genome of *M. denitrificans* FJG1, the transcriptome and proteome data suggests that the FBPA is the main route for the cleavage of fructose-6-phosphate and that the TA pathway is the only route for the regeneration of RuMP (Fig. 22 & 23). The genome of *Methylomicrobium buryatense* 5G also encodes both the FBPA and KDPG pathways and transcriptome analysis on cultures grown under unrestricted aerobic growth correspondingly showed that the FBPA pathway is also the

main route for the cleavage of F6P in this organism (la Torre et al., 2015). Similarly, the proteome of *Methylococcus capsulatus* Bath also suggested that it mainly uses the FBPA pathway for F6P cleavage; all of the proteins for the FBPA pathway were identified in the proteome whereas several of the key proteins for the KDPG pathway were not identified in the proteome (Kao et al., 2004).

At hypoxia induced stationary phase, the differential analysis of the transcriptome and proteome of *M. denitrificans* FJG1 suggest that the first two steps of the RuMP cycle – CH_2O + RuMP →→→ G3P + DHAP – are slower (Fig. 24). This is consistent with slowed or stopped growth that we observed under these conditions, as less carbon would have to be fixed into biomass under these circumstances. The increased abundance of a second copy of the glucose phosphate dehydrogenase may reflect an increase in the amount of carbon flowing through the KDPG pathway during O_2 limitation; however, none of the other transcripts or enzymes of the KDPG pathway were upregulated (Fig. 24).

Carbohydrate metabolism: Entner-Doudoroff and Embden-Meyerhof-Parnas

Expression levels of all the genes of the ED and EMP pathways at the transcript and protein levels indicate that both routes are used by *M. denitrificans* FJG1 for C-1 assimilation (Fig. 22 & 23). The higher protein abundance of the EMP pathway enzymes suggests that EMP is the main route for C-1 assimilation in *M. denitrificans* FJG1. Previous work has confirmed that in *M. alcaliphilum* 20Z most of cellular pyruvate originates from the EMP pathway during growth on CH_4 and that EMP is indeed the main pathway for CH_2O assimilation (Kalyuzhnaya et al., 2013). Our results suggest that this is also the case for *M. denitrificans* FJG1 and that the dominance of the EMP pathway over the ED pathway for C1 assimilation is not restricted to the genus *Methylomicrobium*.

Carbohydrate metabolism: pyruvate metabolism, Krebs cycle, fermentation

It was previously considered that obligate methanotrophic bacteria belonging to the phylum Gammaproteobacteria had multiple enzyme lesions in central carbon pathways that restricted growth and biosynthesis (Trotsenko and Murrell, 2008). The critical lesions included pyruvate kinase, α-ketogluterate dehydrogenase, PEP-synthase, and pyruvate phosphate dikinase (Trotsenko and Murrell, 2008). The absence of α-ketogluterate dehydrogenase meant that Gammaproteobacterial methanotrophs were thought to have an incomplete TCA cycle; in this case the two incomplete branches of the TCA cycle performed an anabolic role for the generation of various amino acids and porphyrins. More recently, however, the presence and activity of α-ketogluterate dehydrogenase has been confirmed in *Methylococcus capsulatus* Bath, *M. alcaliphilum* 20Z, *M. buryatense* 5G, and several other methanotrophs (Kalyuzhnaya et al., 2013; la Torre et al., 2015; Ward et al., 2004). However, little is known about pyruvate metabolism in obligate methanotrophs.

The mRNA and protein from *M. denitrificans* FJG1 cultivated under oxic conditions suggest that the pyruvate dehydrogenase complex is the main route for pyruvate decarboxylation to acetyl-CoA during aerobic growth (Fig. 23). Pyruvate dehydrogenase is generally the enzyme used by aerobic organisms for pyruvate decarboxylation; the NADH produced during the reaction is disadvantageous to fermenting bacteria due to the lack of an externally provided terminal electron acceptor (Clark, 1989). Anaerobic bacteria usually utilize the pyruvate ferredoxin oxidoreductase and/or pyruvate formate lyase for pyruvate decarboxylation; both of which are present in the genome of *M. denitrificans* FJG1 (Gelius Dietrich and Henze, 2004; Knappe and Sawers, 1990). Use of the pyruvate formate lyase is especially advantageous to fermenting bacteria because neither reduced ferredoxin nor NADH are produced in this reaction,

allowing the extra electrons to be dumped as a part of formate. Interestingly, the differential proteome data suggests that pyruvate formate lyase and pyruvate ferredoxin oxidoreductase may be contributing significantly to pyruvate decarboxylation during hypoxic conditions and that formate may be a produced directly from pyruvate to facilitate the expenditure of electrons under formaldehyde-fermenting conditions (Fig. 24).

Fermenting bacteria often utilize the PTA-ACK (**p**hospha**t**e **a**cetyl transferase-**ac**etate **k**inase) for the oxidation of pyruvate to acetate to make ATP and then excrete the produced acetate into the medium. Acetate was previously identified as one of the main fermentation products in *M. alcaliphilum* 20Z and has also been detected in the metabolome of *M. buryatense* 5G (Kalyuzhnaya et al., 2013; la Torre et al., 2015). The proteome of *M. denitrificans* FJG1 suggests that acetate is made through the PTA-ACK system as a part of the excreted fermentation products in response to hypoxia induced stationary phase (Fig. 24).

Both the transcriptome and proteome suggest that a complete TCA cycle is operational during aerobic growth in *M. denitrificans* FJG1. The differential transcriptome and proteome analysis actually suggests that more carbon is flowing through the TCA cycle under hypoxic stationary phase than during aerobic growth and that oxaloacetate is replenished from pyruvate (via pyruvate carboxylase) during O_2 limitation and from PEP (via PEP carboxylase) during aerobic growth (Fig. 24). It is unusual to find both genes for oxaloactetate replenishment in one organism and it seems that *M. denitrificans* FJG1 may use one preferentially over the other during O_2 starvation.

To our knowledge, very few studies have so far addressed the diversity of fermentation products that are excreted by aerobic methanotrophs during formaldehyde-fermentation. Formate, acetate, succinate, H_2, 3-hydroxyburyrate, and lactate have previously been reported as

fermentation products in *Methylomicrobium* species (Kalyuzhnaya et al., 2013). The annotation of a pyruvate decarboxylase and three alcohol dehydrogenases in the genome of *M. denitrificans* FJG1 opened the possibility of formaldehyde fermentation to ethanol (Fig. 24). Pyruvate decarboxylase is rarely found in bacteria, the enzyme of *Zymomonas mobilis* being perhaps the best characterized, but is quite common in eukaryotes and used by yeast during ethanol fermentation to decarboxylase pyruvate to CO_2 and acetaldehyde (Dobritzsch et al., 1998; Eram and Ma, 2013). The significantly increased abundance of the putative pyruvate decarboxylase and two alcohol dehydrogenases in response to hypoxia induced stationary phase suggests that ethanol may be an end product of formaldehyde fermentation in *M. denitrificans* FJG1 (Fig. 24). Conversion of CH_4 to ethanol by aerobic methanotrophic bacteria may be noteworthy for the microbial production of liquid biofuels from single carbon sources; currently we are unaware of another microbial source for bioethanol production from CH_4 gas.

Energy metabolism: C1 oxidation – CH_4 to CO_2

It is typical for the first two steps for the oxidation of CH_4, catalyzed by methane monooxygenase and methanol dehydrogenase respectively, to have very high expression. Previous studies have shown that *pmoCAB* transcripts can make up 12-21% of all mapped reads and a significantly smaller proportion of the (6-7%) of the total identified protein (Dalton, 1977; la Torre et al., 2015; Matsen et al., 2013; Patel et al., 2009). The transcriptome and proteome of *M. denitrificans* FJG1 is consistent with these previous observations, though the PmoCAB peptides made up only ~1.3% of the total identified protein in our study perhaps due to the greater amount of total protein identifications. The asymmetrical response of pMMO transcripts and proteins under hypoxia may be a result of a reduced rate of protein degradation, decreased rate of transcription, or increased rate of mRNA degradation. Presumably, since cell division has

slowed greatly or stopped altogether after O_2 depletion, very limited pMMO synthesis is required. However, the significant change in the pool of the transcripts and protein implies that at least two of the processes mentioned previously occur during hypoxia. The increased protein abundance of pMMO and both methanol dehydrogenases in response to hypoxia-induced stationary phase suggests that the cells become physiologically poised to consume CH_4 and O_2 when substrate availability increases. This is consistent with previous observations in an isolated methanotrophic strain WP12 which showed no measureable decrease in intracellular protein after even 10 days of anaerobic starvation while during the same period aerobically starved cells degraded 24% of intracellular protein (Roslev and King, 1995). Similarly, methanotrophic strain WP12, *Methylomicrobium album* BG8, and *Methylocystis trichosporium* OB3b had a much greater capacity (by 35%) for CH_4 oxidation after 10 days of anaerobic starvation when compared to the same period of aerobic starvation (Roslev and King, 1995).

Energy metabolism: oxidative phosphorylation

Whole transcriptome analysis on formaldehyde fermenting cells of *M. alcaliphilum* 20Z demonstrated significant downregulation of the NADH:ubiquinone oxidoreductase and cytochrome *c* oxidase. Contrastingly, we did not observe downregulation of complex I or IV in hypoxic cultures of *M. denitrificans* FJG1 at the mRNA or protein levels (Fig. 24). The differential transcriptome and proteome both demonstrate that the cytochrome *c* oxidase is more abundant during hypoxia and that the expression of the high affinity cytochrome *bd* ubiquinol oxidase does not change (Fig. 24). This may well be due to the different physiological state of the cells in our study; we utilized a batch culture approach where the cells are O_2 starved in stationary phase while others have employed a continuous culture approach during which dissolved O_2 levels are maintained at $\leq 0.1\%$. However, the downregulation of ATP synthase at

both the mRNA and proteins levels suggests that, during hypoxia, substrate level phosphorylation may be of increasing importance for the re-oxidation of reduced cellular cofactors (i.e. NADH) relative to respiration using an exogenous terminal electron acceptor (Fig. 24).

Energy metabolism: Hydrogenases

Hydrogen production and uptake in both the membrane and soluble fractions have been confirmed and the structural genes for the membrane bound hydrogenase characterized in *Methylococcus capsulatus* Bath (Csáki et al., 2001; Hanczár et al., 2002). The completed genome sequence revealed that three hydrogenases – the formatehydrogen lyase complex, the [NiFe] membrane bound hydrogenase, and the cytoplasmic [NiFe] NAD^+ reducing hydrogenase – were present in the genome of *M. capsulatus* Bath (Ward et al., 2004). While it is accepted that the membrane bound hydrogenase in *M. capsulatus* Bath functions as an uptake hydrogenase *in vivo*, the *in vivo* function of the cytoplasmic hydrogenase is not known. H_2 production in *M. capsulatus* Bath is likely accomplished through nitrogenase activity, which forms H_2 as a byproduct of N_2 fixation, and activity of the cytoplasmic hydrogenase, which can apparently accept electrons from NADH to produce H_2 (Hanczár et al., 2002).

Nevertheless, robust H_2 production has been observed in methanotrophs that lack a nitrogenase. In *M. alcaliphilum* 20Z, significant amounts of H_2 (2.2 ± 0.4 mM) accumulated during CH_4 dependent fermentative metabolism (Kalyuzhnaya et al., 2013). Analysis of the *M. alcaliphilum* 20Z transcriptome showed that the cytoplasmic NAD^+ reducing hydrogenase was significantly upregulated under microaerobic conditions (Kalyuzhnaya et al., 2013). Stimulation of the membrane bound and cytoplasmic hydrogenase in *M. denitrificans* FJG1 during hypoxia-induced stationary phase suggests that hydrogen is a fermentation product during low-oxygen

metabolism (Fig. 24).

Nitrogen metabolism

The general decrease in the abundance of transcripts and proteins belonging to the pathway for assimilatory nitrate reduction to ammonia during O_2 limitation is consistent with previous KEGG classification data. The massive slowdown or stoppage of growth results in lower expression of assimilatory pathways that are needed for the synthesis of cellular components such as amino acids and DNA. Interestingly, mRNA and protein levels for many of the nitrogen assimilation conversions including all three copies of the assimilatory nitrite reductase and the glutamine synthase are not congruent. A large increase in the stability of the proteins even if the mRNA pool is relatively small may explain this observation, though the present data set cannot explain the regulatory mechanism in this instance.

Previous work on respiratory nitrate reduction in *M. denitrificans* FJG1 showed that steady state mRNA levels of the respiratory electrogenic nitrate reductase (*narGHJI*), copper-containing nitrite reductase (*nirK*), and cytochrome *c* linked nitric oxide reductase (*norBC*) increase in response to hypoxia if NO_3^- is present (Kits et al., 2015b). The proteome presented here confirms that the NirK and NorC are expressed at the protein level and that those proteins are upregulated in response to hypoxia (Fig. 24). Taken together with the increased abundance of the periplasmic nitrate reductase NapA protein in the hypoxic cultures, we conclude that a complete denitrification pathway for the respiration of NO_3^- to N_2O is expressed at the protein level and upregulated in response to hypoxia (Fig. 24). Though only *narGHJI* but not *napABC* responded at the transcript level to hypoxia, we only identified the periplasmic nitrate reductase in the proteome. This may be due to the nature of the NarGHI complex being membrane bound; membrane bound proteins often present challenges as they are frequently present in lower

abundance and can be difficult to solubilize (Fischer et al., 2006). Separate proteomic analyses of *Mycobacterium tuberculosis* culture filtrate, whole cell lysate, and membrane fraction succeeded in identifying NarGHI in only the enriched membrane fraction (de Souza et al., 2011). It was previously thought that only one respiratory nitrate reductase is active in *M. denitrificans* FJG1 during O_2 limitation. However, the proteomic analysis here opens up the possibility that both respiratory nitrate reductases may be active.

Storage molecules

Bacterioferritins (BFRs) are a member of the ferritin family of proteins that store large quantities of iron in the cytoplasm by reducing hydrated Fe^{2+} to Fe^{3+} which is insoluble under physiological conditions (10^{-18} M) (Carrondo, 2003). Canonically, it was hypothesized that the principal role of BFRs is to supply cells with required iron when external supply of iron is limited(Le Brun et al., 1995). However, recently it has emerged that BFRs play a critical role in the maintenance of iron homeostasis in aerobic organisms (Honarmand Ebrahimi et al., 2015). Organisms that use iron under oxic conditions require a mechanism to remove free Fe^{2+}, which spontaneously reacts with O_2 to form toxic reactive oxygen species (ROS) that cause oxidative damage to the cell (Wahlgren et al., 2012). Unexpectedly, all three copies of Bfr in the genome of *M. denitrificans* FJG1 respond significantly to hypoxia induced stationary phase despite the low availability of O_2 and high availability of iron in the culture medium (Fig. 24). Indeed, the significantly decreased abundance of ROS detoxification mechanisms such as the superoxide dismutase (Sod) and catalase (Kat) proteins demonstrates that oxidative stress is diminished under hypoxic conditions when compared to oxic growth (Fig. 24). In fact, utilization of BfrS under these conditions to convert Fe^{2+} to Fe^{3+} would titrate valuable O_2 away from the pMMO and complex IV. One possibility is that Bfrs increase in expression as a result of slowed/stopped

growth and this may act as a physiological starvation signal for the cell to start storing iron.

The presence of polyphosphate granules has been reported in various aerobic methanotrophs belonging to phyla Gammaproteobacteria, Alphaproteobacteria, and Verrucomicrobia (Calhoun and King, 1998; Lindner et al., 2007; van Teeseling et al., 2014). *Methylomonas methanica* accumulates up to 5.73 mg/g dry weight of mostly high molecular weight (>20 $PolyP_i$) polyphosphate, which is similar to values reported for *E. coli* (Trotsenko and Shishkina, 1990). To our knowledge, the expression of polyphosphate and its relevance during hypoxia or stationary phase in methanotrophic bacteria has not been studied before. While the exact physiological function of polyphosphate in methanotrophs is not known, for *E. coli* polyphosphate enhances stationary phase survival and resistance, promotes the degradation of ribosomal proteins, and is necessary for biofilm formation during stationary phase (Grillo-Puertas et al., 2012; Kuroda et al., 2001; Rao and Kornberg, 1996). Taken together, the significant upregulation of polyphosphate kinase in the proteome during hypoxia induced stationary phase is likely a response to promote survival during starvation (Fig. 24).

Conclusions

We utilized both RNA-Seq and label free protein quantification to assess the physiological response of a denitrifying methanotroph – *M. denitrificans* FJG1 – to hypoxia-induced stationary phase. The data from this study expands current knowledge on the strategies that obligate aerobic methanotrophs utilize to overcome O_2 scarcity. While some of our observations match well with previous literature, we also characterized several new processes. Here we demonstrate that:

1) The agreement between the mRNA and protein pools in aerobic methanotrophs may be significantly lower than for classical bacterial models (i.e. *E. coli*).

2) The EMP pathway is likely the main route for C-1 assimilation in *M. denitrificans* FJG1.
3) The importance of pyruvate ferredoxin oxidoreductase and pyruvate formate lyase is intensified relative to pyruvate dehydrogenase under low O_2 conditions, likely to facilitate the expenditure of electrons through the direct production of CHOOH from pyruvate.
4) Oxaloacetate is likely replenished mainly from pyruvate during O_2 limitation (by pyruvate carboxylase) and mostly from PEP (by PEP carboxylase) during aerobic growth.
5) Terminal reductases (i.e. Nar, Nap, Nir, Nor) are expressed at the mRNA and protein level in addition to the terminal oxidase, rather than in place of.
6) Enzymes encoding denitrification machinery (NapA, NirK, NorC) are expressed in the proteome during denitrifying conditions.
7) *M. denitrificans* FJG1 carries out formaldehyde-based fermentation and denitrification simultaneously – the likely fermentation products we identified are formate, acetate, succinate, H_2, and ethanol.
8) Bacterioferritin and polyphosphate kinase, the functions of which has not previously been studied in methanotrophs, are utilized by *M. denitrificans* FJG1, especially under hypoxia-induced stationary phase.

Acknowledgements:

This work was supported by a grant to L.Y.S. from the Natural Sciences and Engineering Research Council of Canada (RGPIN-2014-03745), fellowship support to K.D.K. from Alberta Innovates Technology Futures, and an NSERC Banting Postdoctoral Fellowship to Manuel Kleiner. We would also like to thank Dr. Marc Strous for access to the proteomics equipment. The purchase of the proteomics equipment was supported by a grant of the Canadian Foundation

for Innovation to Marc Strous.

4.6: Tables and Figures

Transcriptome classification				
	Description of expression level	TPM range	% Orfs	# Orfs
>5000	very high	very high	0.3%	16
1000-5000	high	high	1.8%	82
500-1000	intermediate	intermediate	2.0%	94
200-1000	low	low	6.8%	319
50-200	very low	very low	34.2%	1597
0-50	not expressed	not expressed	54.8%	2556
			100.0%	4664
Proteome classification				
	Description of expression level	NSAFx10,000 range	% Orfs	# Orfs
>50	very high	very high	0.3%	14
20->50	high	high	1.7%	77
4->20	intermediate	intermediate	12.8%	596
2->4	low	low	8.6%	400
1->2	very low	very low	7.7%	359
<1	not expressed	not expressed	8.3%	385
ND	not detected	not detected	60.7%	2833
			100.0%	4664

Figure 18: **Classification of transcript and protein expression levels based on TPM and NSAFx10,000 values from mRNA and total protein extracted from aerobic cultures of *Methylomonas denitrificans* FJG1.**

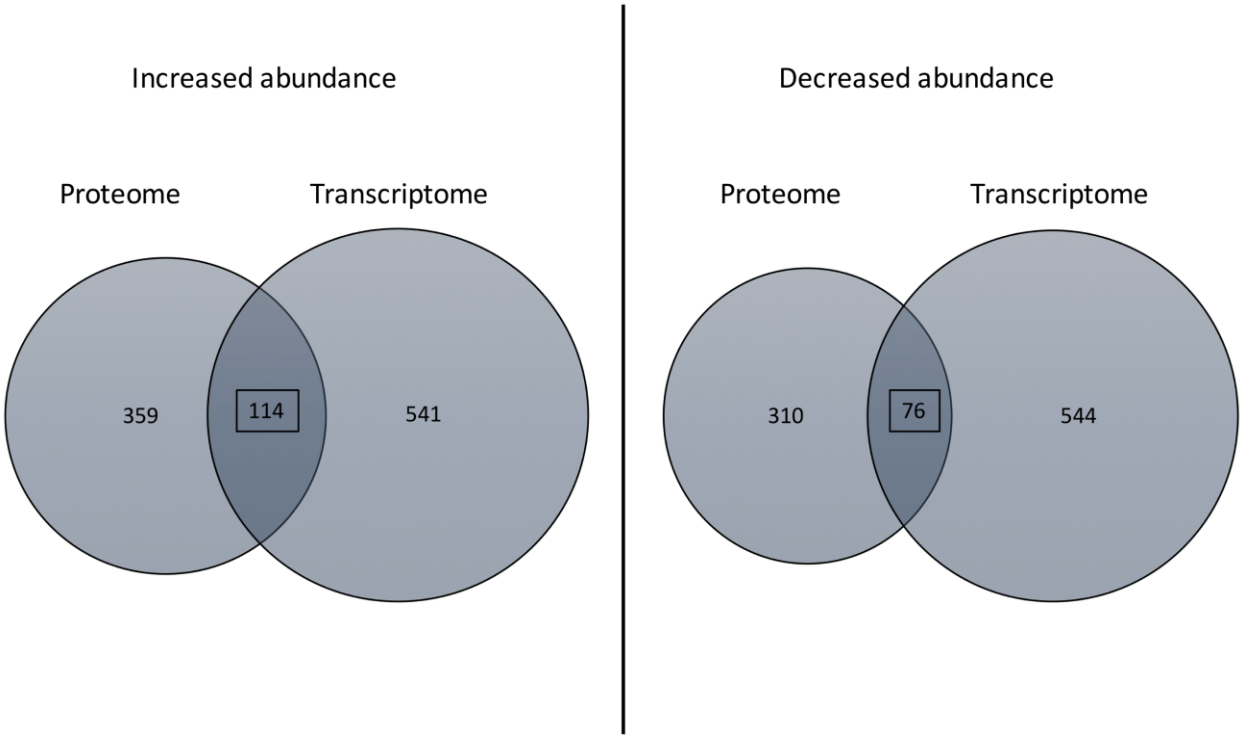

Figure 19: **Overlap of differentially expressed transcripts and proteins identified in the transcriptome and proteome of *Methylomonas denitrificans* FJG1 cultivated under hypoxic conditions.**

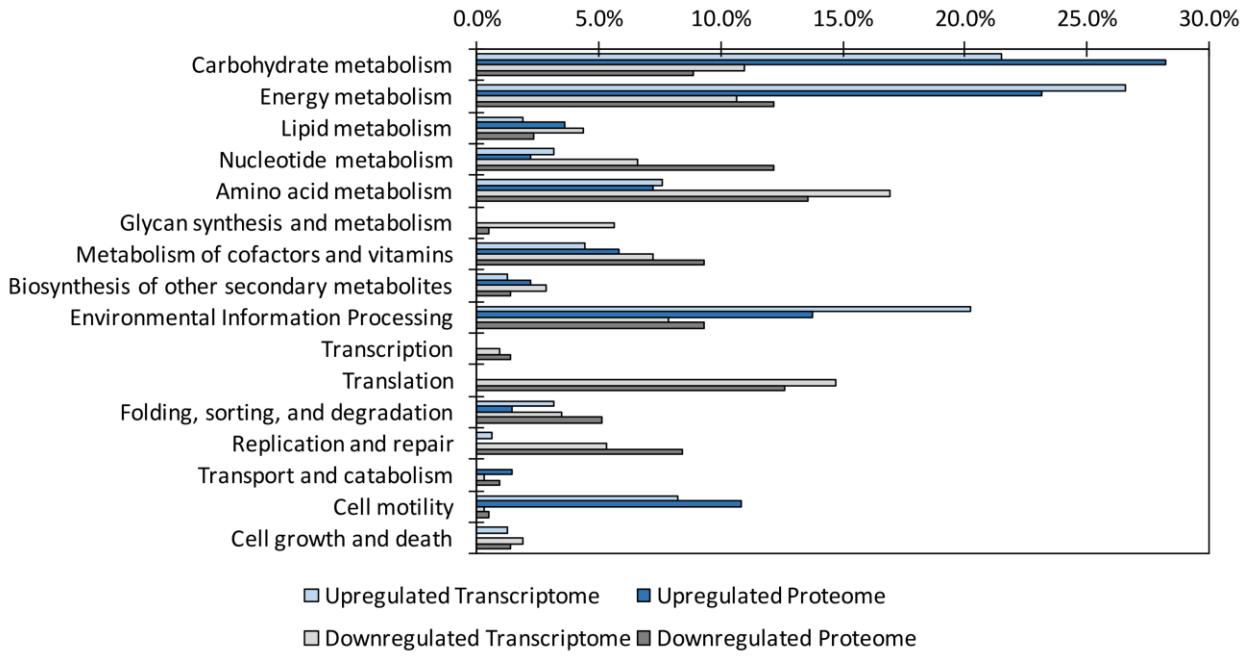

Figure 20: **KEGG classification of differentially expressed transcripts and proteins identified in hypoxic replicate cultures of *Methylomonas denitrificans* FJG1.**

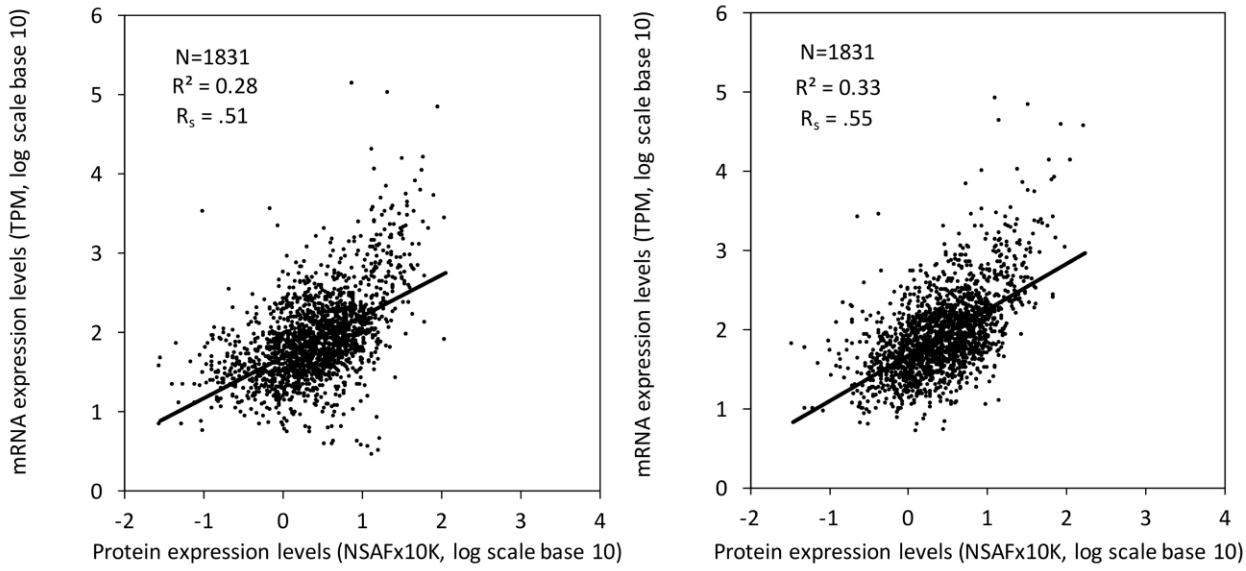

Figure 21: **Correlation between protein expression and mRNA expression levels during aerobic growth and hypoxia for 1831 protein coding genes from *Methylomonas denitrificans* FJG1.**

The R_s and R^2 values represent, respectively, the Spearman Correlation coefficient and the square of the Pearson Correlation coefficient.

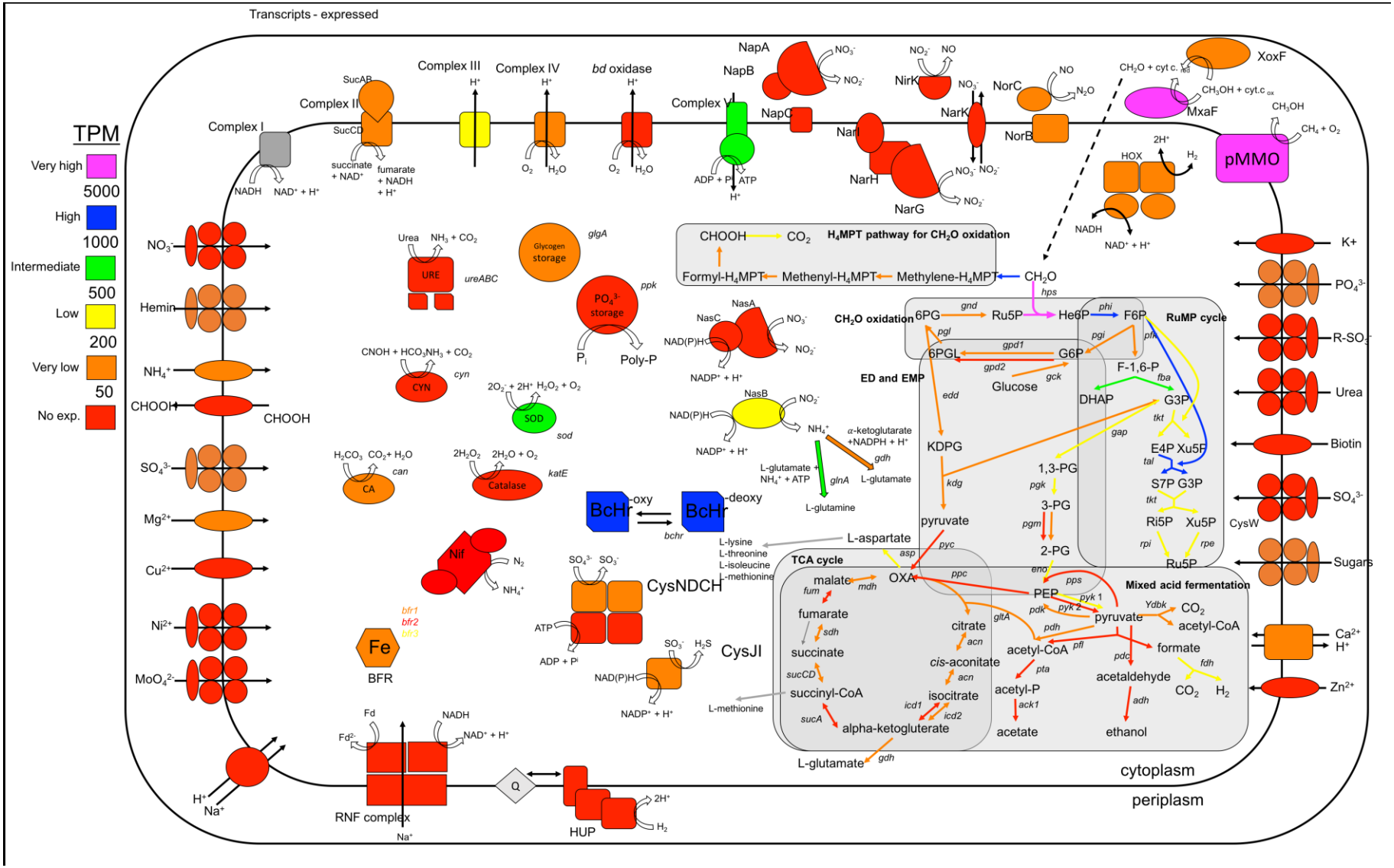
Transcripts - expressed
TPM
Very high
5000
High
1000
Intermediate
500
Low
200
Very low
50
No exp.
Complex I
Complex II
Complex III
Complex IV
bd oxidase
Complex V
NapA
NapB
NapC
NirK
NorC
NorB
NarI
NarK
NarH
NarG
XoxF
MxaF
pMMO
HOX
NADH
NAD+ + H+
succinate + NAD+
fumarate + NADH + H+
ADP + Pi
ATP
NO3-
NO2-
NO
N2O
CH4 + O2
CH3OH
CH2O + cyt c red
CH3OH + cyt.c ox
2H+
H2
O2
H2O
NO3-
Hemin
NH4+
CHOOH
SO4 3-
Mg2+
Cu2+
Ni2+
MoO4 2-
K+
PO4 3-
R-SO3-
Urea
Biotin
SO4 3-
CysW
Sugars
Ca2+
H+
Zn2+
Urea
NH3 + CO2
URE
ureABC
Glycogen storage
glgA
PO4 3- storage
ppk
Pi
Poly-P
CNOH + HCO3NH3 + CO2
CYN
cyn
2O2- + 2H+ H2O2 + O2
SOD
sod
H2CO3 CO2+ H2O
CA
can
2H2O2 2H2O + O2
Catalase
katE
NasA
NasC
NasB
NAD(P)H
NADP+ + H+
NH4+
α-ketoglutarate +NADPH + H+
gdh
L-glutamate
L-glutamate + NH4+ + ATP
glnA
L-glutamine
BcHr-oxy
BcHr-deoxy
bchr
L-lysine
L-threonine
L-isoleucine
L-methionine
L-aspartate
asp
Nif
N2
NH4+
bfr1
bfr2
bfr3
Fe
BFR
SO4 3- SO3-
CysNDCH
ATP
ADP + Pi
SO3- H2S
CysJI
L-methionine
Fd
Fd2-
NADH
NAD+ + H+
RNF complex
Na+
H+
Na+
Q
HUP
2H+
H2
CHOOH
CO2
H4MPT pathway for CH2O oxidation
Formyl-H4MPT
Methenyl-H4MPT
Methylene-H4MPT
CH2O
hps
CH2O oxidation
6PG
gnd
Ru5P
He6P
phi
F6P
RuMP cycle
pgl
pgi
6PGL
gpd1
G6P
ED and EMP
gpd2
gck
Glucose
F-1,6-P
fba
DHAP
G3P
edd
tkt
gap
KDPG
E4P Xu5P
tal
kdg
1,3-PG
pgk
S7P G3P
tkt
3-PG
pgm
Ri5P Xu5P
2-PG
rpi
rpe
Ru5P
eno
pyruvate
pyc
ppc
pps
TCA cycle
malate
mdh
fum
OXA
PEP
pyk 1
pyk 2
Mixed acid fermentation
Ydbk
CO2
pdh
pyruvate
acetyl-CoA
fumarate
sdh
gltA
citrate
acn
pfl
formate
succinate
sucCD
cis-aconitate
acn
pta
pdc
fdh
acetaldehyde
CO2
H2
succinyl-CoA
isocitrate
acetyl-P
ack1
sucA
icd1
icd2
adh
alpha-ketogluterate
acetate
ethanol
L-glutamate
gdh
cytoplasm
periplasm

Figure 22: **Cellular diagram representing steady state mRNA levels of major metabolic pathways in *Methylomonas denitrificans* FJG1 during aerobic growth.**

Colors represent the steady state mRNA levels (in TPM) for predicted gene products; red – not expressed, orange – very low expression, yellow – low expression, green – intermediate expression, blue – high expression, purple – very high expression.

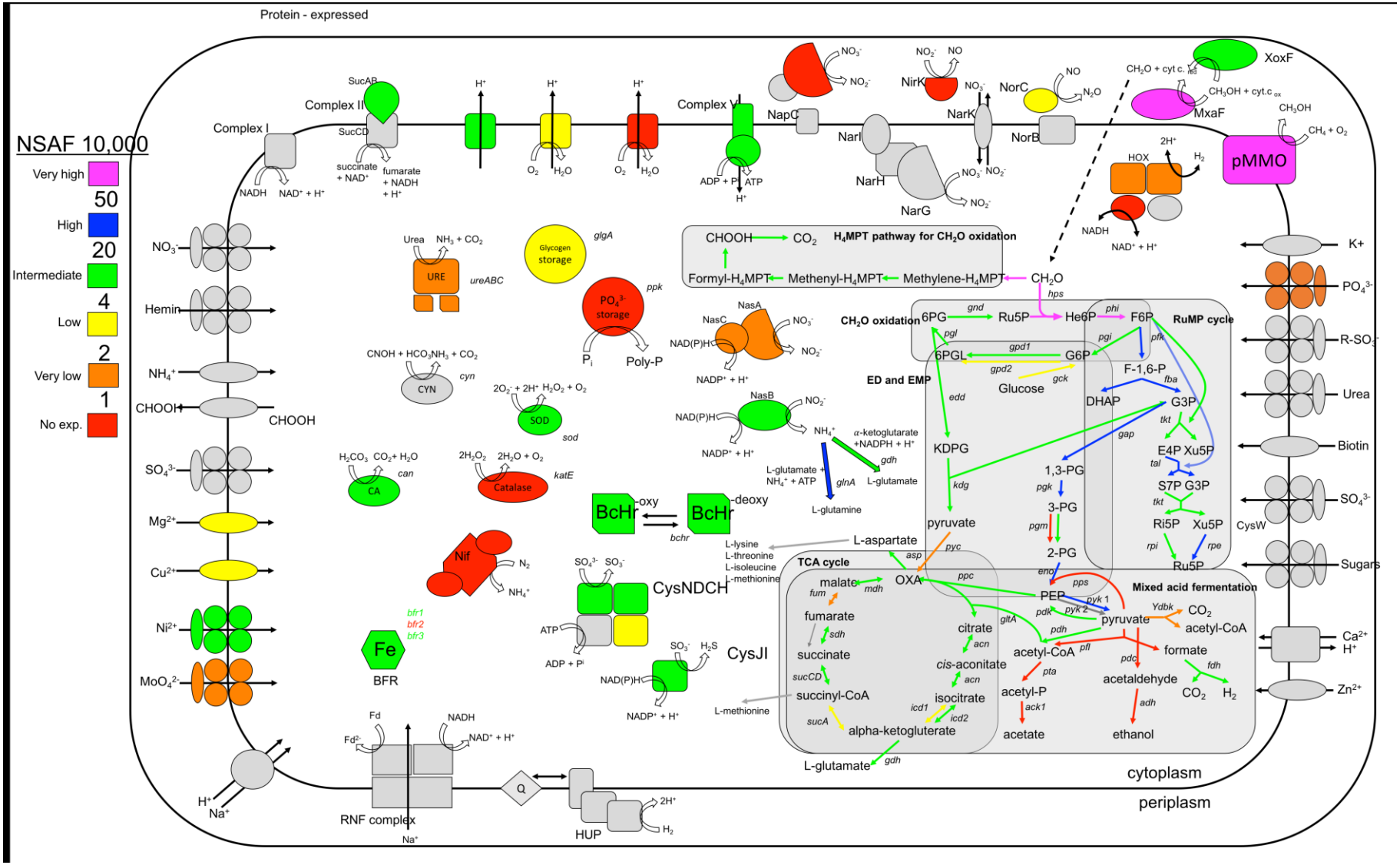
Protein - expressed
NSAF 10,000
Very high
50
High
20
Intermediate
4
Low
2
Very low
1
No exp.
Complex I
Complex II
Complex V
SucAB
SucCD
succinate + NAD+
fumarate + NADH + H+
NADH
NAD+ + H+
ADP + Pi
ATP
NapC
NarI
NarH
NarG
NarK
NirK
NorC
NorB
XoxF
MxaF
pMMO
HOX
CH2O + cyt c red
CH3OH + cyt.c ox
CH3OH
CH4 + O2
NO3-
NO2-
NO
N2O
H2O
O2
H+
2H+
H2
K+
PO4 3-
R-SO3-
Urea
Biotin
SO4 3-
CysW
Sugars
Ca2+
Zn2+
Mg2+
Cu2+
Ni2+
MoO4 2-
Hemin
NH4+
CHOOH
Urea
NH3 + CO2
URE
ureABC
Glycogen storage
glgA
PO4 3- storage
ppk
Poly-P
Pi
CNOH + HCO3NH3 + CO2
CYN
cyn
2O2- + 2H+ H2O2 + O2
SOD
sod
H2CO3 CO2+ H2O
CA
can
2H2O2 2H2O + O2
Catalase
katE
NasA
NasC
NasB
NAD(P)H
NADP+ + H+
NO2-
NO3-
CHOOH
CO2
H4MPT pathway for CH2O oxidation
Formyl-H4MPT
Methenyl-H4MPT
Methylene-H4MPT
CH2O
hps
CH2O oxidation
6PG
gnd
Ru5P
He6P
phi
F6P
RuMP cycle
pgl
pgi
pfk
6PGL
gpd1
G6P
gpd2
gck
Glucose
ED and EMP
F-1,6-P
fba
DHAP
G3P
edd
KDPG
tkt
gap
E4P Xu5P
tal
1,3-PG
kdg
pgk
S7P G3P
3-PG
pgm
tkt
Ri5P Xu5P
2-PG
rpi
rpe
Ru5P
pyruvate
pyc
asp
L-aspartate
eno
ppc
pps
PEP
pyk 1
pyk 2
pdk
pdh
Mixed acid fermentation
Ydbk
CO2
acetyl-CoA
pyruvate
pfl
formate
pdc
fdh
acetaldehyde
CO2
H2
adh
ethanol
acetyl-P
pta
ack1
acetate
TCA cycle
malate
mdh
fum
OXA
fumarate
sdh
gltA
citrate
acn
succinate
cis-aconitate
acn
sucCD
succinyl-CoA
isocitrate
icd1
icd2
sucA
alpha-ketogluterate
gdh
L-glutamate
α-ketoglutarate +NADPH + H+
L-glutamate + NH4+ + ATP
glnA
L-glutamine
gdh
L-glutamate
L-lysine
L-threonine
L-isoleucine
L-methionine
BcHr-oxy
BcHr-deoxy
bchr
Nif
N2
NH4+
Fe
BFR
bfr1
bfr2
bfr3
SO4 3- SO3-
CysNDCH
ATP
ADP + Pi
SO3- H2S
CysJI
L-methionine
Fd
Fd2-
NADH
NAD+ + H+
RNF complex
Na+
H+
Q
HUP
2H+
H2
cytoplasm
periplasm

Figure 23: **Cellular diagram representing steady state protein levels for major metabolic pathways in *Methylomonas denitrificans* FJG1 during aerobic growth.**

Proteins identified in the 1D-LC-MS/MS are highlighted in colors other than grey; proteins/pathways in grey were not identified in our analysis. Colors represent the steady state protein levels (in NSAFx10K) for predicted gene products; red – not expressed, orange – very low expression, yellow – low expression, green – intermediate expression, blue – high expression, purple – very high expression.

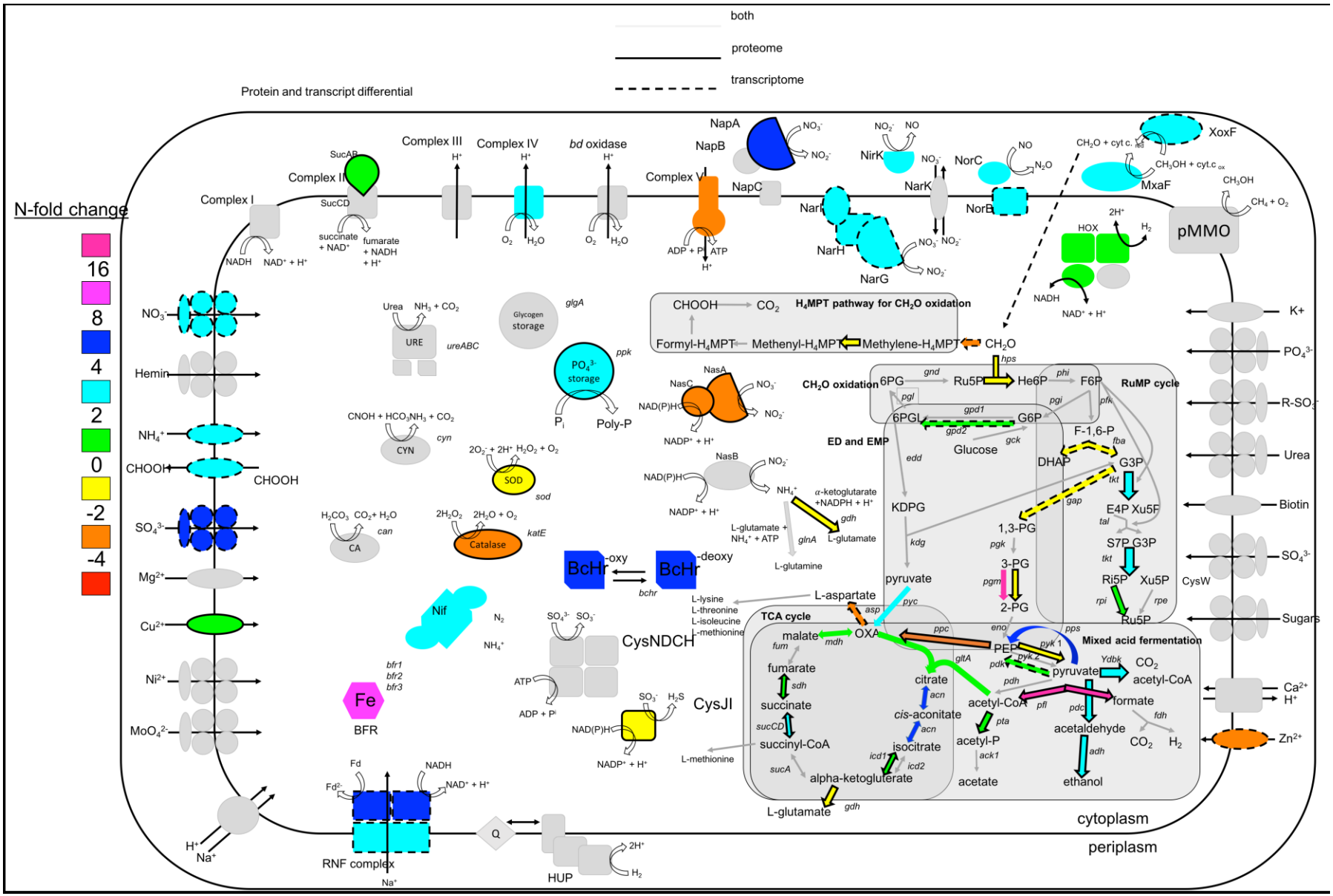
both
proteome
transcriptome
Protein and transcript differential
N-fold change
16
8
4
2
0
-2
-4
Complex I
Complex II
SucAB
SucCD
Complex III
Complex IV
bd oxidase
Complex V
NapA
NapB
NapC
NirK
NarK
NarI
NarH
NarG
NorC
NorB
XoxF
MxaF
pMMO
HOX
CH4 + O2
CH3OH
CH2O + cyt c. red
CH3OH + cyt.c ox
succinate + NAD+
fumarate + NADH + H+
NADH
NAD+ + H+
ADP + Pi
ATP
O2
H2O
H+
2H+
H2
NO3-
NO2-
NO
N2O
Urea
NH3 + CO2
URE
ureABC
Glycogen storage
glgA
PO4 3- storage
ppk
Poly-P
Pi
CNOH + HCO3NH3 + CO2
CYN
cyn
2O2- + 2H+ H2O2 + O2
SOD
sod
H2CO3 CO2+ H2O
CA
can
2H2O2 2H2O + O2
Catalase
katE
NasA
NasC
NasB
NAD(P)H
NADP+ + H+
NO2-
NH4+
α-ketoglutarate +NADPH + H+
gdh
L-glutamate
L-glutamine
L-glutamate + NH4+ + ATP
glnA
BcHr
-oxy
-deoxy
bchr
Nif
N2
NH4+
bfr1
bfr2
bfr3
Fe
BFR
SO4 3-
SO3-
CysNDCH
ATP
ADP + Pi
CysJI
H2S
L-lysine
L-threonine
L-isoleucine
L-methionine
L-aspartate
asp
pyruvate
pyc
CHOOH
CO2
H4MPT pathway for CH2O oxidation
Formyl-H4MPT
Methenyl-H4MPT
Methylene-H4MPT
CH2O
hps
CH2O oxidation
6PG
gnd
Ru5P
He6P
phi
F6P
RuMP cycle
pgl
pgi
pfk
6PGL
gpd1
G6P
gpd2
gck
Glucose
F-1,6-P
fba
ED and EMP
edd
DHAP
G3P
tkt
KDPG
gap
E4P Xu5F
tal
kdg
pgk
1,3-PG
S7P G3P
3-PG
pgm
2-PG
Ri5P
Xu5P
rpi
rpe
Ru5P
CysW
TCA cycle
malate
mdh
OXA
ppc
eno
PEP
pps
Mixed acid fermentation
fum
fumarate
sdh
succinate
sucCD
succinyl-CoA
sucA
alpha-ketogluterate
gltA
citrate
acn
cis-aconitate
isocitrate
icd1
icd2
pdk
pyk 1
pyk 2
pyruvate
pdh
acetyl-CoA
pfl
pdc
formate
fdh
CO2
H2
pta
acetyl-P
ack1
acetate
acetaldehyde
adh
ethanol
Ydbk
gdh
L-glutamate
Fd
Fd2-
NADH
NAD+ + H+
RNF complex
Na+
H+
Q
HUP
cytoplasm
periplasm
K+
PO4 3-
R-SO3-
Urea
Biotin
SO4 3-
Sugars
Ca2+
H+
Zn2+

Figure 24: **Cellular diagram representing differential expression of transcripts and proteins for major metabolic pathways in *Methylomonas denitrificans* FJG1 during hypoxia induced stationary phase.**

Proteins/transcripts identified in the analysis are color-filled (red, orange, yellow, green, turquoise, blue, violet, magenta) while those that were not identified are filled in grey. Color represents the N-fold change for gene products (transcripts and proteins) that belong to the represented proteins and protein complexes. The outline of each predicted protein/reaction indicates whether the mRNA and protein were differentially expressed at hypoxia induced stationary phase when compared to aerobic growth; the grey outline indicates that both the mRNA and protein were significantly differentially expressed, the solid black outline indicates that only the protein was differentially expressed, and the dashed black outline represents that only the mRNA was differentially expressed.

	Transcriptome	Proteome	sum
Total Carbohydrate metabolism depressed	35	19	54
Total Carbohydrate metabolism stimulated	34	39	73
TCA cycle + pyruvate metabolism depressed	3	4	7
TCA cycle + pyruvate metabolism stimulated	17	18	35
Total energy metabolism depressed	34	26	60
Total energy metabolism stimulated	42	32	74
Nitrogen metabolism depressed	0	8	8
Nitrogen metabolism stimulated	18	6	24
Total EIP depressed	25	20	45
Total EIP stimulated	32	19	51
Two component system depressed	5	6	11
Two component system stimulated	22	12	34

Absolute numbers	Upregulated Transcriptome	Upregulated Proteome	Downregulated Transcriptome	Downregulated Proteome
Carbohydrate metabolism	34	39	35	19
Energy metabolism	42	32	34	26
Lipid metabolism	3	5	14	5
Nucleotide metabolism	5	3	21	26
Amino acid metabolism	12	10	54	29
Glycan synthesis and metabolism	0	0	18	1
Metabolism of cofactors and vitamins	7	8	23	20
Biosynthesis of other secondary metabolites	2	3	9	3
Environmental Information Processing	32	19	25	20
Transcription	0	0	3	3
Translation	0	0	47	27
Folding, sorting, and degradation	5	2	11	11
Replication and repair	1	0	17	18
Transport and catabolism	0	2	1	2
Cell motility	13	15	1	1
Cell growth and death	2	0	6	3
Total	158	138	319	214

Percentages	Upregulated Transcriptome	Upregulated Proteome	Downregulated Transcriptome	Downregulated Proteome
Carbohydrate metabolism	21.5%	28.3%	11.0%	8.9%
Energy metabolism	26.6%	23.2%	10.7%	12.1%
Lipid metabolism	1.9%	3.6%	4.4%	2.3%
Nucleotide metabolism	3.2%	2.2%	6.6%	12.1%
Amino acid metabolism	7.6%	7.2%	16.9%	13.6%
Glycan synthesis and metabolism	0.0%	0.0%	5.6%	0.5%
Metabolism of cofactors and vitamins	4.4%	5.8%	7.2%	9.3%
Biosynthesis of other secondary metabolites	1.3%	2.2%	2.8%	1.4%
Environmental Information Processing	20.3%	13.8%	7.8%	9.3%
Transcription	0.0%	0.0%	0.9%	1.4%
Translation	0.0%	0.0%	14.7%	12.6%
Folding, sorting, and degradation	3.2%	1.4%	3.4%	5.1%
Replication and repair	0.6%	0.0%	5.3%	8.4%
Transport and catabolism	0.0%	1.4%	0.3%	0.9%
Cell motility	8.2%	10.9%	0.3%	0.5%
Cell growth and death	1.3%	0.0%	1.9%	1.4%
Total	100.0%	100.0%	100.0%	100.0%

Carb. + Energy + EIP	68.4%	65.2%	29.5%	30.4%
Nucleotide metabolism	3.2%	2.2%	6.6%	12.1%
Translation	0.0%	0.0%	14.7%	12.6%
Replication and repair	0.6%	0.0%	5.3%	8.4%
Nucleotide metabolism, translation, replication and repair	3.8%	2.2%	26.6%	33.2%

Table 3: **Analysis of some KEGG gene classifications from differentially expressed transcripts and proteins of *M. denitrificans* FJG1 during hypoxia induced stationary phase.**

Transcriptome

Functional category

	Whole Genome	Upregulated transcriptome	Downregulated transcriptome
Carbohydrate metabolism			
00010 Glycolysis / Gluconeogenesis	24	2	3
00020 Citrate cycle (TCA cycle)	24	9	0
00030 Pentose phosphate pathway	21	2	1
00040 Pentose and glucuronate interconversions	2	0	0
00051 Fructose and mannose metabolism	10	1	3
00052 Galactose metabolism	6	0	2
00053 Ascorbate and aldarate metabolism	2	0	0
00500 Starch and sucrose metabolism	20	1	2
00520 Amino sugar and nucleotide sugar metabolism	32	2	11
00620 Pyruvate metabolism	32	8	3
00630 Glyoxylate and dicarboxylate metabolism	22	5	2
00640 Propanoate metabolism	13	0	2
00650 Butanoate metabolism	10	2	1
00660 C5-Branched dibasic acid metabolism	8	2	4
00562 Inositol phosphate metabolism	2	0	1
Energy metabolism			
00190 Oxidative phosphorylation	28	2	13
00195 Photosynthesis	8	1	8
00710 Carbon fixation in photosynthetic organisms	12	3	3
00720 Carbon fixation pathways in prokaryotes	27	9	2
00680 Methane metabolism	41	7	7
00910 Nitrogen metabolism	28	18	0
00920 Sulfur metabolism	21	2	1
Lipid metabolism			
00061 Fatty acid biosynthesis	13	0	7
00071 Fatty acid degradation	2	0	0
00100 Steroid biosynthesis	1	0	0
00561 Glycerolipid metabolism	7	1	2

00564 Glycerophospholipid metabolism	13	1	4
00600 Sphingolipid metabolism	1	0	0
00590 Arachidonic acid metabolism	1	1	0
01040 Biosynthesis of unsaturated fatty acids	2	0	1
Nucleotide metabolism			
00230 Purine metabolism	56	4	11
00240 Pyrimidine metabolism	36	1	10
Amino acid metabolism			
00250 Alanine, aspartate and glutamate metabolism	19	2	6
00260 Glycine, serine and threonine metabolism	23	1	8
00270 Cysteine and methionine metabolism	28	5	8
00280 Valine, leucine and isoleucine degradation	4	0	0
00290 Valine, leucine and isoleucine biosynthesis	11	0	5
00300 Lysine biosynthesis	13	1	8
00310 Lysine degradation	4	0	0
00220 Arginine biosynthesis	12	1	1
00330 Arginine and proline metabolism	16	2	3
00340 Histidine metabolism	11	0	7
00350 Tyrosine metabolism	6	0	1
00360 Phenylalanine metabolism	8	0	1
00380 Tryptophan metabolism	6	0	0
00400 Phenylalanine, tyrosine and tryptophan biosynth	18	0	6
Glycan synthesis and metabolism			
00510 N-Glycan biosynthesis	1	0	0
00531 Glycosaminoglycan degradation	1	0	0
00540 Lipopolysaccharide biosynthesis	18	0	7
00550 Peptidoglycan biosynthesis	19	0	11
00511 Other glycan degradation	1	0	0
Metabolism of cofactors and vitamins			
00730 Thiamine metabolism	8	1	2
00740 Riboflavin metabolism	7	0	2
00750 Vitamin B6 metabolism	4	0	3
00760 Nicotinate and nicotinamide metabolism	13	1	1

00770 Pantothenate and CoA biosynthesis	14	2	4
00780 Biotin metabolism	11	0	3
00785 Lipoic acid metabolism	2	0	0
00790 Folate biosynthesis	18	0	3
00670 One carbon pool by folate	11	0	1
00830 Retinol metabolism	1	0	0
00860 Porphyrin and chlorophyll metabolism	34	2	2
00130 Ubiquinone and other terpenoid-quinone biosynth	9	1	2
Biosynthesis of other secondary metabolites			
00940 Phenylpropanoid biosynthesis	2	0	1
00950 Isoquinoline alkaloid biosynthesis	2	0	0
00960 Tropane, piperidine and pyridine alkaloid biosynthesis	2	0	1
00965 Betalain biosynthesis	1	1	0
00311 Penicillin and cephalosporin biosynthesis	2	0	1
00332 Carbapenem biosynthesis	2	0	1
00261 Monobactam biosynthesis	6	0	2
00521 Streptomycin biosynthesis	8	1	1
00524 Butirosin and neomycin biosynthesis	1	0	0
00401 Novobiocin biosynthesis	3	0	2
Environmental Information Processing			
Membrane transport			
02010 ABC transporters	49	5	9
03070 Bacterial secretion system	33	3	9
Signal transduction			
02020 Two-component system	74	22	5
04011 MAPK signaling pathway	1	0	0
04066 HIF-1 signaling pathway	4	0	1
04068 FoxO signaling pathway	2	0	0
04020 Calcium signaling pathway	1	0	0
04070 Phosphatidylinositol signaling system	3	1	1
04072 Phospholipase D signaling pathway	1	0	0

04151 PI3K-Akt signaling pathway	1	1	0
04152 AMPK signaling pathway	1	0	0
Genetic Information processing			
Transcription			
03020 RNA polymerase	4	0	3
Translation			
03010 Ribosome	49	0	40
00970 Aminoacyl-tRNA biosynthesis	25	0	6
03013 RNA transport	1	0	0
03008 Ribosome biogenesis	3	0	1
Folding, sorting and degradation			
03060 Protein export	16	0	10
04141 Protein processing	2	1	0
04122 Sulfur relay system	12	1	0
03018 RNA degradation	15	3	1
Replication and repair			
03030 DNA replication	14	1	5
03410 Base excision repair	9	0	0
03420 Nucleotide excision repair	7	0	0
03430 Mismatch repair	16	0	5
03440 Homologous recombination	22	0	7
Cellular Processes			
Transport and catabolism			
04142 Lysosome	1	0	0
04146 Peroxisome	5	0	1
Cell motility			
02030 Bacterial chemotaxis	16	8	0
02040 Flagellar assembly	35	5	1
Cell growth and death			
04112 Cell cycle - Caulobacter	12	2	6
04113 Meiosis	1	0	0
04214 Apoptosis	1	0	0

Proteome

	Whole Genome	Upregulated proteome	Downregulated proteome
Carbohydrate metabolism			
00010 Glycolysis / Gluconeogenesis	24	3	2
00020 Citrate cycle (TCA cycle)	24	10	1
00030 Pentose phosphate pathway	21	1	1
00040 Pentose and glucuronate interconversions	2	0	0
00051 Fructose and mannose metabolism	10	1	1
00052 Galactose metabolism	6	1	0
00053 Ascorbate and aldarate metabolism	2	0	0
00500 Starch and sucrose metabolism	20	1	0
00520 Amino sugar and nucleotide sugar metabolism	32	4	1
00620 Pyruvate metabolism	32	8	3
00630 Glyoxylate and dicarboxylate metabolism	22	4	5
00640 Propanoate metabolism	13	2	1
00650 Butanoate metabolism	10	3	1
00660 C5-Branched dibasic acid metabolism	8	1	2
00562 Inositol phosphate metabolism	2	0	1
Energy metabolism			
00190 Oxidative phosphorylation	28	3	3
00195 Photosynthesis	8	1	3
00710 Carbon fixation in photosynthetic organisms	12	3	1
00720 Carbon fixation pathways in prokaryotes	27	10	2
00680 Methane metabolism	41	7	7
00910 Nitrogen metabolism	28	6	8
00920 Sulfur metabolism	21	2	2
Lipid metabolism			
00061 Fatty acid biosynthesis	13	2	2
00071 Fatty acid degradation	2	1	0
00100 Steroid biosynthesis	1	0	0
00561 Glycerolipid metabolism	7	2	1

00564 Glycerophospholipid metabolism	13	0	2
00600 Sphingolipid metabolism	1	0	0
00590 Arachidonic acid metabolism	1	0	0
01040 Biosynthesis of unsaturated fatty acids	2	0	0
Nucleotide metabolism			
00230 Purine metabolism	56	2	15
00240 Pyrimidine metabolism	36	1	11
Amino acid metabolism			
00250 Alanine, aspartate and glutamate metabolism	19	1	5
00260 Glycine, serine and threonine metabolism	23	1	3
00270 Cysteine and methionine metabolism	28	3	2
00280 Valine, leucine and isoleucine degradation	4	0	0
00290 Valine, leucine and isoleucine biosynthesis	11	0	3
00300 Lysine biosynthesis	13	0	5
00310 Lysine degradation	4	0	0
00220 Arginine biosynthesis	12	0	3
00330 Arginine and proline metabolism	16	1	0
00340 Histidine metabolism	11	0	2
00350 Tyrosine metabolism	6	0	1
00360 Phenylalanine metabolism	8	2	0
00380 Tryptophan metabolism	6	2	1
00400 Phenylalanine, tyrosine and tryptophan biosynthesis	18	0	4
Glycan synthesis and metabolism			
00510 N-Glycan biosynthesis	1	0	0
00531 Glycosaminoglycan degradation	1	0	0
00540 Lipopolysaccharide biosynthesis	18	0	1
00550 Peptidoglycan biosynthesis	19	0	0
00511 Other glycan degradation	1	0	0
Metabolism of cofactors and vitamins			
00730 Thiamine metabolism	8	0	3
00740 Riboflavin metabolism	7	0	0
00750 Vitamin B6 metabolism	4	0	0
00760 Nicotinate and nicotinamide metabolism	13	2	0

00770 Pantothenate and CoA biosynthesis	14	0	3
00780 Biotin metabolism	11	1	1
00785 Lipoic acid metabolism	2	0	0
00790 Folate biosynthesis	18	1	1
00670 One carbon pool by folate	11	0	2
00830 Retinol metabolism	1	0	0
00860 Porphyrin and chlorophyll metabolism	34	3	8
00130 Ubiquinone and other terpenoid-quinone biosynthesis	9	1	2
Biosynthesis of other secondary metabolites			
00940 Phenylpropanoid biosynthesis	2	0	0
00950 Isoquinoline alkaloid biosynthesis	2	0	0
00960 Tropane, piperidine and pyridine alkaloid biosynthesis	2	0	0
00965 Betalain biosynthesis	1	0	0
00311 Penicillin and cephalosporin biosynthesis	2	1	0
00332 Carbapenem biosynthesis	2	0	0
00261 Monobactam biosynthesis	6	0	2
00521 Streptomycin biosynthesis	8	2	1
00524 Butirosin and neomycin biosynthesis	1	0	0
00401 Novobiocin biosynthesis	3	0	0
Environmental Information Processing			
Membrane transport			
02010 ABC transporters	49	0	6
03070 Bacterial secretion system	33	6	3
Signal transduction			
02020 Two-component system	74	12	6
04011 MAPK signaling pathway	1	0	1
04066 HIF-1 signaling pathway	4	1	0
04068 FoxO signaling pathway	2	0	2
04020 Calcium signaling pathway	1	0	0
04070 Phosphatidylinositol signaling system	3	0	1
04072 Phospholipase D signaling pathway	1	0	0
04151 PI3K-Akt signaling pathway	1	0	1
04152 AMPK signaling pathway	1	0	0

Genetic Information processing			
Transcription			
03020 RNA polymerase	4	0	3
Translation			
03010 Ribosome	49	0	16
00970 Aminoacyl-tRNA biosynthesis	25	0	11
03013 RNA transport	1	0	0
03008 Ribosome biogenesis	3	0	0
Folding, sorting and degradation			
03060 Protein export	16	0	4
04141 Protein processing	2	1	1
04122 Sulfur relay system	12	1	2
03018 RNA degradation	15	0	4
Replication and repair			
03030 DNA replication	14	0	4
03410 Base excision repai	9	0	2
03420 Nucleotide excision repair	7	0	2
03430 Mismatch repair	16	0	7
03440 Homologous recombination	22	0	3
Cellular Processes			
Transport and catabolism			
04142 Lysosome	1	0	0
04146 Peroxisome	5	2	2
Cell motility			
02030 Bacterial chemotaxis	16	11	0
02040 Flagellar assembly	35	4	1
Cell growth and death			
04112 Cell cycle - Caulobacter	12	0	3
04113 Meiosis	1	0	0
04214 Apoptosis	1	0	0

Table 4: **Complete KEGG classification of differentially expressed transcripts and proteins of *M. denitrificans* FJG1 during hypoxia induced stationary phase.**

4.7: References

Achbergerová, L., and Nahálka, J. (2011). Polyphosphate--an ancient energy source and active metabolic regulator. *Microb. Cell Fact.* 10, 63. doi:10.1186/1475-2859-10-63.

Bodelier, P. L. E., and Steenbergh, A. K. (2014). Interactions between methane and the nitrogen cycle in light of climate change. *Current Opinion in Environmental Sustainability* 9-10, 26–36.

Calhoun, A., and King, G. M. (1998). Characterization of Root-Associated Methanotrophs from Three Freshwater Macrophytes: *Pontederia cordata, Sparganium eurycarpum*, and *Sagittaria latifolia*. *Appl. Environ. Microbiol.* 64, 1099–1105.

Campbell, M. A., Nyerges, G., Kozlowski, J. A., Poret Peterson, A. T., Stein, L. Y., and Klotz, M. G. (2011). Model of the molecular basis for hydroxylamine oxidation and nitrous oxide production in methanotrophic bacteria. *FEMS Microbiology Letters* 322, 82–89. doi:10.1111/j.1574-6968.2011.02340.x.

Carrondo, M. A. (2003). Ferritins, iron uptake and storage from the bacterioferritin viewpoint. *EMBO J.* 22, 1959–1968. doi:10.1093/emboj/cdg215.

Chu, F., and Lidstrom, M. E. (2016). XoxF acts as the predominant methanol dehydrogenase in the type I methanotroph *Methylomicrobium buryatense*. *J. Bacteriol.* 198, 1317–1325. doi:10.1128/JB.00959-15.

Clark, D. P. (1989). The fermentation pathways of *Escherichia coli. FEMS Microbiol. Rev.* 5, 223–234. doi:10.1111/j.1574-6968.1989.tb03398.x.

Conrad, R. (2009). The global methane cycle: Recent advances in understanding the microbial processes involved. *Environ Microbiol Rep* 1, 285–292. doi:10.1111/j.1758-2229.2009.00038.x/asset/j.1758-2229.2009.00038.x.pdf.

Corbin, R. W., Paliy, O., Yang, F., Shabanowitz, J., Platt, M., Lyons, C. E., et al. (2003). Toward a protein profile of *Escherichia coli*: comparison to its transcription profile. *Proc. Natl. Acad. Sci. U.S.A.* 100, 9232–9237. doi:10.1073/pnas.1533294100.

Cox, J., and Mann, M. (2012). 1D and 2D annotation enrichment: a statistical method integrating quantitative proteomics with complementary high-throughput data. *BMC Bioinformatics* 13 Suppl 16, S12. doi:10.1186/1471-2105-13-S16-S12.

Csáki, R., Hanczár, T., Bodrossy, L., Murrell, J. C., and Kovács, K. L. (2001). Molecular characterization of structural genes coding for a membrane bound hydrogenase in *Methylococcus capsulatus* (Bath). *FEMS Microbiology Letters* 205, 203–207. doi:10.1016/S0378-1097(01)00469-4.

Dalton, H. (1977). Ammonia oxidation by the methane oxidising bacterium *Methylococcus capsulatus* strain bath. *Arch. Microbiol.* 114, 273–279. doi:10.1007/BF00446873.

de Sousa Abreu, R., Penalva, L. O., Marcotte, E. M., and Vogel, C. (2009). Global signatures of protein and mRNA expression levels. *Mol Biosyst* 5, 1512–1526. doi:10.1039/b908315d.

de Souza, G. A., Leversen, N. A., Målen, H., and Wiker, H. G. (2011). Bacterial proteins with cleaved or uncleaved signal peptides of the general secretory pathway. *J Proteomics* 75, 502–510. doi:10.1016/j.jprot.2011.08.016.

Dillies, M.-A., Rau, A., Aubert, J., Hennequet-Antier, C., Jeanmougin, M., Servant, N., et al. (2013). A comprehensive evaluation of normalization methods for Illumina high-throughput RNA sequencing data analysis. *Brief. Bioinformatics* 14, 671–683. doi:10.1093/bib/bbs046.

Dobritzsch, D., König, S., Schneider, G., and Lu, G. (1998). High resolution crystal structure of pyruvate decarboxylase from *Zymomonas mobilis*. Implications for substrate activation in pyruvate decarboxylases. *J. Biol. Chem.* 273, 20196–20204. doi:10.1074/jbc.273.32.20196.

Eram, M. S., and Ma, K. (2013). Decarboxylation of pyruvate to acetaldehyde for ethanol production by hyperthermophiles. *Biomolecules* 3, 578–596. doi:10.3390/biom3030578.

Fischer, F., Wolters, D., Rögner, M., and Poetsch, A. (2006). Toward the complete membrane proteome: High coverage of integral membrane proteins through transmembrane peptide detection. *Mol. Cell Proteomics* 5, 444–453. doi:10.1074/mcp.M500234-MCP200.

Florens, L., Carozza, M. J., Swanson, S. K., Fournier, M., Coleman, M. K., Workman, J. L., et al. (2006). Analyzing chromatin remodeling complexes using shotgun proteomics and normalized spectral abundance factors. *Methods* 40, 303–311. doi:10.1016/j.ymeth.2006.07.028.

Gelius Dietrich, G., and Henze, K. (2004). Pyruvate Formate Lyase (PFL) and PFL Activating Enzyme in the Chytrid Fungus *Neocallimastix frontalis*: A Free-Radical Enzyme System Conserved Across Divergent Eukaryotic Lineages. *Journal of Eukaryotic Microbiology* 51, 456–463. doi:10.1111/j.1550-7408.2004.tb00394.x.

Gilman, A., Laurens, L. M., Puri, A. W., Chu, F., Pienkos, P. T., and Lidstrom, M. E. (2015). Bioreactor performance parameters for an industrially-promising methanotroph *Methylomicrobium buryatense* 5GB1. *Microb. Cell Fact.* 14, 182. doi:10.1186/s12934-015-0372-8.

Grillo-Puertas, M., Villegas, J. M., Rintoul, M. R., and Rapisarda, V. A. (2012). Polyphosphate Degradation in Stationary Phase Triggers Biofilm Formation via LuxS Quorum Sensing System in *Escherichia coli*. *PLoS ONE* 7, e50368. doi:10.1371/journal.pone.0050368.

Hamilton, R., Kits, K. D., Ramonovskaya, V. A., Rozova, O. N., Yurimoto, H., Iguchi, H., et al. (2015). Draft genomes of gammaproteobacterial methanotrophs isolated from terrestrial ecosystems. *Genome Announc* 3, e00515–15. doi:10.1128/genomeA.00515-15.

Hanczár, T., Csáki, R., Bodrossy, L., Murrell, J. C., and Kovács, K. L. (2002). Detection and localization of two hydrogenases in *Methylococcus capsulatus* (Bath) and their potential role in methane metabolism. *Arch. Microbiol.* 177, 167–172. doi:10.1007/s00203-001-0372-4.

Honarmand Ebrahimi, K., Hagedoorn, P.-L., and Hagen, W. R. (2015). Unity in the biochemistry of the iron-storage proteins ferritin and bacterioferritin. *Chem. Rev.* 115, 295–326. doi:10.1021/cr5004908.

Jayapal, K. P., Philp, R. J., Kok, Y.-J., Yap, M. G. S., Sherman, D. H., Griffin, T. J., et al. (2008). Uncovering genes with divergent mRNA-protein dynamics in Streptomyces coelicolor. *PLoS ONE* 3, e2097. doi:10.1371/journal.pone.0002097.

Kalyuzhnaya, M. G., Yang, S., Rozova, O. N., Smalley, N. E., Clubb, J., Lamb, A., et al. (2013). Highly efficient methane biocatalysis revealed in a methanotrophic bacterium. *Nat Comms* 4, 2785. doi:10.1038/ncomms3785.

Kao, W.-C., Chen, Y.-R., Yi, E. C., Lee, H., Tian, Q., Wu, K.-M., et al. (2004). Quantitative proteomic analysis of metabolic regulation by copper ions in *Methylococcus capsulatus* (Bath). *J. Biol. Chem.* 279, 51554–51560. doi:10.1074/jbc.M408013200.

Kearse, M., Moir, R., Wilson, A., Stones-Havas, S., Cheung, M., Sturrock, S., et al. (2012). Geneious Basic: an integrated and extendable desktop software platform for the organization and analysis of sequence data. *Bioinformatics* 28, 1647–1649. doi:10.1093/bioinformatics/bts199.

Khadem, A. F., van Teeseling, M. C. F., van Niftrik, L., Jetten, M. S. M., Op den Camp, H. J. M., and Pol, A. (2012). Genomic and Physiological Analysis of Carbon Storage in the Verrucomicrobial Methanotroph "Ca. *Methylacidiphilum fumariolicum*" SolV. *Front. Microbiol.* 3, 345. doi:10.3389/fmicb.2012.00345.

Kits, K. D., Campbell, D. J., Rosana, A. R., and Stein, L. Y. (2015a). Diverse electron sources support denitrification under hypoxia in the obligate methanotroph *Methylomicrobium album* strain BG8. *Front. Microbiol.* 6, 1072. doi:10.3389/fmicb.2015.01072.

Kits, K. D., Klotz, M. G., and Stein, L. Y. (2015b). Methane oxidation coupled to nitrate reduction under hypoxia by the Gammaproteobacterium *Methylomonas denitrificans*, sp. nov. type strain FJG1. *Environ. Microbiol.* 17, 3219–3232. doi:10.1111/1462-2920.12772.

Knappe, J., and Sawers, G. (1990). A radical-chemical route to acetyl-CoA: the anaerobically induced pyruvate formate-lyase system of *Escherichia coli*. *FEMS Microbiol. Rev.* 6, 383–398.

Kuroda, A., Nomura, K., Ohtomo, R., Kato, J., Ikeda, T., Takiguchi, N., et al. (2001). Role of inorganic polyphosphate in promoting ribosomal protein degradation by the Lon protease in E. coli. *Science* 293, 705–708. doi:10.1126/science.1061315.

la Torre, de, A., Metivier, A., Chu, F., Laurens, L. M. L., Beck, D. A. C., Pienkos, P. T., et al. (2015). Genome-scale metabolic reconstructions and theoretical investigation of methane conversion in *Methylomicrobium buryatense* strain 5G(B1). *Microb. Cell Fact.* 14, 188. doi:10.1186/s12934-015-0377-3.

Le Brun, N. E., Andrews, S. C., Guest, J. R., Harrison, P. M., Moore, G. R., and Thomson, A. J. (1995). Identification of the ferroxidase centre of *Escherichia coli* bacterioferritin. *Biochem. J.* 312 (Pt 2), 385–392.

Lindner, A. S., Pacheco, A., Aldrich, H. C., Staniec, A. C., Uz, I., and Hodson, D. J. (2007). *Methylocystis hirsuta* sp. nov., a novel methanotroph isolated from a groundwater aquifer. *International Journal of Systematic and Evolutionary Microbiology* 57, 1891–1900. doi:10.1099/ijs.0.64541-0.

Lu, P., Vogel, C., Wang, R., Yao, X., and Marcotte, E. M. (2007). Absolute protein expression profiling estimates the relative contributions of transcriptional and translational regulation. *Nat. Biotechnol.* 25, 117–124. doi:10.1038/nbt1270.

Matsen, J. B., Yang, S., Stein, L. Y., Beck, D., and Kalyuzhnaya, M. G. (2013). Global Molecular Analyses of Methane Metabolism in Methanotrophic Alphaproteobacterium, *Methylosinus trichosporium* OB3b. Part I: Transcriptomic Study. *Front. Microbiol.* 4. doi:10.3389/fmicb.2013.00040.

Murrell, J. C., and Dalton, H. (1983). Nitrogen Fixation in Obligate Methanotrophs. *J Gen Microbiol* 129, 3481–3486.

Nazaries, L., Murrell, J. C., and Millard, P. (2013). Methane, microbes and models: fundamental understanding of the soil methane cycle for future predictions - Nazaries - 2013 - Environmental Microbiology - Wiley Online Library. *Environmental …*. doi:10.1111/1462-2920.12149/pdf.

Nie, L., Wu, G., and Zhang, W. (2006). Correlation of mRNA expression and protein abundance affected by multiple sequence features related to translational efficiency in Desulfovibrio vulgaris: a quantitative analysis. *Genetics* 174, 2229–2243. doi:10.1534/genetics.106.065862.

Nyerges, G., and Stein, L. Y. (2009). Ammonia cometabolism and product inhibition vary considerably among species of methanotrophic bacteria. *FEMS Microbiology Letters* 297, 131–136. doi:10.1111/j.1574-6968.2009.01674.x.

Oberg, A. L., and Vitek, O. (2009). Statistical design of quantitative mass spectrometry-based proteomic experiments. *J. Proteome Res.* 8, 2144–2156. doi:10.1021/pr8010099.

Olsen, J. V., de Godoy, L. M. F., Li, G., Macek, B., Mortensen, P., Pesch, R., et al. (2005). Parts

per million mass accuracy on an Orbitrap mass spectrometer via lock mass injection into a C-trap. *Mol. Cell Proteomics* 4, 2010–2021. doi:10.1074/mcp.T500030-MCP200.

Patel, N. A., Crombie, A., Slade, S. E., Thalassinos, K., Hughes, C., Connolly, J. B., et al. (2012). Comparison of one- and two-dimensional liquid chromatography approaches in the label-free quantitative analysis of *Methylocella silvestris*. *J. Proteome Res.* 11, 4755–4763. doi:10.1021/pr300253s.

Patel, V. J., Thalassinos, K., Slade, S. E., Connolly, J. B., Crombie, A., Murrell, J. C., et al. (2009). A comparison of labeling and label-free mass spectrometry-based proteomics approaches. *J. Proteome Res.* 8, 3752–3759. doi:10.1021/pr900080y.

Poret Peterson, A. T., Graham, J. E., Gulledge, J., and Klotz, M. G. (2008). Transcription of nitrification genes by the methane-oxidizing bacterium, *Methylococcus capsulatus* strain Bath. *ISME J* 2, 1213–1220. doi:10.1038/ismej.2008.71.

Rao, N. N., and Kornberg, A. (1996). Inorganic polyphosphate supports resistance and survival of stationary-phase *Escherichia coli*. *J. Bacteriol.* 178, 1394–1400.

Rao, N. N., and Kornberg, A. (1999). Inorganic polyphosphate regulates responses of *Escherichia coli* to nutritional stringencies, environmental stresses and survival in the stationary phase. *Prog. Mol. Subcell. Biol.* 23, 183–195.

Roslev, P., and King, G. M. (1995). Aerobic and anaerobic starvation metabolism in methanotrophic bacteria. *Appl. Environ. Microbiol.* 61, 1563–1570.

Serang, O., MacCoss, M. J., and Noble, W. S. (2010). Efficient marginalization to compute protein posterior probabilities from shotgun mass spectrometry data. *J. Proteome Res.* 9, 5346–5357. doi:10.1021/pr100594k.

Skennerton, C. T., Ward, L. M., Michel, A., Metcalfe, K., Valiente, C., Mullin, S., et al. (2015).

Genomic reconstruction of an uncultured hydrothermal vent gammaproteobacterial methanotroph (Family Methylothermaceae) indicates multiple adaptations to oxygen limitation. *Front. Microbiol.* 6, 1425. doi:10.3389/fmicb.2015.01425.

Spivak, M., Weston, J., Bottou, L., Käll, L., and Noble, W. S. (2009). Improvements to the percolator algorithm for Peptide identification from shotgun proteomics data sets. *J. Proteome Res.* 8, 3737–3745. doi:10.1021/pr801109k.

Tavormina, P. L., Orphan, V. J., Kalyuzhnaya, M. G., Jetten, M. S. M., and Klotz, M. G. (2011). A novel family of functional operons encoding methane/ammonia monooxygenase-related proteins in gammaproteobacterial methanotrophs. *Environ Microbiol Rep* 3, 91–100. doi:10.1111/j.1758-2229.2010.00192.x.

Trotsenko, Y. A., and Murrell, J. C. (2008). Metabolic aspects of aerobic obligate methanotrophy. *Adv. Appl. Microbiol.* 63, 183–229. doi:10.1016/S0065-2164(07)00005-6.

Trotsenko, Y. A., and Shishkina, V. N. (1990). Studies on phosphate metabolism in obligate methanotrophs. *FEMS Microbiology Letters* 87, 267–271. doi:10.1016/0378-1097(90)90465-3.

Tusher, V. G., Tibshirani, R., and Chu, G. (2001). Significance analysis of microarrays applied to the ionizing radiation response. *Proc. Natl. Acad. Sci. U.S.A.* 98, 5116–5121. doi:10.1073/pnas.091062498.

van Teeseling, M. C. F., Pol, A., Harhangi, H. R., van der Zwart, S., Jetten, M. S. M., Op den Camp, H. J. M., et al. (2014). Expanding the verrucomicrobial methanotrophic world: description of three novel species of *Methylacidimicrobium* gen. nov. *Appl. Environ. Microbiol.* 80, 6782–6791. doi:10.1128/AEM.01838-14.

Vizcaíno, J. A., Deutsch, E. W., Wang, R., Csordas, A., Reisinger, F., Ríos, D., et al. (2014).

ProteomeXchange provides globally coordinated proteomics data submission and dissemination. *Nat. Biotechnol.* 32, 223–226. doi:10.1038/nbt.2839.

Wagner, G. P., Kin, K., and Lynch, V. J. (2012). Measurement of mRNA abundance using RNA-seq data: RPKM measure is inconsistent among samples. *Theory Biosci.* 131, 281–285. doi:10.1007/s12064-012-0162-3.

Wahlgren, W. Y., Omran, H., Stetten, von, D., Royant, A., van der Post, S., and Katona, G. (2012). Structural Characterization of Bacterioferritin from *Blastochloris viridis*. *PLoS ONE* 7, e46992. doi:10.1371/journal.pone.0046992.

Ward, N., Larsen, Ø., Sakwa, J., Bruseth, L., Khouri, H., Durkin, A. S., et al. (2004). Genomic Insights into Methanotrophy: The Complete Genome Sequence of *Methylococcus capsulatus* (Bath). *PLoS Biol* 2, e303. doi:10.1371/journal.pbio.0020303.

Wiśniewski, J. R., Zougman, A., Nagaraj, N., and Mann, M. (2009). Universal sample preparation method for proteome analysis. *Nat. Methods* 6, 359–362. doi:10.1038/nmeth.1322.

Zhu, J., Wang, Q., Yuan, M., Tan, G.-Y. A., Sun, F., Wang, C., et al. (2016). Microbiology and potential applications of aerobic methane oxidation coupled to denitrification (AME-D) process: A review. *Water Res.* 90, 203–215. doi:10.1016/j.watres.2015.12.020.

Chapter 5: Conclusions and future research

5.1: Overview

The original research work presented in this thesis utilized various microbial physiology techniques, microrespirometry, genome assembly and annotation, transcriptome sequencing and analysis, and proteomics to investigate the potential for CH_4 driven denitrification in aerobic methanotrophic bacteria. The objectives of this research were to (**i**) to determine whether aerobic methanotrophs can denitrify at the expense of methane, (**ii**) to unravel what genes and enzymes are involved in methane-dependent denitrification, (**iii**) what environmental conditions govern methane-dependent denitrification in aerobic methanotrophs, (**iv**) to assess the diversity of denitrification in aerobic methanotrophs in terms of energy sources and terminal electron acceptors, (**v**) to elucidate the bioenergetic function of denitrification in aerobic methanotrophs, and (**vi**) to characterize the genome wide metabolic regulation by oxygen in a model aerobic methanotroph using transcriptomics, proteomics, and metabolomics

5.2: General Conclusions

One hundred and ten years ago, Söhngen realized that CH_4 is produced in abundance in anaerobic environments and postulated that the vastly lower concentration of CH_4 in the atmosphere is due to the presence of unicellular microorganisms that could consume this carbon compound for growth (Söhngen). He isolated the first methanotroph – *Bacillus methanicus* – and began the study of methane consuming microbes (Söhngen). Aerobic methanotrophs are ubiquitous and abundant in nearly all terrestrial and aquatic environments where mixtures of CH_4 and O_2 are present and it is now appreciated that aerobic methanotrophic bacteria are critical players in the carbon and nitrogen cycles; methanotrophs attenuate CH_4 before it can escape to the atmospheric reservoir, serve as a significant sink for atmospheric CH_4, help form the base of

the food chain in many hydrothermal vent ecosystems which do not depend on sunlight for energy, and participate in nitrogen cycling by fixing atmospheric N_2 into NH_4^+ and oxidizing NH_3 to NO_2^- (Colin Murrell and Jetten, 2009; Conrad, 2009; Knief, 2015; Murrell, 2010; Nazaries et al., 2013; Stein and Klotz, 2011).

Since Söhngen, a massive diversity of methanotrophic bacteria have been isolated and cultivated from the phyla Proteobacteria and Verrucomicrobia. Moreover, over 55 closed completed genomes of aerobic methanotrophic bacteria are now available in public databases (IMG/ER - https://img.jgi.doe.gov/cgi-bin/mer/main.cgi) (Boden et al., 2011; Chen et al., 2010; Dam et al., 2013; Hamilton et al., 2015; Hou et al., 2008; Khadem et al., 2012; Khmelenina et al., 2013; Kits et al., 2013; Stein et al., 2010; Svenning et al., 2011; Vuilleumier et al., 2012; Ward et al., 2004). However, it has always been thought that aerobic methanotrophs require O_2 for CH_4 oxidation and respiration. Yoshinari (1985) was the first to glimpse anaerobic respiration in aerobic methanotrophs when he observed that *Methylosinus trichosporium* OB3b consumed NO_2^- and produced N_2O; however, the results were dismissed as abiotic decay of various nitrogen species (Yoshinari, 1985). Later, it was observed that cultures of three obligate methanotrophs consumed NO and produced minor quantities of N_2O (Ren et al., 2000). However, PCR analysis did not detect any denitrification genes and, once again, it was concluded that the activity was abiotic. The discovery of putative nitrite and nitric oxide reductases in the genome of *Methylomonas* sp. 16a continued to perplex researchers and then the study of denitrification in aerobic methanotrophs turned to investigating consortia in which, presumably, exudates from methanotrophic bacteria fed heterotrophic denitrifiers (Knowles, 2005; Ye and Thomas, 2001). Later, methanol driven denitrification was demonstrated in *Methylocystis* sp. strain SC2 under anaerobic conditions but CH_4 driven NO_3^- respiration

remained unidentified and uncharacterized (Dam et al., 2013).

The genome sequence of the obligate aerobic methanotroph *Methylomonas denitrificans* FJG1 hinted at the presence of an anaerobic metabolism; the genome encoded a complete pathway for the respiration of NO_3^- to N_2O via potentially two nitrate reductases (*narGHJI,* and *napABC*), two nitrite reductases (*nirS* and *nirK*), and a cytochrome *c* linked nitric oxide reductase (*norCB*) (Kits et al., 2015). Chapter 2 then showed that *M. denitrificans* FJG1 produced N_2O during batch growth on CH_4 but only after O_2 had been depleted and only in the presence of NO_3^-. To probe the metabolism further, microrespirometry was used to determine that NO_3^- consumption was stoichiometric with N_2O production in a ratio of 2:1 under hypoxic conditions exactly as would be expected for denitrification and that NO_2^- and NO were intermediates of the pathway – showing conclusively that *M. denitrificans* FJG1 can couple CH_4 oxidation to NO_3^- respiration. Gene expression then uncovered that mRNA levels for the membrane bound nitrate reductase (*narGHJI*), copper-containing nitrite reductase (*nirK*), and nitric oxide reductase (*norCB*) were elevated only under hypoxia and in the presence of NO_3^- (or denitrifying conditions). Chapter 2 also demonstrated that denitrification is bioenergetically advantageous under O_2 limiting conditions, suggesting a possible evolutionary driving force for the acquisition of denitrification gene modules in methanotrophs. Surprisingly, this work also revealed that expression of an operon encoding a divergent monooxygenase *pxmABC,* which is found in the genome of *M. denitrificans* FJG1 as well as many other aerobic methanotrophs, was responsive only to denitrifying conditions. This last observation suggested that the uncharacterized monooxygenase may play a role under O_2 limiting conditions. Taken together, chapter 2 demonstrated that CH_4 dependent NO_3^- respiration does exist and that aerobic methanotrophs are surprisingly able to execute this process. The research also identified a

putative pathway for denitrification in *M. denitrificans* FJG1 and suggested a novel function for the uncharacterized *pxmABC* gene cluster.

Chapter 3 investigated the diversity of denitrification activity in aerobic methanotrophs in terms of the modularity of denitrification pathways and the supporting electron donors. The model methanotroph utilized in chapter 3 was *Methylomicrobium album* BG8 – a Gammaproteobacterial methanotroph that encodes only a cytochrome cd_1 containing nitrite reductase (*nirS*) and cytochrome c linked nitric oxide reductase but lacks any dissimilatory nitrate reductases. While NO_3^- respiration in M. denitrificans FJG1 is likely coupled to generation of Δp because the NAR complex is electrogenic, NO_2^- respiration is likely not. Ergo, chapter 3 investigated whether a methanotroph whose genome only encodes a NIR and NOR exhibited denitrification activity. Using microrespirometry, we demonstrated that *M. album* BG8 coupled CH_4 oxidation to NO_2^- respiration under hypoxia and found that steady state mRNA levels of the the putative *nirS* and *norB* homologs were upregulated as well as *pxmA* in response to NO_2^- and not hypoxia. Unlike *M. denitrificans* FJG1, *M. album* BG8 oxidizes NH_3 to NO_2^- using pMMO and hydroxylamine dehydrogenase (*hao*). *M. album* BG8 cannot grow on NH_3 as the sole energy source but the electrons from NH_3 oxidation do enter the electron transport chain. To answer whether electron sources other than CH_4 could support denitrification, we again employed respirometry. We found that NH_3, ethanol, ethane and intermediates of the CH_4 oxidation pathway (CH_3OH, CH_2O, CHOOH) could all support denitrification activity. As a whole, we demonstrated that denitrification is modular in aerobic methanotrophs and that a large variety of electron sources can be utilized by the organisms to support the process.

The objective of chapter 4 was: i) to test whether formaldehyde fermentation and denitrification represent mutually exclusive strategies to deal with hypoxia or whether both can

be utilized simultaneously, and ii) to assess the diversity of fermentation pathways and possible products in *M. denitrificans* FJG1. Also, to test our hypothesis that denitrification genes should be expressed under denitrifying conditions, we analyzed the proteome of *M. denitrificans* FJG1 under hypoxia induced-stationary phase. In chapter 4, we were the first to measure the agreement between the mRNA and protein pools in an aerobic methanotroph and we found that the agreement is significantly lower than for classical bacterial models like *E. coli* and *Streptomyces* (Corbin et al., 2003; de Sousa Abreu et al., 2009; Jayapal et al., 2008; Lu et al., 2007; Nie et al., 2006). The combined transcriptome and proteome analysis suggested that the main route for carbon assimilation in *M. denitrificans* FJG1 is the EMP pathway and implied that pyruvate ferredoxic oxidoreductase and pyruvate formate lyase play an important role in pyruvate decarboxylation during hypoxia. Analysis of the genomic inventory necessary for fermentation and denitrification indicated that NO_3^- respiration and formaldehyde fermentation likely occur simultaneously during hypoxia, with the predicted fermentation products being formate, acetate, succinate, H_2, and ethanol. In terms of the respiratory chain, the combined transcriptome-proteome showed that enzymes encoding denitrification machinery were expressed in much higher abundance during denitrifying conditions and that, surprisingly, the terminal reductases are expressed and functional in addition to the terminal oxidase.

5.3 Future directions

The original research encapsulated in this thesis answered many questions about adaptations of aerobic methanotrophs to hypoxia and vastly expanded our comprehension of how methanotrophs attenuate and emit greenhouse gases and also how methanotrophs might influence their community members in low oxygen environments. Nonetheless, there still remain important directions for future research on the topic, which could include:

1) **Mutagenesis of *nar*, *nap*, *nirS*, *nirK*, and *norB* in *M. denitrificans* FJG1.** Currently, we have presented evidence that both the *nar* and *nap* nitrate reductases are expressed during denitrification. However, it is now known whether one or both catalyze NO_3^- reduction and whether one has a catalytic advantage under certain conditions. The transcriptome and proteome data suggest that *nirK* is responsible for NO_2^- respiration; a knockout of the *nirS* gene could definitively confirm this.
2) **Metabolomics analysis of formaldehyde fermenting cultures of *M. denitrificans* FJG1.** The –omics analyses in chapter 4 indicated that acetate, succinate, formate, H_2, and ethanol are the main fermentation products in *M. denitrificans* FJG1 but the metabolites were not measured. Work to identify the complete metabolome of this organism could identify the actual fermentation products and, if ethanol is a metabolite, contribute significantly to the field of CH_4 bioconversion to liquid fuels.
3) **Functional characterization of the Pxm gene cluster.** Chapter 2 and 3 presented evidence that transcription of the *pxmABC* operon, which encodes an uncharacterized monooxygenase, is upregulated in response to hypoxic conditions in two different aerobic denitrifying methanotrophs. We hypothesize that the Pxm protein is a CH_4 monooxygenase with a high affinity for O_2 and that it plays an important role under O_2 depleted conditions. Work to express this enzyme heterologouslym or purify the protein (apart from the pMMO), or mutagenize the gene to disrupt its function would greatly expand current knowledge of copper containing monooxygenases.
4) **Environmental significance of CH_4 driven NO_3^- respiration.** In this thesis we were the first to provide rigorous evidence for NO_3^- respiration in aerobic methanotrophs and characterized not only the environmental conditions that govern the process (O_2, NO_3^-)

but also the expression of the genes and gene products that are likely responsible for this activity. Methanotrophs are found in high abundance in hypoxic oceans, permafrost, and soils. However, the contribution of those methanotrophs to N_2O flux through the denitrification pathway is unknown. Environmental microbiology work to measure the activity and abundance of NO_3^--respiring aerobic methanotrophs in various environments would further our understanding of microbial greenhouse sinks and sources.

5.4 References

Boden, R., Cunliffe, M., Scanlan, J., Moussard, H., Kits, K. D., Klotz, M. G., et al. (2011). Complete genome sequence of the aerobic marine methanotroph *Methylomonas methanica* MC09. *J. Bacteriol.* 193, 7001–7002. doi:10.1128/JB.06267-11.

Chen, Y., Crombie, A., Rahman, M. T., Dedysh, S. N., Liesack, W., Stott, M. B., et al. (2010). Complete genome sequence of the aerobic facultative methanotroph *Methylocella silvestris* BL2. *J. Bacteriol.* 192, 3840–3841. doi:10.1128/JB.00506-10.

Colin Murrell, J., and Jetten, M. S. M. (2009). The microbial methane cycle. *Environ Microbiol Rep* 1, 279–284. doi:10.1111/j.1758-2229.2009.00089.x/asset/j.1758-2229.2009.00089.x.pdf.

Conrad, R. (2009). The global methane cycle: Recent advances in understanding the microbial processes involved. *Environ Microbiol Rep* 1, 285–292. doi:10.1111/j.1758-2229.2009.00038.x/asset/j.1758-2229.2009.00038.x.pdf.

Corbin, R. W., Paliy, O., Yang, F., Shabanowitz, J., Platt, M., Lyons, C. E., et al. (2003). Toward a protein profile of *Escherichia coli*: comparison to its transcription profile. *Proc. Natl. Acad. Sci. U.S.A.* 100, 9232–9237. doi:10.1073/pnas.1533294100.

Dam, B., Dam, S., Blom, J., and Liesack, W. (2013). Genome Analysis Coupled with Physiological Studies Reveals a Diverse Nitrogen Metabolism in *Methylocystis* sp. Strain SC2. *PLoS ONE* 8, e74767. doi:10.1371/journal.pone.0074767.

de Sousa Abreu, R., Penalva, L. O., Marcotte, E. M., and Vogel, C. (2009). Global signatures of protein and mRNA expression levels. *Mol Biosyst* 5, 1512–1526. doi:10.1039/b908315d.

Hamilton, R., Kits, K. D., Ramonovskaya, V. A., Rozova, O. N., Yurimoto, H., Iguchi, H., et al. (2015). Draft genomes of gammaproteobacterial methanotrophs isolated from terrestrial ecosystems. *Genome Announc* 3, e00515–15. doi:10.1128/genomeA.00515-15.

Hou, S., Makarova, K. S., Saw, J. H., Senin, P., and Ly, B. V. (2008). Complete genome sequence of the extremely acidophilic methanotroph isolate V4, *Methylacidiphilum infernorum*, a representative of the bacterial phylum …. *Biol* ….

Jayapal, K. P., Philp, R. J., Kok, Y.-J., Yap, M. G. S., Sherman, D. H., Griffin, T. J., et al. (2008). Uncovering genes with divergent mRNA-protein dynamics in *Streptomyces coelicolor*. *PLoS ONE* 3, e2097. doi:10.1371/journal.pone.0002097.

Khadem, A. F., Wieczorek, A. S., Pol, A., Vuilleumier, S., Harhangi, H. R., Dunfield, P. F., et al. (2012). Draft genome sequence of the volcano-inhabiting thermoacidophilic methanotroph *Methylacidiphilum fumariolicum* strain SolV. *J. Bacteriol.* 194, 3729–3730. doi:10.1128/JB.00501-12.

Khmelenina, V. N., Beck, D. A. C., Munk, C., Davenport, K., Daligault, H., Erkkila, T., et al. (2013). Draft Genome Sequence of *Methylomicrobium buryatense* Strain 5G, a Haloalkaline-Tolerant Methanotrophic Bacterium. *Genome Announc* 1, e00053–13. doi:10.1128/genomeA.00053-13.

Kits, K. D., Kalyuzhnaya, M. G., Klotz, M. G., Jetten, M. S. M., Op den Camp, H. J. M., Vuilleumier, S., et al. (2013). Genome Sequence of the Obligate Gammaproteobacterial Methanotroph *Methylomicrobium album* Strain BG8. *Genome Announc* 1, e0017013–e00170–13. doi:10.1128/genomeA.00170-13.

Kits, K. D., Klotz, M. G., and Stein, L. Y. (2015). Methane oxidation coupled to nitrate reduction under hypoxia by the Gammaproteobacterium *Methylomonas denitrificans*, sp. nov. type strain FJG1. *Environ. Microbiol.* 17, 3219–3232. doi:10.1111/1462-2920.12772.

Knief, C. (2015). Diversity and Habitat Preferences of Cultivated and Uncultivated Aerobic Methanotrophic Bacteria Evaluated Based on pmoA as Molecular Marker. *Front. Microbiol.* 6, 1346. doi:10.3389/fmicb.2015.01346.

Knowles, R. (2005). Denitrifiers associated with methanotrophs and their potential impact on the nitrogen cycle. *Ecological Engineering* 24, 441–446. doi:10.1016/j.ecoleng.2005.01.001.

Lu, P., Vogel, C., Wang, R., Yao, X., and Marcotte, E. M. (2007). Absolute protein expression profiling estimates the relative contributions of transcriptional and translational regulation. *Nat. Biotechnol.* 25, 117–124. doi:10.1038/nbt1270.

Murrell, J. C. (2010). The aerobic methane oxidizing bacteria (methanotrophs). *Handbook of Hydrocarbon and Lipid Microbiology*. doi:10.1007/978-3-540-77587-4_143.pdf.

Nazaries, L., Murrell, J. C., and Millard, P. (2013). Methane, microbes and models: fundamental understanding of the soil methane cycle for future predictions - Nazaries - 2013 - Environmental Microbiology - Wiley Online Library. *Environmental ….* doi:10.1111/1462-2920.12149/pdf.

Nie, L., Wu, G., and Zhang, W. (2006). Correlation of mRNA expression and protein abundance affected by multiple sequence features related to translational efficiency in *Desulfovibrio vulgaris*: a quantitative analysis. *Genetics* 174, 2229–2243. doi:10.1534/genetics.106.065862.

Ren, T., Roy, R., and Knowles, R. (2000). Production and consumption of nitric oxide by three methanotrophic bacteria. *Appl. Environ. Microbiol.* 66, 3891–3897. doi:10.1128/AEM.66.9.3891-3897.2000.

Söhngen, N. L. Uber bakterien, welche methan ab kohlenstoffnahrung and energiequelle gebrauchen. *Parasitenkd. Infectionskr.* 2, 513–517.

Stein, L. Y., and Klotz, M. G. (2011). Nitrifying and denitrifying pathways of methanotrophic bacteria. *Biochemical Society Transactions*.

Stein, L. Y., Yoon, S., Semrau, J. D., Dispirito, A. A., Crombie, A., Murrell, J. C., et al. (2010). Genome sequence of the obligate methanotroph *Methylosinus trichosporium* strain OB3b. *J. Bacteriol.* 192, 6497–6498. doi:10.1128/JB.01144-10.

Svenning, M. M., Hestnes, A. G., Wartiainen, I., Stein, L. Y., Klotz, M. G., Kalyuzhnaya, M. G., et al. (2011). Genome sequence of the Arctic methanotroph *Methylobacter tundripaludum* SV96. *J. Bacteriol.* 193, 6418–6419. doi:10.1128/JB.05380-11.

Vuilleumier, S., Khmelenina, V. N., Bringel, F., Reshetnikov, A. S., Lajus, A., Mangenot, S., et al. (2012). Genome sequence of the haloalkaliphilic methanotrophic bacterium *Methylomicrobium alcaliphilum* 20Z. *J. Bacteriol.* 194, 551–552. doi:10.1128/JB.06392-11.

Ward, N., Larsen, Ø., Sakwa, J., Bruseth, L., Khouri, H., Durkin, A. S., et al. (2004). Genomic Insights into Methanotrophy: The Complete Genome Sequence of *Methylococcus capsulatus* (Bath). *PLoS Biol* 2, e303. doi:10.1371/journal.pbio.0020303.

Ye, R. W., and Thomas, S. M. (2001). Microbial nitrogen cycles: physiology, genomics and

applications. *Curr. Opin. Microbiol.* 4, 307–312. doi:10.1016/S1369-5274(00)00208-3.

Yoshinari, T. (1985). Nitrite and nitrous oxide production by *Methylosinus trichosporium*. *Can. J. Microbiol.* 31, 139–144.

REFERENCES

Achbergerová, L., and Nahálka, J. (2011). Polyphosphate--an ancient energy source and active metabolic regulator. *Microb. Cell Fact.* 10, 63. doi:10.1186/1475-2859-10-63.

Balasubramanian, R., Smith, S. M., Rawat, S., Yatsunyk, L. A., Stemmler, T. L., and Rosenzweig, A. C. (2010). Oxidation of methane by a biological dicopper centre. *Nature* 465, 115–119. doi:10.1038/nature08992.

Beal, E. J., House, C. H., and Orphan, V. J. (2009). Manganese- and iron-dependent marine methane oxidation. *Science* 325, 184–187. doi:10.1126/science.1169984.

Bédard, C., and Knowles, R. (1989). Physiology, biochemistry, and specific inhibitors of CH_4, NH_4^+, and CO oxidation by methanotrophs and nitrifiers. *Microbiol. Rev.* 53, 68–84.

Bodelier, P. L. E., and Laanbroek, H. J. (2004). Nitrogen as a regulatory factor of methane oxidation in soils and sediments. *FEMS Microbiol. Ecol.* 47, 265–277. doi:10.1016/S0168-6496(03)00304-0.

Bodelier, P. L. E., and Steenbergh, A. K. (2014). Interactions between methane and the nitrogen cycle in light of climate change. *Current Opinion in Environmental Sustainability* 9-10, 26–36.

Bodelier, P. L., Roslev, P., Henckel, T., and Frenzel, P. (2000). Stimulation by ammonium-based fertilizers of methane oxidation in soil around rice roots. *Nature* 403, 421–424. doi:10.1038/35000193.

Boden, R., Cunliffe, M., Scanlan, J., Moussard, H., Kits, K. D., Klotz, M. G., et al. (2011). Complete genome sequence of the aerobic marine methanotroph *Methylomonas methanica* MC09. *J. Bacteriol.* 193, 7001–7002. doi:10.1128/JB.06267-11.

Boetius, A., Ravenschlag, K., Schubert, C. J., Rickert, D., Widdel, F., Gieseke, A., et al. (2000). A marine microbial consortium apparently mediating anaerobic oxidation of methane. *Nature* 407, 623–626. doi:10.1038/35036572.

Borisov, V. B., Gennis, R. B., Hemp, J., and Verkhovsky, M. I. (2011). The cytochrome *bd* respiratory oxygen reductases. *Biochimica et Biophysica Acta (BBA) - Bioenergetics* 1807, 1398–1413. doi:10.1016/j.bbabio.2011.06.016.

Calhoun, A., and King, G. M. (1998). Characterization of Root-Associated Methanotrophs from Three Freshwater Macrophytes: *Pontederia cordata, Sparganium eurycarpum*, and *Sagittaria latifolia*. *Appl. Environ. Microbiol.* 64, 1099–1105.

Cammack, R., Joannou, C. L., Cui, X.-Y., Torres Martinez, C., Maraj, S. R., and Hughes, M. N. (1999). Nitrite and nitrosyl compounds in food preservation. *Biochimica et Biophysica Acta (BBA) - Bioenergetics* 1411, 475–488. doi:10.1016/S0005-2728(99)00033-X.

Campbell, M. A., Nyerges, G., Kozlowski, J. A., Poret Peterson, A. T., Stein, L. Y., and Klotz, M. G. (2011). Model of the molecular basis for hydroxylamine oxidation and nitrous oxide production in methanotrophic bacteria. *FEMS Microbiology Letters* 322, 82–89. doi:10.1111/j.1574-6968.2011.02340.x.

Canfield, D. E., Glazer, A. N., and Falkowski, P. G. (2010). The evolution and future of Earth's nitrogen cycle. *Science* 330, 192–196. doi:10.1126/science.1186120.

Carrondo, M. A. (2003). Ferritins, iron uptake and storage from the bacterioferritin viewpoint. *EMBO J.* 22, 1959–1968. doi:10.1093/emboj/cdg215.

Chen, J., and Strous, M. (2013). Denitrification and aerobic respiration, hybrid electron transport chains and co-evolution. *Biochimica et Biophysica Acta (BBA) - Bioenergetics* 1827, 136–144. doi:10.1016/j.bbabio.2012.10.002.

Chen, Y., Crombie, A., Rahman, M. T., Dedysh, S. N., Liesack, W., Stott, M. B., et al. (2010). Complete genome sequence of the aerobic facultative methanotroph *Methylocella silvestris* BL2. *J. Bacteriol.* 192, 3840–3841. doi:10.1128/JB.00506-10.

Chistoserdova, L., and Lidstrom, M. E. (2013). "Aerobic methylotrophic prokaryotes," in *The Prokaryotes: Prokaryotic Physiology and Biochemistry* (Berlin, Heidelberg: Springer Berlin Heidelberg), 267–285. doi:10.1007/978-3-642-30141-4_68.

Chu, F., and Lidstrom, M. E. (2016). XoxF acts as the predominant methanol dehydrogenase in the type I methanotroph *Methylomicrobium buryatense*. *J. Bacteriol.* 198, 1317–1325. doi:10.1128/JB.00959-15.

Clark, D. P. (1989). The fermentation pathways of *Escherichia coli. FEMS Microbiol. Rev.* 5, 223–234. doi:10.1111/j.1574-6968.1989.tb03398.x.

Colin Murrell, J., and Jetten, M. S. M. (2009). The microbial methane cycle. *Environ Microbiol Rep* 1, 279–284. doi:10.1111/j.1758-2229.2009.00089.x/asset/j.1758-2229.2009.00089.x.pdf.

Conrad, R. (2009). The global methane cycle: Recent advances in understanding the microbial processes involved. *Environ Microbiol Rep* 1, 285–292. doi:10.1111/j.1758-2229.2009.00038.x/asset/j.1758-2229.2009.00038.x.pdf.

Corbin, R. W., Paliy, O., Yang, F., Shabanowitz, J., Platt, M., Lyons, C. E., et al. (2003). Toward a protein profile of *Escherichia coli*: comparison to its transcription profile. *Proc. Natl. Acad. Sci. U.S.A.* 100, 9232–9237. doi:10.1073/pnas.1533294100.

Costa, C., Dijkema, C., Friedrich, M., García-Encina, P., Fernández-Polanco, F., and Stams, A. J. (2000). Denitrification with methane as electron donor in oxygen-limited bioreactors. *Appl. Microbiol. Biotechnol.* 53, 754–762.

Cox, J., and Mann, M. (2012). 1D and 2D annotation enrichment: a statistical method integrating quantitative proteomics with complementary high-throughput data. *BMC Bioinformatics* 13 Suppl 16, S12. doi:10.1186/1471-2105-13-S16-S12.

Cramm, R., Siddiqui, R. A., and Friedrich, B. (1997). Two isofunctional nitric oxide reductases in *Alcaligenes eutrophus* H16. *J. Bacteriol.* 179, 6769–6777.

Csáki, R., Hanczár, T., Bodrossy, L., Murrell, J. C., and Kovács, K. L. (2001). Molecular characterization of structural genes coding for a membrane bound hydrogenase in *Methylococcus capsulatus* (Bath). *FEMS Microbiology Letters* 205, 203–207. doi:10.1016/S0378-1097(01)00469-4.

Dalton, H. (1977). Ammonia oxidation by the methane oxidising bacterium *Methylococcus capsulatus* strain bath. *Arch. Microbiol.* 114, 273–279. doi:10.1007/BF00446873.

Dalton, H. (1980). Oxidation of Hydrocarbons by Methane Monooxygenases from a Variety of Microbes. *Adv. Appl. Microbiol.* 26, 71–87. doi:10.1016/S0065-2164(08)70330-7.

Dam, B., Dam, S., Blom, J., and Liesack, W. (2013). Genome Analysis Coupled with Physiological Studies Reveals a Diverse Nitrogen Metabolism in *Methylocystis* sp. Strain SC2. *PLoS ONE* 8, e74767. doi:10.1371/journal.pone.0074767.

Dam, B., Dam, S., Kube, M., Reinhardt, R., and Liesack, W. (2012). Complete genome sequence of *Methylocystis* sp. strain SC2, an aerobic methanotroph with high-affinity methane oxidation potential. *J. Bacteriol.* 194, 6008–6009. doi:10.1128/JB.01446-12.

de Sousa Abreu, R., Penalva, L. O., Marcotte, E. M., and Vogel, C. (2009). Global signatures of protein and mRNA expression levels. *Mol Biosyst* 5, 1512–1526. doi:10.1039/b908315d.

de Souza, G. A., Leversen, N. A., Målen, H., and Wiker, H. G. (2011). Bacterial proteins with cleaved or uncleaved signal peptides of the general secretory pathway. *J Proteomics* 75,

502–510. doi:10.1016/j.jprot.2011.08.016.

Demirbas, A. (2010). *Methane Gas Hydrate*. London: Springer London doi:10.1007/978-1-84882-872-8.

Dillies, M.-A., Rau, A., Aubert, J., Hennequet-Antier, C., Jeanmougin, M., Servant, N., et al. (2013). A comprehensive evaluation of normalization methods for Illumina high-throughput RNA sequencing data analysis. *Brief. Bioinformatics* 14, 671–683. doi:10.1093/bib/bbs046.

Dobritzsch, D., König, S., Schneider, G., and Lu, G. (1998). High resolution crystal structure of pyruvate decarboxylase from *Zymomonas mobilis*. Implications for substrate activation in pyruvate decarboxylases. *J. Biol. Chem.* 273, 20196–20204. doi:10.1074/jbc.273.32.20196.

Dunfield, P., and Knowles, R. (1995). Kinetics of inhibition of methane oxidation by nitrate, nitrite, and ammonium in a humisol. *Appl. Environ. Microbiol.* 61, 3129–3135.

Eram, M. S., and Ma, K. (2013). Decarboxylation of pyruvate to acetaldehyde for ethanol production by hyperthermophiles. *Biomolecules* 3, 578–596. doi:10.3390/biom3030578.

Ettwig, K. F., Butler, M. K., Le Paslier, D., Pelletier, E., Mangenot, S., Kuypers, M. M. M., et al. (2010). Nitrite-driven anaerobic methane oxidation by oxygenic bacteria. *Nature* 464, 543–548. doi:10.1038/nature08883.

Fischer, F., Wolters, D., Rögner, M., and Poetsch, A. (2006). Toward the complete membrane proteome: High coverage of integral membrane proteins through transmembrane peptide detection. *Mol. Cell Proteomics* 5, 444–453. doi:10.1074/mcp.M500234-MCP200.

Florens, L., Carozza, M. J., Swanson, S. K., Fournier, M., Coleman, M. K., Workman, J. L., et al. (2006). Analyzing chromatin remodeling complexes using shotgun proteomics and normalized spectral abundance factors. *Methods* 40, 303–311. doi:10.1016/j.ymeth.2006.07.028.

Gelius Dietrich, G., and Henze, K. (2004). Pyruvate Formate Lyase (PFL) and PFL Activating Enzyme in the Chytrid Fungus Neocallimastix frontalis: A Free-Radical Enzyme System Conserved Across Divergent Eukaryotic Lineages. *Journal of Eukaryotic Microbiology* 51, 456–463. doi:10.1111/j.1550-7408.2004.tb00394.x.

Gilman, A., Laurens, L. M., Puri, A. W., Chu, F., Pienkos, P. T., and Lidstrom, M. E. (2015). Bioreactor performance parameters for an industrially-promising methanotroph *Methylomicrobium buryatense* 5GB1. *Microb. Cell Fact.* 14, 182. doi:10.1186/s12934-015-0372-8.

González, P. J., Correia, C., Moura, I., Brondino, C. D., and Moura, J. J. G. (2006). Bacterial nitrate reductases: Molecular and biological aspects of nitrate reduction. *J. Inorg. Biochem.* 100, 1015–1023. doi:10.1016/j.jinorgbio.2005.11.024.

Grillo-Puertas, M., Villegas, J. M., Rintoul, M. R., and Rapisarda, V. A. (2012). Polyphosphate Degradation in Stationary Phase Triggers Biofilm Formation via LuxS Quorum Sensing System in *Escherichia coli*. *PLoS ONE* 7, e50368. doi:10.1371/journal.pone.0050368.

Gu, W., Haque, M. F. U., Dispirito, A. A., and Semrau, J. D. (2016). Uptake and Effect of Rare Earth Elements on Gene Expression in *Methylosinus trichosporium* OB3b. *FEMS Microbiology Letters*. doi:10.1093/femsle/fnw129.

Hamilton, R., Kits, K. D., Ramonovskaya, V. A., Rozova, O. N., Yurimoto, H., Iguchi, H., et al. (2015). Draft genomes of gammaproteobacterial methanotrophs isolated from terrestrial ecosystems. *Genome Announc* 3, e00515–15. doi:10.1128/genomeA.00515-15.

Hanczár, T., Csáki, R., Bodrossy, L., Murrell, J. C., and Kovács, K. L. (2002). Detection and localization of two hydrogenases in *Methylococcus capsulatus* (Bath) and their potential role in methane metabolism. *Arch. Microbiol.* 177, 167–172. doi:10.1007/s00203-001-0372-4.

Hanson, R. S., and Hanson, T. E. (1996). Methanotrophic bacteria. *Microbiol. Rev.* 60, 439–471.

Hanson, T. E., Campbell, B. J., Kalis, K. M., Campbell, M. A., and Klotz, M. G. (2013). Nitrate ammonification by Nautilia profundicola AmH: experimental evidence consistent with a free hydroxylamine intermediate. *Front. Microbiol.* 4, 180. doi:10.3389/fmicb.2013.00180.

Haroon, M. F., Hu, S., Shi, Y., Imelfort, M., Keller, J., Hugenholtz, P., et al. (2013). Anaerobic oxidation of methane coupled to nitrate reduction in a novel archaeal lineage. *Nature* 500, 567–570. doi:10.1038/nature12375.

Hinrichs, K. U., Hayes, J. M., Sylva, S. P., Brewer, P. G., and DeLong, E. F. (1999). Methane-consuming archaebacteria in marine sediments. *Nature* 398, 802–805. doi:10.1038/19751.

Hoefman, S., van der Ha, D., Boon, N., Vandamme, P., De Vos, P., and Heylen, K. (2014). Niche differentiation in nitrogen metabolism among methanotrophs within an operational taxonomic unit. *BMC Microbiology* 14, 83. doi:10.1186/1471-2180-14-83.

Hoehler, T. M., Alperin, M. J., Albert, D. B., and Martens, C. S. (1994). Field and laboratory studies of methane oxidation in an anoxic marine sediment: Evidence for a methanogen-sulfate reducer consortium. *Global Biogeochemical Cycles* 8, 451–463. doi:10.1029/94GB01800.

Holmes, A. J., Costello, A., Lidstrom, M. E., and Murrell, J. C. (1995). Evidence that particulate methane monooxygenase and ammonia monooxygenase may be evolutionarily related. *FEMS Microbiology Letters* 132, 203–208.

Honarmand Ebrahimi, K., Hagedoorn, P.-L., and Hagen, W. R. (2015). Unity in the biochemistry of the iron-storage proteins ferritin and bacterioferritin. *Chem. Rev.* 115, 295–326. doi:10.1021/cr5004908.

Hou, S., Makarova, K. S., Saw, J. H., Senin, P., and Ly, B. V. (2008). Complete genome

sequence of the extremely acidophilic methanotroph isolate V4, *Methylacidiphilum infernorum*, a representative of the bacterial phylum …. *Biol ….*

Jayapal, K. P., Philp, R. J., Kok, Y.-J., Yap, M. G. S., Sherman, D. H., Griffin, T. J., et al. (2008). Uncovering genes with divergent mRNA-protein dynamics in *Streptomyces coelicolor*. *PLoS ONE* 3, e2097. doi:10.1371/journal.pone.0002097.

Kalyuzhnaya, M. G., Yang, S., Rozova, O. N., Smalley, N. E., Clubb, J., Lamb, A., et al. (2013). Highly efficient methane biocatalysis revealed in a methanotrophic bacterium. *Nat Comms* 4, 2785. doi:10.1038/ncomms3785.

Kanehisa, M., Sato, Y., and Morishima, K. (2016). BlastKOALA and GhostKOALA: KEGG Tools for Functional Characterization of Genome and Metagenome Sequences. *J. Mol. Biol.* 428, 726–731. doi:10.1016/j.jmb.2015.11.006.

Kao, W.-C., Chen, Y.-R., Yi, E. C., Lee, H., Tian, Q., Wu, K.-M., et al. (2004). Quantitative proteomic analysis of metabolic regulation by copper ions in *Methylococcus capsulatus* (Bath). *J. Biol. Chem.* 279, 51554–51560. doi:10.1074/jbc.M408013200.

Kearse, M., Moir, R., Wilson, A., Stones-Havas, S., Cheung, M., Sturrock, S., et al. (2012). Geneious Basic: an integrated and extendable desktop software platform for the organization and analysis of sequence data. *Bioinformatics* 28, 1647–1649. doi:10.1093/bioinformatics/bts199.

Khadem, A. F., Pol, A., Wieczorek, A. S., Jetten, M. S. M., and Op den Camp, H. J. M. (2012a). Metabolic regulation of "Ca. *Methylacidiphilum fumariolicum*" soIV cells grown under different nitrogen and oxygen limitations. *Front. Microbiol.* 3.

Khadem, A. F., Pol, A., Wieczorek, A., Mohammadi, S. S., Francoijs, K.-J., Stunnenberg, H. G., et al. (2011). Autotrophic methanotrophy in verrucomicrobia: *Methylacidiphilum*

fumariolicum SolV uses the Calvin-Benson-Bassham cycle for carbon dioxide fixation. *J. Bacteriol.* 193, 4438–4446. doi:10.1128/JB.00407-11.

Khadem, A. F., van Teeseling, M. C. F., van Niftrik, L., Jetten, M. S. M., Op den Camp, H. J. M., and Pol, A. (2012b). Genomic and Physiological Analysis of Carbon Storage in the Verrucomicrobial Methanotroph "Ca. *Methylacidiphilum fumariolicum*" SolV. *Front. Microbiol.* 3, 345. doi:10.3389/fmicb.2012.00345.

Khadem, A. F., Wieczorek, A. S., Pol, A., Vuilleumier, S., Harhangi, H. R., Dunfield, P. F., et al. (2012c). Draft genome sequence of the volcano-inhabiting thermoacidophilic methanotroph *Methylacidiphilum fumariolicum* strain SolV. *J. Bacteriol.* 194, 3729–3730. doi:10.1128/JB.00501-12.

Khmelenina, V. N., Beck, D. A. C., Munk, C., Davenport, K., Daligault, H., Erkkila, T., et al. (2013). Draft Genome Sequence of *Methylomicrobium buryatense* Strain 5G, a Haloalkaline-Tolerant Methanotrophic Bacterium. *Genome Announc* 1, e00053–13. doi:10.1128/genomeA.00053-13.

King, G. M., and Schnell, S. (1994). Ammonium and Nitrite Inhibition of Methane Oxidation by *Methylobacter albus* BG8 and *Methylosinus trichosporium* OB3b at Low Methane Concentrations. *Appl. Environ. Microbiol.* 60, 3508–3513.

Kits, K. D., Campbell, D. J., Rosana, A. R., and Stein, L. Y. (2015a). Diverse electron sources support denitrification under hypoxia in the obligate methanotroph *Methylomicrobium album* strain BG8. *Front. Microbiol.* 6, 1072. doi:10.3389/fmicb.2015.01072.

Kits, K. D., Kalyuzhnaya, M. G., Klotz, M. G., Jetten, M. S. M., Op den Camp, H. J. M., Vuilleumier, S., et al. (2013). Genome Sequence of the Obligate Gammaproteobacterial Methanotroph *Methylomicrobium album* Strain BG8. *Genome Announc* 1, e0017013–

e00170–13. doi:10.1128/genomeA.00170-13.

Kits, K. D., Klotz, M. G., and Stein, L. Y. (2015b). Methane oxidation coupled to nitrate reduction under hypoxia by the Gammaproteobacterium *Methylomonas denitrificans,* sp. nov. type strain FJG1. *Environ. Microbiol.* 17, 3219–3232. doi:10.1111/1462-2920.12772.

Knappe, J., and Sawers, G. (1990). A radical-chemical route to acetyl-CoA: the anaerobically induced pyruvate formate-lyase system of *Escherichia coli*. *FEMS Microbiol. Rev.* 6, 383–398.

Knief, C. (2015). Diversity and Habitat Preferences of Cultivated and Uncultivated Aerobic Methanotrophic Bacteria Evaluated Based on pmoA as Molecular Marker. *Front. Microbiol.* 6, 1346. doi:10.3389/fmicb.2015.01346.

Knowles, R. (2005). Denitrifiers associated with methanotrophs and their potential impact on the nitrogen cycle. *Ecological Engineering* 24, 441–446. doi:10.1016/j.ecoleng.2005.01.001.

Kozlowski, J. A., Price, J., and Stein, L. Y. (2014). Revision of N_2O-producing pathways in the ammonia-oxidizing bacterium *Nitrosomonas europaea* ATCC 19718. *Appl. Environ. Microbiol.* 80, 4930–4935. doi:10.1128/AEM.01061-14.

Kraft, B., Tegetmeyer, H. E., Sharma, R., Klotz, M. G., Ferdelman, T. G., Hettich, R. L., et al. (2014). Nitrogen cycling. The environmental controls that govern the end product of bacterial nitrate respiration. *Science* 345, 676–679. doi:10.1126/science.1254070.

Kuroda, A., Nomura, K., Ohtomo, R., Kato, J., Ikeda, T., Takiguchi, N., et al. (2001). Role of inorganic polyphosphate in promoting ribosomal protein degradation by the Lon protease in E. coli. *Science* 293, 705–708. doi:10.1126/science.1061315.

la Torre, de, A., Metivier, A., Chu, F., Laurens, L. M. L., Beck, D. A. C., Pienkos, P. T., et al. (2015). Genome-scale metabolic reconstructions and theoretical investigation of methane

conversion in *Methylomicrobium buryatense* strain 5G(B1). *Microb. Cell Fact.* 14, 188. doi:10.1186/s12934-015-0377-3.

Le Brun, N. E., Andrews, S. C., Guest, J. R., Harrison, P. M., Moore, G. R., and Thomson, A. J. (1995). Identification of the ferroxidase centre of *Escherichia coli* bacterioferritin. *Biochem. J.* 312 (Pt 2), 385–392.

Lieberman, R. L., and Rosenzweig, A. C. (2005). Crystal structure of a membrane-bound metalloenzyme that catalyses the biological oxidation of methane. *Nature* 434, 177–182. doi:10.1038/nature03311.

Lindner, A. S., Pacheco, A., Aldrich, H. C., Staniec, A. C., Uz, I., and Hodson, D. J. (2007). *Methylocystis hirsuta* sp. nov., a novel methanotroph isolated from a groundwater aquifer. *International Journal of Systematic and Evolutionary Microbiology* 57, 1891–1900. doi:10.1099/ijs.0.64541-0.

Lipscomb, J. D. (1994). Biochemistry of the soluble methane monooxygenase. *Annual Reviews in Microbiology*.

Liu, J., Sun, F., Wang, L., Ju, X., Wu, W., and Chen, Y. (2014). Molecular characterization of a microbial consortium involved in methane oxidation coupled to denitrification under micro-aerobic conditions. *Microb Biotechnol* 7, 64–76. doi:10.1111/1751-7915.12097.

Lu, P., Vogel, C., Wang, R., Yao, X., and Marcotte, E. M. (2007). Absolute protein expression profiling estimates the relative contributions of transcriptional and translational regulation. *Nat. Biotechnol.* 25, 117–124. doi:10.1038/nbt1270.

Mackelprang, R., Waldrop, M. P., DeAngelis, K. M., David, M. M., Chavarria, K. L., Blazewicz, S. J., et al. (2011). Metagenomic analysis of a permafrost microbial community reveals a rapid response to thaw. *Nature* 480, 368–371. doi:10.1038/nature10576.

Martens, C. S., and Berner, R. A. (1974). Methane production in the interstitial waters of sulfate-depleted marine sediments. *Science* 185, 1167–1169. doi:10.1126/science.185.4157.1167.

Matsen, J. B., Yang, S., Stein, L. Y., Beck, D., and Kalyuzhnaya, M. G. (2013). Global Molecular Analyses of Methane Metabolism in Methanotrophic Alphaproteobacterium, *Methylosinus trichosporium* OB3b. Part I: Transcriptomic Study. *Front. Microbiol.* 4. doi:10.3389/fmicb.2013.00040.

McGlynn, S. E., Chadwick, G. L., Kempes, C. P., and Orphan, V. J. (2015). Single cell activity reveals direct electron transfer in methanotrophic consortia. *Nature* 526, 531–535. doi:10.1038/nature15512.

Mesa, S., Velasco, L., Manzanera, M. E., Delgado, M. J., and Bedmar, E. J. (2002). Characterization of the *norCBQD genes*, encoding nitric oxide reductase, in the nitrogen fixing bacterium *Bradyrhizobium japonicum*. *J Gen Microbiol* 148, 3553–3560.

Milucka, J., Ferdelman, T. G., Polerecky, L., Franzke, D., Wegener, G., Schmid, M., et al. (2012). Zero-valent sulphur is a key intermediate in marine methane oxidation. *Nature* 491, 541–546. doi:10.1038/nature11656.

Mountfort, D. O. (1990). Oxidation of aromatic alcohols by purified methanol dehydrogenase from *Methylosinus trichosporium*. *J. Bacteriol.* 172, 3690–3694.

Murrell, J. C. (2010). The aerobic methane oxidizing bacteria (methanotrophs). *Handbook of Hydrocarbon and Lipid Microbiology*. doi:10.1007/978-3-540-77587-4_143.pdf.

Murrell, J. C., and Dalton, H. (1983). Nitrogen Fixation in Obligate Methanotrophs. *J Gen Microbiol* 129, 3481–3486.

Murrell, J. C., and Jetten, M. S. M. (2009). The microbial methane cycle. *Environ Microbiol Rep* 1, 279–284. doi:10.1111/j.1758-2229.2009.00089.x.

Nazaries, L., Murrell, J. C., and Millard, P. (2013). Methane, microbes and models: fundamental understanding of the soil methane cycle for future predictions - Nazaries - 2013 - Environmental Microbiology - Wiley Online Library. *Environmental ….* doi:10.1111/1462-2920.12149/pdf.

Nie, L., Wu, G., and Zhang, W. (2006). Correlation of mRNA expression and protein abundance affected by multiple sequence features related to translational efficiency in *Desulfovibrio vulgaris*: a quantitative analysis. *Genetics* 174, 2229–2243. doi:10.1534/genetics.106.065862.

Nyerges, G., and Stein, L. Y. (2009). Ammonia cometabolism and product inhibition vary considerably among species of methanotrophic bacteria. *FEMS Microbiology Letters* 297, 131–136. doi:10.1111/j.1574-6968.2009.01674.x.

Nyerges, G., Han, S.-K., and Stein, L. Y. (2010). Effects of ammonium and nitrite on growth and competitive fitness of cultivated methanotrophic bacteria. *Appl. Environ. Microbiol.* 76, 5648–5651. doi:10.1128/AEM.00747-10.

Oberg, A. L., and Vitek, O. (2009). Statistical design of quantitative mass spectrometry-based proteomic experiments. *J. Proteome Res.* 8, 2144–2156. doi:10.1021/pr8010099.

Olsen, J. V., de Godoy, L. M. F., Li, G., Macek, B., Mortensen, P., Pesch, R., et al. (2005). Parts per million mass accuracy on an Orbitrap mass spectrometer via lock mass injection into a C-trap. *Mol. Cell Proteomics* 4, 2010–2021. doi:10.1074/mcp.T500030-MCP200.

Patel, N. A., Crombie, A., Slade, S. E., Thalassinos, K., Hughes, C., Connolly, J. B., et al. (2012). Comparison of one- and two-dimensional liquid chromatography approaches in the label-free quantitative analysis of *Methylocella silvestris*. *J. Proteome Res.* 11, 4755–4763. doi:10.1021/pr300253s.

Patel, V. J., Thalassinos, K., Slade, S. E., Connolly, J. B., Crombie, A., Murrell, J. C., et al. (2009). A comparison of labeling and label-free mass spectrometry-based proteomics approaches. *J. Proteome Res.* 8, 3752–3759. doi:10.1021/pr900080y.

Pol, A., Barends, T. R. M., Dietl, A., Khadem, A. F., Eygensteyn, J., Jetten, M. S. M., et al. (2014). Rare earth metals are essential for methanotrophic life in volcanic mudpots. *Environ. Microbiol.* 16, 255–264. doi:10.1111/1462-2920.12249.

Poret Peterson, A. T., Graham, J. E., Gulledge, J., and Klotz, M. G. (2008). Transcription of nitrification genes by the methane-oxidizing bacterium, *Methylococcus capsulatus* strain Bath. *ISME J* 2, 1213–1220. doi:10.1038/ismej.2008.71.

Rao, N. N., and Kornberg, A. (1996). Inorganic polyphosphate supports resistance and survival of stationary-phase *Escherichia coli*. *J. Bacteriol.* 178, 1394–1400.

Rao, N. N., and Kornberg, A. (1999). Inorganic polyphosphate regulates responses of *Escherichia coli* to nutritional stringencies, environmental stresses and survival in the stationary phase. *Prog. Mol. Subcell. Biol.* 23, 183–195.

Reeburgh, W. S. (2007). Oceanic Methane Biogeochemistry. *Chem. Rev.* 107, 486–513. doi:10.1021/cr050362v.

Reith, F., Drake, H. L., and Küsel, K. (2002). Anaerobic activities of bacteria and fungi in moderately acidic conifer and deciduous leaf litter. *FEMS Microbiol. Ecol.* 41, 27–35. doi:10.1111/j.1574-6941.2002.tb00963.x.

Ren, T., Roy, R., and Knowles, R. (2000). Production and consumption of nitric oxide by three methanotrophic bacteria. *Appl. Environ. Microbiol.* 66, 3891–3897. doi:10.1128/AEM.66.9.3891-3897.2000.

Richardson, D. J., Berks, B. C., Russell, D. A., Spiro, S., and Taylor, C. J. (2001). Functional,

biochemical and genetic diversity of prokaryotic nitrate reductases. *Cell. Mol. Life Sci.* 58, 165–178.

Roslev, P., and King, G. M. (1994). Survival and recovery of methanotrophic bacteria starved under oxic and anoxic conditions. *Appl. Environ. Microbiol.* 60, 2602–2608.

Roslev, P., and King, G. M. (1995). Aerobic and anaerobic starvation metabolism in methanotrophic bacteria. *Appl. Environ. Microbiol.* 61, 1563–1570.

Saidi-Mehrabad, A., He, Z., Tamas, I., Sharp, C. E., Brady, A. L., Rochman, F. F., et al. (2013). Methanotrophic bacteria in oilsands tailings ponds of northern Alberta. *ISME J* 7, 908–921. doi:10.1038/ismej.2012.163.

Scheller, S., Yu, H., Chadwick, G. L., McGlynn, S. E., and Orphan, V. J. (2016). Artificial electron acceptors decouple archaeal methane oxidation from sulfate reduction. *Science* 351, 703–707. doi:10.1126/science.aad7154.

Semrau, J. D., Dispirito, A. A., and Yoon, S. (2010). Methanotrophs and copper. *FEMS Microbiol. Rev.* 34, 496–531. doi:10.1111/j.1574-6976.2010.00212.x.

Serang, O., MacCoss, M. J., and Noble, W. S. (2010). Efficient marginalization to compute protein posterior probabilities from shotgun mass spectrometry data. *J. Proteome Res.* 9, 5346–5357. doi:10.1021/pr100594k.

Simon, J., and Klotz, M. G. (2013). Diversity and evolution of bioenergetic systems involved in microbial nitrogen compound transformations. *Biochim. Biophys. Acta* 1827, 114–135. doi:10.1016/j.bbabio.2012.07.005.

Skennerton, C. T., Ward, L. M., Michel, A., Metcalfe, K., Valiente, C., Mullin, S., et al. (2015). Genomic reconstruction of an uncultured hydrothermal vent gammaproteobacterial methanotroph (Family Methylothermaceae) indicates multiple adaptations to oxygen

limitation. *Front. Microbiol.* 6, 1425. doi:10.3389/fmicb.2015.01425.

Söhngen, N. L. Uber bakterien, welche methan ab kohlenstoffnahrung and energiequelle gebrauchen. *Parasitenkd. Infectionskr.* 2, 513–517.

Spivak, M., Weston, J., Bottou, L., Käll, L., and Noble, W. S. (2009). Improvements to the percolator algorithm for Peptide identification from shotgun proteomics data sets. *J. Proteome Res.* 8, 3737–3745. doi:10.1021/pr801109k.

Stein, L. Y., and Klotz, M. G. (2011a). Nitrifying and denitrifying pathways of methanotrophic bacteria. *Biochemical Society Transactions*.

Stein, L. Y., and Klotz, M. G. (2011b). Nitrifying and denitrifying pathways of methanotrophic bacteria. *Biochemical Society Transactions* 39, 1826–1831. doi:10.1042/BST20110712.

Stein, L. Y., Bringel, F., Dispirito, A. A., Han, S., Jetten, M. S. M., Kalyuzhnaya, M. G., et al. (2011). Genome sequence of the methanotrophic Alphaproteobacterium, *Methylocystis* sp. Rockwell (ATCC 49242). *J. Bacteriol.* 193, 2668–2669. doi:10.1128/JB.00278-11.

Stein, L. Y., Yoon, S., Semrau, J. D., Dispirito, A. A., Crombie, A., Murrell, J. C., et al. (2010). Genome sequence of the obligate methanotroph *Methylosinus trichosporium* strain OB3b. *J. Bacteriol.* 192, 6497–6498. doi:10.1128/JB.01144-10.

Stieglmeier, M., Mooshammer, M., Kitzler, B., Wanek, W., Zechmeister-Boltenstern, S., Richter, A., et al. (2014). Aerobic nitrous oxide production through N-nitrosating hybrid formation in ammonia-oxidizing archaea. *ISME J* 8, 1135–1146. doi:10.1038/ismej.2013.220.

Sutka, R. L., Ostrom, N. E., Ostrom, P. H., Gandhi, H., and Breznak, J. A. (2003). Nitrogen isotopomer site preference of N_2O produced by *Nitrosomonas europaea* and *Methylococcus capsulatus* Bath. *Rapid Commun. Mass Spectrom.* 17, 738–745. doi:10.1002/rcm.968.

Svenning, M. M., Hestnes, A. G., Wartiainen, I., Stein, L. Y., Klotz, M. G., Kalyuzhnaya, M. G., et al. (2011). Genome sequence of the Arctic methanotroph *Methylobacter tundripaludum* SV96. *J. Bacteriol.* 193, 6418–6419. doi:10.1128/JB.05380-11.

Tavormina, P. L., Orphan, V. J., Kalyuzhnaya, M. G., Jetten, M. S. M., and Klotz, M. G. (2011). A novel family of functional operons encoding methane/ammonia monooxygenase-related proteins in gammaproteobacterial methanotrophs. *Environ Microbiol Rep* 3, 91–100. doi:10.1111/j.1758-2229.2010.00192.x.

Teraguchi, S., and Hollocher, T. C. (1989). Purification and some characteristics of a cytochrome c-containing nitrous oxide reductase from *Wolinella succinogenes*. *J. Biol. Chem.* 264, 1972–1979.

Thauer, R. K., Jungermann, K., and Decker, K. (1977). Energy conservation in chemotrophic anaerobic bacteria. *Bacteriol Rev* 41, 809–180.

Theisen, A. R., and Murrell, J. C. (2005). Facultative methanotrophs revisited. *J. Bacteriol.* 187, 4303–4305. doi:10.1128/JB.187.13.4303-4305.2005.

Trotsenko, Y. A., and Murrell, J. C. (2008). Metabolic aspects of aerobic obligate methanotrophy. *Adv. Appl. Microbiol.* 63, 183–229. doi:10.1016/S0065-2164(07)00005-6.

Trotsenko, Y. A., and Shishkina, V. N. (1990). Studies on phosphate metabolism in obligate methanotrophs. *FEMS Microbiology Letters* 87, 267–271. doi:10.1016/0378-1097(90)90465-3.

Tsugawa, W., Shimizu, H., Masahiro Tata, R. A., Ueno, Y., Kojima, K., and Sode, K. (2012). Nitrous oxide sensing using oxygen-Insensitive direct-electron-transfer- type Nitrous oxide reductase. *Electrochemistry* 80, 371–374. doi:10.5796/electrochemistry.80.371.

Tusher, V. G., Tibshirani, R., and Chu, G. (2001). Significance analysis of microarrays applied

to the ionizing radiation response. *Proc. Natl. Acad. Sci. U.S.A.* 98, 5116–5121. doi:10.1073/pnas.091062498.

Tveit, A. T., Urich, T., and Svenning, M. M. (2014). Metatranscriptomic analysis of arctic peat soil microbiota. *Appl. Environ. Microbiol.* 80, 5761–5772. doi:10.1128/AEM.01030-14.

Tveit, A., Schwacke, R., Svenning, M. M., and Urich, T. (2013). Organic carbon transformations in high-Arctic peat soils: key functions and microorganisms. *ISME J* 7, 299–311. doi:10.1038/ismej.2012.99.

van Teeseling, M. C. F., Pol, A., Harhangi, H. R., van der Zwart, S., Jetten, M. S. M., Op den Camp, H. J. M., et al. (2014). Expanding the verrucomicrobial methanotrophic world: description of three novel species of *Methylacidimicrobium* gen. nov. *Appl. Environ. Microbiol.* 80, 6782–6791. doi:10.1128/AEM.01838-14.

Vizcaíno, J. A., Deutsch, E. W., Wang, R., Csordas, A., Reisinger, F., Ríos, D., et al. (2014). ProteomeXchange provides globally coordinated proteomics data submission and dissemination. *Nat. Biotechnol.* 32, 223–226. doi:10.1038/nbt.2839.

Vuilleumier, S., Khmelenina, V. N., Bringel, F., Reshetnikov, A. S., Lajus, A., Mangenot, S., et al. (2012). Genome sequence of the haloalkaliphilic methanotrophic bacterium *Methylomicrobium alcaliphilum* 20Z. *J. Bacteriol.* 194, 551–552. doi:10.1128/JB.06392-11.

Wagner, G. P., Kin, K., and Lynch, V. J. (2012). Measurement of mRNA abundance using RNA-seq data: RPKM measure is inconsistent among samples. *Theory Biosci.* 131, 281–285. doi:10.1007/s12064-012-0162-3.

Wahlgren, W. Y., Omran, H., Stetten, von, D., Royant, A., van der Post, S., and Katona, G. (2012). Structural Characterization of Bacterioferritin from *Blastochloris viridis*. *PLoS ONE* 7, e46992. doi:10.1371/journal.pone.0046992.

Ward, N., Larsen, Ø., Sakwa, J., Bruseth, L., Khouri, H., Durkin, A. S., et al. (2004). Genomic Insights into Methanotrophy: The Complete Genome Sequence of *Methylococcus capsulatus* (Bath). *PLoS Biol* 2, e303. doi:10.1371/journal.pbio.0020303.

Wegener, G., Krukenberg, V., Riedel, D., Tegetmeyer, H. E., and Boetius, A. (2015). Intercellular wiring enables electron transfer between methanotrophic archaea and bacteria. *Nature* 526, 587–590. doi:10.1038/nature15733.

Wei, W., Isobe, K., Nishizawa, T., Zhu, L., Shiratori, Y., Ohte, N., et al. (2015). Higher diversity and abundance of denitrifying microorganisms in environments than considered previously. *ISME J*. doi:10.1038/ismej.2015.9.

White, D., Drummond, J., and Fuqua, C. (2012). "The Physiology and Biochemistry of Prokaryotes," in (New York: Oxford University Press), 358–382.

Whittenbury, R., Phillips, K. C., and Wilkinson, J. F. (1970). Enrichment, Isolation and Some Properties of Methane-utilizing Bacteria. *J Gen Microbiol* 61, 205–218. doi:10.1099/00221287-61-2-205.

Wiśniewski, J. R., Zougman, A., Nagaraj, N., and Mann, M. (2009). Universal sample preparation method for proteome analysis. *Nat. Methods* 6, 359–362. doi:10.1038/nmeth.1322.

Ye, R. W., and Thomas, S. M. (2001). Microbial nitrogen cycles: physiology, genomics and applications. *Curr. Opin. Microbiol.* 4, 307–312. doi:10.1016/S1369-5274(00)00208-3.

Yoshinari, T. (1985). Nitrite and nitrous oxide production by *Methylosinus trichosporium*. *Can. J. Microbiol.* 31, 139–144.

Zahn, J. A., and DiSpirito, A. A. (1996). Membrane-associated methane monooxygenase from *Methylococcus capsulatus* (Bath). *J. Bacteriol.* 178, 1018–1029.

Zhu, J., Wang, Q., Yuan, M., Tan, G.-Y. A., Sun, F., Wang, C., et al. (2016). Microbiology and potential applications of aerobic methane oxidation coupled to denitrification (AME-D) process: A review. *Water Res.* 90, 203–215. doi:10.1016/j.watres.2015.12.020.

Zumft, W. G. (1997). Cell biology and molecular basis of denitrification. *Microbiol. Rev.* 61, 533–616.

Zumft, W. G. (2005). Nitric oxide reductases of prokaryotes with emphasis on the respiratory, heme-copper oxidase type. *J. Inorg. Biochem.* 99, 194–215. doi:10.1016/j.jinorgbio.2004.09.024.

Appendix A

Citation: Kits, K. D., Kalyuzhnaya, M. G., Klotz, M. G., Jetten, M. S. M., Op den Camp, H. J. M., Vuilleumier, S., et al. (2013). Genome Sequence of the Obligate Gammaproteobacterial Methanotroph Methylomicrobium album Strain BG8. *Genome Announc* 1, e0017013–e00170–13. doi:10.1128/genomeA.00170-13.

genomeA
Journals.ASM.org

Genome Sequence of the Obligate Gammaproteobacterial Methanotroph *Methylomicrobium album* Strain BG8

K. Dimitri Kits,[a] Marina G. Kalyuzhnaya,[b] Martin G. Klotz,[c] Mike S. M. Jetten,[d] Huub J. M. Op den Camp,[d] Stéphane Vuilleumier,[e] Françoise Bringel,[e] Alan A. DiSpirito,[f] J. Colin Murrell,[g] D. Bruce,[h] J.-F. Cheng,[i] A. Copeland,[i] Lynne Goodwin,[h] Loren Hauser,[j] Aurélie Lajus,[k] M. L. Land,[j] A. Lapidus,[i] S. Lucas,[i] Claudine Médigue,[k] S. Pitluck,[i] Tanja Woyke,[i] A. Zeytun,[h] Lisa Y. Stein[a]

Department of Biological Sciences, University of Alberta, Edmonton, Alberta, Canada[a]; Department of Microbiology, University of Washington, Seattle, Washington, USA[b]; Department of Biology, University of North Carolina, Charlotte, North Carolina, USA[c]; Department of Microbiology, IWWR, Radboud University Nijmegen, Nijmegen, the Netherlands[d]; Université de Strasbourg, UMR, CNRS, Strasbourg, France[e]; Department of Biochemistry, Biophysics and Molecular Biology, Ames, Iowa, USA[f]; School of Environmental Sciences, University of East Anglia, Norwich, United Kingdom[g]; Los Alamos National Lab, Los Alamos, New Mexico, USA[h]; U.S. Department of Energy (DOE), Joint Genome Institute, Walnut Creek, California, USA[i]; Oak Ridge National Lab, Biosciences Division, Oak Ridge, Tennessee, USA[j]; Laboratoire d'Analyse Bioinformatique en Génomique et Métabolisme, Genoscope-IG-CEA, Evry, France[k]

The complete genome sequence of *Methylomicrobium album* strain BG8, a methane-oxidizing gammaproteobacterium isolated from freshwater, is reported. Aside from a conserved inventory of genes for growth on single-carbon compounds, *M. album* BG8 carries a range of gene inventories for additional carbon and nitrogen transformations but no genes for growth on multicarbon substrates or for N fixation.

Received 7 March 2013 **Accepted** 13 March 2013 **Published** 11 April 2013

Citation Kits KD, Kalyuzhnaya MG, Klotz MG, Jetten MSM, Op den Camp HJM, Vuilleumier S, Bringel F, DiSpirito AA, Murrell JC, Bruce D, Cheng J-F, Copeland A, Goodwin L, Hauser L, Lajus A, Land ML, Lapidus A, Lucas S, Médigue C, Pitluck S, Woyke T, Zeytun A, Stein LY. 2013. Genome sequence of the obligate gammaproteobacterial methanotroph *Methylomicrobium album* strain BG8. Genome Announc. 1(2):e00170-13. doi:10.1128/genomeA.00170-13.

Address correspondence to Lisa Y. Stein, lisa.stein@ualberta.ca.

Methanotrophic bacteria are found in diverse environments and utilize methane as their sole source of energy, reductants, and carbon (1). Methanotrophs attenuate the emission of methane, the second most important greenhouse gas (2), and have applications in bioremediation and bioprocessing (3). *Methylomicrobium album* strain BG8 (also known as *Methylobacter albus*, *Methylomonas albus*, and *Methylomonas alba*) is a mesophilic, aerobic gammaproteobacterium isolated from freshwater by Roger Whittenbury et al. (4).

The *M. album* BG8 genome was sequenced, assembled, and annotated by the U.S. Department of Energy Joint Genome Institute (http://www.jgi.doe.gov/sequencing/). Illumina GA II and 454 Titanium standard libraries with paired-end reads were generated, representing 30-fold coverage. Using Newbler v2.3, a chromosomal sequence of 2 contigs and 1 scaffold and a complete plasmid sequence were assembled. Automatic annotation was performed using Prodigal and GenePRIMP (5). The draft genome is 4.49 Mbp, with a mean G+C content of 56.2%. Two copies of the rRNA operon, 42 tRNA genes, and 3,984 predicted protein-coding genes are present. Manual annotation and comparative analysis are under way with assistance from the MicroScope annotation platform at Genoscope (6).

The *M. album* BG8 genome contains one operon (*pmoCAB*) with genes encoding particulate methane monooxygenase and a *pxm* operon (*pxmABC*) with genes encoding a copper membrane monooxygenase of unknown function (7). Genes encoding the enzyme methanol dehydrogenase and accessory proteins (*mxaYDFGIRSACKL-mxaB*) and a Xox-type methanol dehydrogenase (*xoxFJ*) (8) were identified. Genes encoding enzymes for C_1 metabolism include those for the tetrahydrofolate (H_4-folate) and tetrahydromethanopterin (H_4MPT)-linked C_1 transfer pathways, glutathione-dependent formaldehyde dehydrogenases (GD-FALDH) and accessory functions, and a NAD-dependent formate dehydrogenase (encoded by *fdh5A*). A membrane-bound formate dehydrogenase (encoded by *fdh3DABC*) is typically absent in strict methanotrophs, but it is expressed in "*Candidatus* Methylacidiphilum fumariolicum" SolV of the phylum *Verrucomicrobia*. Also similar to "*Ca.* Methylacidiphilum fumariolicum" SolV, *M. album* BG8 was found to have a complete set of genes for glycogen biosynthesis (9). Genes encoding the complete ribulose monophosphate (RuMP) pathway for formaldehyde assimilation, a complete tricarboxylic acid (TCA) cycle, the pentose phosphate pathway, and the Embden-Meyerhof-Parnas pathway were identified. A complement of genes for a complete serine cycle, with the exception of phosphoenolpyruvate carboxylase, was identified; key genes for the Calvin-Benson-Bassham cycle were absent.

Genes encoding enzymes for nitrogen metabolism were identified, including those for direct ammonium uptake (*amtB*), nitrate transport (*narK*), nitrate or nitrite reduction (*nasCA*, *nasB*, and *nirBD*), and glutamine synthetase/glutamate synthase (*glnA*, *gltB*) and alanine dehydrogenase (*ald*) for ammonium assimilation. Tandem genes encoding proteins implicated in the oxidation of hydroxylamine to nitrite (*haoAB*) were identified, which likely facilitate the detoxification of hydroxylamine produced from the oxidation of ammonia by membrane-bound methane monooxygenase (pMMO) (10). Genes encoding a cytochrome cd_1 nitrite reductase (*nirS*) and accessory functions, as well as nitric oxide redutase (*norCB*), were found, perhaps explaining the capacity of this strain to tolerate high nitrite concentrations (11). The *nirS* and *norCB* genes in this strain share high sequence identities with

homologues in other methanotrophs (12, 13). Analysis of the *M. album* BG8 genome sequence enables further understanding of single-carbon metabolism and the environmental adaptation strategies of methanotrophs.

Nucleotide sequence accession numbers. The genome sequences of the chromosome and plasmid of *M. album* BG8 have been deposited in GenBank under accession no. CM001475 and CM001476, respectively.

ACKNOWLEDGMENTS

The work conducted by the U.S. Department of Energy Joint Genome Institute is supported by the Office of Science of the U.S. Department of Energy under contract no. DE-AC02-05CH11231.

We thank additional members of the Organization for Methanotroph Genome Analysis (OMeGA).

L.Y.S. was supported by a Discovery Grant from the Natural Sciences and Engineering Research Council of Canada. M.G.K. was supported by the U.S. NSF (0541797 and 0948202).

REFERENCES

1. **Trotsenko YA, Murrell JC.** 2008. Metabolic aspects of aerobic obligate methanotrophy. Adv. Appl. Microbiol. **63**:183–229.
2. **Conrad R.** 2009. The global methane cycle: recent advances in understanding the microbial processes involved. Environ. Microbiol. Rep. **1**:285–292.
3. **Han JI, Lontoh S, Semrau JD.** 1999. Degradation of chlorinated and brominated hydrocarbons by *Methylomicrobium album* BG8. Arch. Microbiol. **172**:393–400.
4. **Whittenbury R, Phillips KC, Wilkinson JF.** 1970. Enrichment, isolation and some properties of methane-utilizing bacteria. J. Gen. Microbiol. **61**: 205–218.
5. **Hyatt D, Chen GL, LoCascio PF, Land ML, Larimer FW, Hauser LJ.** 2010. Prodigal: prokaryotic gene recognition and translation initiation site identification. BMC Bioinformatics **11**:119.
6. **Vallenet D, Engelen S, Mornico D, Cruveiller S, Fleury L, Lajus A, Rouy Z, Roche D, Salvignol G, Scarpelli C, Médigue C.** 2009. MicroScope: a platform for microbial genome annotation and comparative genomics. Database **2009**:bap021. doi:http://dx.doi.org/10.1093/database/bap021.
7. **Tavormina PL, Orphan VJ, Kalyuzhnaya MG, Jetten M, Klotz MG.** 2011. A novel family of functional operons encoding methane/ammonia monooxygenase-related proteins in gammaproteobacterial methanotrophs. Environ. Microbiol. Rep. **3**:91–100.
8. **Schmidt S, Christen P, Kiefer P, Vorholt JA.** 2010. Functional investigation of methanol dehydrogenase-like protein XoxF in *Methylobacterium extorquens* AM1. Microbiology **156**:2575–2586.
9. **Khadem AF, van Teeseling MCF, Jetten M, Op den Camp HJM, Pol A.** 2012. Genomic and physiological analysis of carbon storage in the verrucomicrobial methanotroph "*Ca.* Methylacidiphilum fumariolicum" SolV. Front. Microbiol. **3**:345.
10. **Stein LY, Bringel F, DiSpirito AA, Han S, Jetten MS, Kalyuzhnaya MG, Kits KD, Klotz MG, Op den Camp HJ, Semrau JD, Vuilleumier S, Bruce DC, Cheng JF, Davenport KW, Goodwin L, Han S, Hauser L, Lajus A, Land ML, Lapidus A, Lucas S, Médigue C, Pitluck S, Woyke T.** 2011. Genome sequence of the methanotrophic alphaproteobacterium *Methylocystis* sp strain Rockwell (ATCC 49242). J. Bacteriol. **193**:2668–2669.
11. **Nyerges G, Han SK, Stein LY.** 2010. Effects of ammonium and nitrite on growth and competitive fitness of cultivated methanotrophic bacteria. Appl. Environ. Microbiol. **76**:5648–5651.
12. **Svenning MM, Hestnes AG, Wartiainen I, Stein LY, Klotz MG, Kalyuzhnaya MG, Spang A, Bringel F, Vuilleumier S, Lajus A, Médigue C, Bruce DC, Cheng JF, Goodwin L, Ivanova N, Han J, Han CS, Hauser L, Held B, Land ML, Lapidus A, Lucas S, Nolan M, Pitluck S, Woyke T.** 2011. Genome sequence of the Arctic methanotroph *Methylobacter tundripaludum* SV96. J. Bacteriol. **193**:6418–6419.
13. **Boden R, Cunliffe M, Scanlan J, Moussard H, Kits KD, Klotz MG, Jetten MS, Vuilleumier S, Han J, Peters L, Mikhailova N, Teshima H, Tapia R, Kyrpides N, Ivanova N, Pagani I, Cheng JF, Goodwin L, Han C, Hauser L, Land ML, Lapidus A, Lucas S, Pitluck S, Woyke T, Stein L, Murrell JC.** 2011. Complete genome sequence of the aerobic marine methanotroph *Methylomonas methanica* MC09. J. Bacteriol. **193**: 7001–7002.

Appendix B: Culture origin and background of *Methylomonas denitrificans* FJG1

The strain *Methylomonas denitrificans* str. FJG1 was received from Dr. Jay Gulledge in 2002 when he was a professor at University of Louisville. The strain was identified by Dr. Gulledge as *Methylomonas methanica* and we published the strain under this name in Nyerges & Stein, 2009 (FEMS Lett. 297:131-136). The strain was subsequently genome-sequenced, which revealed a different phylogeny than the *Methylomonas methanica* strain. With the physiological examination of its denitrifying activity and its robust phylogenetic placement outside of the *Methylomonas methanica* species, the name *Methylomonas denitrificans* str. FGJ1 ("from Jay Gulledge") was adopted.

In conversation with Dr. Gulledge, it is speculated that this strain was part of a larger collection that he isolated from wetlands in Massachusetts in the 1990's. However, the environmental origin of the strain can not be verified.

Appendix C: Inventory of denitrification genes found in aerobic methanotrophs

Genome	narG	nirS	nirK	norB	norSY
Methylacidiphilum fumariolicum SolV			+	+	
Methylacidiphilum infernorum V4			+	+	
Methylobacter luteus IMV-B-3098T		+		+	
Methylobacter sp. BBA5.1		+			
Methylobacter tundripaludum 21/22	+	+	+		+
Methylobacter tundripaludum 21/22		+			
Methylobacter tundripaludum 31/32	+	+	+		+
Methylobacter tundripaludum SV96	+	+			+
Methylobacter whittenburyi ACM 3310		+			
Methylocaldum sp. 175		+			
Methylocaldum szegediense O-12			+	+	
Methylococcaceae sp. 73a					
Methylococcus capsulatus ATCC 19069				+	
Methylococcus capsulatus Bath				+	
Methylococcus capsulatus Texas				+	
Methyloferula stellata AR4					
Methyloglobulus morosus KoM1					
Methylohalobius crimeensis 10Ki			+	+	
Methylomicrobium agile ATCC 35068		+		+	
Methylomicrobium album BG8		+		+	
Methylomicrobium alcaliphilum 20Z				+	
Methylomicrobium buryatense 5G				+	
Methylomicrobium kenyense AMO1					
***Methylomonas denitrificans* FJG1**	+	+	+	+	
Methylomonas methanica MC09		+		+	
Methylomonas sp. 11b		+		+	
Methylomonas sp. LW13		+		+	
Methylomonas sp. MK1		+		+	
Methylosarcina fibrata AML-C10	+		+	+	
Methylosarcina lacus LW14		+		+	
Methylovulum miyakonense HT12		+		+	
Methylocapsa acidiphila B2					
Methylocapsa aurea KYG T					
Methylocella silvestris BL2	+		+	+	
Methylocystis parvus OBBP				+	
Methylocystis rosea SV97T					
Methylocystis sp. LW5					
Methylocystis sp. Rockwell, ATCC 49242			+		
Methylocystis sp. SC2					
Methylocystis sp. strain SB2					
Methylosinus sp. LW3					
Methylosinus sp. LW4					
Methylosinus sp. PW1					
Methylosinus trichosporium OB3b				+	

Table 5: **Presence of putative denitrification genes in publically available genomes of aerobic methanotrophic bacteria.**

Publically available complete genome sequences of 44 aerobic methane-oxidizing bacteria were downloaded from the Integrated Microbial Genomes (IMG) database (https://img.jgi.doe.gov/cgi-bin/mer/main.cgi). Organism names under the "Genome" column indicate the respective organism and genome sequence downloaded from IMG. Verrucomicrobia are shaded in green, Gammaproteobacteria are shaded in blue, and Alphaproteobacteria are shaded in orange. BlastP was used to search for putative homologs of *narG, nirS, nirK, norB, norSY* in all 44 downloaded genomes using an E-value of 1e-20. Blast hits were then manually curated/annotated. The *narG, nirS, nirK,* and *norB* of *M. denitrificans* FJG1 were used as the seeds for the blast search for those respective genes while the *norSY* of *N. europaea* was used as the seed to identify homologs of *norSY*. A "+" in the genes column indicates whether a putative homolog of *narG, nirS, nirK, norB* or *norSY* was identified in a particular genome sequence. A fully shaded row (in grey) under the gene columns indicates that the genome of that organism encodes all necessary genetic inventory for NO_3^- respiration to N_2O.